THE UNIVERSITY OF CHICAGO

MOLECULARLY DEFINING VESICULAR TRAFFICKING PATHWAYS AT THE GOLGI APPARATUS

A DISSERTATION SUBMITTED TO
THE FACULTY OF THE DIVISION OF THE BIOLOGICAL SCIENCES
AND THE PRITZKER SCHOOL OF MEDICINE
IN CANDIDACY FOR THE DEGREE OF
DOCTOR OF PHILOSOPHY

GRADUATE PROGRAM IN CELL AND MOLECULAR BIOLOGY

BY
ADAM HAINES KRAHN

CHICAGO, ILLINOIS
DECEMBER 2025

ABSTRACT

The Golgi apparatus functions as the heart of the eukaryotic cellular endomembrane system, sorting newly made, ER-exported proteins and lipids while circulating and recycling older ones from other organelles. Many membrane traffic machinery proteins reside at the Golgi, with their localizations polarized across the set of cisternae comprising this organelle. A suite of resident Golgi enzymes is likewise polarized. These enzymes sequentially modify proteins and lipids passing through the Golgi, fine-tuning them for their appropriate functions at other organelles or the cell exterior. To perform these functions, the Golgi organizes itself through cisternal maturation, a process by which individual Golgi cisternae are assembled, biochemically altered over time, and then disassembled. Retrograde intra-Golgi vesicular transport pathways are essential for the fidelity of this maturation process, because they both polarize and recycle resident Golgi proteins by allowing younger cisternae to receive these proteins from older cisternae. In spite of this understanding, the number of intra-Golgi vesicular transport pathways and their molecular characteristics have not yet been identified.

In this thesis, I identify and characterize three molecularly distinct intra-Golgi vesicular trafficking pathways at the *Saccharomyces cerevisiae* Golgi. To accomplish this, I designed vesicle capture and tethering assays that concentrate distinct vesicle populations at the yeast bud neck based on cargo content or affinity with a vesicle tether. Both assay types reveal three populations of vesicles containing largely unique sets of transmembrane resident Golgi proteins. Each of these vesicle populations presumably belongs to a distinct intra-Golgi trafficking pathway. The first two pathways employ coat protein complex I (COPI) for vesicle formation and operate at early and intermediate stages of cisternal maturation. The early COPI pathway apparently uses the golgin Rud3 to tether its vesicles prior to their fusion with cisternae, and the intermediate COPI

pathway likewise uses the Sgm1 golgin tether. At the late Golgi, an intra-Golgi trafficking pathway is operated by the clathrin coat and its AP-1 and Ent5 adapter proteins. This AP-1/Ent5 pathway utilizes the Imh1 golgin and Golgi-associated retrograde protein (GARP) complex to coordinately tether its vesicles. Cargo-based vesicle capture analysis further differentiates the intra-Golgi AP-1/Ent5 pathway from other transport pathways that traffic proteins between the late Golgi and prevacuolar endosome (PVE). The PVE-to-Golgi pathway notably utilizes Imh1 but apparently not GARP to tether its vesicles at cisternae. Altogether, the findings presented in this thesis grant us important insights into the molecular mechanisms of Golgi self-organization, particularly with regard to resident protein retention and polarization. Collectively, this work comprises the first systematic molecular characterization of intra-Golgi trafficking pathways.

A substantial amount of data presented in this thesis is from fluorescence time lapse microscopy of live yeast cells. Such experiments showcase the dynamic nature of cisternal maturation, and their data are naturally depicted as videos. Cryo-electron tomography data obtained for this thesis can also be represented as videos revealing a continuum of sections through the 3D volume. Representative videos for both experiment types have been archived online as supplementary files. As a reference, the first frame of each video and an accompanying legend are included at the end of each pertinent chapter.

The earth is the Lord's and the fullness thereof,

the world and those who dwell therein

~ Psalm 24:1 (ESV)

Soli Deo Gloria

TABLE OF CONTENTS

LIST OF FIGURES

LIST OF TABLES

LIST OF MOVIES

ACKNOWLEDGMENTS

While conducting my thesis research, I received the support of numerous scientific colleagues, family members, and friends. I would like to recognize their contributions that enabled and empowered me to complete this work.

I want to first thank my advisor, Ben Glick, for his invaluable mentorship and unwavering support. Ben is an exceptional scientist who has patiently guided me throughout my PhD journey. He has been extremely generous with his time, attention, and professional assistance, allowing me to mature as a scientist. I am also grateful for the members of the Glick lab, both past and present, who have worked alongside and collaborated with me during my PhD training.

I also wish to specifically express my appreciation for Areti Pantazopoulou. Areti first mentored me during my rotation in the Glick lab, and she subsequently became my closest colleague in the lab. I cannot count the number of lessons and pieces of advice Areti gave me while I worked on my thesis research. Our many conversations shaped my scientific growth and helped me hold to the highest possible standards of our discipline.

My thesis committee has been a wonderful source of intellectual support and personal encouragement. Our periodic meetings invariably left me with new perspectives and a renewed sense of accomplishment as I progressed in my work. Christine Labno at the Light Microscopy Core and Joe Austin at the Electron Microscopy Core greatly supported me through their technical expertise and assistance with experiments.

I am blessed to have many friends who have helped provide the crucial support necessary for my personal health and well-being. My friends at the Hyde Park Vineyard Church and University of Chicago Graduate Christian Fellowship (GCF) supported my spiritual, emotional, social, and mental health as I navigated my PhD. Brian Hempel and Carolyn Zhang, two of my

best friends, graduated with their doctoral degrees before I did and were excellent role models. Their empathy and close companionship helped me persist through periods of adversity, whether scientific in nature or otherwise.

My family has always been a safe haven of holistic support and tangible love. They have been extremely patient and understanding, allowing me to work uninterrupted for long periods of time before visiting and vacationing with them. I specifically want to express my utmost appreciation for my parents, Brian and Stacy Krahn. They raised and empowered me to be my authentic self, and always encouraged me to pursue my academic interests, however exotic they became. They made untold sacrifices so that I could pursue my education. I am forever grateful for their love.

Finally, as a man of faith, I want to recognize Jesus Christ as the source of all life. He is the reason I live, the reason I became interested in cell biology, and the reason I maintained the strength, motivation, and vitality to complete my PhD. He is my eternal Savior, Lord, and Friend. All ultimate credit and glory from my accomplishment are His.

CHAPTER 1

INTRODUCTION

Internal compartmentation has been a defining organizational feature of eukaryotic cells across their evolutionary history (Thattai, 2023). The ability of cells to spatially partition their plethora of macromolecules has allowed them to perform specialized functions in optimized subcellular locales. Consequently, they are capable of precisely responding to environmental perturbations on short timescales, a feat that has granted them the fitness required to survive and evolve across untold cellular generations. This is especially evident in the context of multicellular organisms, where cells must concern themselves with the health status of their cellular neighbors which themselves comprise a part of the immediate environment (Marijuán et al., 2013). The intricate compartmentation within eukaryotic cells is both astoundingly beautiful and strikingly utilitarian. Indeed, it is hard to imagine how the diverse life forms on our planet could exist without some form of internal organization facilitated by compartmentation.

To achieve their internal compartmentation and optimize molecular functionality, cells use membrane bound structures called organelles. The many organelles utilized by eukaryotic cells have been subjected to intense study by the scientific community in recent decades. We now know that organelles are not isolated entities. Rather, they interact and communicate with each other through the exchange of proteins and lipids mediated by numerous vesicular and non-vesicular transport mechanisms (Thattai, 2023; Prinz et al., 2020). These communication and trafficking networks allow organelles to maintain their homeostatic identities by establishing personalized proteome and lipidome profiles (Hein et al., 2025; Sarmento et al., 2023). When organelle homeostasis is properly maintained in this manner, a cell can thrive since organelle compartmentation allows it to function optimally at the molecular level.

The Endomembrane System and Golgi Apparatus

Various transport networks exist between different organelles in eukaryotic cells. Perhaps the most well-known transport network is the endomembrane system, which contains the secretory and endocytic trafficking pathways. The major organelles participating in these pathways include the endoplasmic reticulum (ER), Golgi apparatus, endosomes, lysosomes (vacuoles in yeast), and the plasma membrane (not strictly an endomembrane organelle). The ER and Golgi specialize in the enzymatic modification and sorting of proteins and lipids within the cell (Stanley, 2011). They are commonly categorized as secretory organelles since they export macromolecules to endosomes, lysosomes, the plasma membrane, and the extracellular space. The endosomes and plasma membrane specialize in the regulated transport of proteins, lipids, and other molecules between the cell interior and exterior (Naslavsky and Caplan, 2018). These organelles largely organize the endocytic pathways. Lysosomes receive material from both the Golgi and endosomes, allowing them to function as a station for macromolecule decomposition and recycling as well as related metabolic signaling (Settembre and Perera, 2024). Together, these endomembrane organelles regulate the spatial organization of most of the cellular lipidome and roughly one quarter of the cellular proteome (Krogh et al., 2001).

Of all the organelles participating in eukaryotic endomembrane homeostasis, the Golgi Apparatus plays the most centralized role by connecting the endocytic and secretory pathways. The Golgi is considered a single organelle, but it actually consists of multiple membrane bound compartments called cisternae. These cisternae vary in their biochemical compositions, yet collectively participate in protein and lipid processing, sorting, and export (Mironov and Pavelka, 2008). Through an abundance of vesicular transport pathways, the Golgi sorts newly synthesized proteins received from the ER while concurrently retrieving and relocating older ones from other

organelles. Incredibly, the Golgi is simultaneously able to dynamically retain and organize its own proteins and lipids across its set of cisternae (Pantazopoulou and Glick, 2019). This self-organizational feat further establishes the Golgi as a master regulator of endomembrane homeostasis.

The mechanisms of protein and lipid transport through the Golgi and between Golgi cisternae have been studied extensively over the past few decades. Chapter two of this thesis contains a published encyclopedia article on vesicular transport at the Golgi. An emphasis is placed on knowledge obtained from the budding yeast, *Saccharomyces cerevisiae*, the model organism used in this thesis research. The reader should peruse the article for a comprehensive summary of information on Golgi transport, which will provide valuable context for later chapters. When writing the article, the authors were not aware of the experimental findings presented in this thesis. The final model in Figure 2.1A is consequently outdated, and parts of it will be revised in Chapters 3 and 4 using the experimental evidence presented therein. After viewing the article, the reader can return to this first chapter and read the following detailed literature summary describing the molecular tethers investigated in this thesis.

Golgin Tethers

Golgin Localization and Structure

Golgins are a family of Golgi-associated proteins known for their ability to tether vesicles destined for fusion with cisternae (Gillingham, 2017). The name "golgin" associated with these proteins is derived from studies that initially identified some of them as human autoantigens (Fritzler et al.,

1993). Subsequently, the definition of a golgin was not concrete, although researchers have since agreed on certain characteristics that all possess.

Golgins localize to the cytosolic face of cisternal membranes via their C-termini using one or more of three mechanisms. The most common means of attachment is through binding a GTPase of the Rab, Arl or Arf families (Witkos and Lowe, 2016). The other two mechanisms are tail anchoring with a transmembrane sequence, and association with other peripheral membrane proteins on the cisternal surface. Some golgins (e.g. GM130, Coy1) use multiple localization mechanisms (Moyer et al., 2001; Bekier et al., 2017; Anderson et al., 2017; Anderson and Barlowe, 2019), although GTPase binding is typically required for cisternal association when a golgin utilizes it. Like other resident Golgi proteins, golgins are polarized across the cisternal stack. However, due to limitations in experimental techniques, localization assignments for golgins have largely been limited to the *cis*-Golgi, *trans*-Golgi, or the medial Golgi and/or Golgi rims (Tie et al., 2018; Witkos and Lowe, 2016; Su et al., 2025; Goud and Gleeson, 2010).

Aside from their localization to Golgi cisternae, another characteristic common to all golgins is the presence of an extended series of coiled coil domains along most of their length (Munro, 2011). Many proteins involved in membrane traffic possess coiled coil domains, but golgins each appear to have at least 300 amino acids comprising a series of these domains. This lengthy structure gives golgins enough rigidity to protrude 100 to 600 nm from the cisternal membrane to tether vesicles. Short, unstructured 'linker' sequences are often positioned between coiled coil domains, and Rab GTPase binding sites are sometimes present along the golgin length (Muschalik and Munro, 2018; Sinka et al., 2008). These are thought to grant intrinsic and Rab GTPase-regulated flexibility to golgins so they can move vesicles closer to cisternal membranes and promote their fusion (Witkos and Lowe, 2017; Ishida et al., 2015; Lesa et al., 2000).

Another property of golgins is their predicted tendency to form parallel oligomers using the coiled coil domains along their lengths. Published data has verified the oligomerization status for two golgins (Cheung et al., 2015; Ishida et al., 2015), and there is a consensus that golgins at least form parallel homodimers. Of note, a recent preprint from the Rothman research group has reported that six mammalian golgins form parallel dimers *in vitro*, with a subset of these golgins additionally forming anti-parallel dimers (Su et al., 2025).

Golgin Functions in Golgi Structure and Cellular Polarization

Like many proteins, golgins perform multiple functions in various cellular contexts. These functions range from tethering vesicles to supporting cellular polarization. A common theme is the promotion of cellular and tissue-level organization as demonstrated by studies across multiple cell types and model organisms (Lowe, 2019).

Golgins were first recognized for their role in establishing and regulating Golgi structure. Early electron microscopy studies observed string-like structures spanning the inter-cisternal spaces of Golgi stacks and protruding from cisternal rims (Franke et al., 1972; Orci et al., 1998). These were interpreted to be golgins. Subsequently, golgins were assigned as major members of the Golgi matrix, a set of proteins thought to maintain Golgi structural integrity and create an observed ribosome exclusion zone around the organelle (Staehelin and Kang, 2008; Lowe, 2011). More recent studies have confirmed roles for golgins in promoting cisternal stacking in the budding yeast *Pichia pastoris* (Jain et al., 2019; Dahara and Bhattacharyya, 2025) and regulating Golgi cisternal morphology, stacking, and ribbon formation in mammalian cells (Diao et al., 2003; Brown et al., 2011; Lee et al., 2014). Those studies examining the impact of golgin depletion on Golgi morphology in higher eukaryotes have sometimes been confounded by the relatively large

number of partially functionally redundant golgins present in these organisms (Reddy et al., 2006; Goud and Gleeson, 2010). In such cases, multiple golgins and/or other Golgi matrix proteins must be removed to substantially perturb Golgi morphology and function. These complications notwithstanding, there is a consensus that at least some golgins play a role in maintaining Golgi structural integrity (Xiang and Wang, 2011).

Through their ability to engage the cytoskeleton, golgins also play a role in regulating Golgi architecture, positioning, and cell polarization (Thyberg and Moskalewski, 1999; Goud and Gleeson, 2010). An abundance of studies have discovered interactions between golgins and microtubules (Kulkarni-Gosavi et al., 2019). These interactions link Golgi membranes and polarized microtubules, allowing the Golgi ribbon to be formed and maintained in the perinuclear region of the cell. This is especially apparent during cell division, when obligate Golgi disassembly necessitates re-formation of Golgi stacks and ribbons from Golgi membranes inherited by both daughter cells (Ayala et al., 2020). Golgin mediated Golgi-microtubule connections also play critical roles in maintaining cell polarity through the polarization of anterograde membrane trafficking from the Golgi (Ravichandran et al., 2020). Some golgins have been reported to help create or stabilize microtubule organizing centers, providing a possible mechanism for Golgi-assisted cytoskeletal polarization (Rios, 2014; Sanders and Kaverina, 2015). However, it remains unclear whether golgin-microtubule interactions help establish cellular polarization or merely serve to support it. Interactions between golgins and actin have also been described, but these serve to expand the Golgi ribbon and maintain flattened cisternal morphology rather than directly influence cell polarization (Lázaro-Diéguez et al., 2006; Makhoul et al., 2019).

Vesicle Tethering by Golgins

Arguably, golgins are best known for their ability to tether vesicles destined for fusion with Golgi cisternae (Gillingham, 2017). Such tethering activity was first demonstrated *in vivo* by the Munro group using ectopic localization assays in mammalian cells (Wong and Munro, 2014; Shin et al., 2020). A later study also demonstrated vesicle tethering by golgins in Drosophila (Park et al., 2022). In the mammalian cell experiments, ten golgins were individually anchored to mitochondria at their C-termini, and seven of them were observed to capture transport vesicles with Golgi resident proteins and/or ER exported cargo. Most golgins showed tethering specificity for vesicles with different protein compositions, suggesting they act in different Golgi trafficking pathways. However, some proteins were present in multiple tethered vesicle populations, confounding nuanced interpretations of the data. The authors concluded that golgin-mediated vesicle tethering aids in membrane trafficking organization at the Golgi.

The molecular mechanisms of vesicle tethering by golgins are incompletely understood, although some studies have provided concrete insights. It is known that the N-terminal 21 to 49 amino acids of at least six mammalian golgins are necessary and sufficient for vesicle capture (Wong et al., 2017). The cis-Golgi localized GMAP-210 golgin uniquely possesses an amphipathic lipid-packing sensor (ALPS) motif at its N-terminus. This motif is known to recognize regions of high membrane curvature and apparently mediates vesicle tethering by GMAP-210 (Sato et al., 2015; Magdeleine et al., 2016). Of note, the GMAP-210 ALPS motif is not fully conserved in invertebrates, yet residues flanking the motif assist in vesicle tethering and are conserved (Wong et al., 2017). These insights suggest the presence of undiscovered molecular interactions that grant tethering activity to GMAP-210 and its orthologs.

At the *trans*-Golgi network (TGN), a different mechanism allows golgin-97 and golgin-245 to tether Golgi-destined carriers arriving from endosomes (Gillingham, 2017). A catalytically inactive Rab GTPase activating protein, TBC1D23, was found to bind the N-termini of these golgins, and link them to the FAM21A subunit of the WASH complex (Shin et al., 2017). This is significant, as the WASH complex localizes to carriers emerging from endosomes (Seaman et al., 2013). In addition, the C-terminal domain of TBC1D23 was found to interact with a threonine-leucine-tyrosine (TLY) sequence present in several endosome-to-Golgi trafficked proteins like carboxypeptidase D and syntaxin-16 (Cattin-Ortolá et al., 2024). The current understanding is that TBC1D23 serves as a bridge for tethering by linking golgin-97 and golgin-245 to the WASH complex and/or TLY motif containing cargo proteins present in incoming endosome-derived carriers.

Similar to the WASH complex, the WDR11 complex also plays a role in linking TBC1D23 to Golgi-bound vesicles (Navarro Negredo et al., 2018; Lowe, 2019). Researchers found that the WDR11 complex specifically assists in golgin-245 vesicle tethering, potentially through direct recruitment of TBC1D23 onto vesicles. Although removal of WDR11 only partially abolished ectopic vesicle tethering by golgin-245, a near quantitatively identical result was obtained in cells lacking adaptor protein complex 1 (AP-1), which forms vesicles with the aid of the clathrin coat (Duncan, 2022). These data suggest that the WDR11 complex may work with TBC1D23 to specifically aid in the tethering of AP-1 vesicles at the TGN.

Golgin Contributions to Organismal Physiology

The cellular organization promoted by golgins is paralleled by their influence on tissue organization and cellular specialization during organismal development. Studies in mice and

zebrafish have demonstrated devastating physiological consequences upon the loss of a golgin (Lowe, 2019). For example, loss of golgin GM130 causes neuromuscular defects in zebrafish (Shamseldin et al., 2016) and slow growth, ataxia, lung and liver fibrosis, and postnatal death in mice (Liu et al., 2017; Park et al., 2018). Removal of mouse GMAP-210 causes lethal skeletal dysplasia (Smits et al., 2010), while removal of the golgin Giantin causes a milder version of the same disease in zebrafish (Stevenson et al., 2017). On the level of cellular specialization, golgin-160 and golgin TMF both play critical roles in mouse sperm development (Lerer-Goldshtein et al., 2010; Bentson et al., 2013). Male mice lacking either of these golgins are infertile due to deficiencies in sperm motility and acrosome formation. Collectively, studies like these examining the physiological roles of golgins highlight their importance for healthy organismal development.

Although golgins clearly promote organization at the level of cells and tissues, not all golgins appear equally critical in this regard. For example, removal of golgin-84 in mice showed no obvious physiological impact (McGee et al., 2017). There are also no reports of organismal phenotypes for the individual loss of golgin-97, golgin-245, GCC88, GCC185, and CASP. It appears that these golgins are either less functionally critical and/or are functionally redundant. A recent study in Drosophila supports the latter concept for golgins in general, demonstrating pre-eclosion lethality only when all three of GMAP (GMAP-210 ortholog), golgin-84, and TMF were removed (Park et al., 2022). Researchers in the field currently favor the idea that most golgins are partially redundant in function, and this perspective is supported by numerous experiments showing little to no impact of single golgin knockdowns or knockouts in cells (Witkos and Lowe, 2016; Muschalik and Munro, 2018).

Golgins in Saccharomyces cerevisiae

The budding yeast, *S. cerevisiae*, possesses five known golgins that have been characterized to varying extents (Munro, 2011). These golgins are listed in Table 1.1 alongside their human orthologs and plausible functions in vesicular trafficking. As the research in Chapter 4 largely examines Rud3, Sgm1, and Imh1, a detailed summary of the literature for these three golgins is provided below.

***S. cerevisiae* Golgin**	**Human Ortholog(s)**	**Likely *S. cerevisiae* Golgin Function(s) In Vesicular Transport**
Bug1	GM130	Promotes COPII vesicle fusion with the early Golgi (Behnia et al., 2007)
Rud3	GMAP-210	Promotes fusion of COPII and intra-Golgi vesicles with the early Golgi (Siniossoglou and Pelham, 2001; Anderson et al., 2017)
Coy1	CASP	Regulates COG-dependent, intra-Golgi vesicle fusion (Anderson et al., 2017; Anderson and Barlowe, 2019)
Sgm1	TMF	Contributes to COG-dependent intra-Golgi vesicular transport (Siniossoglou and Pelham, 2001; Anderson et al., 2017)
Imh1	Golgin-97, Golgin-245, GCC88, and GCC185	Supports vesicular transport between the late Golgi and endosomes (Chen et al., 2019)

Table 1.1: ***Saccharomyces cerevisiae* has five golgins with corresponding human orthologs.** The names of human and yeast golgins are provided alongside a summary of the likely functions of *S. cerevisiae* golgins.

Golgin Imh1

The *S. cerevisiae* golgin Imh1 possesses a C-terminal GRIP domain, an extended region of coiled coil domains, and an unstructured N-terminal region. The GRIP domain, as its name implies,

promotes Imh1 association with Golgi cisternae (Kjer-Nielsen et al., 1999; Setty et al., 2003). *Pichia pastoris* Imh1 forms parallel homodimers with splayed N-terminal ends, and this dimerization is apparently mediated by its GRIP domain and central coiled coil region (Jain et al., 2018). All of these biochemical properties are likely true for *S. cerevisiae* Imh1, as one study found evidence of Imh1 dimerization in vivo (Tsukada et al., 1999).

S. cerevisiae Imh1 localization requires binding of its GRIP domain to the activated Arl1 GTPase at the late Golgi (Setty et al., 2003; Panic et al., 2003). The mechanism of Arl1 activation has not been fully elucidated, but it requires the Golgi resident transmembrane receptor Sys1 which recruits the acetylated Arl3 GTPase, potentially through a direct interaction (Behnia et al., 2004). Through an unknown mechanism, Golgi-associated Arl3 recruits Arl1-GTP, likely with the aid of one or both of the guanine nucleotide exchange factor proteins Syt1 and Gea2 (Chen et al., 2010; Hsu et al., 2016; Duan et al., 2024). In total, research efforts have revealed the importance of the Arl3 to Arl1 GTPase cascade for late Golgi Imh1 localization. They have further underscored the importance of Sys1 in initiating this cascade. However, the precise temporal localization of Imh1 during cisternal maturation, and the vesicular trafficking pathway(s) that deliver Sys1 to cisternae have not yet been definitively identified.

Research efforts over the past few decades have yielded evidence suggesting that *S. cerevisiae* Imh1 functions as a vesicle tether for endosome-to-Golgi transport. As with studies on mammalian golgins, these investigations were sometimes hampered by a lack of detectable phenotypes upon deletion of Imh1 alone. However, one of the earliest studies observed improper secretion of carboxypeptidase Y (CPY) upon Imh1 removal (Tsukada et al., 1999). This is significant, as CPY sorting depends on the Vps10 receptor that recycles between the late Golgi and yeast prevacuolar endosome (Cooper and Stevens, 1996). The same study reported a synthetic

growth defect as well as degradation of the late Golgi Kex2 protease upon additional deletion of Ypt6, a GTPase that was later found to support intra-Golgi and endosome-to-Golgi transport (Luo and Gallwitz, 2003). Using fluorescence and electron microscopy experiments, the authors observed an accumulation of vesicles and fragmented vacuoles in cells lacking Imh1 and Ypt6. These data provided initial evidence that Imh1 assists in vesicular transport between the Golgi and endosomes.

Subsequent studies further clarified the role of Imh1 as an Arl1 effector that promotes vesicular transport at the late Golgi. One research group discovered that a cold sensitive growth defect occurring due to overactive Arl1 could be rescued by Imh1 overexpression (Benjamin et al., 2011). Another group reported that Arl1 or Imh1 overexpression could completely restore normal trafficking of the late Golgi resident proteins Sft2, Tlg1, and Snc1 in cells lacking Ypt6 (Chen et al., 2019; Lai et al., 2023). Interestingly, the authors noted that deletion of the N-terminal 100 amino acids of Imh1 abrogated its ability to restore proper transport of these three proteins. They mechanistically explained this by suggesting that the Imh1 N-terminus is responsible for aiding in the cisternal recruitment of the GARP complex, a multi-subunit tether thought to function in endosome-to-Golgi transport (Dubuke and Munson, 2016; Chen et al., 2019). However, another non-mutually exclusive explanation is that the Imh1 N-terminus recognizes incoming vesicles, and its deletion therefore eliminates Imh1 vesicle tethering and perturbs late Golgi protein transport.

In total, these studies suggest that Imh1 regulates vesicular trafficking between the Golgi and endosomes. Whether this regulation occurs via vesicle tethering and/or another mechanism (e.g. GARP recruitment) is an open question that requires investigation. Assuming Imh1 plays a direct role in vesicular transport at the late Golgi, it will also be important to determine which trafficking pathway(s) it operates in. In particular, the hypothesis that Imh1 functions in intra-

Golgi transport should be tested as the *S. cerevisiae* late Golgi acts as an early endosome (Day et al., 2018).

Golgin Sgm1

Compared to Imh1, *S. cerevisiae* Sgm1 has not been extensively studied. Sgm1 was initially characterized through an affinity purification screen for Ypt6 effectors (Siniossoglou and Pelham, 2001). Using GTPase binding assays and microscopy experiments, the authors confirmed that Sgm1 is a bona fide effector of Ypt6 and requires this GTPase for its Golgi localization. The C-terminal coiled coil domain of Sgm1 was later found to bind activated Ypt6 (Fridmann-Sirkis et al., 2004). The localization of Sgm1 during cisternal maturation has not been determined, although Ypt6-GTP is apparently present at both the early and late Golgi (Suda et al., 2013).

The exact function of Sgm1 has been elusive, with minimal data implicating a role in intra-Golgi transport. The authors who initially characterized Sgm1 noted its predicted coiled-coil architecture, and consequently suspected it might act in vesicle tethering and endosome-to-Golgi trafficking (Siniossoglou and Pelham, 2001). However, they did not observe a trafficking defect of the endocytic SNARE Snc1 upon deletion of Sgm1 alone or Sgm1 and Imh1 in combination. Another study presented evidence that Sgm1 may act with the golgins Coy1 and Rud3 to promote the COG-dependent fusion of intra-Golgi vesicles (Anderson et al., 2017). The deletion of Sgm1 in combination with the removal of Coy1 and/or Rud3 caused moderate to large glycosylation and growth defects. Furthermore, membrane fractionation experiments revealed that deletion of Coy1, Sgm1, or both golgins caused a significant loss of COG from Golgi membranes. These data, although sparse, suggest that Sgm1 coordinates with COG, Coy1, and Rud3 to promote the fusion of retrograde intra-Golgi transport vesicles containing glycosyltransferases. The precise

function(s) of Sgm1, whether vesicle tethering or otherwise, and the trafficking pathway(s) in which it operates have remained important topics for future investigation.

Golgin Rud3

The *S. cerevisiae* golgin Rud3 was first discovered and researched over twenty years ago as a suppressor of temperature sensitive Uso1 and Cog3 alleles (VanRheenen et al., 1999; Kim et al., 1999). Since then, it has received little attention despite published data suggesting it functions in critical stages of Golgi transport. Rud3, like other golgins, is predicted to contain central coiled coil domains flanked by less structured N- and C-terminal regions (VanRheenen et al., 1999). A landmark study found that Rud3 contains a C-terminal GRIP-related Arf binding (GRAB) domain that binds active Arf1 GFPase at the Golgi (Gillingham et al., 2004). The GRAB domain is conserved in Rud3 orthologs from a wide range of species. It is required for Rud3 membrane association as the mutation of a key residue (L410A) within this domain abolishes *in vitro* Arf1-GTP binding and *in vivo* Rud3 Golgi localization. Rud3 also contains two GRAB-associated (GA) motifs, GA1 and GA2. These motifs are less conserved across other species, but GA1 nevertheless contributes to Rud3 function (Gillingham et al., 2004).

The precise localization of Rud3 during cisternal maturation has not been described, but single time point localization data places it at the early Golgi. Rud3 colocalizes partially with Uso1, a protein that supports the ER-to-Golgi transport of COPII vesicles (Cao et al., 1998; Gillingham et al., 2004). In addition, Rud3 colocalizes well with the early Golgi mannosyltransferase Och1 but minimally with the intermediate Golgi mannosyltransferase Mnn1 and late Golgi exomer component Chs5 (Kim, 2003). The apparent restriction of Rud3 to the early Golgi is puzzling, since cisternal Arf1-GTP levels increase during maturation and peak at the late Golgi (Manzer and

Fromme, 2023). In fact, Rud3 does not completely colocalize with Arf1-GTP and additionally requires the ER cargo receptor Erv14 for its Golgi localization (Gillingham et al., 2004). It is a formal possibility that Rud3 obligately binds both Erv14 and Arf1-GTP to associate with cisternae. However, it is also possible that Erv14 instead enables the ER-to-Golgi transport of another receptor for Rud3 which itself recycles constitutively through the ER. The exact mechanism which restricts Rud3 to the early Golgi is therefore incompletely understood.

ER-to-Golgi transport is a critical stage in the formation of new Golgi cisternae, and Rud3 may play a role in this transport step. As mentioned earlier, Rud3 genetically interacts with the COG complex and Uso1, both of which reportedly function in COPII ER-to-Golgi vesicle transport (Cao et al., 1998; VanRheenen et al., 1998, 1999). Cells lacking Rud3 exhibit slowed growth at temperatures over 30°C, and Rud3 overexpression partially suppresses temperature sensitive alleles of Bos1 and Sec22, both of which are SNAREs that promote the fusion of COPII vesicles with Golgi cisternae (Newman et al., 1990; Kim, 2003). These data imply that Rud3, while not essential for ER-to-Golgi transport, may contribute to the efficacy of this crucial trafficking step.

Some data also suggest Rud3 may promote the fusion of intra-Golgi transport vesicles. First, genetic interactions between COG and Rud3 can be interpreted as evidence for this as COG is known to mediate the fusion of intra-Golgi vesicles (Blackburn et al., 2019). Second, Rud3 was reported to physically interact with the COG binding partner Coy1 by yeast two-hybrid analysis (Zhang et al., 2009). Finally, loss of both Sgm1 and Rud3 causes a synthetic growth defect which is greatly exacerbated upon further loss of Coy1 (Anderson et al., 2017). As Coy1 apparently does not promote ER-to-Golgi transport (Anderson et al., 2017), it is reasonable to hypothesize that Rud3 aids in the fusion of intra-Golgi vesicles. If so, it will be critical to understand which intra-

Golgi trafficking pathway(s) Rud3 acts in, and whether vesicle tethering is a mechanism employed by Rud3.

Multisubunit Tethering Complexes at the Golgi

The conserved oligomeric Golgi (COG) complex is a Golgi-localized multisubunit tethering complex (MTC) thought to tether vesicles and promote their SNARE-mediated fusion with cisternae (Dubuke and Munson, 2016; Witkos and Lowe, 2017). COG is an hetero-octameric complex consisting of two tetrameric subcomplexes called lobe A and lobe B (Blackburn et al., 2019). Evidence for vesicle tethering by COG has been found both *in vitro* and *in vivo* (Willett et al., 2013; Cottam et al., 2014). This tethering capability is presumably mediated by some of the many interactions between COG subunits and Golgi proteins including SNAREs, Rab GTPases, and golgins (Willett et al., 2013). The identities of the trafficking pathways assisted by COG are unknown. However, given the broad distribution of COG across the Golgi stack (Vasile et al., 2006), it is likely that this MTC tethers vesicles from many if not most intra-Golgi trafficking pathways.

The Golgi-associated retrograde protein (GARP) complex is an MTC that is structurally and evolutionarily related to COG (Bonifacino and Hierro, 2011). GARP forms a single heterotetramer resembling one of the COG lobes, and it consists of the subunits Vps51, Vps52, Vps53, and Vps54. Like COG, GARP associates with Golgi cisternae and is thought to tether vesicles. Less research has currently examined GARP compared to COG, and the ability of GARP to tether vesicles has not been clearly demonstrated. Nevertheless, documented interactions between GARP and resident Golgi SNAREs and GTPases suggest that GARP and COG function similarly as vesicle tethers (Khakurel and Lupashin, 2023). As the research in this thesis examines

GARP and not COG, the following literature review covers our present knowledge about GARP in greater detail.

GARP Structure

The structure of GARP has not been empirically determined in detail, but reasonable models have been proposed. An initial study of *S. cerevisiae* GARP using negative stain electron microscopy found evidence of a flexible Y-shaped structure (Chou et al., 2016). To achieve this structure, the N-terminal domains of all four GARP subunits interact to form a central bundle from which the C-terminal segments of Vps52, Vps53, and Vps54 protrude. A later study corroborated these results using a computational approach combining the RoseTAAFold and AlphaFold protein interaction and structure prediction programs (Humphreys et al., 2021). The computed structure of GARP possessed the same Y-shape configuration and subunit distribution as the one visualized by electron microscopy. This structure for GARP, although plausible, does not reveal any conformational changes which may occur as the complex functions during the vesicle tethering and fusion processes. Advanced experimentation examining GARP structure *in situ* will be required to observe these dynamics and elucidate precisely how this MTC functions.

GARP Localization

GARP localizes to the late Golgi/TGN in yeast and mammalian cells, yet its localization mechanism somewhat differs between cell types and is not fully understood (Khakurel and Lupashin, 2023). In yeast, efficient GARP recruitment to cisternae requires Ypt6 but not Arl1 (Siniossoglou and Pelham, 2001; Panic et al., 2003). *In vitro* experiments indicate that Ypt6-GTP interacts with Vps52, and Arl1-GTP interacts with Vps53 (Siniossoglou and Pelham, 2002; Panic

et al., 2003). However, only the Ypt6-Vps52 interaction is GTP nucleotide preferential. These data suggest that Ypt6 and not Arl1 is responsible for GARP recruitment to cisternae in yeast, although the presence of Ypt6 at early Golgi cisternae suggests that another factor is necessary to restrict GARP to the late Golgi (Conibear and Stevens, 2000; Suda et al., 2013). Interestingly, overexpression of Arl1 completely restores GARP localization to Sec7-positive cisternae in yeast cells lacking Ypt6 (Chen et al., 2019). Arl1 may therefore support Ypt6-mediated GARP cisternal recruitment and help restrict GARP to the late Golgi. Future studies should determine the precise localization of GARP during cisternal maturation and identify other factors specifying its timing of cisternal association.

In mammalian cells, GARP localization depends on Arl5, a GTPase that is absent from *S. cerevisiae*. Knockout of Arl5 largely displaces GARP from the Golgi to the cytosol (Ishida and Bonifacino, 2019). The same study found that knockouts of Arl1 or the Ypt6 homolog Rab6 do not displace GARP, even though Vps52 physically interacts with Rab6-GTP (Liewen et al., 2005). A separate study also documented a loss of GARP from the mammalian Golgi upon knockdown of Arl5, corroborating the Arl5 knockout phenotype (Rosa-Ferreira et al., 2015). These studies distinguish the GARP localization mechanism in mammalian cells from that used by yeast.

As a final note, mammalian cells possess an endosome-associated recycling protein (EARP) complex that only differs from GARP by the substitution of Vps54 with another subunit, Vps50 (Schindler et al., 2015). EARP localizes to recycling and/or early endosomes and presumably functions in an analogous way to GARP, although it has not been studied extensively (Spang, 2016). *S. cerevisiae* does not possess an EARP complex, presumably because it has a minimal endomembrane system with a late Golgi that performs the functions of early and recycling endosomes (Day et al., 2018).

GARP Contributions to Organismal Physiology

The GARP complex is crucial for normal organismal development and physiology. Complete loss of Vps54 causes embryonic lethality in mice, infertility or non-viability in *Caenorhabditis elegans*, and male infertility in *Drosophila melanogaster* (Khakurel and Lupashin, 2023). In mice, a recessive mutant allele of VPS54 causes a wobbler phenotype characterized by a gradual loss of motor neurons as well as accompanying muscle atrophy and motility defects (Moser et al., 2013). The wobbler allele destabilizes the GARP complex and causes its degradation, providing a logical explanation for its detriment. On the tissue and cellular levels, the resulting GARP deficiency causes endomembrane transport defects, reduced axonal transport, neurofilament aggregation, neuronal hyperexcitability, and neuroinflammation. These phenotypes are similar to those seen in the human disease amyotrophic lateral sclerosis, prompting researchers to use the wobbler mouse as a model organism to study this disease (Schmitt-John, 2015).

Deficiencies in GARP/EARP function also cause severe cerebellar atrophy and developmental deficiencies in humans. Using whole exome sequencing, one study found an intragenic deletion in VPS51 as the likely cause of postnatal microcephaly, delayed psychomotor development, and severe intellectual disability in two siblings (Uwineza et al., 2019). Another study reported multiple heterozygous mutations within VPS51 in an individual suffering from global developmental delay, microcephaly, and epilepsy among other conditions (Gershlick et al., 2019). It was determined that the mutations either caused Vps51 degradation by the proteasome or prevented efficient association of Vps51 with the other GARP and EARP subunits. Additional studies have found mutations in VPS53 that are thought to cause progressive cerebello-cerebral atrophy 2 and Hereditary spastic paraparesis (Feinstein et al., 2014; Hausman-Kedem et al., 2019). Collectively, these reports have implicated the GARP and/or EARP complexes as crucial

contributors to human development, and in particular, to proper cerebellar growth and maintenance.

General GARP Contributions to Cell Physiology

Multiple studies have reported varying endomembrane system perturbations upon partial or complete loss of GARP function (Khakurel and Lupashin, 2023). Several studies demonstrated reduced secretion in mammalian cell lines with knockouts of different GARP subunits (Hirata et al., 2015; Homma and Fukuda, 2021). GARP removal also causes the depletion of Golgi glycosylation machinery and SNAREs, as well as the displacement of COPI and some of its regulating protein partners from cisternae (Khakurel et al., 2021, 2022). GARP even plays a role in sphingolipid homeostasis, with its functional deficiency causing the accumulation of sphingolipid synthesis intermediates in mammalian cells (Fröhlich et al., 2015). It should be noted that all but one of the above studies in mammalian cells perturbed both GARP and EARP in their experiments, obscuring functional distinctions between the complexes. In addition, as GARP has been mechanistically implicated in facilitating endosome-to-TGN vesicular transport (more on this below), some of the reported GARP-deficiency phenotypes are likely indirect effects. Nevertheless, they highlight the critical role GARP plays as a multisubunit tethering complex operating at an interface of the secretory and endocytic pathways.

GARP Contributions to Membrane Trafficking

GARP was initially identified in *S. cerevisiae* as a complex required for vacuolar protein sorting at the late Golgi (Conibear and Stevens, 2000). Yeast lacking GARP have fragmented vacuoles, secrete the vacuolar enzyme carboxypeptidase Y (CPY), and partially missort the late Golgi

protease Kex2 to the vacuole. They also grow and secrete more slowly than their wild type counterparts. The localizations of the CPY receptor, Vps10, and the Snc1 SNARE, both of which traffic through the late Golgi, are also perturbed in GARP deficient yeast (Conibear et al., 2003). At the time of these initial studies, researchers thought Snc1, Vps10, and Kex2 all trafficked through the early and/or late endosomes to the late Golgi. GARP was therefore proposed to function in promoting vesicular transport from endosomes to the late Golgi. This understanding of GARP function may need refinement, because Snc1, Vps10, and Kex2 potentially recycle in three different pathways (Papanikou et al., 2015; Day et al., 2018; Casler et al., 2021).

Subsequent studies in mammalian cells provided further evidence for the hypothesized role of GARP in endosome-to-TGN transport. One research group observed a substantial mislocalization of TGN resident proteins upon knockdown or knockout of different GARP/EARP subunits (Pérez-Victoria and Bonifacino, 2009; Ishida and Bonifacino, 2019). They also discovered an inability of GARP deficient cells to efficiently transport endocytosed cargos to the TGN. Since endocytosed cargos first arrive at early endosomes and some TGN residents recycle through endosomes, the data in these studies support a role for GARP in promoting endosome-to-TGN transport. However, even in GARP knockout experiments, trafficking deficiencies were only partial, indicating that other trafficking machinery proteins and/or transport pathways can compensate for the loss of GARP function.

In an effort to more precisely examine the role of GARP in membrane traffic, researchers have employed the auxin inducible degradation system to uncover the immediate impacts of GARP removal on membrane trafficking. One study was performed in *S. cerevisiae*, and utilized a quantitative proteomics approach to query for the mislocalization of GARP-dependent proteins to the vacuole (Eising et al., 2019). Interestingly, the authors failed to observe significant vacuolar

missorting of most late Golgi localizing proteins (e.g. Vps10) after 30, 60, and 90 minutes of auxin induced GARP depletion. They instead found that aminophospholipid flippases and cell wall synthesis proteins were mislocalized from the plasma membrane to the vacuole. Other studies have also implicated the GARP complex in regulating phospholipid flipping and cell wall composition (Conde et al., 2003; Takagi et al., 2012). It is therefore plausible that *S. cerevisiae* GARP directly aids in the trafficking of lipid flippases and cell wall synthesis proteins from the plasma membrane to the late Golgi. Degradation of GARP could gradually arrest this transport step and cause the eventual vacuolar mislocalization of these proteins.

A second GARP degron study, performed in mammalian cells, used microscopy to examine the localization of TGN proteins after three or more hours of auxin treatment (Khakurel et al., 2022). The authors reported a partial mislocalization of some but not all glycosylation enzymes and TGN resident proteins examined. In particular, the cation-independent mannose-6-phosphate receptor (CI-MPR), functionally analogous to yeast Vps10, was not depleted from the TGN. Cisternal dissociation of the COPI coat as well as the Gga2 and AP-1 adaptors also occurred after three hours of auxin application. These observations likely reveal indirect effects of GARP depletion on Golgi function. Nevertheless, the collective data from this study suggests that GARP promotes the retrieval of certain Golgi resident proteins to cisternae.

In summary, research on the GARP complex highlights its role in promoting vesicular transport from endosomes to the TGN. Nevertheless, neither the precise identities of distinct endosome-to-TGN trafficking pathways nor which of these pathways GARP acts in are currently known. To rectify this knowledge gap, the GARP degradation-related data described above may be useful in formulating working hypotheses. For example, GARP in yeast will likely operate in a trafficking pathway with vesicles carrying phospholipid flippases and/or cell wall synthesis

proteins. On the other hand, a pathway with vesicles containing Vps10 may not involve GARP. Of additional investigative importance is the hypothesis that GARP assists with intra-Golgi recycling. The endocytic SNARE Tlg1, once thought to recycle from early endosomes to the late Golgi in *S. cerevisiae*, likely recycles using an intra-Golgi route (Casler et al., 2021). Since an interaction between Tlg1 and Vps51 has been well documented (Siniossoglou and Pelham, 2002; Conibear et al., 2003; Fridmann-Sirkis et al., 2006), it is possible that GARP aids in the fusion of Tlg1-containing, intra-Golgi vesicles.

Proposed Molecular Mechanisms of GARP Function

The fusion of transport vesicles with their target organelles requires the bundling of four different SNARE proteins in *trans* (Baker and Hughson, 2016). To drive lipid mixing and membrane fusion, these SNAREs must be collectively contributed by both the organelle and vesicle membranes. MTCs like GARP are thought to facilitate the formation of the pre-fusion, trans-SNARE complex. If this occurs, the molecular mechanism will likely include a transient tethering event during which the MTC simultaneously engages the SNAREs embedded in both opposing membranes. Evidence presented below suggests that GARP employs such a mechanism as it promotes the fusion of vesicles with Golgi cisternae.

Interactions between GARP and SNAREs involved in endocytic trafficking have been detected. As stated previously, the Vps51 GARP subunit is known to interact with the Tlg1 SNARE in *S. cerevisiae* (Siniossoglou and Pelham, 2002). An analogous interaction between mammalian GARP and Stx6, the Tlg1 homolog, was also found (Abascal-Palacios et al., 2013). A landmark study found that Stx16, Vti1, and Vamp4, the three other endocytic SNAREs known to form a complex with Stx6, also individually interact with GARP (Pérez-Victoria and Bonifacino,

2009). The authors determined these interactions occur via the SNARE motif of each SNARE, and that GARP-SNARE interactions persist after SNARE bundling. GARP depleted cells also experience a reduction in the formation of this SNARE complex as detected by co-immunoprecipitation. This is correlated with a partial loss of Stx16 and Vamp4 from the TGN. In total, these data support a hypothetical mechanism for GARP function that involves simultaneous SNARE coordination followed by SNARE complex formation and concomitant membrane fusion.

Assuming GARP aids in SNARE pairing, the question remains whether it acts as a bona fide vesicle tether. Although definitive evidence of vesicle tethering by GARP has been lacking, at least two studies have reported mislocalization to the cytosol of TGN resident proteins in GARP-deficient yeast and mammalian cells (Conboy and Cyert, 2000; Pérez-Victoria et al., 2008). The cytosolic haze observed likely originated from vesicles that require GARP for their timely fusion with cisternae. The implication is that GARP normally catalyzes vesicle fusion with the TGN, potentially by tethering them to cisternae. Another study ectopically localized Vps51 to mitochondria and observed the concurrent accumulation of Stx6-containing vesicles at this organelle (Koike and Jahn, 2019). The authors plausibly claimed that GARP tethered these vesicles, but they did not rule out the possibility that EARP was at least partially responsible for their observation. In conclusion, while it is likely that GARP plays a vesicle tethering role during the vesicle fusion process, further research is required to robustly support this hypothesis.

Summary of Research Objectives and Motivation

Years of research have largely uncovered the set of proteins that operate vesicular transport pathways between Golgi cisternae as well as between the Golgi and other organelles

(Pantazopoulou and Glick, 2019). The logical next objective is to molecularly define these trafficking pathways, a challenge researchers have not yet rigorously tackled. A complication is the lack of a consensus definition for a vesicular trafficking pathway adopted by the scientific community. The definition I present here is therefore preliminary, and is proposed to conceptually frame and motivate the research performed for this thesis.

Vesicular trafficking pathways at the Golgi can be defined using a combination of five general attributes: 1) The organellar origin and destination of the vesicular transport intermediates, 2) The time windows during cisternal maturation when vesicles of each pathway bud and/or fuse with cisternae, 3) The cargo molecules present in the vesicles of each pathway, 4) The molecules involved in the processes of vesicle formation and fission, and 5) The molecules involved in the processes of vesicle transport, tethering, and fusion. It should be noted that the first attribute is not strictly required in the case of intra-Golgi transport between two cisternae. However, it will be important to include when considering transport pathways between the Golgi and other organelles (e.g. the ER).

The research findings presented in this thesis address all five of the above attributes to characterize vesicular trafficking pathways at the Golgi in the budding yeast, *S. cerevisiae*. In particular, the experiments in Chapter 3 query the protein cargo content of Golgi-derived vesicles and clarify some of the previously identified molecular coats and adaptors that mediate their formation and fission. These data are used to hypothesize molecularly distinct vesicular trafficking pathways at the Golgi. Subsequently, Chapter 4 examines molecular tethers that assist in the fusion processes for vesicles of each proposed trafficking pathway. Both chapters additionally examine the timing of trafficking pathways during cisternal maturation and ultimately achieve progress towards holistically defining them in molecular terms.

CHAPTER 2

INTRA-GOLGI TRANSPORT

Abstract

Many newly synthesized proteins pass through the Golgi apparatus. This passage is driven by the maturation of Golgi cisternae, which are disk-shaped membrane compartments that contain the newly synthesized proteins together with resident Golgi processing enzymes. Golgi cisternae continually form, transform, and then dissolve into transport carriers. Meanwhile, resident Golgi proteins recycle by pathways that involve either intra-Golgi recycling or transport to another organelle and back. These processes are regulated by multiple GTPases. The different kinetics of the various recycling pathways generate polarized distributions of resident Golgi proteins. An ongoing challenge is to elucidate the mechanisms that control Golgi dynamics.

This chapter is a version of an article published in the Encyclopedia of Cell Biology Second Edition, 2023. The authors are A. H. Krahn and B. S. Glick. I wrote the first draft. B.S. Glick and I revised it and subsequent drafts.
B. S. Glick designed the figure. *Reprinted from Encyclopedia of Cell Biology, Second Edition, Adam H. Krahn and Benjamin S. Glick, Intra-Golgi Transport, 495-506, Copyright 2023, with permission from Elsevier.*

Introduction

Organelles of the cellular endomembrane system constantly exchange membrane, and a central component of this system is the Golgi apparatus. Disk-shaped Golgi compartments called cisternae receive newly synthesized proteins from the endoplasmic reticulum (ER) and subsequently deliver newly synthesized proteins and lipids to the cell surface and to endosomes, lysosomes, and vacuoles (Chou et al., 2016). The protein and lipid cargoes that pass through the Golgi undergo various types of processing. For example, in the Golgi, glycoproteins are remodeled by the addition and trimming of sugars, and glycosphingolipids are synthesized (D'Angelo et al., 2013; Orlean, 2012; Schjoldager et al., 2020). In addition to these transient cargoes, the Golgi contains resident proteins that employ recycling pathways to remain within the organelle. Thus, intra-Golgi transport involves the forward movement of newly synthesized cargoes as well as the retrograde movement of resident Golgi proteins.

Cell biologists view the Golgi as a machine (Nicholson, 2019) with the core components being cisternae. But human-made machines are built from stable components that operate in a fixed way, whereas Golgi cisternae undergo rapid transformation and turnover (Pantazopoulou and Glick, 2019). The full implications of this insight are only gradually being appreciated. Because dynamics are key to understanding how the Golgi works, we will use this perspective to synthesize the available information.

Golgi Structure

Although the basic functions and characteristics of the Golgi are conserved, the structure of this organelle varies between species. The vertebrate Golgi consists of stacks of cisternae linked

laterally by tubular membrane connections into a "Golgi ribbon" (Rambourg and Clermont, 1997; Wei and Seemann, 2010). These lateral connections make the Golgi more efficient at synthesizing certain large secretory cargoes (Lavieu et al., 2014). By contrast, most invertebrates, fungi, and plants possess individual Golgi stacks throughout the cytoplasm (Mollenhauer and Morré, 1991). Some eukaryotes, including the budding yeast *Saccharomyces cerevisiae*, have non-stacked cisternae (Mowbrey and Dacks, 2009; Papanikou and Glick, 2009). These observations imply that the basic functions of the Golgi are carried out by individual cisternae, which can be arranged in various ways to meet the needs of different cell types.

A given cisterna is not homogeneous in composition. In the stacked mammalian Golgi, glycosylation enzymes are concentrated in the interiors of the cisternae while trafficking components are concentrated at the rims (Tie et al., 2018). Lateral segregation of trafficking components is also seen in non-stacked yeast cisternae (Kurokawa et al., 2019), suggesting that this phenomenon is a general property of Golgi membranes.

Stacking of Golgi cisternae apparently involves proteins called golgins, which are rod-shaped dimers that project from the cisternae into the cytoplasm (Gillingham and Munro, 2016). Golgins have mainly been implicated in vesicle tethering as described below. In addition, a study of the yeast *Pichia pastoris* showed that deletion of a peripherally membrane-associated golgin caused partial unstacking of the Golgi (Jain et al., 2019). The authors suggested that the two subunits of a dimeric golgin might link adjacent cisternae. Studies in mammalian cells support this general concept, although the inactivation of multiple golgins and/or golgin-binding proteins is required to unstack the mammalian Golgi (Lee et al., 2014). The physiological role of cisternal stacking is

unknown, but a plausible idea is that close association of cisternae facilitates the regulation of intra-Golgi transport.

The vertebrate Golgi ribbon is generated with the aid of microtubules, which emanate from the microtubule-organizing center (MTOC) (Thyberg and Moskalewski, 1999). Additional microtubules are nucleated by the Golgi membranes themselves (Sanders and Kaverina, 2015). In many cell types, the Golgi ribbon is positioned near the MTOC. Some of the ER exit sites are associated with the Golgi ribbon while others are in the cell periphery (Budnik and Stephens, 2009; Hammond and Glick, 2000). Elements of the "ER-Golgi intermediate compartment" (ERGIC) carry newly synthesized proteins from peripheral ER exit sites toward the MTOC by means of a golgin linked to a molecular motor (Burkhardt, 1998; Yadav et al., 2012). ERGIC elements are not fully characterized, but they seem to represent ER-derived membranes that have recycled some components to the ER (Appenzeller-Herzog and Hauri, 2006). After newly synthesized proteins traverse the vertebrate Golgi, juxtaposition to the MTOC enables the microtubule network to be harnessed for delivery of secretory vesicles to the plasma membrane, and to specific plasma membrane domains in polarized cells (Fourriere et al., 2020). If microtubules are artificially disrupted, the vertebrate Golgi reorganizes into functional "mini-stacks" that are present throughout the cytoplasm (Cole et al., 1996; Thyberg and Moskalewski, 1999). Thus, the vertebrate Golgi ribbon is a microtubule-dependent enhancement of the stacked Golgi architecture seen in many other eukaryotes.

Golgi Polarity

Golgi cisternae vary in their properties and interactions with other organelles. This phenomenon is most evident for a stacked Golgi, in which cisternae on opposite sides of the stack contain different transmembrane and peripheral membrane proteins as well as distinct lipids (Dunphy and Rothman, 1985; Farquhar and Hauri, 1997). Historically, this polarity led the Golgi to be viewed as an ordered set of compartments labeled *cis*, *medial*, *trans*, and *trans*-Golgi network (TGN). Newly synthesized proteins arrive at the *cis*-Golgi and depart from the TGN. But despite the widespread use of terminology referring to Golgi compartments, those compartments have never been precisely defined with regard to their molecular compositions (Pantazopoulou and Glick, 2019). An alternative terminology, equally suited to stacked and non-stacked Golgi organelles, states that newly synthesized proteins are initially found in "early Golgi" cisternae and are subsequently found in "late Golgi" cisternae. Early Golgi cisternae are associated with ER exit sites in many organisms (Glick, 2014; Kurokawa et al., 2014; Staehelin and Kang, 2008), and this association supports bidirectional membrane traffic (Barlowe and Miller, 2013; Roy Chowdhury et al., 2020). In vertebrate cells, the analogous association is between ERGIC elements and ER exit sites (Budnik and Stephens, 2009; Hammond and Glick, 2000; Raote et al., 2021). Late Golgi cisternae can be considered synonymous with the TGN, where newly synthesized proteins are sorted into export carriers (Di Martino et al., 2019; Ramazanov et al., 2021).

The polarized composition of the Golgi enables the cell to assign different biochemical activities to early or late cisternae. For example, in vertebrate cells, early cisternae support initial oligosaccharide modifications, while late cisternae support terminal oligosaccharide modifications as well as glycosphingolipid synthesis and the proteolytic processing of certain secretory cargoes

(D'Angelo et al., 2013; Tie et al., 2016). Enzymes that carry out these reactions are concentrated in different parts of the Golgi stack, although these enzymes show overlapping distributions rather than being strictly segregated into separate cisternae (Rabouille et al., 1995). The processing and sorting functions of the Golgi depend on membrane trafficking components, which themselves exhibit a polarized distribution (Gillingham and Munro, 2016; Kim et al., 2016; Thomas and Fromme, 2020). As described below, membrane traffic pathways generate the polarized distribution of resident Golgi transmembrane proteins. Therefore, Golgi polarity is both a mechanism for and a consequence of Golgi function.

The Cisternal Maturation Model for Intra-Golgi Transport

After extensive debates about the mechanisms of intra-Golgi transport, most researchers now favor the cisternal maturation model (Glick and Luini, 2011). This model states that Golgi polarity results from progressive changes in the properties of individual cisternae. Golgi cisternae are not stable compartments, but rather transient structures whose compositions and activities evolve in a defined sequence (Figure 2.1). An early cisterna matures into a late cisterna, typically within about 5-30 minutes depending on the cell type. Maturing cisternae serve as forward transport carriers for newly synthesized proteins.

Golgi maturation involves three basic processes: cisternal formation, retrograde vesicular transport, and cisternal dissolution. A cisterna forms by the homotypic fusion of membranes derived from the ER. Then the cisterna receives resident Golgi proteins from older cisternae by retrograde vesicular transport. As the cisterna matures, it continues to import components from older cisternae while exporting other components to younger cisternae. Finally, when the cisterna

reaches the TGN stage, it dissolves into various types of carriers, some of which contain proteins and lipids destined for the cell surface or for endolysosomal organelles.

Microscopy has provided the best evidence for Golgi maturation. Electron microscopy revealed that the Golgi transports large cargoes, including algal scales and procollagen bundles (Becker et al., 1995; Leblond, 1989). A careful study revealed that procollagen remains within the cisternae, implying that cisternae are the forward carriers for this secretory cargo (Bonfanti et al., 1998). Budding yeast provided the first direct visualization of maturing cisternae. In *S. cerevisiae*, individual cisternae are optically resolvable, and dual-color live cell fluorescence microscopy confirmed that a cisterna changes composition over time (Losev et al., 2006; Matsuura-Tokita et al., 2006). Fluorescent secretory cargoes can be visualized within maturing yeast cisternae as the resident Golgi proteins come and go (Casler et al., 2019; Kurokawa et al., 2019). In cells with Golgi stacks, such live-cell imaging experiments are not feasible because the cisternae are too close together to be resolved by light microscopy, so there is still uncertainty about whether mammalian Golgi cisternae behave like their yeast counterparts (Pellett et al., 2013; Pfeffer, 2010). However, the strong conservation of membrane trafficking components suggests that Golgi maturation is also conserved.

The maturation mechanism is probably augmented in mammalian cells (Glick and Luini, 2011). A simple maturation model predicts that all secretory cargoes should traverse the Golgi at the same rate, but albumin traverses the mammalian Golgi about ten times faster than procollagen (Beznoussenko et al., 2014). This albumin “fast track” appears to involve transient tubular connections that connect different cisternae within a stack when cells are actively secreting.

Because albumin is not glycosylated, it derives no benefit from residing in the Golgi, and the tubular connections allow the cell to transport large amounts of albumin without moving corresponding amounts of membrane. In general, different cell types probably adapt the basic cisternal maturation mechanism for their particular requirements.

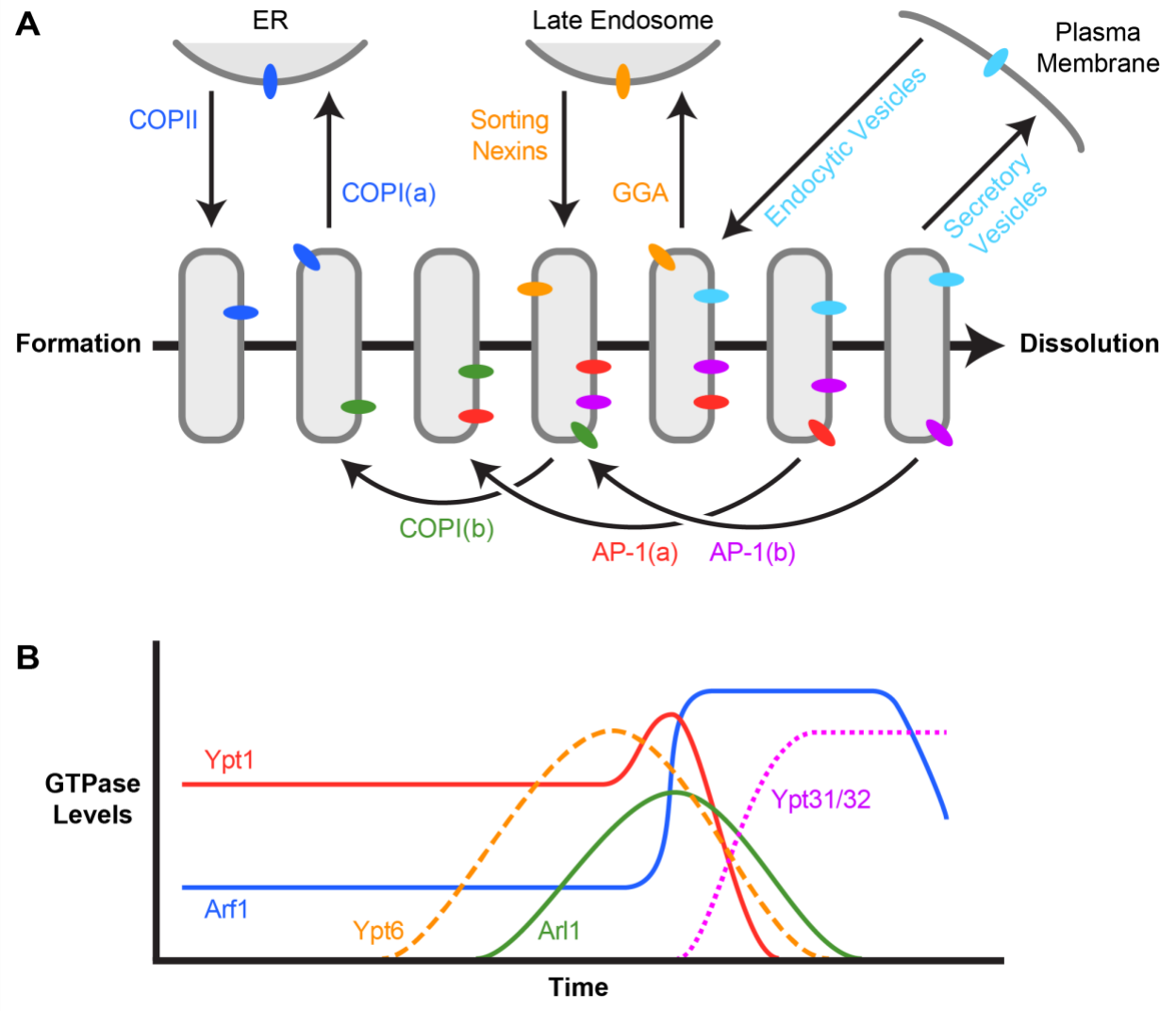

Figure 2.1: **Membrane recycling and GTPase activity during Golgi maturation in S. cerevisiae.** *(continued on next page)*

Figure 2.1: **(A)** Membrane traffic pathways for an individual yeast Golgi cisterna during the time course of maturation. Transmembrane proteins are shown as colored ovals. The thick arrow represents time, and the thin arrows represent six recycling pathways (Casler et al., 2021; Pantazopoulou and Glick, 2019). *Blue*: SNAREs and other transmembrane proteins exit the ER in COPII vesicles, and some of those proteins recycle to the ER in COPI(a) vesicles. *Green*: Glycosylation enzymes and other early Golgi proteins recycle within the Golgi in COPI(b) vesicles. *Red*: Sys1 and other proteins that act at an intermediate stage of maturation recycle within the Golgi in AP-1(a) vesicles. *Orange*: A subset of TGN proteins, including the acid hydrolase receptor Vps10, travel in GGA vesicles to late endosomes and then return in carriers generated by sorting nexins. *Purple*: Many TGN proteins, including processing proteases, recycle within the Golgi in AP-1(b) vesicles. *Light Blue*: Secretory vesicles contain SNAREs and other transmembrane proteins that subsequently recycle to the Golgi in endocytic vesicles. In mammalian cells, Golgi membrane traffic is presumably similar but more elaborate. For example, mammalian endocytic vesicles fuse with early endosomes, which in turn transport material to the Golgi. **(B)** Levels of active GTPases on a yeast Golgi cisterna during maturation. The horizontal axis represents time on the same scale as in (A), and the vertical axis represents the amount of a GTPase at the membrane surface in arbitrary units. These plots are approximations based on the existing data (Lipatova and Segev, 2019; Thomas and Fromme, 2020; Tojima et al., 2019). *Blue*: At the early Golgi, Arf1 recruits COPI and a vesicle tether, and at the late Golgi, additional Arf1 recruits multiple effectors that include coats and adaptors. *Green*: At an intermediate stage of maturation, Arl1 recruits multiple effectors that include vesicle tethers. *Red*: At the early Golgi, Ypt1 recruits vesicle tethers, and during the early-to-late Golgi transition, additional Ypt1 cooperates with Arl1 to recruit an Arf1 GEF. *Orange (dashed)*: At an intermediate stage of maturation, Ypt6 recruits vesicle tethers. *Purple (dotted)*: At the late Golgi, Ypt31/Ypt32 recruits multiple effectors that include a myosin motor for transporting secretory vesicles. In mammalian cells, a larger number of GTPases act at the Golgi, but many of those GTPases are related to the yeast enzymes and likely perform similar functions.

Transport of Newly Synthesized Proteins Through the Golgi

In a stacked Golgi, maturing cisternae carry newly synthesized proteins forward by progressing from the *cis* to the *trans* face (Mollenhauer and Morré, 1991). The mechanism of cisternal progression has not been directly studied, but three processes likely contribute. First, the formation of new cisternae at the *cis* face of the stack may create a pushing force. Second, motor proteins pull maturing cisternae away from the *trans* face during the formation of secretory vesicles, which travel along cytoskeletal tracks to the plasma membrane (Fourriere et al., 2020; Mogelsvang et al.,

2003; Santiago-Tirado et al., 2011; Jin et al., 2011). Third, stacking interactions presumably transmit these pushing and pulling forces to move all of the cisternae forward in synchrony.

For some newly synthesized proteins, a fraction of the molecules partition into retrograde vesicles that otherwise serve to recycle resident Golgi proteins. Retrograde intra-Golgi movement of a secretory cargo has been described in yeast (Casler et al., 2019). A similar pathway may account for the finding that after mammalian cells were artificially fused, a secretory cargo exchanged between the separate Golgi ribbons (Pellett et al., 2013). The significance of this retrograde traffic is unknown, but it slows the departure of newly synthesized proteins from the Golgi, thereby providing more opportunities for correct processing and sorting.

Secretory cargoes exit the Golgi when the TGN produces carriers for delivery to the plasma membrane (Ford et al., 2021; Di Martino et al., 2019). The simplest view is that constitutive secretory vesicles are the remnants of terminally mature TGN cisternae (Glick and Malhotra, 1998). Yeast probably employs this mechanism, although in addition, yeast has a protein complex called exomer that delivers certain proteins from the TGN to the plasma membrane (Paczkowski et al., 2015). The situation is more complex in polarized mammalian cells, where different classes of secretory cargoes are sorted at the TGN into carriers destined for either the apical or the basolateral plasma membrane domain (Stoops and Caplan, 2014). Some mammalian secretory cargoes appear to pass through TGN-like recycling endosomes en route to the cell surface (Ang et al., 2004; Grant and Donaldson, 2009). In many cell types, the TGN also produces regulated secretory granules that fuse with the plasma membrane in a signal-dependent manner (Turkewitz, 2004; Omar-Hmeadi and Idevall-Hagren, 2020). The cargoes of regulated secretory granules undergo progressive aggregation and condensation as the granules form. Sorting at the TGN is

thought to involve calcium-dependent interactions between luminal cargoes and their receptors as well the partitioning of certain cargoes into sphingolipid-rich membrane domains (Ramazanov et al., 2021).

Exit from the TGN to the plasma membrane has been considered a default pathway, but at least for some transmembrane proteins, exit from the TGN requires signals such as glycosylation (Gut et al., 1998; Parmar et al., 2014; Sun et al., 2020). In light of the cisternal maturation model, which postulates that the TGN is a transient compartment, the mechanism that traps proteins in the TGN is not obvious. A possible explanation is that proteins retained in the TGN actually undergo repeated rounds of recycling in intra-Golgi transport vesicles.

Some of the newly synthesized proteins that reach the TGN are not delivered to the plasma membrane, but instead are transported either to endosomes, or to lysosomes in animal cells or vacuoles in fungi and plants. Many transmembrane proteins are delivered directly from the TGN to lysosomes or vacuoles (de Marcos Lousa and Denecke, 2016). Other soluble and transmembrane proteins travel from the TGN to late endosomes and then either remain in late endosomes, or travel further to lysosomes or vacuoles, or recycle to the TGN. In yeast, proteins destined for late endosomes depart from the TGN well before the formation of secretory vesicles (Figure 2.1A) (Casler and Glick, 2020; Daboussi et al., 2012), and in mammalian cells, the kinetics of the TGN-to-late endosome pathway are probably similar (Daboussi et al., 2017).

Newly synthesized proteins begin to segregate from one another in the early Golgi. This phenomenon has been reported for secretory granule proteins (Clermont et al., 1992) and

endolysosomal proteins (Chen et al., 2017). Moreover, there are indications that some secretory cargoes can leave the mammalian Golgi before the terminal TGN stage (Mogelsvang et al., 2004; Tie et al., 2016). Thus, sorting events may occur throughout Golgi maturation.

The sorting and vesicle formation events at the TGN involve a variety of lipid rearrangements (von Blume and Hausser, 2019). Phospholipid flippases of the P4-ATPase family promote membrane curvature during transport carrier formation (Best et al., 2019). During the TGN stage of maturation, lipid kinases generate phosphatidylinositol 4-phosphate (PI4P), which regulates the formation of transport vesicles (Highland and Fromme, 2021; Walch-Solimena and Novick, 1999). Some of the PI4P molecules are transferred to the ER in exchange for sterols, a process that takes place in mammalian cells at contact sites between the ER and the late Golgi (Del Bel and Brill, 2018; Venditti et al., 2020). Sterols are thought to interact with the glycosphingolipids synthesized in the late Golgi to generate lipid domains involved in cargo sorting (D'Angelo et al., 2013; Ford et al., 2021; Rizzo et al., 2021).

Recycling of Golgi Proteins During Cisternal Maturation

As a cisterna matures, resident Golgi proteins arrive and depart in a defined sequence. A peripheral membrane protein typically binds to a cisterna, and then dissociates into the cytosol when its job is finished, and then binds once again to a younger cisterna. By contrast, a transmembrane protein necessarily recycles in a vesicle or vesicle-like carrier. Membrane components are delivered to a maturing cisterna by multiple recycling pathways (Figure 2.1A). A given Golgi transmembrane protein typically follows a single recycling pathway that determines when the protein resides in a cisterna (Pantazopoulou and Glick, 2019). These various recycling pathways have different

kinetics, which give rise to the observed polarity in the distributions of transmembrane proteins across the Golgi (Casler et al., 2021). The machinery that recycles resident Golgi proteins is described below.

GTPases Act as Molecular Switches During Golgi Maturation

In the secretory pathway, the top-level regulators of membrane traffic and membrane composition are small GTPases of the Arf, Arl, and Rab families (Mizuno-Yamasaki et al., 2012; Thomas and Fromme, 2020). The activity of a GTPase is determined by its nucleotide status. While bound to GTP, the GTPase associates with the membrane and recruits effector proteins. Upon hydrolysis of GTP to GDP, the GTPase dissociates from the membrane. Golgi-associated GTPases are regulated by guanine nucleotide exchange factors (GEFs) and GTPase-activating proteins (GAPs). GEFs activate GTPases by promoting the replacement of GDP with GTP, while GAPs inactivate GTPases by catalyzing GTP hydrolysis. Each GEF or GAP localizes to a cisterna during a particular stage of maturation, and as a result, a given GTPase has a characteristic kinetic signature (Figure 2.1B). The various GTPases, GEFs, and GAPs at the Golgi are functionally interconnected, thereby ensuring that trafficking pathways are initiated and terminated at the appropriate times to orchestrate cisternal maturation.

Arf family GTPases include Sar1, which recruits the COPII coat to the ER membrane, and Arf1, which recruits multiple coats and coat adaptors, including the COPI coat at the early Golgi and the AP-1 clathrin adaptor at the late Golgi (Sztul et al., 2019; Adarska et al., 2021). After a coated vesicle forms, a GAP promotes uncoating to enable the vesicle to fuse with its target membrane. The timing of uncoating probably varies between different types of coats—in some cases, the coat

may disassemble immediately after a vesicle pinches off, while in other cases, the coat may persist and may play a role in targeting to the destination membrane (Schröter et al., 2016). Additional Arf1 effectors include a vesicle tether and phosphatidylinositol 4-kinases (Gillingham and Munro, 2016; Highland and Fromme, 2021). Peripherally membrane-associated Arf1 GEFs operate at the early Golgi, and related Arf1 GEFs operate at the late Golgi (Thomas and Fromme, 2020), so Arf1 is present on a cisterna throughout the maturation process (Figure 2.1B).

Arl family GTPases are regulated by a pathway that begins with the transmembrane protein Sys1, which recruits an Arl protein called Arl3 in yeast or ARFRP1 in mammals (Panic et al., 2003; Setty et al., 2003; Shin et al., 2005; Zahn et al., 2006). Arl3/ARFRP1 then recruits Arl1 in yeast or Arl1 and Arl5 in mammals. This pathway merits further study because the mechanisms of Sys1 and Arl3/ARFRP1 action are unknown. The downstream Arl proteins are present on a cisterna during an intermediate stage of maturation (Casler et al., 2021; Tojima et al., 2019) (Figure 2.1B), and they recruit effectors that include vesicle tethers (Gillingham and Munro, 2016; Goud and Gleeson, 2010; Ishida and Bonifacino, 2019).

Rab family GTPases play a central role in Golgi maturation (Figure 2.1B) (Kim et al., 2016; Lipatova and Segev, 2019). Yeast Ypt1, which is related to mammalian Rab1, acts during ER-to-Golgi transport and at the early Golgi to recruit vesicle tethers (Goud et al., 2018). Yeast Ypt6 and mammalian Rab6 act at an intermediate stage of maturation to recruit additional vesicle tethers (Fridmann-Sirkis et al., 2004; Siniossoglou and Pelham, 2001; Suda et al., 2013; Goud et al., 2018). Yeast Ypt31/Ypt32 and mammalian Rab11 promote cargo exit from the TGN, partly by recruiting motor proteins that assist in secretory vesicle formation and transport (Santiago-Tirado

et al., 2011; Welz et al., 2014; Lipatova et al., 2008). Finally, yeast Sec4 and mammalian Rab8 promote the tethering of secretory vesicles at the plasma membrane with the aid of the multi-subunit exocyst complex (Wu and Guo, 2015). At least in some cases, Rab proteins operate in a cascade that involve one Rab recruiting a GEF for the next Rab, which in turn recruits a GAP for the first Rab (Rivera-Molina and Novick, 2009; Suda et al., 2013). The result of a Rab cascade is a change in the composition and activity of the cisterna.

A Golgi-associated GTPase may interact functionally with GTPases from other families. For example, at the late Golgi, Ypt1/Rab1 and Arl1 help to recruit an Arf1 GEF (Christis and Munro, 2012, 201; McDonold and Fromme, 2014), and the resulting Golgi-associated Arf1 then recruits a GAP to inactivate Ypt1 (Thomas et al., 2021). These GTPase networks are part of the system that controls Golgi maturation (Pantazopoulou and Glick, 2019; Thomas and Fromme, 2020).

Peripheral membrane proteins of the Golgi, including the coats, adaptors, and tethers described below, are typically recruited with the aid of GTPases. A given peripheral membrane protein binds to a cisterna in response to GTPase activation and subsequently dissociates into the cytosol in response to GTPase inactivation. Thus, GTPases directly control the recycling and the polarized distribution of many resident Golgi peripheral membrane proteins.

Coats and Adaptors Form Multiple Types of Transport Carriers

The movement of transmembrane proteins between different Golgi cisternae, and between the Golgi and other organelles, is usually mediated by vesicles or vesicle-like carriers (Figure 2.1A). These carriers are formed by peripherally membrane-associated coats and adaptors.

COPII mediates ER-to-Golgi traffic

Newly synthesized proteins are transported from the ER to the Golgi with the aid of the COPII coat (Barlowe and Miller, 2013; Jensen and Schekman, 2011). COPII consists of an inner layer of subunits that bind ER-localized cargoes plus an outer layer of subunits that polymerize to form a curved lattice. In yeast, COPII generates spherical vesicles, and in animal cells, COPII also helps to generate tubules (Mironov et al., 2003; Mogelsvang et al., 2003; Shomron et al., 2021; Weigel et al., 2021). COPII binds directly to some transmembrane cargoes, and it binds indirectly via cargo receptors to other transmembrane cargoes and to luminal cargoes. When COPII generates vesicles, the bound cargoes are selectively captured in the vesicles. Alternatively, when COPII assembles at the base of ER-derived tubules, the turnover and directed flow of COPII subunits may drive selective transport of COPII-bound cargoes into the tubules. The COPII system also supports a nonselective "bulk flow" delivery of newly synthesized proteins to the Golgi (Barlowe and Helenius, 2016).

COPII is unusually flexible in two ways. First, COPII can polymerize with different levels of curvature to generate spherical coats of varying size (Stagg et al., 2008). Second, COPII can assemble in a different geometry to form tubular lattices (Zanetti et al., 2013). This flexibility is needed to enable the ER export of diverse cargoes, including some that would not fit inside conventional COPII vesicles (McCaughey and Stephens, 2019). Most notably, animal cells produce procollagens that form elongated rods. In vertebrate and insect cells, procollagen export from the ER is facilitated by a transmembrane ER protein called TANGO1, which both recognizes procollagen and helps to shape COPII into tubules that can accommodate this cargo (Feng et al., 2021; Raote et al., 2021). TANGO1 has also been implicated in fusing ERGIC elements with

COPII-containing ER exit sites to generate "tunnels" for the transport of cargoes such as procollagen (Raote and Malhotra, 2021). Ongoing studies aim to clarify the relative contributions of COPII vesicles, COPII-generated tubules, and ER-to-ERGIC tunnels in the exit of newly synthesized proteins from the ER.

COPI mediates Golgi-to-ER and intra-Golgi recycling

Proteins are recycled from the Golgi to the ER with the aid of the COPI coat, also known as coatomer (Popoff et al., 2011). COPI is a heptameric complex that has both cargo-binding and lattice-forming activities. Proteins recycled by COPI include escaped ER transmembrane proteins, as well as receptors that capture newly synthesized proteins in the ER for delivery to the Golgi (Barlowe and Miller, 2013). Some of the proteins recycled by COPI have C-terminal dilysine (KKxx or KxKxx) peptides that are recognized directly by COPI (Cosson and Letourneur, 1997; Jackson, 2014). Other proteins are recycled indirectly by COPI, which binds to Golgi-localized receptors that recognize escaped ER proteins for retrieval to the ER. One retrieval receptor is Rer1, which recognizes the membrane-embedded segments of certain transmembrane ER proteins (Annaert and Kaether, 2020; Sato et al., 2001). A second retrieval receptor is the mammalian KDEL receptor and the related yeast HDEL receptor, which recognize C-terminal tetrapeptides present on many soluble ER proteins (Bräuer et al., 2019; Pelham, 1995). In the case of the KDEL receptor, binding to a KDEL-containing ligand induces redistribution from the Golgi to the ER (Lewis and Pelham, 1992). COPI-dependent Golgi-to-ER retrograde traffic is sometimes referred to as the COPI(a) pathway (Donohoe et al., 2007) (Figure 2.1A). Because the KDEL receptor can mediate retrieval from Golgi cisternae as late as the TGN (Miesenböck and Rothman, 1995), the COPI(a) pathway probably operates during a large part of the maturation process.

A second COPI-dependent process, sometimes referred to as the COPI(b) pathway, mediates the intra-Golgi recycling of resident Golgi proteins such as glycosylation enzymes (Donohoe et al., 2007; Glick and Luini, 2011) (Figure 2.1A). This pathway ensures that glycosylation enzymes remain in the Golgi as newly synthesized cargoes pass through. COPI(b)-dependent recycling is largely restricted to proteins of the early Golgi (Adolf et al., 2019; Papanikou et al., 2015; Tojima et al., 2019). The mechanism of COPI(b)-dependent recycling is incompletely understood, but the available evidence suggests that the cytosolic tails of glycosylation enzymes are recognized either directly by COPI (Liu et al., 2018), or indirectly via an adaptor called Vps74 in yeast or GOLPH3 in mammals (Rizzo et al., 2021; Schmitz et al., 2008; Tu et al., 2008; Welch et al., 2021). Transmembrane domain length also plays a role in the recycling of glycosylation enzymes, perhaps by influencing how efficiently the enzymes partition into the curved COPI vesicle membrane (Welch and Munro, 2019). It is not known how the same COPI machinery generates distinct COPI(a) and COPI(b) vesicles, which differ in both their contents and their target organelles.

The AP-1 clathrin adaptor mediates intra-Golgi recycling downstream of COPI

The tetrameric AP-1 adaptor recognizes signals in the cytosolic tails of transmembrane proteins, and it captures those proteins into vesicles by simultaneously binding clathrin (Paczkowski et al., 2015; Tan and Gleeson, 2019). In yeast, the intra-Golgi recycling of many resident Golgi transmembrane proteins is mediated by AP-1 (Casler et al., 2021; Liu et al., 2008; Valdivia et al., 2002). Yeast AP-1 seems to be involved in two sequential pathways, termed the AP-1(a) and AP-1(b) pathways, that recycle Golgi transmembrane proteins traditionally designated medial/*trans* residents or TGN residents, respectively (Figure 2.1A) (Casler et al., 2021). As with COPI, it is

unknown how the AP-1 adaptor generates two types of vesicles. Mammalian AP-1 has not yet been shown to mediate intra-Golgi recycling, but it does mediate retrograde traffic in the late secretory pathway (Hinners and Tooze, 2003; Hirst et al., 2012; Matsudaira et al., 2015). Both yeast and mammalian AP-1 operate in conjunction with epsin-related clathrin adaptors (Casler et al., 2021; Duncan et al., 2003; Hirst et al., 2015; Myers and Payne, 2013).

Mammalian AP-1 has also been implicated in the forward traffic of certain secretory cargoes from the TGN to the plasma membrane (Tan and Gleeson, 2019; Fölsch, 2015). The mechanisms remain to be clarified, and some of the actions ascribed to mammalian AP-1 might be indirect, but AP-1 likely has more diverse functions in mammalian cells than in yeast.

GGA clathrin adaptors mediate transport from the TGN to late endosomes

GGAs are large monomeric clathrin adaptors that capture acid hydrolase receptors and other transmembrane proteins into clathrin-coated vesicles for transport from the TGN to late endosomes (Dell'Angelica et al., 2000; Myers and Payne, 2013). The formation of GGA-containing vesicles begins early in TGN maturation, before the formation of AP-1-containing vesicles (Figure 2.1A) (Casler and Glick, 2020; Daboussi et al., 2017, 2012). Newly synthesized acid hydrolases bind in the Golgi lumen to transmembrane receptors. In mammals, acid hydrolases are modified on their oligosaccharide side chains with mannose 6-phosphate, which is recognized by mannose 6-phosphate receptors (Ghosh et al., 2003). In yeast, acid hydrolases contain peptide signals that are recognized by the Vps10 receptor (Bowers and Stevens, 2005). The cytosolic tails of acid hydrolase receptors are recognized in turn by GGAs.

Acid hydrolase receptors are recycled from late endosomes to the Golgi in tubular carriers generated by coat-like sorting nexin complexes (Ma and Burd, 2020; McNally and Cullen, 2018). Kinetic studies of yeast revealed that the late endosome-to-Golgi pathway delivers Vps10 to maturing cisternae prior to GGA arrival, thereby enabling Vps10 to bind acid hydrolases before departing from the TGN (Figure 2.1A) (Casler and Glick, 2020; Casler et al., 2021). The timing is probably similar for the late endosome-to-Golgi pathway in mammalian cells.

Late endosomes receive not only acid hydrolases, but also proteins internalized by endocytosis. In mammalian cells, internalized proteins are delivered first to early endosomes. Some internalized proteins are then transported to the TGN (Bonifacino and Hierro, 2011; Hong and Lev, 2014), whereas internalized proteins destined for degradation remain in place as the early endosomes mature into late endosomes (Huotari and Helenius, 2011) . In yeast, the situation is different because the Golgi also serves as an early endosome (Day et al., 2018). Yeast endocytic vesicles fuse with the Golgi shortly before GGA arrival so that internalized proteins destined for degradation can be transported from the TGN to late endosomes (Figure 2.1A).

The AP-3 adaptor mediates direct delivery from the TGN to lysosomes or vacuoles

Whereas soluble acid hydrolases are transported to lysosomes or vacuoles via late endosomes, many transmembrane proteins are transported directly from the TGN to lysosomes or vacuoles in vesicles generated by the tetrameric AP-3 complex (Odorizzi et al., 1998; Tan and Gleeson, 2019). AP-3 is an Arf1 effector, and it appears not to interact with clathrin, suggesting that AP-3 has properties of both an adaptor and a coat (Schoppe et al., 2021). Like AP-1, AP-3 recognizes peptide signals in the cytosolic tails of transmembrane proteins.

Exomer delivers a subset of cargoes from the TGN to the plasma membrane in yeast

Yeast cells employ an Arf1 effector called exomer to deliver certain transmembrane cargoes from the TGN to the plasma membrane (Paczkowski et al., 2015). Exomer has properties of an adaptor-coat complex. This complex is absent from metazoans and plants (Trautwein et al., 2006), but it exemplifies one way that cells can achieve selective TGN-to-plasma membrane trafficking.

Tethers Capture Transport Vesicles at the Golgi

A transport vesicle is captured with the aid of tether proteins, which are thought to enhance both the efficiency and the specificity of vesicle targeting. Golgi-associated tethers fall into two categories: rod-like golgins and multi-subunit tethers.

The golgins belong to several protein families, but they share the property of being dimers with long coiled-coil domains (Gillingham and Munro, 2016). Some golgins are recruited to cisternae by the binding of their C-terminal domains to Arf, Arl, or Rab GTPases, while other golgins have C-terminal transmembrane anchors. Vesicle tethering is mediated by N-terminal domains of the golgins (Wong et al., 2017). The mechanisms of vesicle recognition by golgins are still obscure, although bridging proteins have been identified in some cases (Navarro Negredo et al., 2018; Shin et al., 2017). A given golgin localizes to a cisterna at a particular stage of maturation, suggesting that each golgin acts selectively in one or more membrane traffic pathways. Indeed, ectopic localization experiments revealed that different golgins capture vesicles that contain distinct subsets of recycling Golgi proteins (Wong and Munro, 2014). The rigid coiled-coil regions of the golgins have gaps that allow the golgins to bend, presumably to allow transfer of vesicles to the

membrane surface (Cheung and Pfeffer, 2016). The current view is that golgins act as "tentacles" during the initial step of vesicle capture.

Multi-subunit tethers are peripheral membrane proteins. The multi-subunit tethers at the Golgi are the octameric COG complex and the tetrameric GARP complex (Blackburn et al., 2019; Bonifacino and Hierro, 2011). These complexes are evolutionarily related, and they act downstream of the golgins to coordinate vesicle fusion by interacting with the SNARE proteins described below (Hong and Lev, 2014). The precise roles of COG and GARP are not yet known, but COG probably acts in early pathways such as COPI-mediated intra-Golgi recycling while GARP acts in late pathways such as the fusion of vesicles arriving from the endocytic system.

SNAREs Provide Energy and Specificity for Vesicle Fusion

SNARE proteins are the main drivers of vesicle fusion (Zhang and Hughson, 2021). Most SNAREs have transmembrane domains, and they all possess motifs that enable them to form complexes with complementary SNAREs. A SNARE complex contains one member each of the R-SNARE, Qa-SNARE, Qb-SNARE, and Qc-SNARE protein families. Typically, an R-SNARE in the vesicle binds Q-SNAREs in the target membrane to generate a *trans*-SNARE complex. This assembly is initiated with the aid of SM family proteins, which catalyze the pairing of an R-SNARE in one membrane with a complementary Qa-SNARE in the opposing membrane (Zhang and Hughson, 2021). SNARE complex assembly pulls the opposing membranes together and provides energy for membrane fusion (Song et al., 2021; Südhof and Rothman, 2009). The fused membrane contains a *cis*-SNARE complex that needs to be disassembled, a process that is carried out by the

hexameric ATPase NSF and its partner protein α-SNAP (Khan et al., 2022). Monomeric SNAREs are then recycled for another round of membrane fusion.

SNAREs act downstream of vesicle tethers and provide an additional level of specificity. Each vesicle targeting step is thought to involve a unique SNARE complex, although a given SNARE can function in more than one pathway. For example, in yeast, the same R-SNARE that assembles with Q-SNAREs in the plasma membrane to mediate fusion of secretory vesicles also assembles with different Q-SNAREs in the Golgi to mediate fusion of endocytic vesicles (Lewis et al., 2000; Paumet et al., 2001; Protopopov et al., 1993). Other SNARE complexes have been shown to mediate fusion during ER-to-Golgi transport and intra-Golgi recycling (Grissom et al., 2020; Nichols and Pelham, 1998). However, for several of the pathways shown in Figure 2.1A, the assignment of SNARE complexes is still tentative.

Outlook

Decades of research have substantially illuminated the functions and features of the Golgi (Farquhar and Hauri, 1997; Lujan and Campelo, 2021). It now seems evident that the Golgi can be viewed as a set of maturing cisternae, and that multiple membrane traffic pathways are switched on and off during the maturation process (Pantazopoulou and Glick, 2019). For the next phase of Golgi research, we envision three objectives.

1. Characterize the membrane traffic pathways that operate at the Golgi. This task is well advanced for yeast (Figure 2.1A), but key questions remain. For example, it is unclear how the same COPI machinery mediates two traffic pathways with distinct passengers and destinations, and the same

is true for the AP-1 machinery. Mammalian Golgi traffic is presumably similar to that in yeast but more complex.

2. Determine which components operate in each membrane traffic pathway. Significant progress has been made in this regard as described above, but much remains to be learned. In particular, each membrane traffic pathway needs to be defined in molecular terms by identifying its particular set of tethers and SNAREs.

3. Elucidate the processes that choreograph Golgi maturation. As a cisterna matures, the different membrane traffic pathways are switched on and off in a consistent sequence. Perhaps the most interesting challenge for the coming years is to reveal the molecular logic circuit that controls these switches. Part of this circuit is a network of interactions between Golgi-associated GTPases (Figure 2.1B) (Thomas and Fromme, 2020), and we postulate that a second network of interactions enables membrane traffic pathways to regulate one another by delivering or removing key components. This system-level analysis promises to yield an increasingly rich motion picture of the Golgi.

CHAPTER 3

COPI-DEPENDENT INTRA-GOLGI RECYCLING AT AN INTERMEDIATE STAGE OF CISTERNAL MATURATION

Abstract

The traffic pathways that recycle resident Golgi proteins during cisternal maturation are not completely defined. We addressed this challenge using the yeast *Saccharomyces cerevisiae*, in which maturation of individual cisternae can be visualized directly. A new assay captures a specific population of Golgi-derived vesicles at the bud neck, thereby revealing which resident Golgi proteins are carried as cargo in those vesicles. This method supplies evidence for at least three classes of intra-Golgi vesicles with largely distinct cargo compositions. Consistent with our earlier results, one class of vesicles mediates a late pathway of intra-Golgi recycling with the aid of the AP-1 and Ent5 clathrin adaptors, and a second class of vesicles mediates an early pathway of intra-Golgi recycling with the aid of the COPI vesicle coat. Here, we identify another COPI-dependent pathway of intra-Golgi recycling and show that it operates kinetically between the two previously known pathways. Thus, intra-Golgi recycling is mediated by multiple COPI-dependent pathways followed by a clathrin-dependent pathway.

This is a version of a research article that is under review for publication with the following author list: Adam H. Krahn, Areti Pantazopoulou, Jotham Austin II, Natalie Johnson, and Benjamin S. Glick. I contributed to experimental design, performed most of the experimental analysis, and helped create the initial manuscript draft. A. Pantazopoulou performed and analyzed the experiments in Figure 3.8B. J. Austin II performed and analyzed the cryo-electron tomography experiments as well as helped create the relevant figures and movies. N. Johnson performed and analyzed the experiment in Figure 3.1B. B. S. Glick supervised the project, assisted with experimental design, coded the ImageJ plugins used for data analysis, created the final figures, and edited the final manuscript draft.

Introduction

The eukaryotic Golgi apparatus is a central hub for the modification and distribution of proteins and lipids (Farquhar and Hauri, 1997). This organelle consists of disk-like membrane-bound cisternae, which may be stacked or non-stacked depending on the organism (Mowbrey and Dacks, 2009). Two major activities occur in the Golgi. One activity is enzymatic biosynthesis and processing. Secretory proteins passing through the Golgi undergo modifications such as glycan remodeling and proteolytic cleavage, and various lipids are synthesized in the cisternal membranes. The other activity is protein sorting. Multiple classes of vesicles emerge from the Golgi to deliver material to the plasma membrane or the endolysosomal system.

These activities of the Golgi occur in a defined temporal order, and they are coordinated with biochemical changes in the cisternae (Glick and Nakano, 2009). Researchers are still seeking the best way to describe the Golgi system. A traditional approach divides the Golgi into compartments called *cis*, medial, *trans*, and *trans*-Golgi network (TGN). However, those terms have not been rigorously defined, and the compartment-focused view is arguably more of a hindrance than a help (Pantazopoulou and Glick, 2019). We favor a different approach that represents the Golgi as a set of maturing cisternae (Glick and Malhotra, 1998). In this view, each cisterna forms, undergoes a series of transformations, and ultimately disappears, while the resident Golgi proteins continually recycle from older to younger cisternae. Membrane recycling causes a cisterna to mature— vesicles fuse with the cisterna to deliver resident Golgi proteins, and other vesicles bud from the cisterna to remove other resident Golgi proteins, so the composition of the cisterna changes over time. Presumably, a molecular logic circuit links the various membrane recycling pathways to orchestrate the sequential transformations experienced by a cisterna (Pantazopoulou and Glick, 2019). From this perspective, understanding the Golgi will require

characterizing the membrane recycling pathways that drive cisternal maturation. The specific questions are: How many membrane recycling pathways operate at the Golgi? When during maturation does each pathway operate? Which traffic machinery components mediate each pathway? Which resident Golgi proteins follow each pathway?

S. cerevisiae is uniquely suited to answering these questions because it contains non-stacked Golgi cisternae that are optically resolvable (Wooding and Pelham, 1998). To visualize cisternal maturation, resident Golgi proteins are labeled with fluorescent tags, and changes in the composition of an individual cisterna are tracked by 4D microscopy (Losev et al., 2006; Matsuura-Tokita et al., 2006). If two or more resident Golgi proteins are labeled with different fluorophores, then their relative arrival and departure times can be measured, a method that we term "kinetic mapping". The kinetic signature of a resident Golgi protein is useful for assigning that protein to a particular membrane recycling pathway.

A key feature of a membrane recycling pathway is the traffic machinery components that promote vesicle formation, targeting, and fusion. For intra-Golgi recycling pathways, attention has focused on vesicle formation by the COPI coat (Arab et al., 2024). COPI vesicles mediate retrograde intra-Golgi recycling of resident Golgi proteins as well as retrograde Golgi-to-ER recycling (Rabouille and Klumperman, 2005; Barlowe and Miller, 2013). It is thought that multiple COPI-dependent intra-Golgi pathways recycle different subsets of resident Golgi proteins (Sahu et al., 2022), but the number and properties of those pathways have been uncertain. Meanwhile, our studies of the yeast Golgi showed that COPI-dependent recycling is restricted to resident early Golgi proteins, and that resident late Golgi (TGN) proteins recycle with the aid of the AP-1 clathrin adaptor (Papanikou et al., 2015; Day et al., 2018; Casler et al., 2021). Similarly, a recent study of mammalian cells concluded that AP-1 mediates the recycling of late Golgi proteins (Robinson et

al., 2024). In yeast, the Ent5 clathrin adaptor cooperates with AP-1 to drive intra-Golgi recycling (Casler et al., 2021). It therefore seems that recycling of resident Golgi proteins involves the actions of two vesicle budding machineries: COPI early in maturation, and clathrin together with AP-1 (plus Ent5 in yeast) late in maturation.

The question then becomes, how many distinct Golgi recycling pathways utilize each of these vesicle budding machineries? By combining kinetic mapping with functional tests, we previously suggested that two sequential AP-1/Ent5-dependent recycling pathways operate at the yeast Golgi (Casler et al., 2021). We have now revisited this issue using an updated toolkit that reveals whether different resident Golgi proteins travel together in the same vesicles. The new evidence described here points to the existence of a single AP-1/Ent5-dependent recycling pathway plus at least two COPI-dependent recycling pathways. This advance brings us closer to a complete picture of how proteins localize within the Golgi.

Results

Golgi-derived vesicles containing Kex2 can be captured at the yeast bud neck

We devised a method to capture Golgi-derived vesicles that contain a specific resident Golgi transmembrane protein (Figure 3.1A). The chosen capture site is the bud neck because this region is compact, easily identified, and often devoid of Golgi cisternae. Two copies of FK506-binding protein (FKBP) are fused by gene replacement to the bud-neck-localized septin Shs1 (Iwase et al., 2007), which can be tagged without visibly perturbing cytokinesis. Also present in the Shs1 fusion construct is the red fluorescent protein mScarlet (Bindels et al., 2017; Valbuena et al., 2020). The parental yeast strain has mutations that prevent growth arrest by rapamycin (Haruki et al., 2008;

Papanikou et al., 2015). In addition, to facilitate the use of rapamycin and of HaloTag ligands, the parental strain lacks the transcription factors Pdr1 and Pdr3, which drive expression of pleiotropic drug transporters (Schüller et al., 2007; Barrero et al., 2016). For the capture assay, a resident Golgi transmembrane protein is tagged on its cytosolic domain with FK506-rapamycin binding domain (FRB). Addition of rapamycin promotes heterodimerization of FKBP with FRB (Haruki et al., 2008), resulting in capture at the bud neck of vesicles containing the FRB-tagged Golgi protein. If a second resident Golgi protein is tagged with GFP, then rapamycin-dependent accumulation of GFP fluorescence at the bud neck reflects co-capture of the GFP-tagged protein with the FRB-tagged protein, implying that the two proteins are in the same vesicles (Figure 3.1A). The rapamycin treatment time is only 5 min, terminated by aldehyde fixation, to minimize indirect effects that might alter traffic pathways.

A limitation of this approach is that *S. cerevisiae* Golgi cisternae are mobile in the cytoplasm (Wooding and Pelham, 1998; Losev et al., 2006), so a cisterna that collides with the septin ring could be captured by the FKBP-FRB interaction, thereby generating a confounding signal due to GFP-tagged protein molecules present in the cisterna rather than in vesicles. To avoid this problem, cisternae are labeled by appending HaloTag to two Golgi proteins, Ric1 and Sec7, that should be absent from vesicles. Both proteins are peripherally membrane-associated guanine nucleotide exchange factors (Siniossoglou et al., 2000; McDonold and Fromme, 2014). Ric1 is present on early Golgi cisternae (Huh et al., 2003) while Sec7 is present on late Golgi cisternae (Rossanese et al., 1999; Losev et al., 2006), and together those two proteins are expected to mark a cisterna for most of its lifetime. This expectation was verified by three-color 4D confocal microscopy (Losev et al., 2006; Johnson and Glick, 2019). Golgi cisternae were labeled by tagging

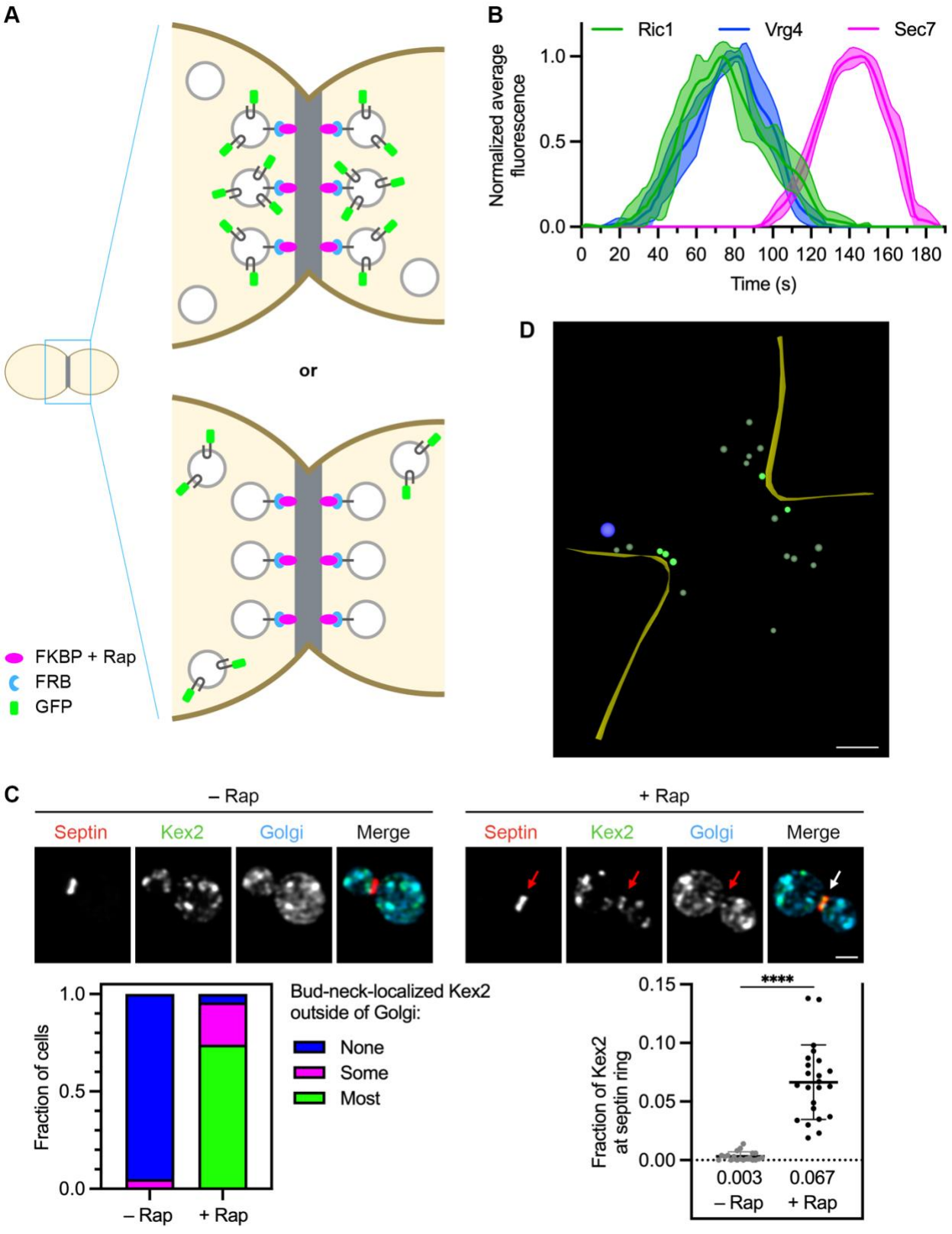

Figure 3.1: **Transport vesicles carrying resident Golgi proteins can be captured at the bud neck.** *(continued on next page)*

Figure 3.1: **(A)** Diagram of the vesicle capture assay. A septin at the bud neck is tagged with FKBP (magenta), and a resident Golgi transmembrane protein is tagged on its cytosolic domain with FRB (blue). When the resident Golgi protein is packaged into transport vesicles in the presence of rapamycin ("Rap"), some of those vesicles will be captured at the bud neck. If a second resident Golgi protein is tagged with GFP (green), then that second protein will either be co-captured at the bud neck if it travels in the same vesicles as the FRB-tagged protein (left) or not co-captured if it travels in different vesicles than the FRB-tagged protein (right). **(B)** Golgi maturation kinetics of GFP-tagged Ric1 compared to HaloTag-labeled Vrg4 and mScarlet-tagged Sec7. Shown are normalized and averaged traces for 11 individual cisternae. **(C)** Rapamycin-dependent capture by an FKBP-tagged septin (red) of Kex2-FRB-GFP (green). Golgi cisternae were marked by HaloTag-labeled Ric1 and Sec7 (blue). Arrows indicate non-Golgi signal at the bud neck after treatment for 5 min with rapamycin. At the lower left, capture of Kex2-FRB-GFP at the bud neck was quantified by assigning cells to categories based on whether any bud-neck-localized Kex2 signal was visible outside of Golgi cisternae, and if so, whether less than half ("Some") or more than half ("Most") of that signal was outside of Golgi cisternae. At the lower right, capture of Kex2-FRB-GFP at the bud neck was quantified by measuring the fraction of the total Kex2 signal within a septin mask, which had been modified by subtraction of a Golgi mask. For this type of numerical quantification, the mean capture values are displayed as thick horizontal bars and are listed numerically below the plots, and the standard deviations are displayed as thin horizontal bars. ****, significant at P value <0.0001. **(D)** Cryo-ET of vesicles captured at the bud neck using Kex2-FRB. A log-phase culture of cells expressing Kex2-FRB and Shs1-FKBP was treated with rapamycin for 5 min followed by cryo-preservation and processing for cryo-ET. Shown is the tomographic model of a SIRT-reconstructed tomogram from a large budded cell. The full data set is provided in Video 3.1. The secretory vesicle was identified by its resemblance to the clustered secretory vesicles seen in other cells with small buds (data not shown). Cell cortex, yellow; secretory vesicle, blue; putatively captured non-secretory vesicles, bright green; other non-secretory vesicles, dull green. Scale bar, 250 nm.

Ric1 with GFP, by tagging the early Golgi protein Vrg4 with HaloTag conjugated to a far-red dye (Grimm et al., 2021), and by tagging Sec7 with mScarlet. Fluorescence traces for individual cisternae were smoothed, aligned, and combined to obtain averaged traces (Casler et al., 2021). The results indicated that Ric1 arrived and departed roughly in synchrony with Vrg4, while Sec7 arrived and departed later after a brief period of overlap with Ric1 (Figure 3.1B).

Quantification of vesicle capture is performed as follows. A mask is created from the red fluorescence of tagged Shs1, and this septin mask is modified by subtracting a Golgi mask created from the far-red fluorescence of HaloTag-labeled Ric1 and Sec7, thereby ensuring that the septin mask excludes any cisternae at the bud neck. The Golgi mask is defined generously to encompass

all of the visible HaloTag signal, based on the rationale that eliminating the contribution from Golgi cisternae is more important than preserving the full signal from the captured vesicles. The criterion for analyzing a cell is that subtraction of the Golgi mask removes less than 65% of the septin mask. For the measurement, the green signal from the GFP-tagged Golgi protein is examined. The green signal within the subtraction-modified septin mask is compared with the total cellular green signal to determine the fraction of the GFP-tagged Golgi protein present in captured vesicles.

As a proof of principle, the late Golgi protein Kex2 (Fuller et al., 1988) was tagged on its cytosolic C-terminus with both FRB and GFP so that capture of Kex2-containing vesicles could be visualized. Kex2 and the other Golgi proteins used in this study were tagged by chromosomal replacement of the endogenous genes with fusion genes under control of the normal promoters. In the absence of rapamycin, tagged Kex2 was found in punctate Golgi cisternae and was usually undetectable at the bud neck (Figure 3.1C, upper left). By contrast, after incubation with rapamycin, Kex2 fluorescence was usually visible not only in punctate Golgi cisternae, but also at the bud neck outside of Golgi cisternae (Figure 3.1C, upper right). This capture of Kex2 was quantified by two methods. For the numerical quantification method, the Kex2 fluorescence that overlapped with the subtraction-modified septin mask was measured as described above. A rapamycin-dependent signal was consistently observed (Figure 3.1C, lower right). Quantification yielded average values of 6.7% of the total Kex2 fluorescence at the bud neck for rapamycin-treated cells versus 0.3% for untreated cells. Such measurements may underestimate the efficiency of rapamycin-dependent capture due to the generous Golgi masks used for subtraction, but we are confident that only a small fraction of the resident Golgi protein molecules were captured at the bud neck, implying that Golgi function was likely unperturbed. For the categorical quantification

method, cells were assigned to categories based on visual estimates of how much of the Kex2 fluorescence at the bud neck was outside of Golgi cisternae. Of the rapamycin-treated cells, 96% showed bud-neck-localized Kex2 fluorescence outside of Golgi cisternae, including 74% of the cells for which a majority of the bud-neck-localized fluorescence was outside of cisternae and 22% of the cells for which a minority of the bud-neck-localized fluorescence was outside of cisternae (Figure 3.1C, lower left). Of the untreated cells, only 5% showed bud-neck-localized Kex2 fluorescence outside of cisternae. Thus, the categorical quantification method is useful for verifying that results from the numerical quantification method reflect effects that are evident by visual inspection. These two methods provide complementary ways to assess the capture of a fluorescent Golgi protein at the bud neck.

To confirm that the Kex2 fluorescence at the bud neck represented vesicles, we performed cryo-electron tomography (cryo-ET; Gan et al., 2019) (Figure 3.1D). Cells expressing Kex2-FRB were examined with or without rapamycin treatment under the conditions of the vesicle capture assay. We analyzed 6 untreated large budded cells and 10 rapamycin-treated large budded cells. Lamellae of thickness ~200-220 nm, representing an estimated 15-30% of the total bud neck volume (Bertin et al., 2012), were imaged and modeled. With or without rapamycin treatment, electron-dense secretory vesicles of diameter ~90 nm were occasionally seen near the bud neck, as expected for this stage of the cell cycle (Finger et al., 1998; Pruyne et al., 2004). Also visible were less electron-dense non-secretory vesicles of diameters ~35-60 nm. To score non-secretory vesicles that had putatively been captured by the FKBP-tagged septin, we used prior ultrastructural evidence that yeast septin rings extend about 200 nm in each direction from the center of the bud neck along the cell cortex (Bertin et al., 2012; Ong et al., 2014). Based on that number and the predicted lengths of the FKBP-tagged Shs1 septin and the FRB-tagged Kex2 cytosolic tail, a

vesicle was counted as putatively captured if its membrane was no more than 106 nm from a point on the plasma membrane within 200 nm from the center of the bud neck. For the non-rapamycin-treated cells, the number of vesicles meeting this criterion ranged from 0 to 2 (mean = 0.7). For the rapamycin-treated cells, the number of putatively captured vesicles ranged from 0 to 7 (mean = 2.6). Such variability was anticipated based on the variable capture signals seen by fluorescence imaging. Figure 3.1D and Video 3.1 show an example of a rapamycin-treated cell for which the lamella included 5 putatively captured vesicles. These results indicate that our assay is suitable for capturing vesicles that contain a specific resident Golgi transmembrane protein.

Two Golgi proteins that have the same recycling kinetics as Kex2 are present in Kex2-containing vesicles

We previously showed that Kex2 recycles within the Golgi in a pathway dependent on the AP-1 and Ent5 clathrin adaptors (Casler et al., 2021). Other late Golgi proteins, including Ste13 and Stv1 (Table 3.1), were proposed to follow the same recycling pathway because they closely resembled Kex2 in their kinetics of arrival and departure during Golgi maturation (Casler et al., 2022). By contrast, the early Golgi protein Vrg4 (Table 3.1) recycles in a COPI-dependent manner (Abe et al., 2004; Mari et al., 2014), and it arrives and departs much sooner than Kex2 (Papanikou et al., 2015). The prediction was therefore that Ste13 and Stv1 should be co-captured in Kex2-containing vesicles whereas Vrg4 should not.

To test this prediction, Kex2 was tagged with FRB alone, and either Ste13, Stv1, or Vrg4 was tagged with GFP. After rapamycin addition, Ste13 was seen to accumulate at the bud neck (Figure 3.2A). The pattern of accumulation was variable—in some cells the Ste13 signal extended across the bud neck, and in other cells the Ste13 signal was concentrated in one part of the bud

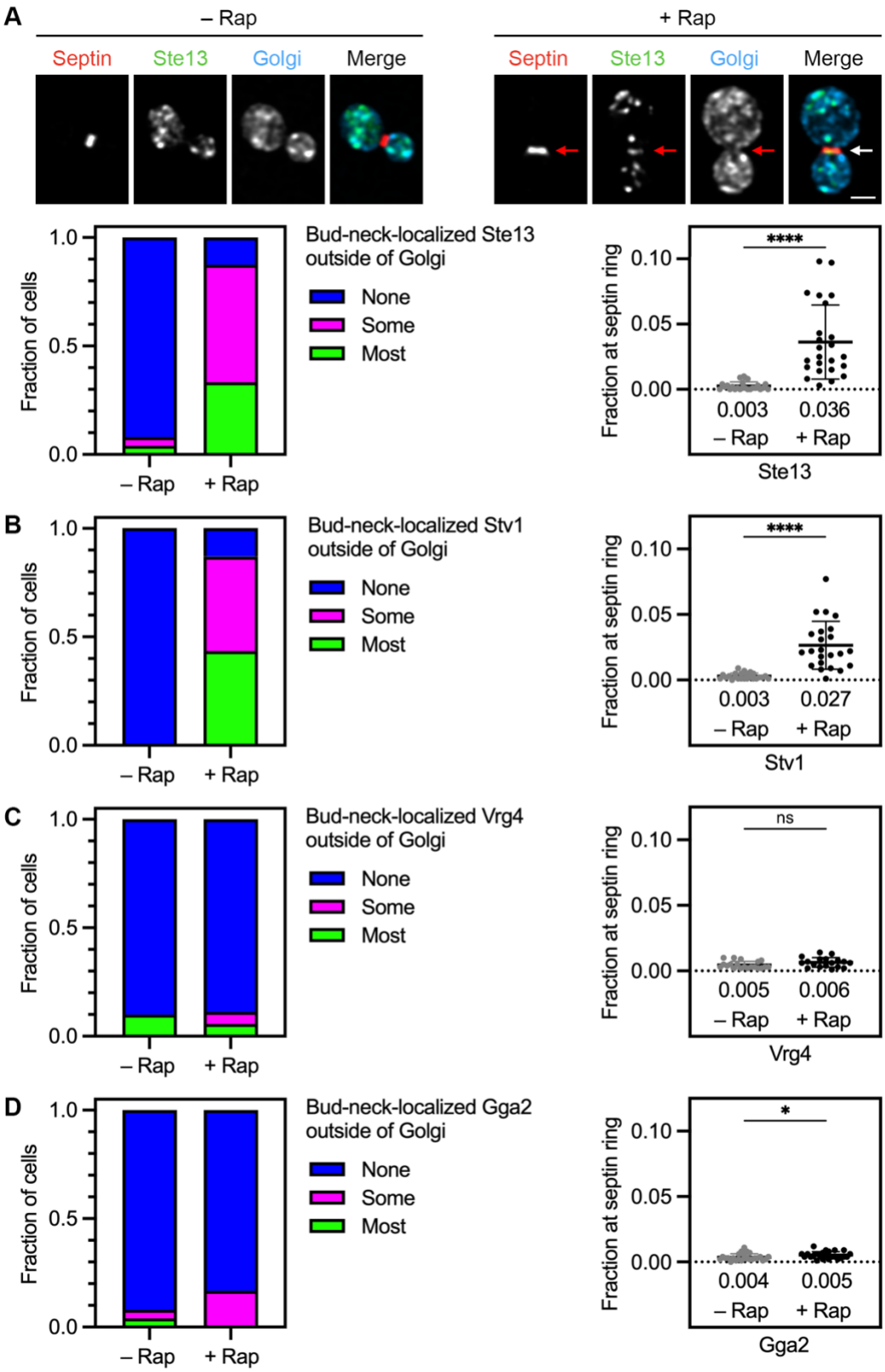

Figure 3.2: **AP-1/Ent5 cargoes can be specifically captured at the bud neck together with Kex2.** *(continued on next page)*

Figure 3.2: **(A)** Rapamycin-dependent capture with Kex2-FRB of GFP-tagged Ste13 (green) by an FKBP-tagged septin (red). Golgi cisternae were marked by HaloTag-labeled Ric1 and Sec7 (blue). Arrows indicate non-Golgi signal at the bud neck in cells treated for 5 min with rapamycin ("Rap"). At the lower left, capture of Ste13 at the bud neck was quantified by assigning cells to categories as described in Figure 3.1C. At the lower right, capture of Ste13 at the bud neck was quantified numerically as described in Figure 3.1C. ****, significant at P value <0.0001. **(B)** Capture with Kex2-FRB of GFP-tagged Stv1. Categorical and numerical quantification was performed as in (A). ****, significant at P value <0.0001. **(C)** No capture with Kex2-FRB of GFP-tagged Vrg4. Categorical and numerical quantification was performed as in (A). ns, not significant. **(D)** Minimal capture with Kex2-FRB of GFP-tagged Gga2. Categorical and numerical quantification was performed as in (A). *, significant at P value 0.04.

Resident Golgi transmembrane protein	Inferred major recycling pathway(s)
Kex2*	**AP-1/Ent5**
Ste13	AP-1/Ent5
Stv1	AP-1/Ent5
Sys1*	COPI(b') + AP-1/Ent5 ‡
Aur1	COPI(b') + AP-1/Ent5 ‡
Tmn1	**COPI(b')**
Gnt1	COPI(b')
Vrg4*	**COPI(b)**
Gda1	COPI(b)
Pmr1	COPI(b)

Table 3.1: **Resident Golgi transmembrane proteins examined in this chapter.** The proteins marked in bold are proposed as reference markers for the three intra-Golgi recycling pathways described here. The proteins marked with an asterisk ("*") were tagged with FRB for use in the vesicle capture assay.

‡ It is possible that native Sys1 and Aur1 traffic mainly in the COPI(b') pathway and that the fluorescent tags divert a fraction of the molecules into the AP-1/Ent5 pathway.

neck (Figure 3.3A, top two rows). We speculate that passage of the nucleus into the daughter cell can affect which parts of the bud neck are accessible for vesicle capture. As judged by the categorical quantification method, 88% of the rapamycin-treated cells showed bud-neck-localized Ste13 with most or some of the signal outside of Golgi cisternae (Figure 3.2A). Examples of cells that were assigned to different categories are shown in Figure 3.3A. As judged by the numerical quantification method, an average of 3.6% of the cellular Ste13 fluorescence was at the bud neck

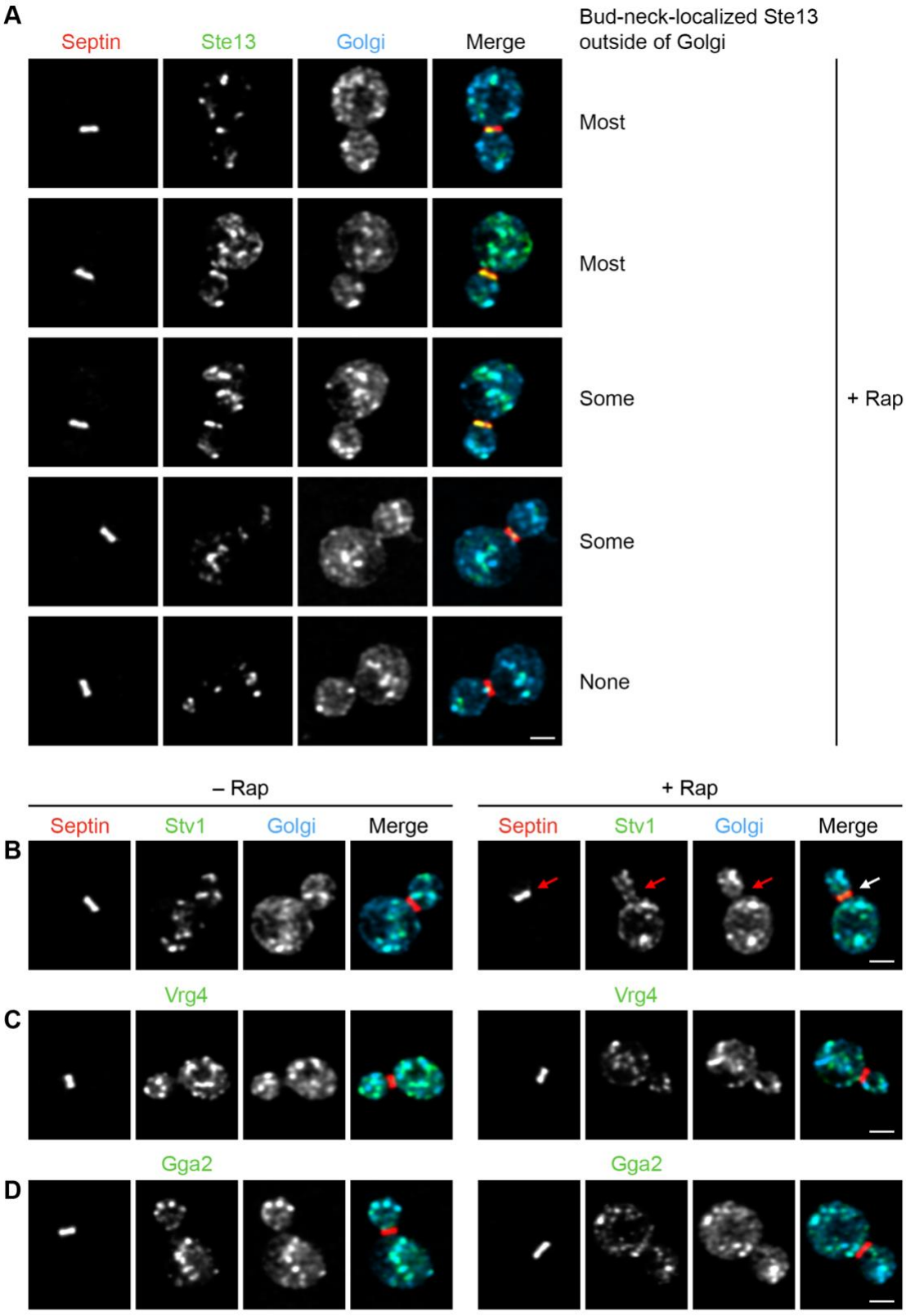

Figure 3.3: **The late Golgi proteins Ste13 and Stv1 can be captured at the septin ring in vesicles with Kex2.** *(continued on next page)*

Figure 3.3: In each part of the figure, Golgi cisternae were marked by HaloTag-labeled Ric1 and Sec7 (blue), and the scale bar is 2 μm. **(A)** A panel of representative images showing capture with Kex2-FRB of GFP-tagged Ste13 (green) by an FKBP-tagged septin (red) after treatment for 5 min with rapamycin ("Rap"). The labels "Most", "Some", and "None" mark representative examples for the image categories used in Figure 3.2A. **(B)** Capture with Kex2-FRB of GFP-tagged Stv1 (green) by an FKBP-tagged septin (red) after treatment for 5 min with rapamycin. Arrows indicate non-Golgi signal at the bud neck. **(C)** No capture with Kex2-FRB of GFP-tagged Vrg4 (green) by an FKBP-tagged septin (red) after treatment for 5 min with rapamycin. **(D)** No capture with Kex2-FRB of GFP-tagged Gga2 (green) by an FKBP-tagged septin (red) after treatment for 5 min with rapamycin.

in rapamycin-treated cells versus 0.3% in untreated cells (Figure 3.2A). For Stv1, similar results were obtained (Figure 3.2B and Figure 3.3B). For Vrg4, as expected, the fluorescence at the bud neck outside of Golgi cisternae was very low both with and without rapamycin addition (Figure 3.2C and Figure 3.3C). Thus, capture of FRB-tagged Kex2 leads to selective co-capture of Ste13 and Stv1.

As described above, subtraction of the Golgi mask ensured that the Ste13 and Stv1 signals seen with FRB-tagged Kex2 resulted from capture of vesicles rather than from capture of late Golgi cisternae at the bud neck. To confirm the effectiveness of this method, we marked late Golgi cisternae with the clathrin adaptor Gga2, which has a kinetic signature largely overlapping that of Kex2 (Daboussi et al., 2012; Casler and Glick, 2020). Gga2 mediates transport from the Golgi to prevacuolar endosomes and should be absent from Kex2-containing AP-1/Ent5 vesicles (Myers and Payne, 2013). For Gga2, the fluorescence at the bud neck outside of Golgi cisternae was very low as judged by both quantification methods (Figure 3.2D and Figure 3.3D), indicating that the subtraction-modified septin masks enable measurement of fluorescence from captured vesicles while excluding nearly all of the fluorescence from Golgi cisternae. This control experiment reinforces the conclusion that Ste13 and Stv1 travel together with Kex2 in vesicles that are largely devoid of Vrg4.

Sys1 and Aur1 arrive at maturing cisternae before Kex2 but are nevertheless found in Kex2-containing vesicles

We previously reported that the resident Golgi transmembrane proteins Sys1 and Aur1 had kinetic signatures between those of Vrg4, which is COPI-dependent, and Kex2, which is AP-1/Ent5-dependent (Casler et al., 2021). The assumption was that Sys1 and Aur1 defined a distinct intra-Golgi recycling pathway. To test this idea, we began by extending the earlier kinetic analysis of Sys1. Golgi cisternae were labeled by tagging Sys1 with HaloTag and by tagging Kex2 with GFP, and then the cells were analyzed by 4D confocal microscopy. A representative example is shown in Figure 3.4A and Video 3.2. Sys1 typically began to arrive at a cisterna about 20 s before Kex2. Then Sys1 typically began to depart from the cisterna sooner than Kex2, although some Sys1 signal remained detectable until Kex2 had almost completely departed. Averaged two-color fluorescence traces are shown in Figure 3.5A. In a separate experiment, Aur1 was tagged with GFP and tracked together with HaloTag-labeled Sys1. The results confirmed that the kinetic signature of Aur1 is very similar to that of Sys1 (Figure 3.5A). Because Sys1 and Aur1 begin to arrive before Kex2, we infer that they travel at least some of the time in vesicles lacking Kex2.

The assumption that Sys1 and Aur1 follow a distinct recycling pathway led us to predict that neither Sys1 nor Aur1 should be co-captured in vesicles containing FRB-tagged Kex2. But surprisingly, both proteins were co-captured with FRB-tagged Kex2 (Figure 3.5B and Figure 3.4B). A possible explanation is that Sys1 and Aur1 partition between two pathways: a pathway with intermediate kinetics of both arrival and departure, and the AP-1/Ent5 pathway followed by Kex2. This hypothesis could explain why Sys1 and Aur1 were co-captured with Kex2. It could also explain the relative kinetic signatures of Sys1 and Kex2, according to the following scenario.

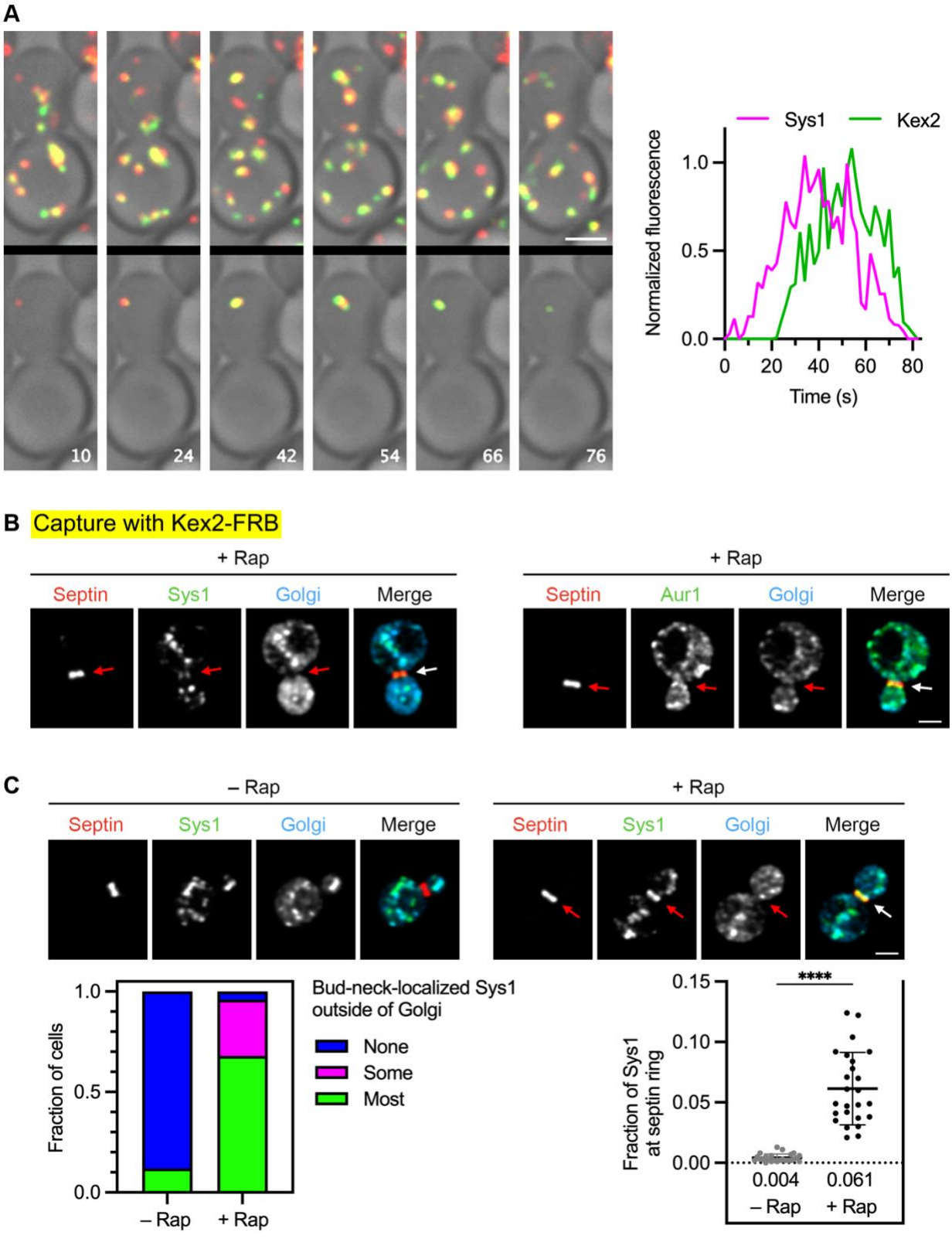

Figure 3.4: **The Sys1 and Kex2 containing vesicle populations do not possess entirely distinct cargo compositions.** *(continued on next page)*

Figure 3.4: **The Sys1 and Kex2 containing vesicle populations do not possess entirely distinct cargo compositions.** *(continued from previous page)*

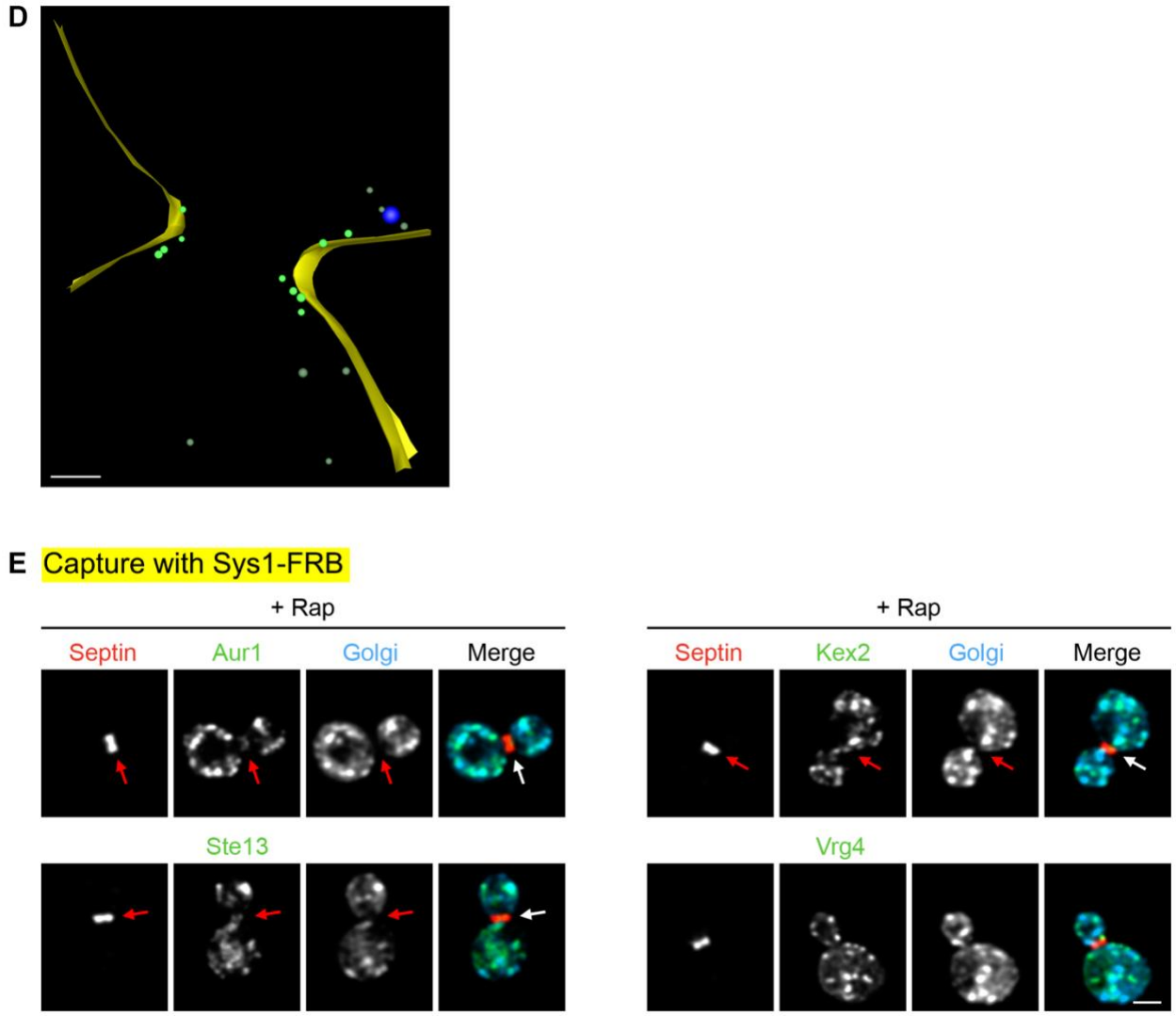

Figure 3.4: **The Sys1 and Kex2 containing vesicle populations do not possess entirely distinct cargo compositions. (A)** Frames from a representative 4D confocal movie of Sys1-HaloTag and Kex2-GFP, and kinetic traces from an individual cisterna in the movie. Depicted at the left are average projected z-stacks from Video 3.2 at the indicated time points. The upper row shows the complete projections, and the lower row shows edited projections that include only the cisterna that was tracked. Scale bar, 2 µm. Plotted at the right are normalized fluorescence intensities for the cisterna tracked in the video. **(B)** Representative images showing capture with Kex2-FRB of GFP-tagged Sys1 or Aur1 (green) by an FKBP-tagged septin (red) after treatment for 5 min with rapamycin. Arrows indicate non-Golgi signal at the bud neck. **(C)** Rapamycin-dependent capture by an FKBP-tagged septin (red) of Sys1-FRB-GFP (green). Arrows indicate non-Golgi signal at the bud neck after treatment for 5 min with rapamycin. At the lower left, capture of Sys1-FRB-GFP at the bud neck was quantified by assigning cells to categories as described in Figure 3.1C. At the lower right, capture of Sys1-FRB-GFP at the bud neck was quantified numerically as described in Figure 3.1C. ****, significant at P value <0.0001.

(continued on next page)

Figure 3.4: **(D)** Cryo-ET of vesicles captured at the bud neck using Sys1-FRB. A log-phase culture of cells expressing Sys1-FRB and Shs1-FKBP was treated with rapamycin for 5 min followed by cryo-preservation and processing for cryo-ET. Shown is the tomographic model of a SIRT-reconstructed tomogram from a large budded cell. The full data set is shown in Video 3. A vesicle was counted as putatively captured if its membrane was no more than 83 nm from a point on the plasma membrane within 200 nm from the center of the bud neck. For the 4 non-rapamycin-treated cells examined, the number of vesicles meeting this criterion ranged from 0 to 2 (mean = 1.0). For the 4 rapamycin-treated cells examined, the number of putatively captured vesicles ranged from 6 to 13 (mean = 10.0). Scale bar, 250 nm. See Fig. 1D for further details. **(E)** Representative images showing capture with Sys1-FRB of GFP-tagged Aur1, Kex2, or Ste13 (green) by an FKBP-tagged septin (red), and minimal capture with Sys1-FRB of Vrg4 (green) by an FKBP-tagged septin (red), all after treatment for 5 min with rapamycin. Arrows indicate non-Golgi signal at the bud neck.

Sys1 arrival occurs in two phases, the first one earlier than Kex2 arrival and the second one synchronous with Kex2 arrival, and then Sys1 departure occurs in two phases, the first one earlier than Kex2 departure and the second one synchronous with Kex2 departure. In this view, the empirical kinetic signature of Sys1 or Aur1 represents the sum of the kinetic signatures for two different recycling pathways.

As an initial test of the new hypothesis, we established a capture assay in which Sys1 was tagged on its cytosolic C-terminus with FRB. To verify that Sys1-containing vesicles could be captured, Sys1 was tagged with both FRB and GFP. Upon rapamycin addition, the dual-tagged Sys1 accumulated in vesicles at the bud neck as judged by fluorescence imaging (Figure 3.4C). Cryo-electron tomography confirmed that capture of Sys1-FRB resulted in the appearance of vesicles at the bud neck (Figure 3.4D and Video 3.3). In cells expressing Sys1 tagged with FRB alone, either Aur1, Kex2, Ste13, or Vrg4 was tagged with GFP. After rapamycin addition, Aur1 showed robust accumulation at the bud neck (Figure 3.5C and Figure 3.4E), confirming that Aur1 travels in vesicles together with Sys1. For Kex2 and Ste13, co-capture with Sys1 was also readily detectable (Figure 3.5C and Figure 3.4E). This result supports the idea that a fraction of the Sys1

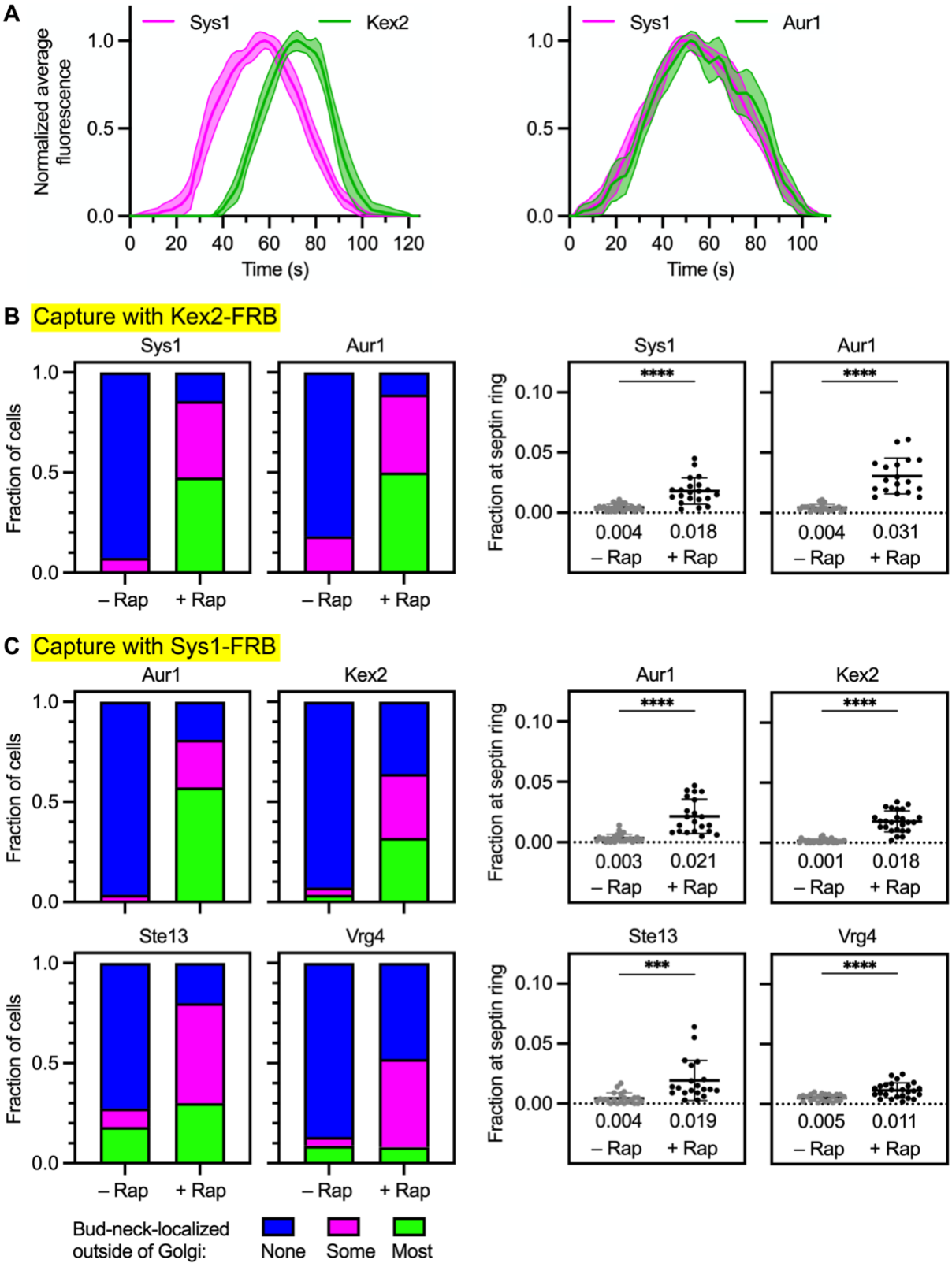

Figure 3.5: **Sys1 and Aur1 are present in AP-1/Ent5 vesicles.** (*continued on next page)*

Figure 3.5: **(A)** Golgi maturation kinetics of HaloTag-labeled Sys1 compared to GFP-tagged Kex2 or Aur1. Shown are normalized and averaged traces for 11 individual cisternae for the Sys1/Kex2 comparison and 10 individual cisternae for the Sys1/Aur1 comparison. **(B)** Capture with Kex2-FRB of GFP-tagged Sys1 and Aur1. Categorical and numerical quantifications were performed as in Figure 3.2A. ****, significant at P value <0.0001. **(C)** Capture with Sys1-FRB of GFP-tagged Aur1 and Kex2 and Ste13, and weak capture with Sys1-FRB of GFP-tagged Vrg4. Categorical and numerical quantifications were performed as in Figure 3.2A. ****, significant at P value <0.0001; ***, significant at P value 0.0008.

molecules recycle in an intermediate pathway while the rest of the Sys1 molecules recycle in a late AP-1/Ent5-dependent pathway together with Kex2 and Ste13.

Interestingly, Vrg4 showed a weak but statistically significant signal for co-capture with Sys1 (Figure 3.5C). This effect was seen in both of the quantitative assays, even though it was hard to discern from qualitative examination of the micrographs (Figure 3.4E). We speculate that the weak Vrg4 signal reflects imperfect fidelity of Golgi traffic pathways. Sys1 is present in a Golgi cisterna when Vrg4 is departing (Figure 3.6A), so Sys1 molecules might occasionally be packaged into the same early pathway vesicles that recycle Vrg4. Alternatively, Vrg4 molecules might occasionally fail to recycle in their “normal” early pathway, in which case they could be salvaged by recycling together with Sys1 in the intermediate pathway. Either event could generate a weak signal for Vrg4 in the assay for co-capture with Sys1. The ability of the vesicle capture method to detect these types of low-frequency events must be kept in mind when seeking to identify the major recycling pathway(s) followed by a given Golgi protein. To interpret the co-capture data, we rely on comparative quantification to distinguish between relatively strong versus weak signals, and we examine complementary data from kinetic analysis.

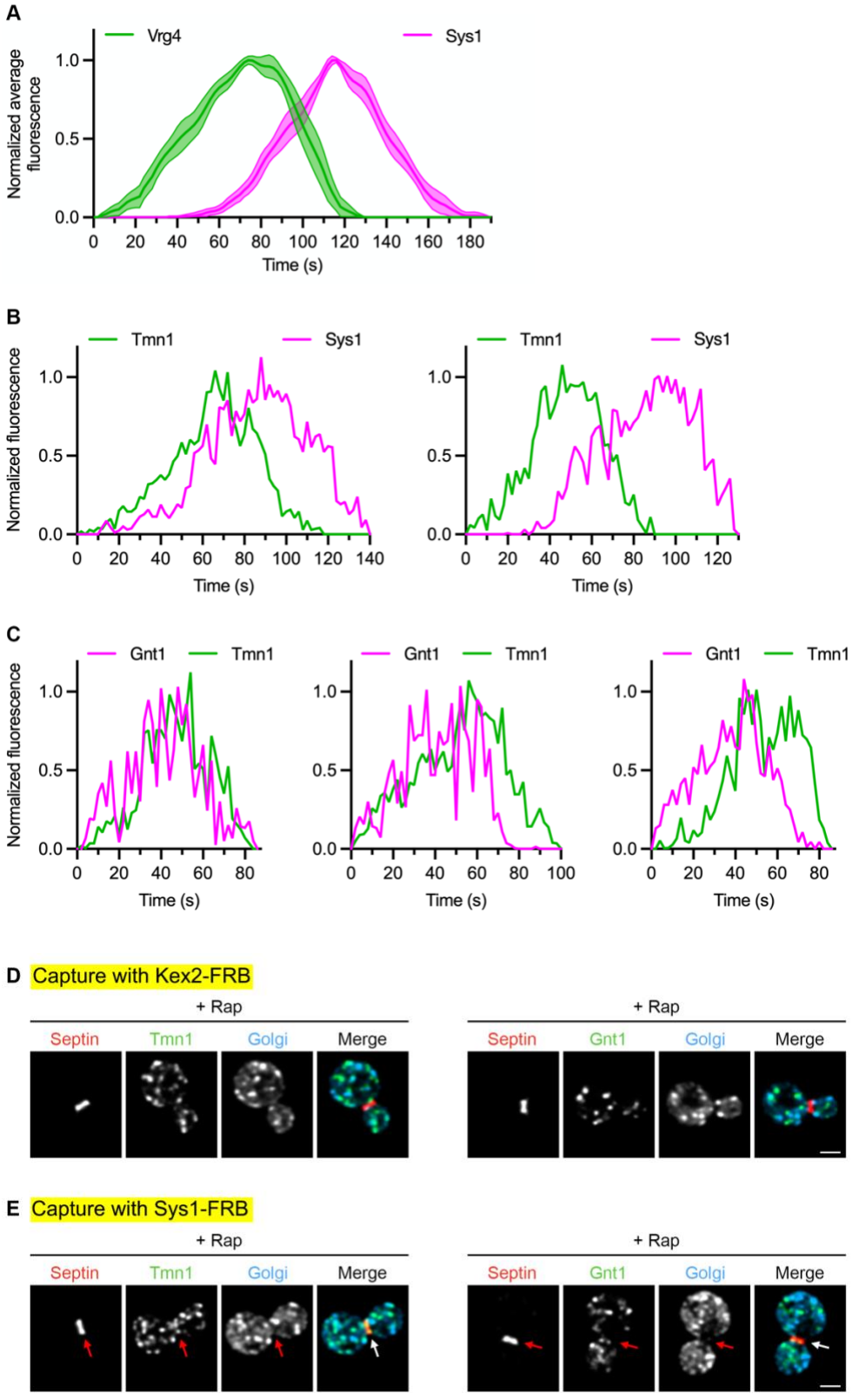

Figure 3.6: **The intermediate Golgi proteins Tmn1 and Gnt1 traffic in vesicles with Sys1 but not Kex2.** *(continued on next page)*

Figure 3.6: **(A)** Golgi maturation kinetics of GFP-tagged Vrg4 compared to HaloTag-labeled Sys1. Shown are normalized and averaged traces for 13 individual cisternae. **(B)** Kinetic traces for two representative cisternae illustrating variations in the relative arrival and departure times of GFP-Tmn1 versus Sys1-HaloTag. Plotted are normalized fluorescence intensities. **(C)** Kinetic traces for three representative cisternae illustrating variations in the relative arrival and departure times of Gnt1-HaloTag versus GFP-Tmn1. Plotted are normalized fluorescence intensities. **(D)** Representative images showing no capture with Kex2-FRB of GFP-tagged Tmn1 or Gnt1 (green) by an FKBP-tagged septin (red) after treatment for 5 min with rapamycin. **(E)** Representative images showing capture with Sys1-FRB of GFP-tagged Tmn1 or Gnt1 (green) by an FKBP-tagged septin (red) after treatment for 5 min with rapamycin. Arrows indicate non-Golgi signal at the bud neck.

Tmn1 and Gnt1 follow an intermediate recycling pathway and are largely absent from Kex2-containing vesicles

Based on the evidence that Sys1 and Aur1 partition between intermediate and late recycling pathways, we looked for proteins that recycle almost exclusively in the intermediate pathway. The evaluation was based on kinetic analysis. A candidate was Tmn1, also known as Emp70 (Singer-Krüger et al., 1993; Schimmöller et al., 1998; Woo et al., 2015). This protein is a member of the evolutionarily conserved but functionally uncharacterized "transmembrane nine" family of Golgi proteins. Tmn1 contains a C-terminal cytosolic tail that reportedly confers COPI-dependent Golgi localization (Woo et al., 2015), so the luminal N-terminus was tagged with GFP. The Ost1 signal sequence was used to ensure efficient co-translational translocation of the GFP tag (Fitzgerald and Glick, 2014). Tmn1 began to arrive after Vrg4 and finished departing after Vrg4, and Tmn1 began to arrive before Kex2 and finished departing before Kex2 (Figure 3.7A). Thus, Tmn1 resembled Sys1 in arriving after Vrg4 and before Kex2 (Figures 3.6A and 3.5A). When Tmn1 and Sys1 were directly compared, the relative arrival and departure times showed notable variability (Figure 3.6B), but Sys1 typically became detectable shortly after Tmn1 and persisted substantially longer than Tmn1 (Figure 3.7A). These results fit with the idea that Tmn1 recycles in an intermediate

pathway together with a fraction of the Sys1 molecules, and that Tmn1 is largely absent from the late pathway followed by Kex2 and the rest of the Sys1 molecules.

In addition to Tmn1, we identified Gnt1 as a candidate cargo of the intermediate pathway. Gnt1 is a type II transmembrane protein that functions as an *N*-acetylglucosaminyltransferase, and it was reported to recycle with intermediate kinetics (Yoko-o et al., 2003; Tojima et al., 2019). Gnt1 was tagged on its luminal C-terminus with HaloTag. When Gnt1 and Tmn1 were directly compared, the two proteins typically began to arrive at about the same time, but for most of the cisternae examined, Gnt1 finished departing earlier than Tmn1 (Figure 3.7A and Figure 3.6C). Thus, our kinetic analysis of Sys1, Tmn1, and Gnt1 indicates that for different cargoes of the putative intermediate recycling pathway, the arrival and departure times are somewhat variable. As explored in the Discussion, such variability can potentially be reconciled with the concept of a single molecularly defined pathway. We favor the idea that Tmn1 and Gnt1 recycle with each other and with a fraction of the Sys1 molecules.

To test whether Tmn1 and Gnt1 primarily follow an intermediate recycling pathway, we would ideally tag one of those proteins with FRB for use in a new vesicle capture assay. Unfortunately, neither Tmn1 nor Gnt1 can be cytosolically tagged without disrupting Golgi localization. As an alternative, we used the existing vesicle capture assays to ask whether Tmn1 and Gnt1 are present in Sys1-containing vesicles but not in Kex2-containing vesicles. In assays for co-capture with Kex2, Tmn1 showed a very weak signal and Gnt1 showed no signal (Figure 3.7B and Figure 3.6D). By contrast, in assays for co-capture with Sys1, both Tmn1 and Gnt1 showed strong signals (Figure 3.7C and Figure 3.6E). The combined data support the interpretation that Tmn1 and Gnt1 follow an intermediate recycling pathway, that Kex2 follows a late recycling pathway, and that Sys1 partitions between those two pathways.

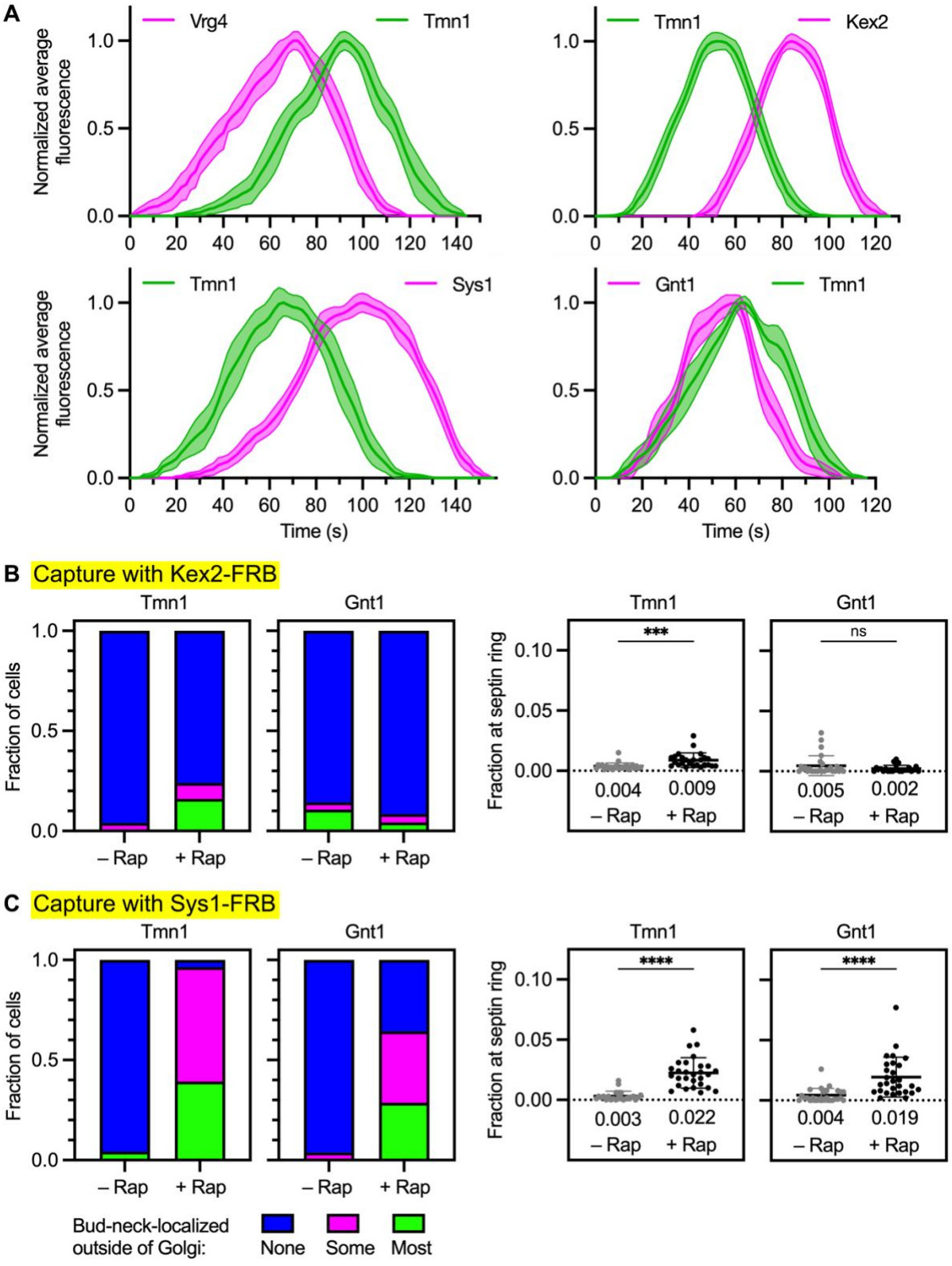

Figure 3.7: **Tmn1 and Gnt1 follow an intermediate recycling pathway that is also followed by a fraction of the Sys1 molecules.** *(continued on next page)*

Figure 3.7: **(A)** Golgi maturation kinetics of GFP-tagged Tmn1 compared to HaloTag-labeled Vrg4, Kex2, Sys1, or Gnt1. Shown are normalized and averaged traces for the following numbers of individual cisternae: 13 for the Tmn1/Vrg4 comparison, 15 for the Tmn1/Kex2 comparison, 11 for the Tmn1/Sys1 comparison, and 14 for the Tmn1/Gnt1 comparison. **(B)** Weak capture with Kex2-FRB of Tmn1, and no capture with Kex2-FRB of Gnt1. Categorical and numerical quantifications were performed as in Figure 3.2A. ***, significant at P value 0.0005; ns, not significant. **(C)** Capture with Sys1-FRB of Tmn1 and Gnt1. Categorical and numerical quantifications were performed as in Figure 3.2A. ****, significant at P value < 0.0001.

The intermediate recycling pathway does not depend directly on the AP-1 and Ent5 adaptors

We previously concluded that recycling of Sys1 and Aur1 involved AP-1 and Ent5 (Casler et al., 2021). That conclusion was based on examination of a strain lacking the AP-1 subunit Apl4 as well as Ent5. In *apl4*Δ *ent5*Δ cells, proteins that would normally recycle within the Golgi in an AP-1/Ent5-dependent manner are expected to travel to the plasma membrane in secretory vesicles and then return to the late Golgi in endocytic vesicles (Day et al., 2018). When endocytosis is inhibited in *apl4*Δ *ent5*Δ cells using the Arp2/3 inhibitor CK-666, exocytosis is also inhibited, and proteins cycling between the Golgi and the plasma membrane become trapped at secretion sites either in secretory vesicles or in the plasma membrane (Casler et al., 2021). During our original analysis of the effects of CK-666 in *apl4*Δ *ent5*Δ cells, Kex2 and Ste13 showed strong effects, Vrg4 showed no effect, and Sys1 and Aur1 showed moderate effects (Casler et al., 2021). In hindsight, the moderate effects can be explained if the AP-1/Ent5-dependent late recycling pathway carries a fraction of the Sys1 and Aur1 molecules.

For the intermediate recycling pathway that carries the remaining fraction of the Sys1 and Aur1 molecules together with Tmn1 and Gnt1, we predicted no dependency on AP-1/Ent5. This idea came from the observation that Tmn1 finished departing from a maturing cisterna around the time that the AP-1 subunit Apl2 began to arrive (Figure 3.8A). Because Ent5 begins to arrive

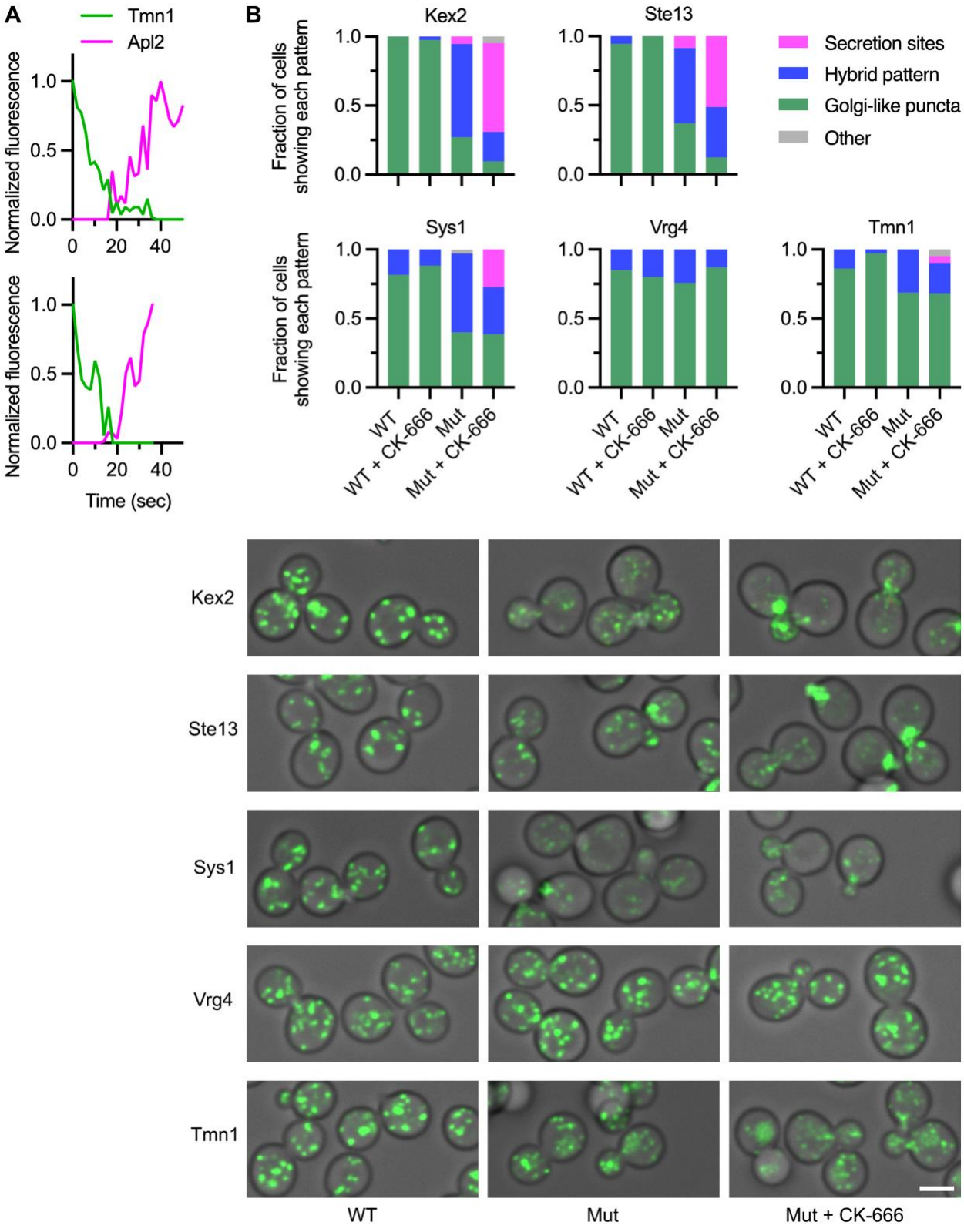

Figure 3.8: **The intermediate recycling pathway does not depend on AP-1/Ent5. (***continued on next page)*

Figure 3.8: **(A)** Partial kinetic traces for two representative cisternae illustrating that the AP-1 subunit Apl2 arrives after Tmn1 has largely departed. For two cisternae that showed detectable kinetic overlap between GFP-tagged Tmn1 and HaloTag-labeled Apl2, the fluorescence signals were quantified for 10-15 s before and after the overlap period. The maximal value obtained for each signal was set to 1.0. **(B)** Plots and representative images showing that in cells lacking AP-1 and Ent5, inhibition of endocytosis with CK-666 affected the localizations of some Golgi proteins but not of Tmn1. Wild-type "WT" or *apl4*Δ *ent5*Δ mutant ("Mut") cells expressing the indicated GFP-tagged Golgi proteins were examined by fluorescence microscopy after either mock treatment or treatment for 15-25 min with CK-666. The fluorescence pattern of each tagged protein was quantified by assigning cells to categories based on whether most of the protein was in Golgi-like puncta, or whether most of the protein was concentrated at secretion sites, or whether the protein was distributed in a hybrid pattern between Golgi-like puncta and secretion sites. Approximately 30-45 cells were examined for each Golgi protein and each condition. In a few cases ("Other"), a cell could not be confidently assigned to any of the three categories. Representative images are shown for mock-treated wild-type cells, mock-treated mutant cells, and CK-666-treated mutant cells. For a given GFP-tagged protein, the images were all captured and processed with the same parameters.

simultaneously with Apl2 (Daboussi et al., 2012; Casler et al., 2021), neither AP-1 nor Ent5 is present at the Golgi during the departure phase of Tmn1, implying that Tmn1 recycling is independent of AP-1/Ent5. To verify this conclusion, we updated the assay in which *apl4*Δ *ent5*Δ mutant cells are treated with CK-666 (Casler et al., 2021). Cells were assigned to three categories based on whether a GFP-tagged Golgi protein was concentrated primarily in Golgi-like puncta distributed throughout the cell, or whether it was concentrated primarily at secretion sites, or whether it showed a hybrid pattern of concentration both in Golgi-like puncta and at secretion sites. For example, Kex2 mainly showed concentration at Golgi-like puncta in untreated or CK-666-treated wild-type cells, and mainly showed concentration at secretion sites in CK-666-treated mutant cells, and mainly showed a hybrid pattern in untreated mutant cells (Figure 3.8B). The hybrid pattern in untreated mutant cells presumably indicates that Kex2 was cycling between the Golgi and the plasma membrane rather than recycling within the Golgi (Casler et al., 2021). Like Kex2, Ste13 showed concentration at secretion sites in CK-666-treated mutant cells (Figure 3.8B). Sys1 also showed concentration at secretion sites in CK-666-treated mutant cells, but as previously

seen (Casler et al., 2021), this effect was weaker than for Kex2 and Ste13 (Figure 3.8B). A likely explanation is that only a fraction of the Sys1 molecules were missorted into secretory vesicles in *apl4*Δ *ent5*Δ mutant cells. Vrg4 showed no concentration at secretion sites in CK-666-treated mutant cells, as expected (Figure 3.8B). Tmn1 showed some accumulation in the vacuole in *apl4*Δ *ent5*Δ mutant cells with or without CK-666, perhaps due to a perturbation of Golgi function, but it showed minimal concentration at secretion sites in CK-666-treated mutant cells (Figure 3.8B). We conclude that recycling of Tmn1 is not mediated by AP-1/Ent5.

The intermediate recycling pathway depends on COPI

It seemed possible that the intermediate recycling pathway employs COPI. If so, then COPI should be present on Golgi cisternae throughout the departure phase of Tmn1. To test this prediction, we first used three-color kinetic mapping to compare the COPI subunit Sec26 to the early and late Golgi reference proteins Vrg4 and Sec7 (Losev et al., 2006; Papanikou et al., 2015). Previous studies indicated that COPI associates with early Golgi cisternae and persists into the arrival phase of Sec7 (Papanikou et al., 2015; Kim et al., 2016; Tojima et al., 2019). Indeed, Sec26 began to arrive on maturing cisternae well before Vrg4, and Sec26 finished departing around the time that Sec7 reached its peak abundance (Figure 3.9A). Kinetic mapping of Sec26 was technically difficult because the earliest COPI-containing cisternae were small and numerous, but the averaged data suggest that COPI may arrive at cisternae in two successive waves. For our purposes, the key point was that Sec26 persisted after Vrg4 had departed, suggesting that COPI was still present during the departure of proteins that follow the intermediate recycling pathway. Indeed, tracking of Sec26 during the residence period of Tmn1 indicated that COPI persisted at a maturing cisterna until Tmn1 had finished departing (Figure 3.9B). Of the 13 individual cisternae examined in this way,

all of them showed Sec26 persisting at least as long as Tmn1. Thus, COPI could be involved in forming the vesicles of the intermediate recycling pathway.

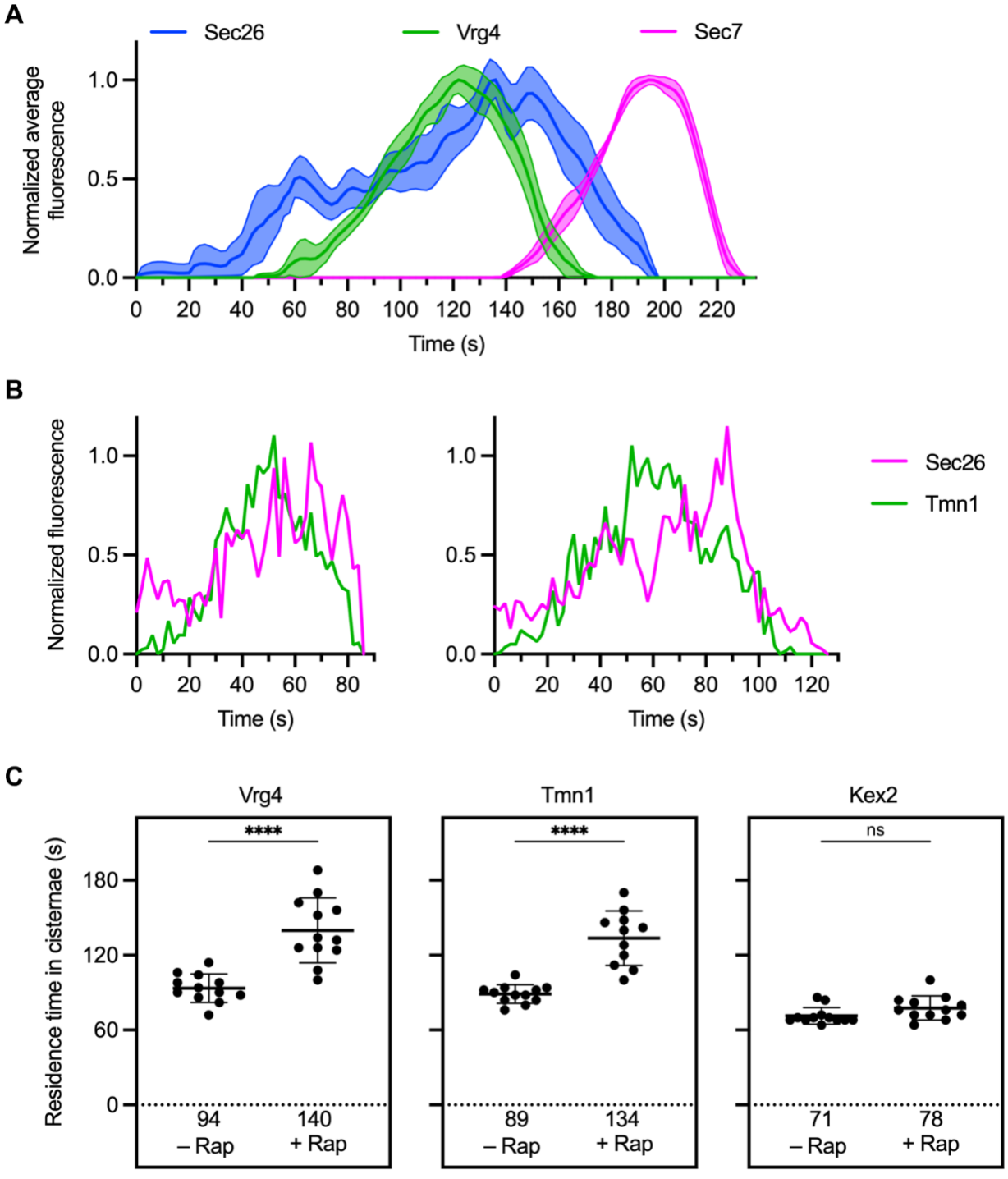

Figure 3.9: **The intermediate recycling pathway depends on COPI.** *(continued on next page)*

Figure 3.9: **(A)** Golgi maturation kinetics of the COPI subunit Sec26 relative to Vrg4 and Sec7. Shown are normalized and averaged traces for 11 individual cisternae marked with GFP-tagged Vrg4, mScarlet-tagged Sec7, and HaloTag-labeled Sec26. **(B)** Kinetic traces for two representative cisternae illustrating that COPI persists long enough to account for the departure of Tmn1. The traces show only the final part of the Sec26 residence times on the cisternae. **(C)** Residence times of Vrg4, Tmn1, and Kex2 in Golgi cisternae after partial inactivation of COPI. For the indicated GFP-tagged Golgi proteins, the residence times were defined as the intervals between the first and last detectable signals in individual maturing cisternae. Where indicated, partial inactivation of COPI was achieved by incubating with rapamycin ("Rap") for 4-7 min before the first detectable signals of the GFP-tagged Golgi protein. The mean residence times are displayed as thick horizontal bars and are listed numerically below the plots, and the standard deviations are displayed as thin horizontal bars. ****, significant at P value <0.0001; ns, not significant.

To determine whether COPI mediates recycling of Tmn1, we modified an earlier approach in which COPI was acutely inactivated (Haruki et al., 2008; Papanikou et al., 2015). The COPI subunit Sec21 was tagged with FRB while a ribosomal subunit was tagged with FKBP, with the result that rapamycin treatment led to ribosomal association and functional inactivation of COPI. Maximal inactivation was previously seen after 10-15 min of rapamycin treatment, but by that time Golgi organization was disrupted (Papanikou et al., 2015). We therefore performed a partial inactivation of COPI by treating cells with rapamycin for only 4 min prior to kinetic mapping. The rationale was that we could track maturing cisternae in the usual way, except that reduced COPI function should slow the departure of proteins whose recycling is COPI-dependent. This approach was validated by examining the COPI-dependent protein Vrg4 and the COPI-independent protein Kex2 (Papanikou et al., 2015). In the absence of rapamycin, the average residence time of Vrg4 in maturing cisternae was 94 s, whereas in the presence of rapamycin, the average residence time of Vrg4 increased about 1.5-fold to 140 s (Figure 3.9C and Figure 3.10 and Video 3.4 and Video 3.5). By contrast, the average residence time of Kex2 was not significantly altered by rapamycin (Figure 3.9C and Figure 3.10). This result indicates that partial inactivation of COPI selectively affected proteins that recycled in a COPI-dependent manner. For Tmn1, the average residence time was

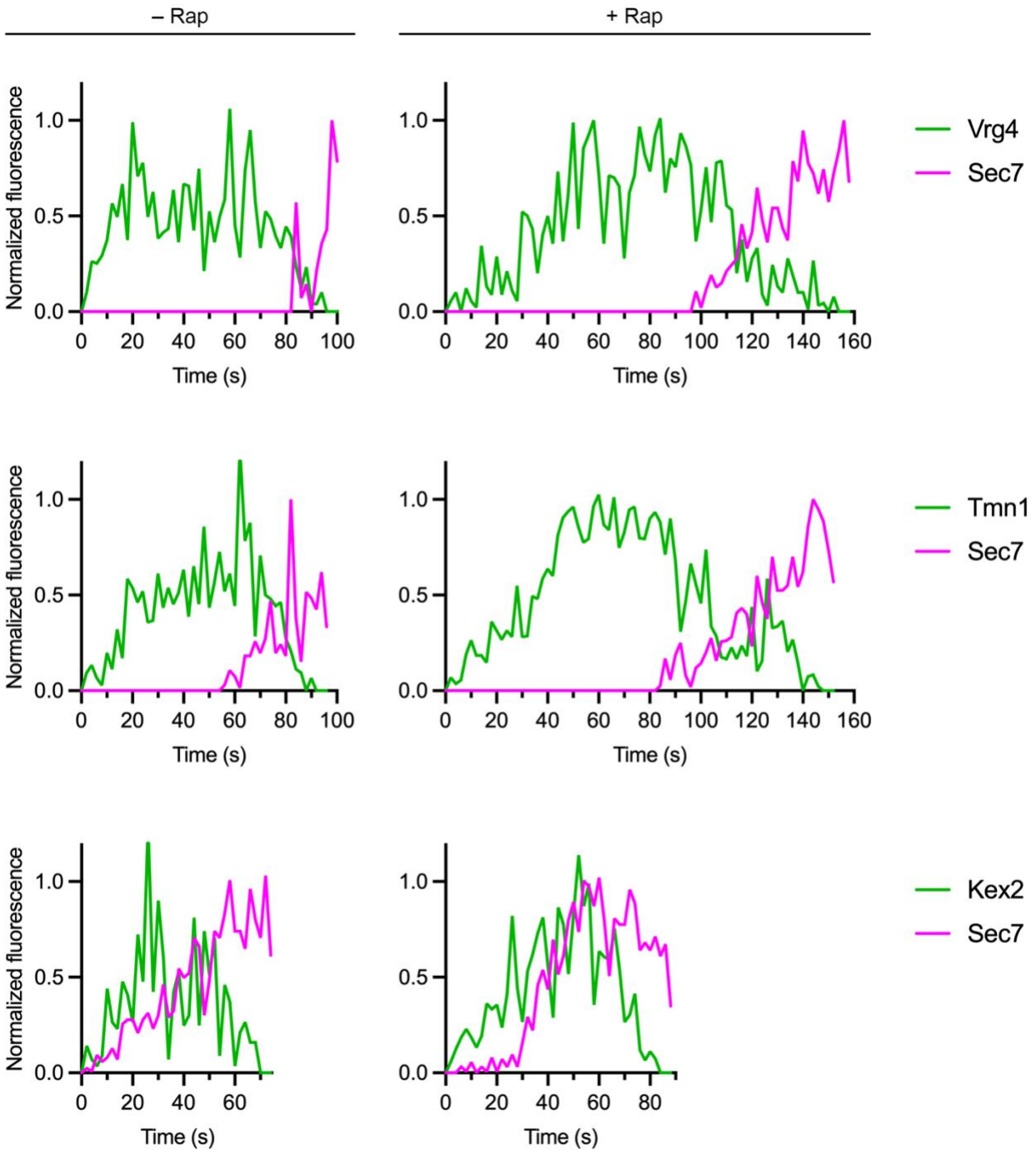

Figure 3.10: **COPI inactivation increases the cisternal residence times of Vrg4 and Tmn1.** Kinetic traces for representative cisternae illustrating the residence times of GFP-tagged Vrg4, Tmn1, and Kex2 in Golgi cisternae either with normal COPI activity ("– Rap") or with reduced COPI activity caused by brief rapamycin treatment ("+ Rap"). The analysis included partial companion traces of the late Golgi marker Sec7-mScarlet. Plotted are normalized fluorescence intensities.

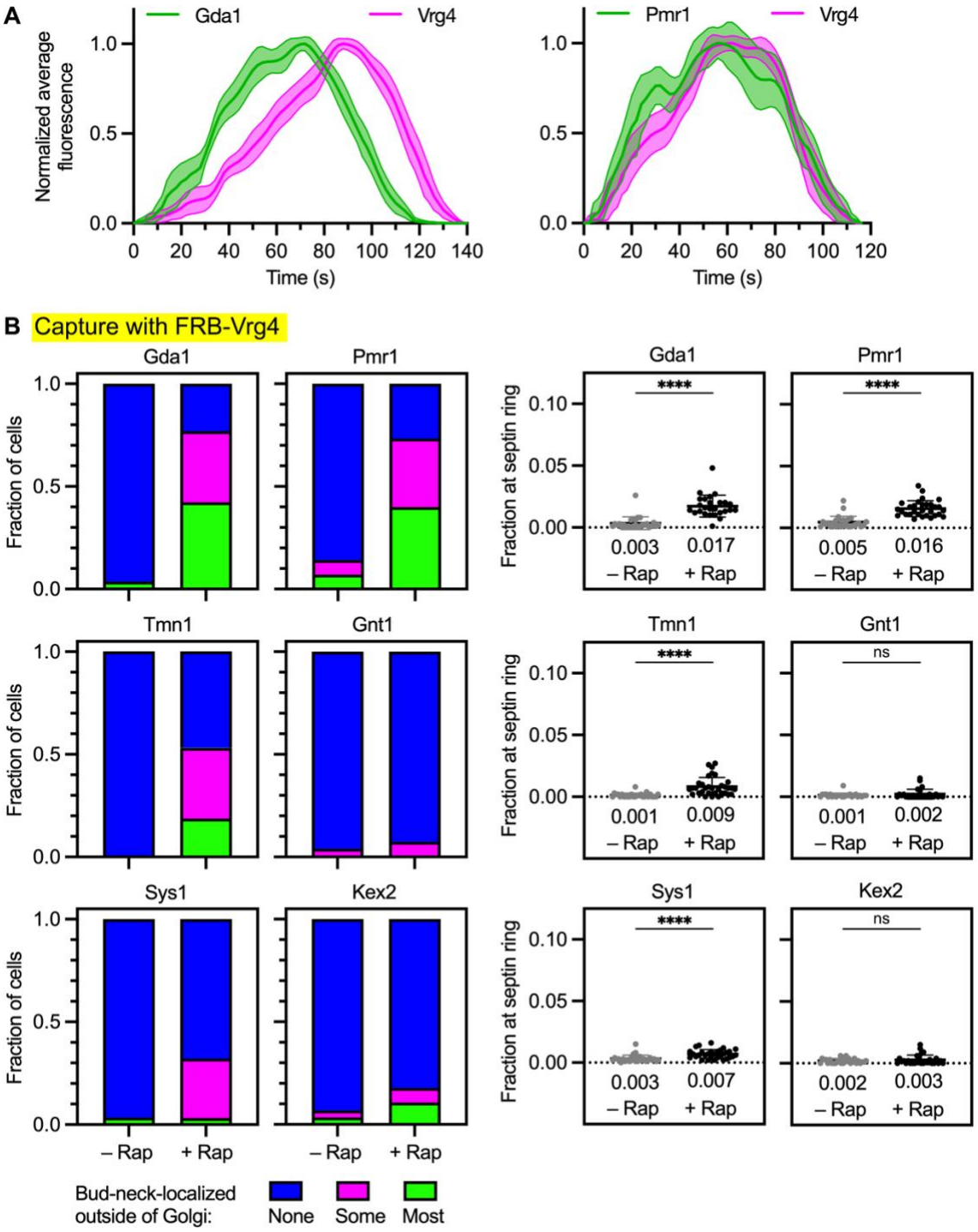

Figure 3.11: **A subset of COPI cargoes can be specifically captured at the bud neck together with Vrg4.** *(continued on next page)*

Figure 3.11: **(A)** Golgi maturation kinetics of HaloTag-labeled Vrg4 compared to GFP-tagged Gda1 or Pmr1. Shown are normalized and averaged traces for 14 individual cisternae for the Vrg4/Gda1 comparison and 11 individual cisternae for the Vrg4/Pmr1 comparison. The strain expressing tagged Gda1 carried the *vps10-104* mutation due to the luminal GFP tag. **(B)** Capture with FRB-Vrg4 of Gda1 and Pmr1, weak capture with FRB-Vrg4 of Tmn1 and Sys1, and no capture with FRB-Vrg4 of Gnt1 or Kex2. Categorical and numerical quantifications were performed as in Figure 3.2A. ****, significant at P value <0.0001; ns, not significant.

89 s in the absence of rapamycin and 134 s in the presence of rapamycin (Figure 3.9C and Figure 3.10). As for Vrg4, the increase was about 1.5-fold. These results strongly suggest that COPI mediates the traffic of Tmn1 and other proteins that follow the intermediate recycling pathway.

Vrg4-containing vesicles and intermediate pathway vesicles have different cargo compositions despite their shared dependency on COPI

The distinct kinetic signatures of Vrg4 and Tmn1 (see Figure 3.7A) could reflect two separate COPI-dependent recycling pathways. If so, then we would expect to find additional resident Golgi transmembrane proteins that begin to arrive together with Vrg4. A likely prospect was Gda1, a guanosine diphosphatase that supports glycosylation (Berninsone et al., 1994). Indeed, kinetic mapping revealed that Gda1 began to arrive at the same time as Vrg4 (Figure 3.11A). Gda1 departed sooner than Vrg4, perhaps reflecting different rates of packaging into COPI vesicles. A second candidate was Pmr1, which also supports glycosylation, in this case by transporting divalent cations into the Golgi lumen (Antebi and Fink, 1992; Dürr et al., 1998). The kinetics of Pmr1 arrival and departure were very similar to those of Vrg4 (Figure 3.11A). We therefore predicted that Gda1 and Pmr1 would be found in the same vesicles as Vrg4.

This prediction was tested by establishing a vesicle capture assay in which Vrg4 was tagged on its cytosolic N-terminus with FRB. To verify that Vrg4-containing vesicles could be captured, Vrg4 was tagged with both FRB and GFP. Upon rapamycin addition, the dual-tagged Vrg4

accumulated in vesicles at the bud neck, as judged by fluorescence imaging (Figure 3.12A). Cryo-electron tomography confirmed that capture of FRB-Vrg4 resulted in the appearance of vesicles at the bud neck (Figure 3.12B and Video 3.6). In cells expressing Vrg4 tagged with FRB alone, either Gda1, Pmr1, Tmn1, Gnt1, Sys1, or Kex2 was tagged with GFP. After rapamycin addition, only Gda1 and Pmr1 showed robust accumulation at the bud neck (Figure 3.11B and Figure 3.12C). No signal was seen with Gnt1 or Kex2, and weak signals were seen with Tmn1 and Sys1

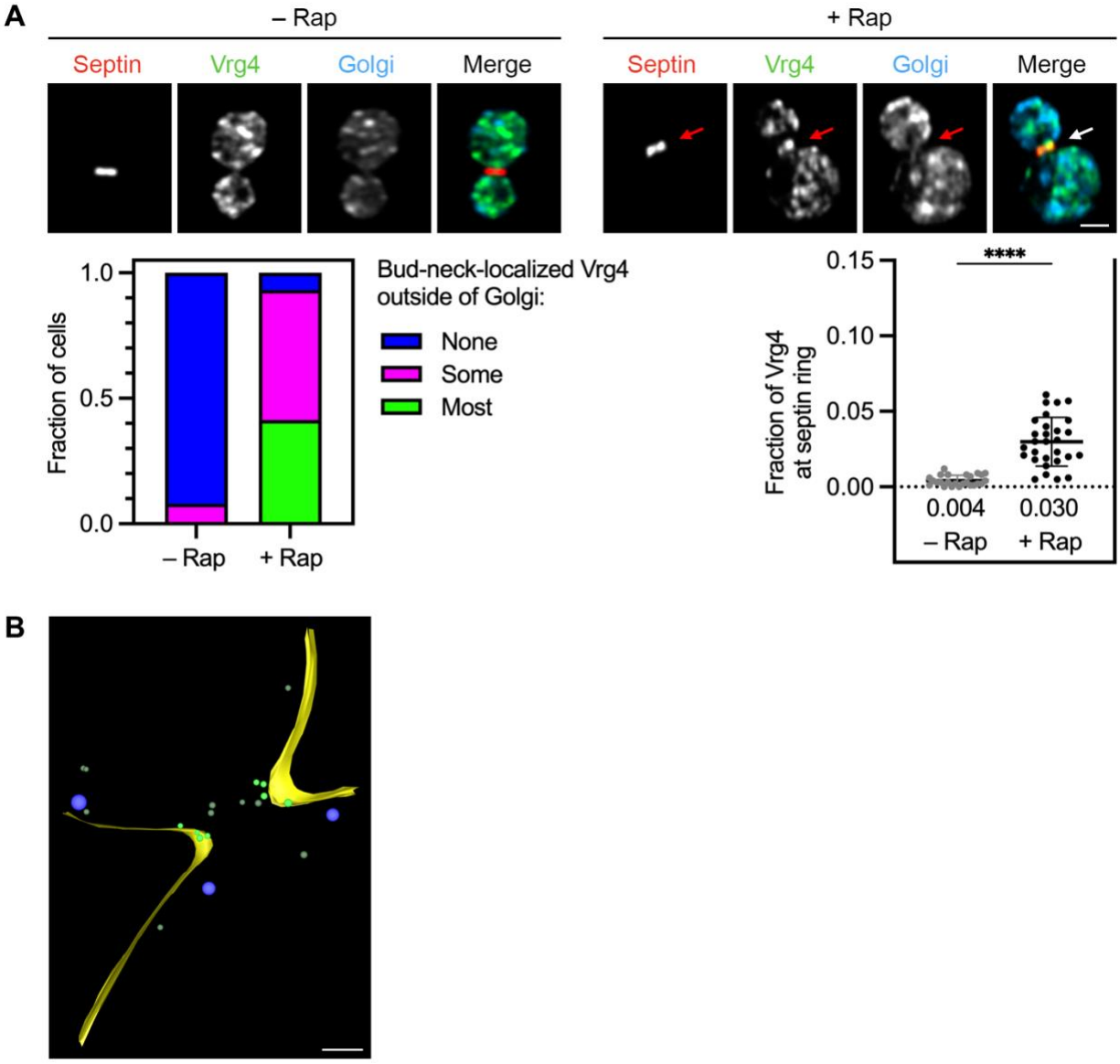

Figure 3.12: **Vrg4 vesicles captured at the septin ring contain substantial amounts of Gda1 and Pmr1.** *(continued on next page)*

Figure 3.12: **Vrg4 vesicles captured at the septin ring contain substantial amounts of Gda1 and Pmr1.** *(continued from previous page)*

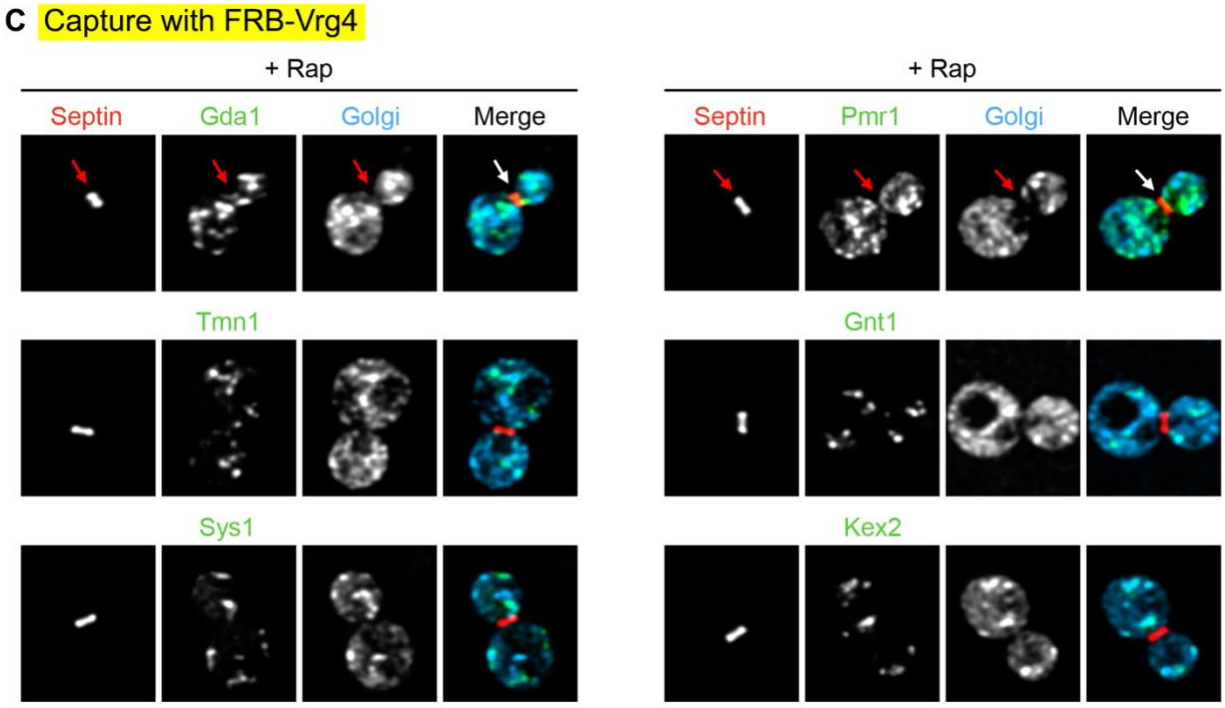

Figure 3.12: **(A)** Rapamycin-dependent capture by an FKBP-tagged septin (red) of FRB-GFP-Vrg4 (green). Arrows indicate non-Golgi signal at the bud neck after treatment for 5 min with rapamycin ("Rap"). At the lower left, capture of FRB-GFP-Vrg4 at the bud neck was quantified by assigning cells to categories as described in Figure 3.1C. At the lower right, capture of FRB-GFP-Vrg4 at the bud neck was quantified numerically as described in Figure 3.1B. ****, significant at P value <0.0001. **(B)** Cryo-ET of vesicles captured at the bud neck using FRB-Vrg4. A log-phase culture of cells expressing FRB-Vrg4 and Shs1-FKBP was treated with rapamycin for 5 min followed by cryo-preservation and processing for cryo-ET. Shown is the tomographic model of a SIRT-reconstructed tomogram from a large budded cell. The full data set is shown in Video 3.6. A vesicle was counted as putatively captured if its membrane was no more than 66 nm from a point on the plasma membrane within 200 nm from the center of the bud neck. For the 6 non-rapamycin-treated cells examined, the number of vesicles meeting this criterion ranged from 0 to 2 (mean = 0.8). For the 6 rapamycin-treated cells examined, the number of putatively captured vesicles ranged from 2 to 7 (mean = 5.0). Scale bar, 250 nm. See Fig. 3.1D for further details. **(C)** Representative images showing capture with FRB-Vrg4 of GFP-tagged Gda1 and Pmr1 (green) by an FKBP-tagged septin (red), minimal capture with FRB-Vrg4 of GFP-tagged Tmn1 and Sys1 (green) by an FKBP-tagged septin (red), and no capture with FRB-Vrg4 of GFP-tagged Gnt1 or Kex2 (green) by an FKBP-tagged septin (red), all after treatment for 5 min with rapamycin. Arrows indicate non-Golgi signal at the bud neck.

(Figure 3.11B). Our interpretation is that Gda1 and Pmr1 frequently travel in vesicles together with Vrg4. The weak signals seen with Tmn1 and Sys1 might reflect occasional leakage of Vrg4

into intermediate pathway vesicles and/or occasional packaging of Tmn1 and Sys1 into early pathway vesicles. Taken together, the kinetic and vesicle capture data suggest that the cargoes recycled by the intermediate COPI-dependent pathway are largely distinct from those recycled by the early COPI-dependent pathway.

Discussion

The polarized distribution of resident Golgi transmembrane proteins (Tie et al., 2016) confers temporal order on the events that occur during cisternal maturation, so a mechanistic understanding of Golgi polarity is crucial. We have proposed that Golgi polarity is generated by multiple membrane recycling pathways that operate with different kinetics during the life cycle of a cisterna (Pantazopoulou and Glick, 2019). Some recycling pathways act within the Golgi to deliver proteins from older to younger cisternae, and some recycling pathways act between the Golgi and other compartments (Figure 3.13).

What defines a Golgi recycling pathway? Our perspective is based on two assumptions. First, each recycling pathway is assumed to employ a specific traffic machinery that mediates the formation, tethering, and fusion of transport vesicles at a particular stage of maturation. Second, each recycling pathway is assumed to generate a distinct population of vesicles carrying a particular set of resident Golgi proteins. For example, our earlier work indicated that the COPI coat is involved in the recycling of Vrg4, which is present early in maturation, and that the clathrin adaptors AP-1 and Ent5 are involved in the recycling of Kex2, which is present late in maturation (Papanikou et al., 2015; Casler et al., 2021). A complication is that an individual component of the traffic machinery might function in multiple pathways. Examples are the role of the COPI coat in both intra-Golgi and Golgi-to-ER traffic (Barlowe and Miller, 2013), and the ability of certain

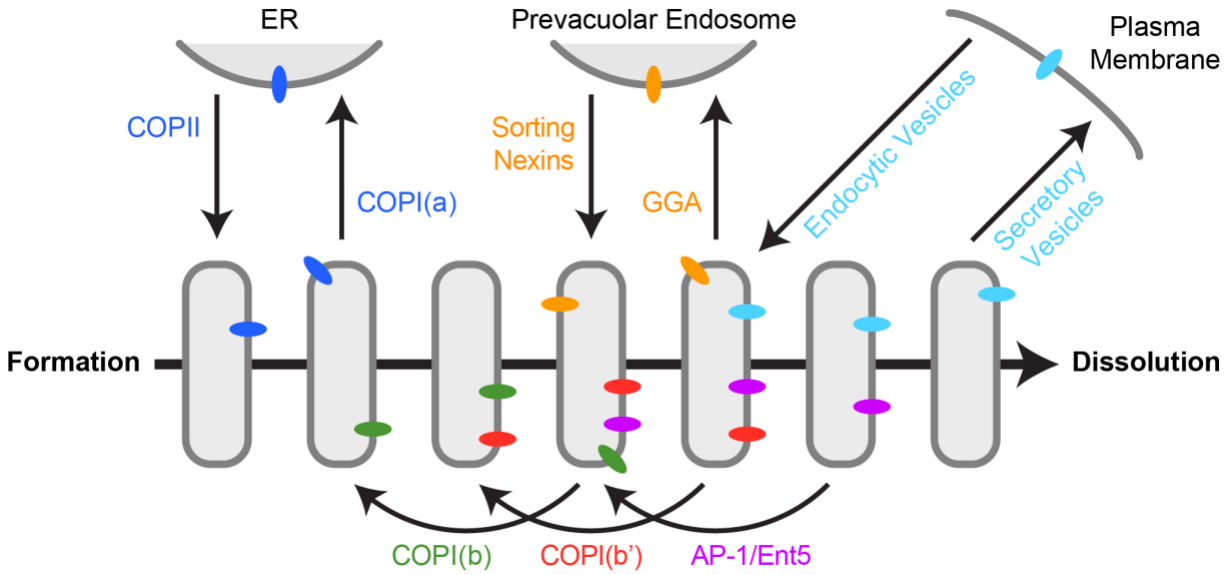

Figure 3.13: **Summary of known recycling pathways that deliver membrane proteins to the yeast Golgi.** The horizontal arrow depicts a timeline of cisternal maturation. During the lifetime of a cisterna, transmembrane proteins are delivered in six recycling pathways: (1) Some proteins (dark blue) are delivered to newly formed Golgi cisternae in COPII vesicles, and then those proteins recycle to the ER in COPI vesicles in a pathway that we term "COPI(a)". (2) At an early stage of maturation, some resident Golgi proteins (green) recycle from older to younger cisternae in COPI vesicles in a pathway that we term "COPI(b)". (3) At an intermediate stage of maturation, some resident Golgi proteins (red) recycle from older to younger cisternae in COPI vesicles in a pathway that we term "COPI(b')". (4) At an intermediate stage of maturation, some proteins (orange) are delivered to prevacuolar endosomes in clathrin-coated vesicles generated with the aid of the GGA adaptors, and then those proteins recycle to the Golgi in carriers generated with the aid of sorting nexins. (5) At a late stage of maturation, some resident Golgi proteins (magenta) recycle from older to younger cisternae in clathrin-coated vesicles generated with the aid of the AP-1 and Ent5 adaptors in a pathway that we term "AP-1/Ent5". (6) At a terminal stage of maturation, some proteins (light blue) travel in secretory vesicles to the plasma membrane, and then those proteins recycle to the Golgi in endocytic vesicles.

Golgi-associated tethering proteins to capture more than one class of transport vesicles (Wong and Munro, 2014). The likely implication is that a given recycling pathway harnesses a unique combination of traffic machinery components.

To characterize Golgi recycling pathways in yeast, we compare the kinetic signatures of various resident Golgi proteins, and we identify transmembrane proteins that can serve as reference markers for different pathways. This approach too has a complication: some resident Golgi

proteins might follow more than one recycling pathway. The fidelity of partitioning into a given pathway is unlikely to be perfect, so many resident Golgi proteins probably follow a major recycling pathway as well as one or more minor salvage pathways. For example, a major pathway for recycling a set of Golgi proteins may also serve to salvage other Golgi proteins that recycle in an earlier pathway but occasionally leak downstream. Moreover, some resident Golgi proteins could partition at high frequency into more than one recycling pathway. This type of multi-pathway recycling might occur normally, e.g., if a resident Golgi protein functions at more than one stage of maturation. Alternatively, fluorescent tagging of a resident Golgi protein might perturb recycling in the major pathway, thereby pushing a fraction of the tagged molecules into a salvage pathway. Because of these caveats, the kinetic signatures of resident Golgi proteins are sometimes challenging to interpret, and additional types of data are needed.

We therefore developed a new functional test that is complementary to kinetic analysis. A specific population of Golgi-derived vesicles is captured at the yeast bud neck by chemically-induced dimerization (Fegan et al., 2010). For this purpose, an FRB-tagged Golgi protein in the vesicles heterodimerizes with an FKBP-tagged septin. Then fluorescence microscopy is used to determine which other resident Golgi proteins are co-captured in the same vesicles as the FRB-tagged protein. Table 3.1 lists the resident Golgi transmembrane proteins that were examined here, together with their inferred intra-Golgi recycling pathways as depicted in Figure 3.13.

The vesicle capture assay gives meaningful results. For example, when Kex2 is tagged with FRB, there is efficient co-capture of Ste13 and Stv1, which have the same kinetic signature and the same AP-1/Ent5 dependency as Kex2 (Casler et al., 2021), and there is no co-capture of Vrg4, which has an earlier kinetic signature and a COPI dependency (Papanikou et al., 2015). But this assay also produces some ambiguous results as indicated below. We can envision possible sources

of ambiguity. Most notably, if the FRB-tagged protein is occasionally missorted into a second type of vesicle, then that second type of vesicle will sometimes be captured at the bud neck, yielding a detectable signal. When interpreting the vesicle capture data, we compare different resident Golgi proteins in order to define strong versus weak co-capture, and we evaluate the findings in the context of kinetic analysis. This exercise has led to the following conclusions.

The available evidence points to a single intra-Golgi recycling pathway mediated by AP-1/Ent5. Our reference protein for this pathway is Kex2, which exhibits perturbed traffic in cells lacking AP-1 and Ent5 but not in cells with inactivated COPI (Papanikou et al., 2015; Casler et al., 2021). We previously suggested that a second AP-1/Ent5-dependent pathway might recycle Sys1 upstream of Kex2 (Casler et al., 2021). The reasoning was that (a) Sys1 arrived at maturing cisternae earlier than Kex2, and (b) Sys1 traffic was altered in cells lacking AP-1 and Ent5. However, we now believe that Sys1 is not a suitable marker for a unique recycling pathway, because the vesicle capture assay reveals that Sys1 is co-captured with Kex2. The combined kinetic and functional data support the idea that Sys1 partitions between two recycling pathways: a late pathway marked by Kex2, and an upstream pathway with intermediate kinetics. This dual partitioning could reflect the physiological behavior of Sys1, but it might be due to the cytosolic tag. When cytosolically-tagged Aur1 (Casler et al., 2021) is analyzed by kinetic mapping and by the vesicle capture assay, it shows the same dual partitioning as Sys1. A possible interpretation is that Sys1 and Aur1 normally recycle in the intermediate pathway and that entry into this pathway is sensitive to bulky cytosolic tags.

This new perspective on Sys1 and Aur1 prompted us to look for other resident Golgi proteins that recycle mainly in the intermediate pathway. We identified Tmn1, which can be luminally tagged. Tmn1 arrives at maturing cisternae before Kex2, and Tmn1 departs before Kex2.

The relative kinetic signatures of Tmn1, Sys1, and Kex2 suggest that tagged Sys1 partitions between an intermediate pathway marked by Tmn1 and a late pathway marked by Kex2. This scenario is bolstered by the finding that Tmn1 is co-captured strongly in vesicles containing FRB-tagged Sys1 but only very weakly in vesicles containing FRB-tagged Kex2. Gnt1 can also be luminally tagged, and it resembles Tmn1 with regard to its kinetic behavior and its selective co-capture with FRB-tagged Sys1. Based on these data, we propose the existence of an intermediate recycling pathway for which Tmn1 can serve as the reference marker.

Is the intermediate pathway mediated by COPI, or is it mediated by AP-1/Ent5? Based on kinetic analysis, COPI remains on a maturing cisterna throughout the departure phase of Tmn1, whereas AP-1 does not arrive at a maturing cisterna until Tmn1 has almost completely departed. This result makes COPI a much better candidate than AP-1/Ent5 for generating vesicles of the intermediate pathway. One way to test this prediction is to block endocytosis in cells lacking AP-1 and Ent5. In such mutant cells, proteins that normally recycle in the AP-1/Ent5 pathway apparently travel to the plasma membrane and then return to the Golgi in endocytic vesicles (Day et al., 2018; Casler et al., 2021). We found that blocking endocytosis in cells lacking AP-1 and Ent5 strongly perturbs the traffic of Kex2 and Ste13 but not of Vrg4 or Tmn1. A moderate effect is seen with Sys1, consistent with the interpretation that some of the tagged Sys1 molecules normally recycle in the AP-1/Ent5 pathway. A second way to test which type of coat generates vesicles of the intermediate pathway is to reduce the activity of COPI by anchoring it to ribosomes (Papanikou et al., 2015). Partial inactivation of COPI slows the departure of Vrg4 and Tmn1 from maturing cisternae but has no effect on the departure of Kex2. That result fits with reports that Vrg4 and Tmn1 have COPI recognition signals (Abe et al., 2004; Woo et al., 2015). The combined

data indicate that Tmn1, and presumably also Gnt1, follow a COPI-dependent recycling pathway with intermediate kinetics.

Because both Vrg4 and Tmn1 show COPI dependency, but they arrive at a maturing cisterna at different times, those two proteins likely recycle in distinct COPI-mediated pathways. To test this prediction, we performed vesicle capture assays using FRB-tagged Vrg4. Gda1 and Pmr1 arrive at maturing cisternae simultaneously with Vrg4, and they show relatively strong co-capture with Vrg4, suggesting that they are present in the same vesicles as Vrg4. By contrast, Gnt1 and Kex2 show no co-capture with Vrg4, consistent with the idea that the intermediate and late recycling pathways are distinct from the early pathway marked by Vrg4. Relatively weak capture with Vrg4 was seen for Tmn1 and Sys1. This result might reflect occasional leakage of Vrg4 into the intermediate pathway or occasional packaging of Tmn1 and Sys1 into vesicles of the early pathway. Thus, while some of the individual results are not definitive, the combination of kinetic and functional analyses supports the existence of two distinct COPI-dependent pathways marked by Vrg4 and Tmn1. One could envision that Vrg4 follows a Golgi-to-ER pathway while Tmn1 follows an intra-Golgi pathway. But if Vrg4 recycled through the ER, it should be visible in the youngest Golgi cisternae, and that result is not observed (Casler et al., 2019). Instead, the appearance of Vrg4 is preceded by that of certain other Golgi markers (Tojima et al., 2024)—including COPI itself, as shown here—suggesting that Vrg4 recycles within the Golgi. Thus, Vrg4 and Tmn1 apparently recycle in successive intra-Golgi pathways, which we provisionally term COPI(b) and COPI(b'), respectively (Figure 3.13 and Table 3.1).

Interestingly, Golgi proteins that follow the same recycling pathway do not always depart with identical kinetics. For example, Gnt1 often departs slightly before Tmn1 in the COPI(b') pathway, and Gda1 departs substantially before Vrg4 in the COPI(b) pathway. These findings can

be rationalized by assuming that different Golgi proteins compete for packaging into a limited number of sites in outgoing COPI vesicles, with the result that the stronger competitors depart sooner (Glick et al., 1997).

Golgi proteins that follow the same recycling pathway would be expected to arrive with similar kinetics. For the most part, that pattern seems to hold true. An apparent exception is the COPI(b') pathway, because accumulation of Sys1 lags behind that of Tmn1. One possible explanation is that Sys1 but not Tmn1 can depart from a cisterna immediately after arrival, with the result that Sys1 accumulates more slowly than Tmn1. Alternatively, our analysis method may be subtly misleading for proteins such as Sys1 that partition between two pathways, based on the following logic. If the partitioning varies such that for some cisternae, a large fraction of the Sys1 molecules follow the COPI(b') pathway together with Tmn1, whereas for other cisternae, only a small fraction of the Sys1 molecules follow the COPI(b') pathway while the rest follow the downstream AP-1/Ent5 pathway, then the averaged kinetic signature will show Sys1 lagging behind Tmn1. This explanation is consistent with the observed variability in the individual traces comparing Sys1 with Tmn1. However, further work is needed to gain a full understanding of Sys1 recycling.

The high-level summary of our findings is that at least two COPI-dependent pathways mediate intra-Golgi recycling early in maturation while an AP-1/Ent5-dependent pathway mediates intra-Golgi recycling late in maturation. It is interesting that even though yeast cells contain just a single species of the COPI coatomer (Gaynor et al., 1998), COPI mediates multiple pathways, including intra-Golgi recycling as well as Golgi-to-ER recycling. The implication is that COPI acts together with partner proteins to ensure specificity for both cargo capture and vesicle targeting. An example of a COPI partner protein is yeast Vps74, which is related to mammalian

GOLPH3 and GOLPH3L (Schmitz et al., 2008; Tu et al., 2008; Welch et al., 2021). Vps74 and its mammalian orthologs interact with COPI and with a subset of the cargo proteins that are packaged into COPI vesicles. We speculate that additional COPI partner proteins assist in specifying the various COPI-dependent recycling pathways.

The insights described here bring us closer to a complete picture of the membrane recycling pathways at the yeast Golgi. A future goal is to identify the tethers and SNAREs that operate in each pathway. The resulting data set will be the framework for an integrated model of the Golgi system.

Materials and methods

Yeast growth and transformation

All strains used in this study were derivatives of JK9-3da (*leu2-3,112 ura3-52 rme1 trp1 his4*; Kunz et al., 1993) with the *pdr1Δ pdr3Δ* mutations to facilitate HaloTag labeling (Barrero et al., 2016; Casler et al., 2021). Rapamycin-resistant strains carrying the *fpr1*Δ and *TOR1-1* mutations were constructed as previously described (Papanikou et al., 2015). If a Golgi protein was luminally tagged with GFP or HaloTag, the strain carried the *vps10-104* mutation to prevent missorting to the vacuole (Fitzgerald and Glick, 2014). Prior to experimental analysis, yeast cells were grown in nonfluorescent minimal glucose medium (NSD) (Bevis et al., 2002) in baffled flasks at 23°C with shaking at 200 rpm unless otherwise noted.

Yeast genes were tagged by chromosomal gene replacement using the pop-in/pop-out method (Rothstein, 1991; Rossanese et al., 1999). The plasmids used for those manipulations were constructed with the aid of SnapGene software (Dotmatics) and the Saccharomyces Genome Database (Wong et al., 2023). Tagged Tmn1 was likely cleaved by Kex2 (Schimmöller et al.,

1998), but the two fragments of the protein are predicted to remain associated based on an AlphaFold Server simulation (Abramson et al., 2024).

Reagents

HaloTag ligands of JFX_{646} and JFX_{650} (Grimm et al., 2021), generously provided by Luke Lavis (Janelia Research Campus, Ashburn, VA), were dissolved in anhydrous DMSO (Invitrogen, catalog no. D12345) at a concentration of 1 mM, and single-use aliquots were stored at -80°C. These stock solutions were diluted 1000-fold to label cells at a final dye concentration of 1 µM. Rapamycin (LC Laboratories, catalog no. R-5000) was prepared as a 1 mg/ml solution in 90% ethanol, 10% Tween 20, and single-use aliquots were stored at -20°C. This stock solution was diluted 100-fold to treat cells at a final rapamycin concentration of 10 µg/ml. CK-666 (Sigma, catalog no. SML0006) was dissolved in anhydrous DMSO to a concentration of 50 mM, and single-use aliquots were stored at 4°C. This stock solution was diluted 500-fold to treat cells at a final CK-666 concentration of 100 µM.

HaloTag labeling

Labeling of HaloTag constructs was performed as previously described (Casler et al., 2021). HaloTag ligand of JFX_{646} or JFX_{650} was diluted by adding 1 µl of a 1 mM DMSO stock solution to 300 µl of NSD. The resulting solution was cleared of precipitate by spinning at 17,000xg (13,000 rpm) in a microcentrifuge for 5 min. Then the supernatant was added to 700 µl of mid-log phase yeast culture to give a final concentration of 1 µM dye, and the cells were incubated for 30-60 min at 23°C with shaking. For live cell imaging experiments, excess dye was removed by filtration and washing with a 0.22-µm syringe filter (Millipore; catalog no. SLGV004SL). The washed cells on

the filter were resuspended in NSD and adhered to a coverglass-bottom dish coated with concanavalin A (ConA) (Johnson and Glick, 2019). Confocal movies were then immediately acquired as described below.

Live cell fluorescence microscopy and analysis

For 4D confocal microscopy, yeast cells were attached to ConA-coated coverglass-bottom dishes that were filled with NSD (Johnson and Glick, 2019). Imaging was performed at 23°C using a Leica Stellaris confocal microscope equipped with a 1.4-NA/63x oil objective. Imaging of cell volumes was performed with 40-80 nm pixels, a 0.30 µm z-step interval, and 20-30 optical sections. z-stacks were obtained at intervals of 2 s.

Confocal movies of Golgi cisternal maturation events were deconvolved using Huygens software (SVI) and quantified with custom ImageJ plugins as previously described (Johnson and Glick, 2019), except that Huygens software was employed for time-based correction of photobleaching prior to deconvolution. Normalization and averaging of kinetic traces from maturing Golgi cisternae were accomplished using custom ImageJ plugins (Casler et al., 2021).

Electron microscopy

Quantifoil R2/2 grids on 200 copper mesh were prepared by glow discharging them. Log-phase yeast cultures in NSD, either mock-treated or treated for 5 min with 10 µg/ml rapamycin, were applied to the grids, which were then cryo-preserved using a Vitrobot Mark IV (Thermo Fisher). The sample chamber was kept at 16 °C and 100% humidity with a 60 s wait time, and grids were blotted for 11 s before being plunged into liquid ethane. Grids were stored under liquid nitrogen.

For cryo-FIB milling, grids were clipped in AutoGrid Rings (Thermo Fisher) with a cut-out to allow for shallower milling angles. Milling was performed on an Aquilos 2 dual-beam instrument (Thermo Fisher). Samples were sputter-coated in-column with platinum for 20 s at 10 Pa and 20 mA, and then they were coated with a layer of organometallic platinum for 35 s using the gas injection system within the instrument. Targets were identified and milled using Maps software and milled using AutoTEM software (Thermo Fisher). The automated protocol included milling of micro-expansion joints at 0.5 nA, followed by rough, fine, and very fine milling at 0.5, 0.3, and 0.1 nA, respectively, followed by two polishing steps at 50 and 30 pA respectively. The result was a lamella with a target thickness of 200-220 nm. Milled samples were stored under liquid nitrogen.

For cryo-ET and modeling, data were collected on a Titan Krios G3i at 300 kV (Thermo Fisher) with a Gatan K3 direct detection camera in CDS mode with the initial dose rate target on the detector between 7.5-8.5 electrons per pixel per second and with the Gatan BioQuantum-K3 energy slit width set to 20 eV. Tomography 5 software (Thermo Fisher) was used for collection. The tilt series was acquired with 3° steps in a bidirectional collection scheme (Hagen et al., 2017) beginning with a lamella pre-tilt of ±9° and extending to ±54°. The total dose for each tilt series was 120 e-/Å^2. Tilts were acquired with a pixel size of 4.45 Å and with 5 µm of defocus. Tilt series data were initially reconstructed using Tomo Live software (Thermo Fisher), which allowed for on-the-fly motion correction, alignment, and SIRT-reconstructed tomograms. We identified target features in the tomograms generated by Tomo Live, and those features were segmented using the 3dmod package in IMOD (Kremer et al., 1996). At least four lamellae from large budded cells were examined for each experimental condition.

To estimate the maximal distance between the plasma membrane beneath the septin ring and a captured vesicle, we used AlphaFold 3 (https://alphafoldserver.com) to simulate the structures of FKBP-tagged Shs1 and the FRB-tagged cytosolic portions of Kex2, Sys1, and Vrg4. Assuming that all of the flexible protein regions were maximally extended, the estimated lengths were 48 nm for Shs1-FKBP, 58 nm for Kex2-FRB, 35 nm for Sys1-FRB, and 18 nm for FRB-Vrg4.

Vesicle capture assay

Cells grown overnight to an OD_{600} of ~0.5 were stained with 1 µM JFX_{650} HaloTag ligand as described above, except that the final volume was 500 µl. After growth with shaking for 1 h at 23°C, either a 100-fold dilution of 90% ethanol, 10% Tween 20 was added as a control or rapamycin was added to a final concentration of 10 µg/ml, and the cells were incubated with shaking for an additional 5 min. Then fixation was performed by adding 250 µl of the culture while vortexing to 750 µl of 1.33-fold concentrated fixative to give final concentrations of 1% paraformaldehyde plus 0.1% glutaraldehyde (Electron Microscopy Sciences, diluted from freshly opened vials), 1 mM $MgCl_2$, 50 mM potassium phosphate, pH 6.5. After fixation on ice for 1 h, the cells were washed twice by centrifuging for 2 min at 1500xg (4000 rpm) and resuspending in 500 µl of phosphate-buffered saline (PBS). Finally, the cells were centrifuged once again and resuspended in 20 µl PBS. Within 30 h of fixation, the fixed cells were compressed under coverslips and imaged with a Leica Stellaris confocal microscope using a 1.4-NA/63x oil objective with 40 nm pixels, a 0.20 µm z-step interval, and 21 optical sections. Cells were chosen for analysis if they were a mother-daughter cell pair with a joined septin ring, and if Golgi cisternae were largely absent from the bud neck region as determined by viewing the Golgi marker channel. The

cell images were deconvolved using Huygens software (Johnson and Glick, 2019). A set of 20-30 cells was then analyzed by the two quantification methods described below.

For categorical quantification of vesicle capture, ImageJ was first used to process the deconvolved images of untreated and rapamycin-treated cells, as follows. The images were average projected, and the contrast of each fluorescence channel was enhanced by choosing a saturation percentage for the pixels (0.3% for the red channel, 0.5% for the green channel, or 0.4% for the blue channel). Then the channels were merged to generate composite images. To ensure objective quantification, the Blind Analysis Tools (v1.0) of ImageJ were employed to hide image identities. Image names were encrypted using basic mode of the File Name Encrypter, and the Analyse & Decide tool was used to assign each budding cell by visual criteria to one of the following categories: 1) No bud-neck localized cargo outside of cisternae, 2) Minority of bud-neck localized cargo outside of cisternae, or 3) Majority of bud-neck localized cargo outside of cisternae.

For numerical quantification of vesicle capture, a confocal image stack of a cell was processed with a custom ImageJ plugin termed "Quantify Overlap", available with source code from https://github.com/bsglicker/4D-Image-Analysis. With this plugin, the user chooses a region of interest (ROI), and the ROI measurements are summed for each image in the z-stack. As used here, the plugin creates a mask from the signal in the red channel and then compares the green signal within the mask to the total green signal in the ROI. The red channel mask can be modified by creating a second mask from the signal in the blue channel and then subtracting the blue channel mask from the red channel mask. Threshold levels are chosen empirically by the user for the red and blue channel masks, from a set of threshold options generated by a custom algorithm. For our purposes, the red threshold was set to the "Lower" level, and the blue threshold was set to the

lowest “Basement” level to create an extensive mask that included all visible Golgi signal. A cell was used for further analysis only if subtraction of the blue channel mask removed less than 65% of the area from the red channel mask.

Representative fluorescence images chosen for display in figures were scaled to the full RGB dynamic range, and then the pixel values were multiplied by 1.5 to ensure adequate visibility of both bright and faint structures.

AP-1/Ent5 dependency assay

To assess whether traffic of a Golgi protein was affected by loss of AP-1 and Ent5, 5-ml cultures of wild-type (*APL4 ENT5*) and mutant (*apl4*Δ *ent5*Δ) yeast strains expressing the GFP-tagged Golgi protein were grown overnight to an OD_{600} of ~0.5. Two 500-µl samples were placed in culture tubes. One sample received 1 µl of DMSO as a control, and the other sample received 1 µl of 50 mM CK-666. After 5-6 min, 250 µl of each sample were transferred to a ConA-coated coverglass-bottom dishes. After an additional 5 min, the medium was removed, and the cells were washed and then overlaid with NSD either lacking or containing CK-666 as appropriate. Confocal z-stacks were captured between 15-25 min after drug addition.

The z-stacks were deconvolved and average projected. For a given Golgi protein, the subsequent quantification was blinded with regard to control versus CK-666-treated samples using ImageJ as described above. Individual cells were visually examined and assigned to categories based on whether (a) most of the GFP-tagged protein was in Golgi-like puncta that were distributed throughout the cytoplasm, or (b) most of the GFP-tagged protein was concentrated at secretion sites (i.e., sites of polarized growth) with little signal in Golgi-like puncta elsewhere in the

cytoplasm, or (c) the GFP-tagged protein was distributed in a hybrid pattern between Golgi-like puncta and secretion sites.

In control experiments, the ability of CK-666 to inhibit endocytosis was confirmed by showing that this drug blocked internalization of the dye FM 4-64 (Casler et al., 2021).

COPI inactivation assay

Live yeast cells expressing Sec21-FRB and Rpl13A-FKBPx2 (Papanikou et al., 2015) plus mScarlet-tagged Sec7 and a GFP-tagged Golgi protein were prepared for confocal imaging by adhering them to ConA-coated coverglass-bottom dishes (Johnson and Glick, 2019). To inhibit COPI activity by anchoring to ribosomes, the medium was replaced with NSD containing 10 µg/ml rapamycin. For the control sample, the medium was replaced with NSD containing 0.9% ethanol, 0.1% Tween 20. Cells were imaged for 6 min starting 4 min after rapamycin addition. Maturation events beginning between 4 and 7 min after rapamycin addition were analyzed to determine the cisternal residence times of the GFP-tagged Golgi protein, where cisternal residence time was defined as the interval between the first and last visible GFP signals in a given cisterna.

Statistical analysis

For vesicle capture experiments, Microsoft Excel was used to compile all of the quantification data. Numerical quantification of mean percentages was performed by first excluding values from cells that exhibited high levels of cisternal interference at the bud neck, where a high level was defined as removal of at least 65% of the red septin mask by subtraction of the blue Golgi mask. The data were then transferred to Prism software (Dotmatics) for plotting and for computing

standard deviations. For cisternal residence time measurements, the data were directly transferred to Prism. The P values of scatter plots were calculated in Prism using Welch's t test.

Videos Associated with Chapter 3

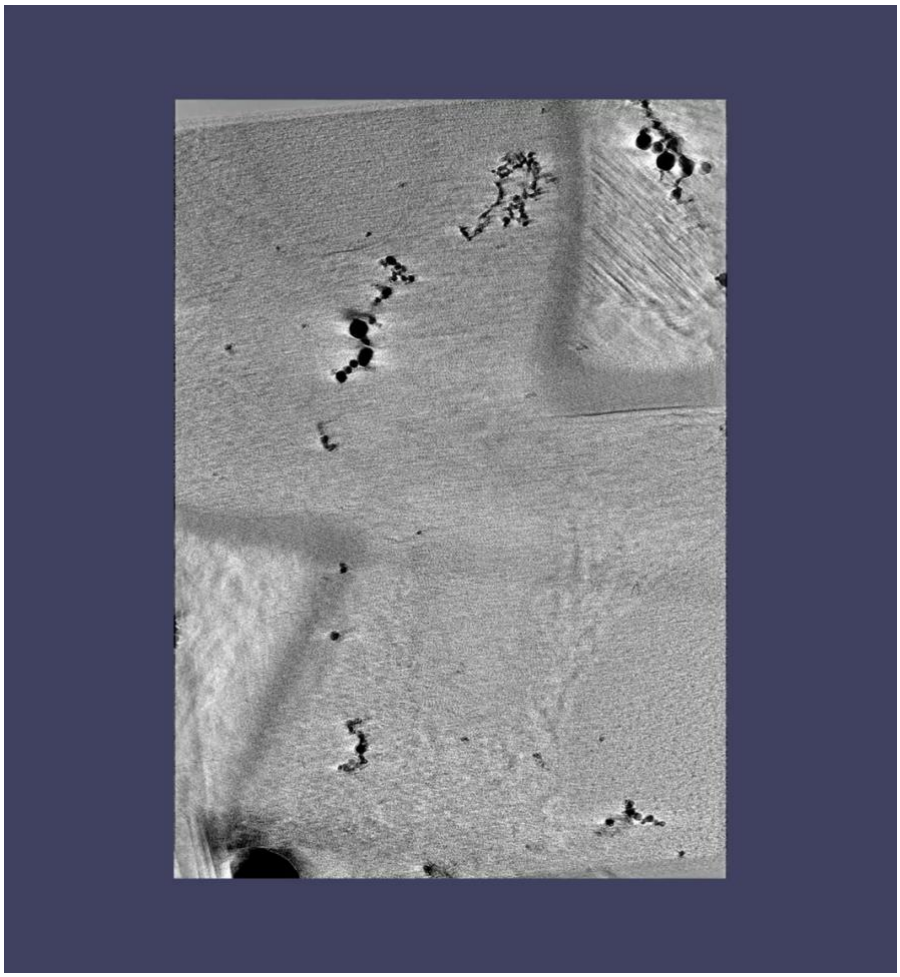

Video 3.1: **Tomographic sections and modeling of part of the bud neck region in a cell with Kex2-FRB-containing vesicles captured by an FKBP-tagged septin.** A log-phase culture of cells expressing Kex2-FRB and Shs1-FKBP was treated for 5 min with rapamycin prior to cryo-preservation and processing for cryo-ET. The first third of the video shows every fifth tomographic section of the SIRT-reconstructed tomogram. The second third of the video shows the same tomographic sections after contours were segmented to mark the cell cortex (yellow), a secretory vesicle (blue), putatively captured non-secretory vesicles (bright green), and other non-secretory vesicles (dull green). Also marked is a mitochondrion (cyan). The final third of the video shows a rotation of the tomographic model.

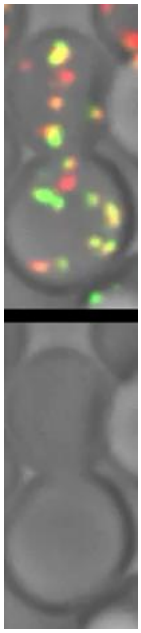

Video 3.2: **Representative 4D confocal movie of Sys1-HaloTag and Kex2-GFP.** 3D z-stacks for the individual time points were average projected. The upper row shows the complete projections, and the lower row shows edited projections that include only the cisterna that was tracked. Intervals between frames are 2 s. The overlaid numbers represent the time in seconds after the cisterna that was tracked first became detectable. See Figure 3.4A for further details.

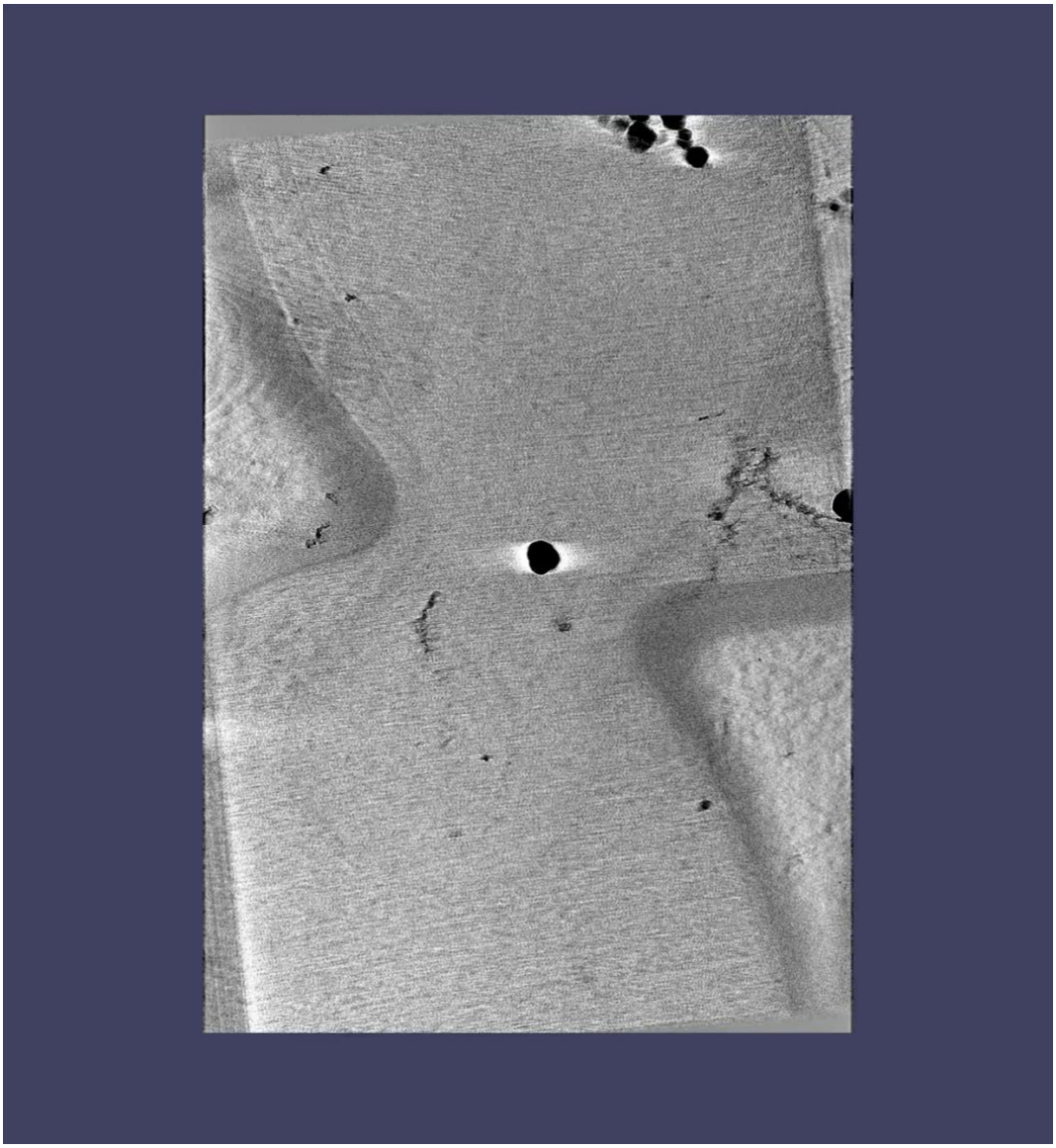

Video 3.3: **Tomographic sections and modeling of part of the bud neck region in a cell with Sys1-FRB-containing vesicles captured by an FKBP-tagged septin.** A log-phase culture of cells expressing Sys1-FRB and Shs1-FKBP was treated for 5 min with rapamycin prior to cryo-preservation and processing for cryo-ET. Further details are as in Video 3.1, except that the nuclear envelope is marked in magenta.

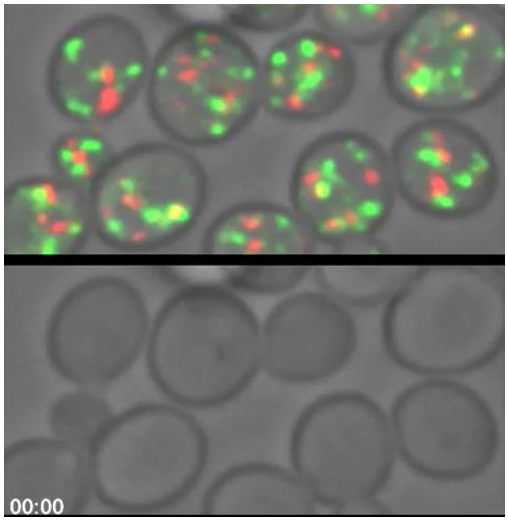

Video 3.4: **Representative 4D confocal movie of Vrg4 dynamics in Golgi cisternae with normal COPI activity.** Intervals between frames are 2 s. This movie corresponds to the "–Rap" trace at the top of Figure 3.10, with time zero in that trace corresponding to 2:22 for the numbering shown here. 3D z-stacks for the individual time points were average projected. The upper row shows the complete projections, and the lower row shows edited projections that include only the single cisterna that was tracked. Vrg4 is green and Sec7 is red.

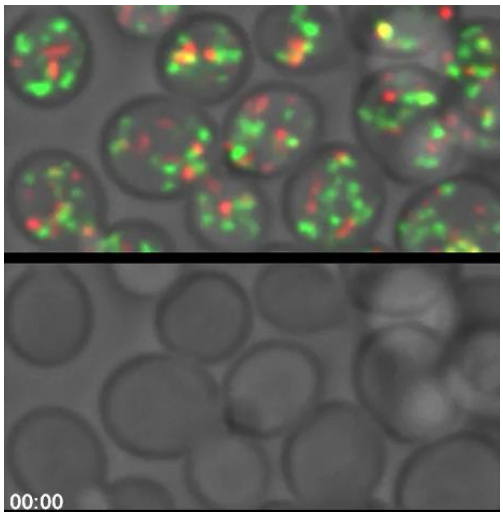

Video 3.5: **Representative 4D confocal movie of Vrg4 dynamics in Golgi cisternae with compromised COPI activity.** Time zero in this movie is 4 min after rapamycin addition, and intervals between frames are 2 s. This movie corresponds to the "+ Rap" trace at the top of Figure 3.10, with time zero in that trace corresponding to 2:56 for the numbering shown here. 3D z-stacks for the individual time points were average projected. The upper row shows the complete projections, and the lower row shows edited projections that include only the single cisterna that was tracked. Vrg4 is green and Sec7 is red.

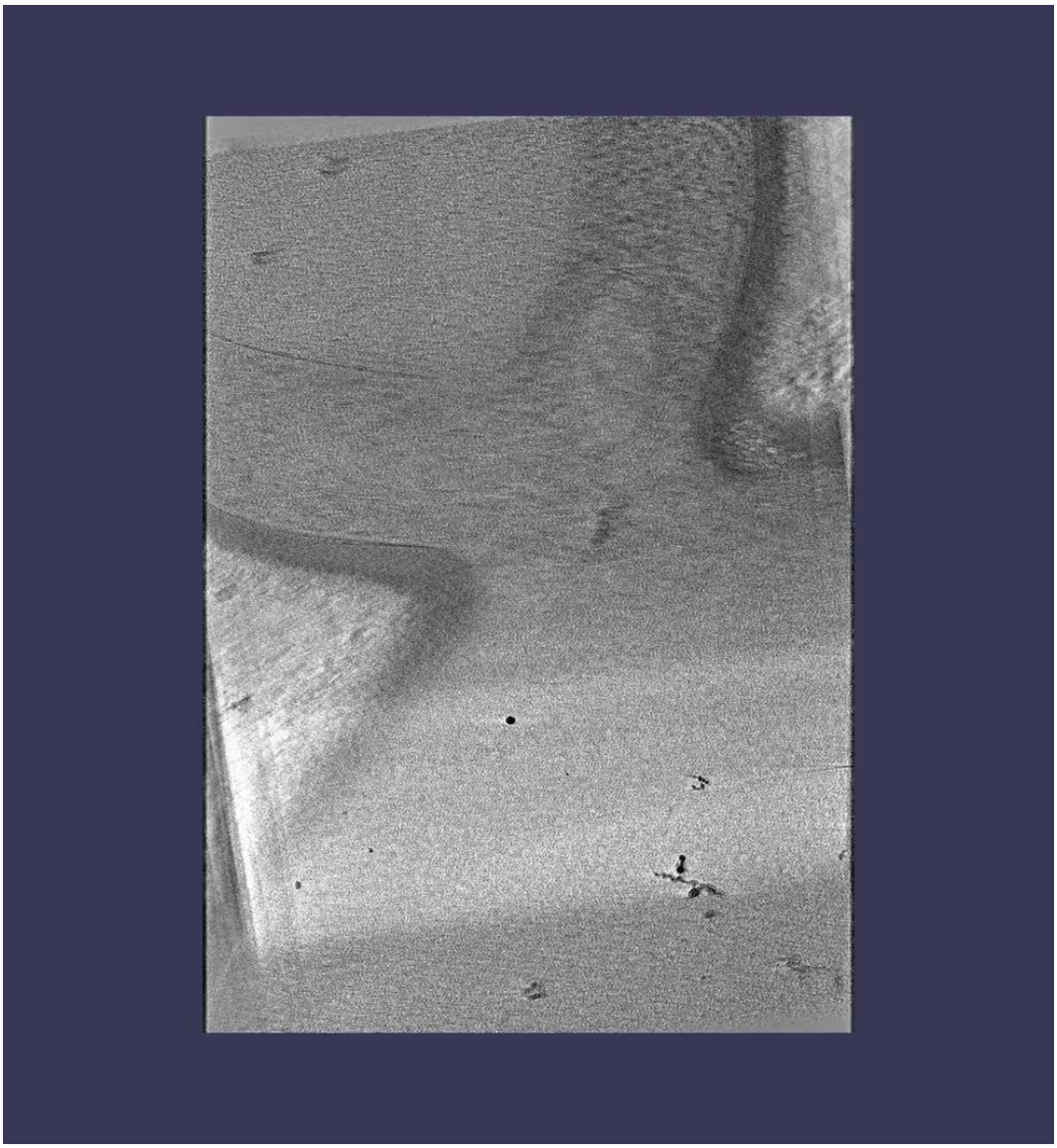

Video 3.6: **Tomographic sections and modeling of part of the bud neck region in a cell with FRB-Vrg4-containing vesicles captured by an FKBP-tagged septin.** A log-phase culture of cells expressing FRB-Vrg4 and Shs1-FKBP was treated for 5 min with rapamycin prior to cryo-preservation and processing for cryo-ET. Further details are as in Video 3.1.

CHAPTER 4

FUNCTIONAL ASSIGNMENT OF GOLGI-ASSOCIATED VESICLE TETHERS TO SPECIFIC MEMBRANE TRAFFIC PATHWAYS

Abstract

During the maturation of a Golgi cisterna, multiple vesicular transport pathways recycle resident Golgi proteins. Recycling vesicles are captured with the aid of Golgi-associated tethers that presumably act in specific pathways. To assign tethers to the different recycling pathways, we assessed tether localization and activity in the yeast *Saccharomyces cerevisiae* using kinetic and functional assays. These two approaches yielded mutually consistent results. Our analysis focused on coiled-coil golgin tethers and the multi-subunit tether GARP. We found that GARP and the golgin Imh1 capture *trans*-Golgi network (TGN) proteins that recycle within the Golgi. This involvement of GARP in intra-Golgi traffic had not previously been documented. Imh1 also captures TGN proteins that recycle from prevacuolar endosome compartments to the Golgi. The golgin Sgm1 exclusively captures vesicles that recycle in a COPI-dependent intra-Golgi pathway with intermediate kinetics, and the golgin Rud3 captures vesicles that recycle in a COPI-dependent intra-Golgi pathway with early kinetics. Our results advance the molecular characterization of membrane traffic pathways at the Golgi.

This is a near complete draft of a research article that will be submitted for publication with the following author list: Adam H. Krahn, Natalie Johnson, Jotham Austin II, and Benjamin S. Glick. I contributed to experimental design, performed most of the experimental analysis, and helped create the initial manuscript draft. N. Johnson contributed to experimental design and performed and analyzed the experiments in Figures 4.1A, 4.2A, 4.7A, 4.10A, and 4.10B (excluding Vrg4 vs Sgm1 kinetics). J. Austin II is performing and analyzing cryo-electron tomography experiments which will be added to complete the manuscript. B. S. Glick supervised the project, assisted with experimental design, coded the ImageJ plugins used for data analysis, created the figures, and revised the draft.

Introduction

A central player in the cellular endomembrane system is the Golgi apparatus (Mironov and Pavelka, 2008; Wilson et al., 2010). This organelle consists of multiple disk-shaped cisternae, which in many eukaryotes are organized into stacks. About 30% of newly synthesized proteins pass through the Golgi, where they encounter a series of processing enzymes that catalyze reactions such as proteolytic cleavage and modification of oligosaccharide side chains. In addition, the Golgi is the site of sphingolipid biosynthesis. Newly synthesized proteins and lipids in the Golgi are sorted at the TGN for delivery to other organelles or to the cell exterior.

A conserved feature of the Golgi is the concentration of each resident protein in a particular subset of the cisternae (Dunphy and Rothman, 1985; Rabouille et al., 1995; Tojima et al., 2024). The resulting polarized distribution of Golgi enzymes ensures that newly synthesized proteins and lipids are processed efficiently in the appropriate sequence. According to the cisternal maturation model, Golgi polarity is established by membrane traffic pathways that recycle resident Golgi proteins (Pantazopoulou and Glick, 2019). The core postulate of cisternal maturation is that Golgi cisternae form *de novo* from ER-derived membranes, then progressively mature while carrying the secretory cargoes forward, and then transform into secretory carriers at the TGN stage. Such events can be directly observed in the budding yeast *Saccharomyces cerevisiae*, which contains non-stacked Golgi cisternae that are individually resolvable by fluorescence microscopy (Wooding and Pelham, 1998; Losev et al., 2006; Matsuura-Tokita et al., 2006). Cisternal maturation is driven by the recycling of resident Golgi proteins from older to younger cisternae. These recycling pathways operate in a defined order, thereby delivering each resident Golgi protein to a cisterna at the appropriate stage of maturation. The distribution of a given resident Golgi protein is determined by the kinetics of its recycling pathway (Pantazopoulou and Glick, 2019).

To understand how this dynamic system works, we need to characterize the membrane traffic pathways that recycle resident Golgi proteins. There are four relevant questions: (1) How many distinct membrane traffic pathways contribute to cisternal maturation? (2) When does each pathway operate? (3) Which traffic machinery components mediate each pathway? (4) Which resident Golgi proteins follow each pathway? *S. cerevisiae* is uniquely powerful for addressing these questions. An initial step in the characterization of recycling pathways at the yeast Golgi is to track various Golgi proteins by 4D fluorescence microscopy to ascertain when they arrive and depart relative to one another (Losev et al., 2006; Papanikou et al., 2015; Tojima et al., 2024). Proteins with similar kinetic signatures are likely to follow the same recycling pathway. However, kinetic analysis is not enough to ascertain whether a given pair of resident Golgi proteins recycle together. We therefore devised a functional assay in which recycling vesicles carrying a tagged resident Golgi protein are captured at the yeast bud neck, and a second tagged resident Golgi protein is examined to see whether it is co-captured with the first protein (see Chapter 3). Based on a combination of kinetic and functional tests, we proposed that there are three intra-Golgi recycling pathways that operate at early, intermediate, and late stages of cisternal maturation, plus a fourth recycling pathway that carries certain resident Golgi proteins to prevacuolar endosome (PVE) compartments and back (Casler et al., 2021) (see Chapter 3 and Figure 4.14).

The next step is to identify the components that mediate each of these yeast Golgi recycling pathways. There is evidence that vesicles generated by the COPI coat retrieve proteins from the Golgi to the ER and also recycle proteins within the Golgi (Rabouille and Klumperman, 2005; Barlowe and Miller, 2013), and indeed, we found that the early and intermediate intra-Golgi recycling pathways depend on COPI (Papanikou et al., 2015) (see Chapter 3). In Chapter 3, those pathways were designated COPI(b) and COPI(b'), respectively (Figure 3.13). The late intra-Golgi

recycling pathway depends on the clathrin adaptors AP-1 and Ent5 (Casler et al., 2021; see Chapter3). For a given recycling pathway, the vesicles need to fuse with maturing cisternae at the appropriate time. The initial capture of incoming vesicles by Golgi cisternae is mediated by tethers, which come in two types: coiled-coil dimeric tethers termed golgins, and multi-subunit tethers that also help to promote the subsequent steps of vesicle fusion (Gillingham and Munro, 2019; Ungermann and Kümmel, 2019). Most of the Golgi tethers are peripheral membrane proteins that are recruited with the aid of small GTPases (Panic et al., 2003; Setty et al., 2003; Fridmann-Sirkis et al., 2004; Ishida and Bonifacino, 2019; Thomas and Fromme, 2020). Thus, the membrane traffic pathways that drive cisternal maturation are coordinated with GTPase cycles (Pantazopoulou and Glick, 2019; Thomas and Fromme, 2020). Pioneering studies of animal cells revealed that Golgi tethers function in specific recycling pathways (Wong and Munro, 2014; Gillingham and Munro, 2019), but the identities of those pathways have not been determined. The yeast system provides an opportunity to assign vesicle tethers to well-defined recycling pathways.

Here, we performed additional vesicle capture assays, and we extended that method by ectopically localizing individual Golgi tethers to the yeast bud neck and allowing those tethers to capture vesicles. The results, in combination with kinetic analysis, reinforced our earlier conclusions about Golgi-associated recycling pathways and enabled us to assign several tethers to particular pathways. This approach enriches our molecular understanding of how resident Golgi proteins are recycled and polarized by vesicular transport.

Results

Imh1 localizes to Golgi cisternae during a late stage of maturation and can be relocalized to the septin ring

We set out to characterize the golgin Imh1. The first step was kinetic analysis, because the time window during which Imh1 is present on maturing Golgi cisternae constrains the possible recycling pathways in which Imh1 could operate. Previous studies revealed that Imh1 is recruited to Golgi membranes by binding the activated form of the Arl1 GTPase (Panic et al., 2003; Setty et al., 2003). The activation and membrane association of Arl1 depend on the transmembrane protein Sys1, which initiates a biochemical cascade that promotes recruitment of Arl1 (Behnia et al., 2004; Setty et al., 2004). Sys1 arrives in the COPI-dependent intermediate intra-Golgi recycling pathway (see Chapter 3), and as expected, Imh1 began to arrive soon thereafter (Figure 4.1A). Under our experimental conditions, Imh1 persisted on a maturing cisterna for about a minute on average. Imh1 was present late in maturation when TGN proteins were arriving (Figure 4.1A and Figure 4.2A). Specifically, Imh1 was present throughout the arrival phases of Vps10, which recycles to the Golgi from PVE compartments (Marcusson et al., 1994; Cooper and Stevens, 1996), and Kex2, which follows the AP-1/Ent5-dependent intra-Golgi recycling pathway (Casler et al., 2021). Those two TGN proteins began to arrive at approximately the same time, although Vps10 accumulated more rapidly (Figure 4.1A). Thus, Imh1 is a candidate tether for more than one recycling pathway.

To analyze the vesicles tethered by Imh1, we took advantage of the rapamycin-inducible heterodimerization system to capture vesicles at the yeast bud neck (Haruki et al., 2008) (see Chapter 3). In brief, the septin subunit Shs1 was endogenously tagged with mScarlet plus two tandem copies of the FK506-binding protein (FKBP). Then Imh1 was endogenously tagged by

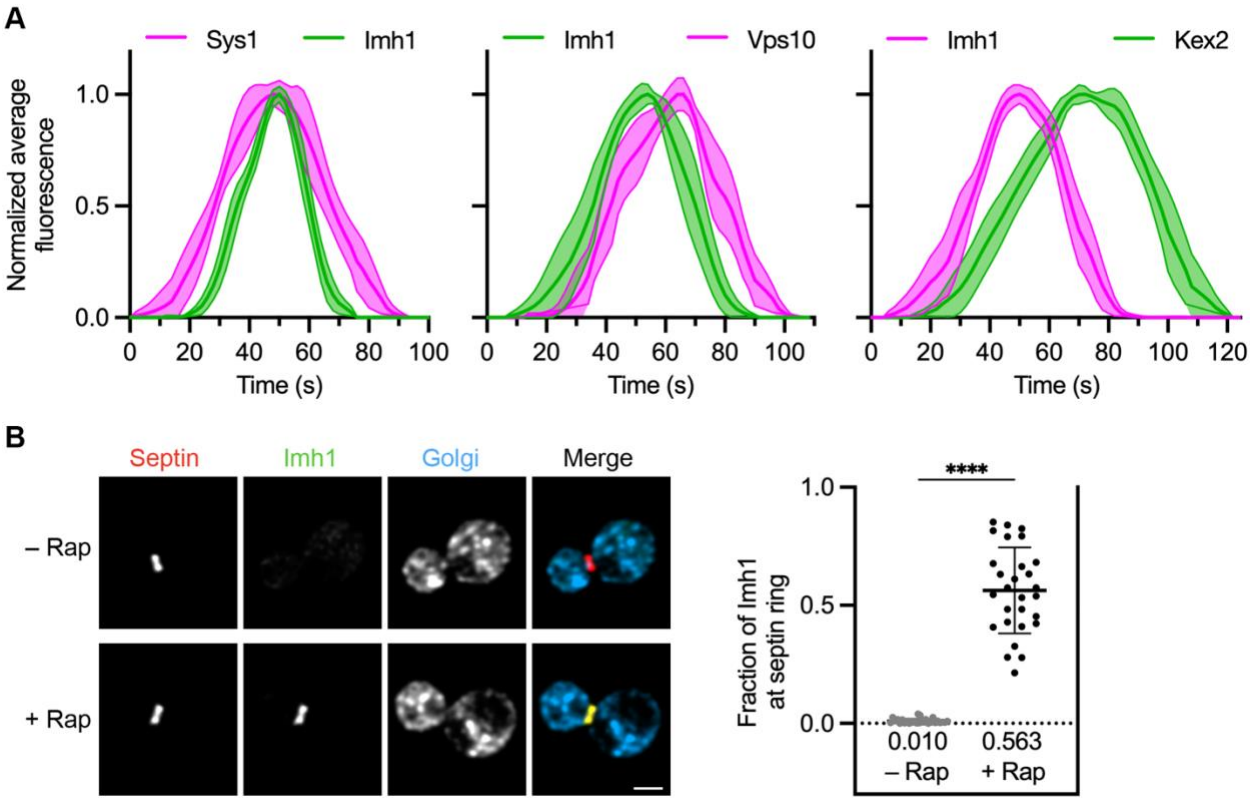

Figure 4.1: **Imh1 is present on maturing cisternae during the arrival of TGN proteins, and a mutant Imh1 can be ectopically localized to the bud neck. (A)** Golgi maturation kinetics of Imh1 relative to Sys1, Vps10, and Kex2. Green represents a GFP label and magenta represents a HaloTag label. Shown are normalized and averaged traces. **(B)** Capture by an FKBP-tagged septin (red) of a truncated Imh1 tagged with FRB-GFP (green). HaloTag-labeled Ric1 and Sec7 (blue) marked Golgi cisternae. Representative images are shown. Imh1-FRB-GFP levels at the bud neck were quantified by measuring the fraction of the total GFP signal present within a septin mask that had been modified by subtraction of a Golgi mask. The mean capture values with or without a 10-min treatment with rapamycin ("Rap") are represented by thick horizontal bars and are listed numerically below the plots, and the standard deviations are represented by thin horizontal bars. ****, significant at P value <0.0001.

replacing the C-terminal GRIP domain, which binds Arl1 to confer Golgi localization (Panic et al., 2003a; b), with GFP plus two copies of the FKBP-rapamycin-binding domain (FRB). The resulting Imh1 fusion protein was largely cytosolic, but it could be ectopically localized to the septin ring after addition of rapamycin (Figure 4.1B). This relocalization was quantified by measuring the fraction of the total cellular GFP signal that overlapped with the mScarlet-labeled septin ring. The results indicated that more than half of the FRB-tagged Imh1 molecules were at

the septin ring after a 10-min rapamycin treatment (Figure 4.1B). We conclude that Imh1 can be localized to the septin ring for tests of its vesicle tethering capability.

Ectopically localized Imh1 tethers vesicles containing TGN proteins

The next objective was to determine which resident Golgi proteins were in the vesicles tethered by Imh1. For this purpose, Imh1 was tagged with FRB alone, and GFP was appended to a transmembrane Golgi protein of interest. The idea was that if the GFP-tagged Golgi protein recycles in vesicles tethered by Imh1, then rapamycin should cause that Golgi protein to accumulate at the septin ring (Figure 4.3A). We treated with rapamycin for only 10 min to minimize perturbations to membrane traffic. To exclude any signal that might be contributed by Golgi cisternae at the bud neck, we generated a mask by linking HaloTag to two peripheral membrane proteins: Ric1, which resides at the early Golgi, and Sec7, which resides at the late Golgi (Figure 3.1B). HaloTag was conjugated to a far-red dye, and the resulting Golgi fluorescence pattern was subtracted from the GFP fluorescence signal (see Chapter 3 methods). The remaining GFP signal that overlapped with the septin fluorescence signal at the bud neck was assumed to represent captured vesicles. Because the HaloTag fluorescence from the labeled Golgi markers did not always fully overlap with the GFP fluorescence in the cisternae, we used a low threshold to create aggressive Golgi masks, thereby minimizing the background signal from cisternae at the expense of excluding some of the genuine vesicle signal.

Empirically, FRB-modified Imh1—and the other ectopically localized tethers described below—captured only a small fraction of the GFP signal from a tagged Golgi protein. A likely reason is that the number of tethering sites at the bud neck is limited by the number of septin molecules and/or the number of tether molecules and/or the number of vesicles that can be

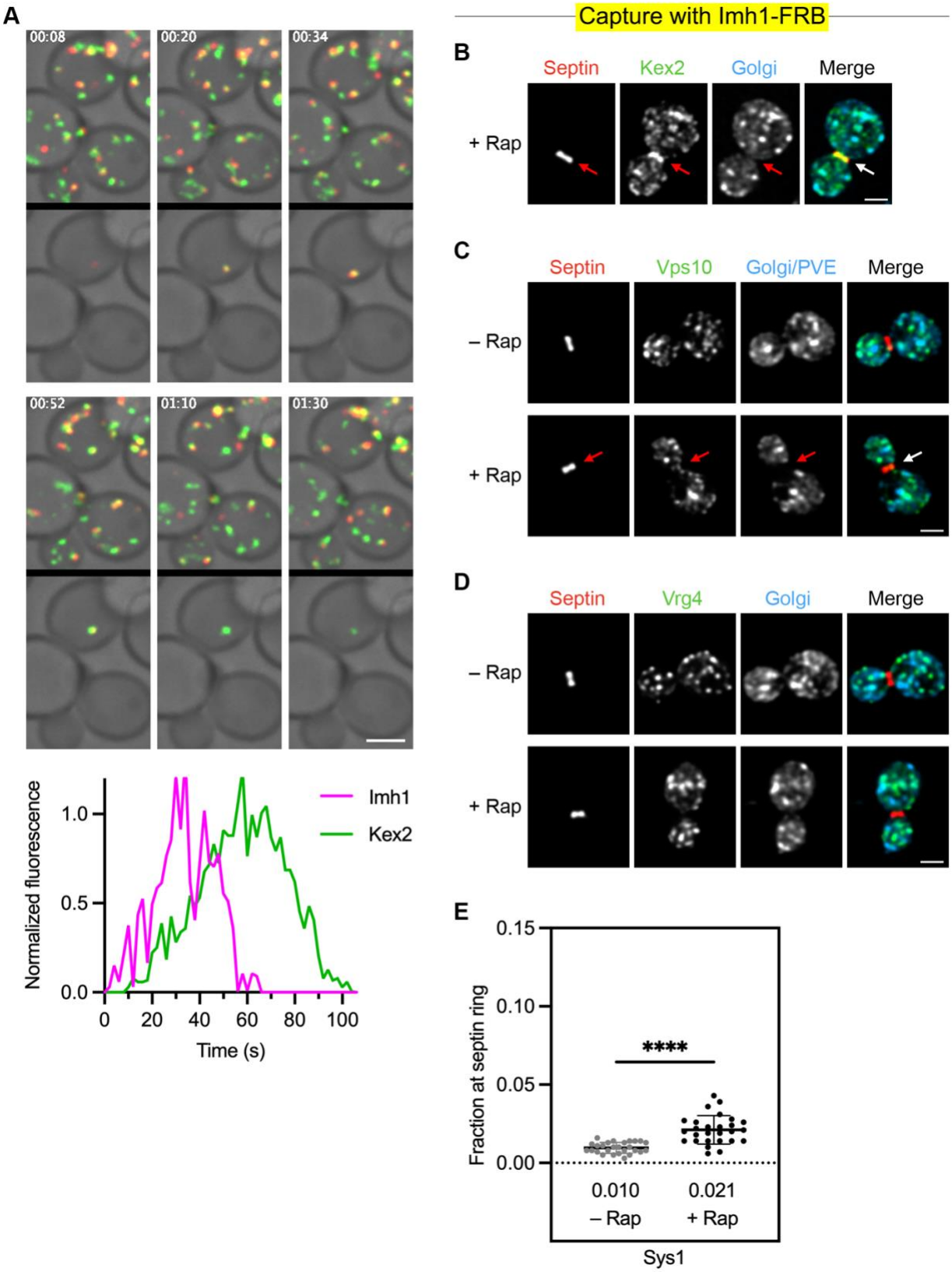

Figure 4.2: **Imh1 arrives at cisternae shortly before Kex2, and ectopically localized Imh1 captures Kex2, Vps10, and Sys1.** *(continued on next page)*

Figure 4.2: **(A)** Frames from a representative 4D confocal movie of HaloTag-Imh1 (red) and Kex2-GFP (green), and kinetic traces from an individual cisterna in the movie. Average projected z-stacks are depicted for the indicated time points from Video 4.1. The upper row shows the complete projections, and the lower row shows edited projections that include only the cisterna that was tracked. Scale bar, 2 μm. Plotted at the bottom are normalized fluorescence intensities for the cisterna tracked in the movie. **(B)** Example of exceptionally strong capture of Kex2 by ectopically localized Imh1 after a 10-min incubation with rapamycin ("Rap"). The analysis was performed as in Figure 4.3C, and this cell corresponds to the highest data point in the quantification from Figure 4.3C. **(C)** Capture of Vps10 by ectopically localized Imh1. Representative images show that localization of Imh1 to the FKBP-tagged septin (red) resulted in rapamycin-dependent accumulation of GFP-tagged Vps10 (green) at the bud neck. HaloTag-labeled Ric1, Sec7, and Vps8 (blue) marked Golgi cisternae and PVE compartments. These images accompany the quantification shown in Figure 4.3D. **(D)** Undetectable capture of Vrg4 by ectopically localized Imh1. Representative images show that localization of Imh1 to the FKBP-tagged septin (red) resulted in no rapamycin-dependent accumulation of GFP-tagged Vrg4 (green) at the bud neck. HaloTag-labeled Ric1 and Sec7 (blue) marked Golgi cisternae. These images accompany the quantification shown in Figure 4.3E. **(E)** Capture of Sys1 by ectopically localized Imh1. Fluorescence at the bud neck for GFP-tagged Sys1 was quantified with or without a 10-min rapamycin treatment as in Figure 4.1B. ****, significant at P value <0.0001.

physically accommodated at the septin ring. Another consideration is that vesicle tethering is reversible, so the capture affinity may be low, especially when a tether is outside its normal environment. Nevertheless, we could robustly detect significant signals by comparisons with the control incubations lacking rapamycin, and we could distinguish between relatively strong versus weak signals.

As a control to confirm that subtraction of the Golgi mask eliminated contaminating GFP signal from cisternae, we appended a GFP tag to Gga2, a clathrin adaptor found at the TGN (Daboussi et al., 2012; Casler and Glick, 2020). Gga2 is not thought to associate stably with vesicles after their fission, so ectopically localized Imh1 should not capture Gga2. Indeed, no vesicle-associated Gga2 was seen at the bud neck after rapamycin addition (Figure 4.3B).

The next step was to test whether ectopically localized Imh1 could capture Kex2 and Ste13, which are TGN proteins that recycle in the AP-1/Ent5 pathway (Casler et al., 2021) (see Chapter

3). Before rapamycin addition, when the mutated Imh1 was in the cytosol, Kex2 and Ste13 fluorescence at the Golgi was weaker than normal (data not shown), but clear Golgi patterns were still visible. After rapamycin addition, both Kex2 and Ste13 reproducibly accumulated at the bud neck (Figure 4.3C). Representative images are shown for Kex2. For these and other representative images, we chose examples with capture signals close to the mean values. As an illustration of an exceptionally strong signal, Figure 4.2B shows the cell with the highest value for capture of Kex2 by Imh1. These results indicate that Imh1 tethers vesicles from the AP-1/Ent5 pathway.

Ectopically localized Imh1 also captured Vps10 and Nhx1 (Figure 4.2C and Figure 4.3D), which are TGN proteins that recycle from PVE compartments (Cooper and Stevens, 1996; Kojima et al., 2012; Casler et al., 2021). As described below, follow-up experiments confirmed that Vps10 and Nhx1 follow a different recycling pathway than Kex2 and Ste13. These results indicate that Imh1 tethers vesicles from two pathways that deliver TGN proteins.

Additional experiments examined resident Golgi proteins that recycle in other pathways. Vrg4 follows the COPI-dependent early intra-Golgi recycling pathway, and it was not captured by ectopically localized Imh1 (Figure 4.2D and Figure 4.3E). However, weak capture was seen for Tmn1 (Figure 4.3E), which follows the COPI-dependent intermediate intra-Golgi recycling pathway. Based on this finding and previous data (Figure 3.7B), we speculate that a fraction of the Tmn1 molecules fail to enter their primary recycling pathway and then are retrieved by the downstream AP-1/Ent5 pathway. Sys1 is a special case. Even though Sys1 is functionally upstream of Imh1 and begins to arrive before Imh1, ectopically localized Imh1 showed moderately strong capture of Sys1 (Figure 4.2E). Our previous work revealed that a substantial fraction of the Sys1 molecules partition into the AP-1/Ent5 pathway (see Chapter 3), so the

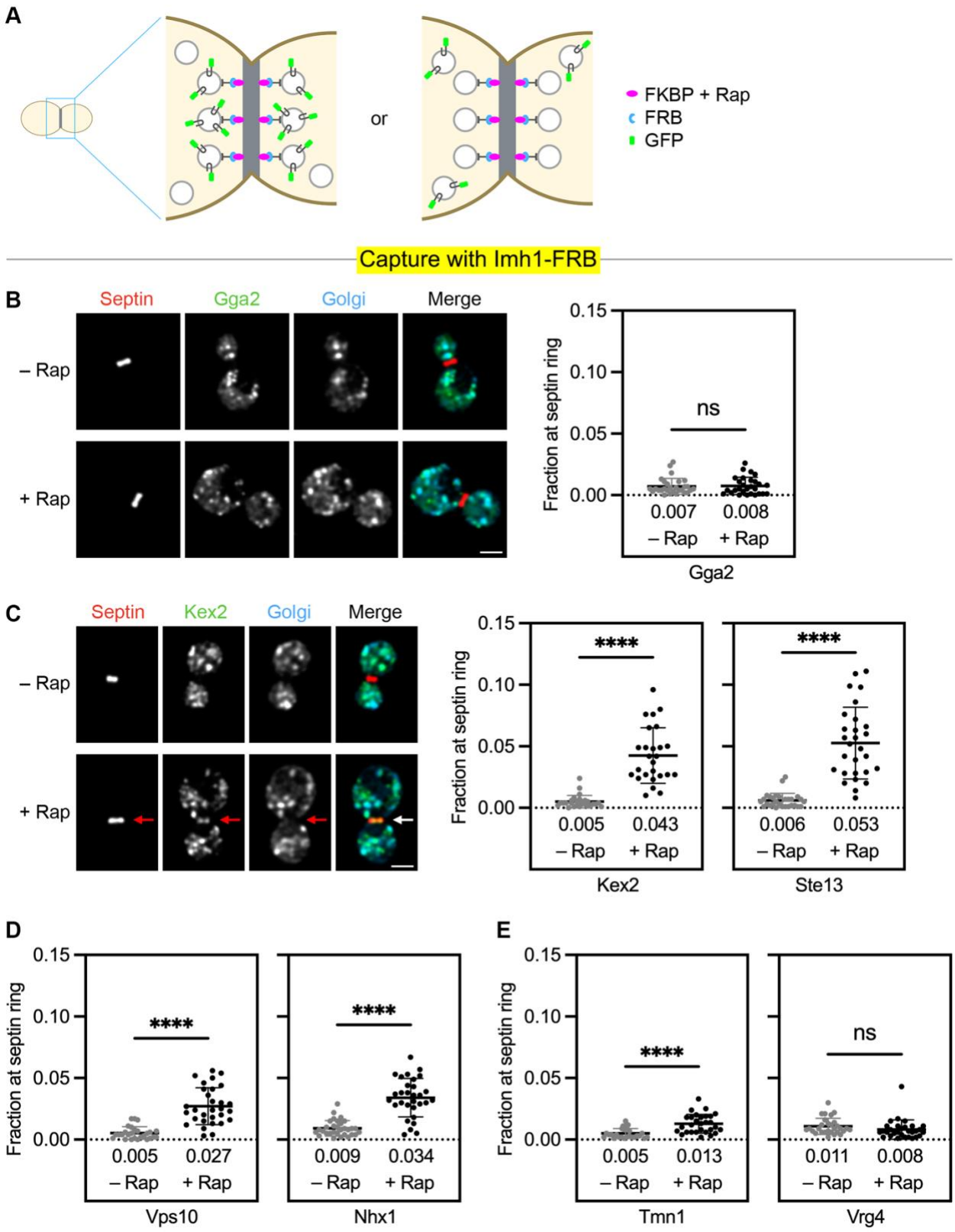

Figure 4.3: **Ectopically localized Imh1 captures two classes of TGN proteins.** *(continued on next page)*

Figure 4.3: For the statistical analyses: ****, significant at P value <0.0001; ns, not significant. **(A)** Diagram of the vesicle capture assay. A septin at the bud neck is tagged with FKBP (magenta), and a Golgi-associated tether is tagged with FRB (blue) to achieve rapamycin-dependent localization of the tether to the bud neck. Meanwhile, a resident Golgi protein is tagged with GFP (green). The ectopically localized tether will capture transport vesicles. If the GFP-tagged Golgi protein travels in vesicles captured by the tether, then green fluorescence will be visible at the bud neck (left). Otherwise, no green fluorescence will be visible at the bud neck (right). **(B)** Control experiment showing that ectopic localization of Imh1 to the FKBP-tagged septin (red) did not result in detectable fluorescence at the bud neck from TGN cisternae marked by GFP-tagged Gga2 (green). HaloTag-labeled Ric1 and Sec7 (blue) marked Golgi cisternae. Representative images are shown. Gga2 fluorescence at the bud neck was quantified with or without a 10-min treatment with rapamycin ("Rap") as in Figure 4.1B. **(C)** Strong capture of AP-1/Ent5 cargoes by ectopically localized Imh1. Representative images show that localization of Imh1 to the FKBP-tagged septin (red) resulted in rapamycin-dependent accumulation of GFP-tagged Kex2 (green) at the bud neck. HaloTag-labeled Ric1 and Sec7 (blue) marked Golgi cisternae. Arrows indicate non-Golgi signal at the bud neck. Kex2 fluorescence at the bud neck was quantified with or without a 10-min rapamycin treatment as in Figure 4.1B. A similar quantification was performed for GFP-tagged Ste13. **(D)** Strong capture of PVE-derived cargoes by ectopically localized Imh1. Fluorescence at the bud neck for GFP-tagged Vps10 or Nhx1 was quantified with or without a 10-min rapamycin treatment as in Figure 4.1B. **(E)** Weak or undetectable capture of COPI cargoes by ectopically localized Imh1. The experiment was performed as in (D) but with GFP-tagged Tmn1 or Vrg4.

AP-1/Ent5 vesicles captured by Imh1 are expected to contain Sys1. Thus, the various results obtained with kinetic analysis and vesicle capture assays are compatible with a coherent interpretation about the tethering specificity of Imh1.

Two classes of TGN proteins follow distinct recycling pathways

After seeing that Imh1 captured all four of the TGN proteins examined, we sought to verify that Kex2 and Ste13 follow a different recycling pathway than Vps10 and Nhx1. This point is important because Kex2 and Ste13 were long thought to recycle together with Vps10 between PVE compartments and the Golgi (Voos and Stevens, 1998; Bowers and Stevens, 2005; Bean et al., 2017). Instead, our data suggest that occasional missorting of Kex2 and Ste13 to PVE compartments had previously diverted attention from the primary recycling route of these proteins within the Golgi in the AP-1/Ent5 pathway. A key piece of evidence for two distinct pathways is

that knocking out AP-1 plus Ent5 perturbs the traffic of Kex2 and Ste13 but not of Vps10 or Nhx1 (Casler et al., 2021). Here, we sought additional ways to characterize the different pathways.

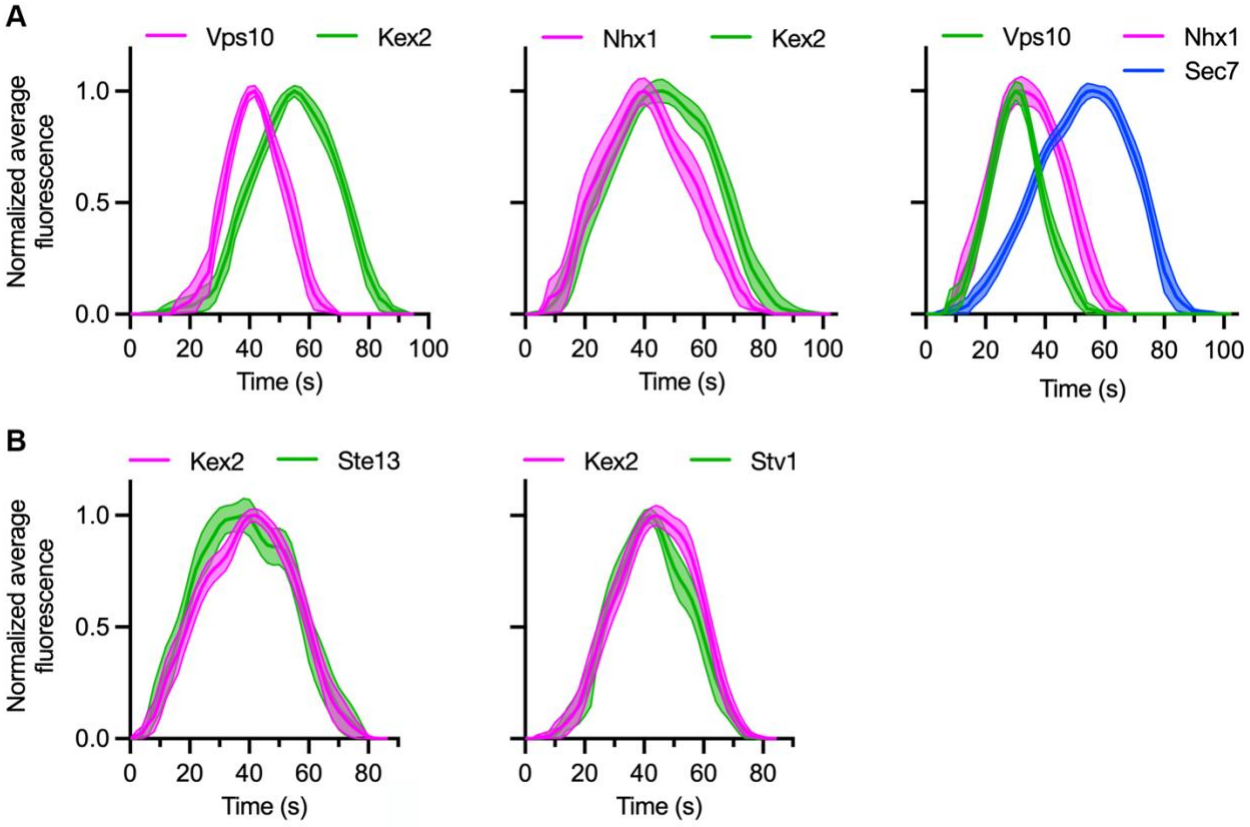

Figure 4.4: **Kinetic analysis distinguishes two classes of TGN proteins.** Green represents a GFP label, magenta represents a HaloTag label, and blue represents an mScarlet label. Shown are normalized and averaged traces. **(A)** Golgi maturation kinetics of Vps10 and Nhx1 relative to Kex2 and relative to each other. Because Vps10 and Nhx1 are present both in the TGN and in PVE compartments, the comparison between these two proteins also included Sec7 to mark TGN structures. **(B)** Golgi maturation kinetics of Kex2 relative to the other AP-1/Ent5 cargoes Ste13 and Stv1.

One approach was to compare kinetic signatures. All four TGN proteins began to arrive at about the same time, slightly before the TGN marker Sec7 (Day et al., 2018; Casler et al., 2021) (Figure 4.4A). However, the departure times varied. Vps10 departed much earlier than Kex2, and Nhx1 departed somewhat earlier than Kex2 (Figure 4.4A). By contrast, Ste13 departed synchronously with Kex2 (Figure 4.4B). This latter phenomenon may be general because Stv1, another cargo of the AP-1/Ent5 pathway (Casler et al., 2021), also departed synchronously with

Kex2 (Figure 4.4B). Thus, Vps10 and Nhx1, which localize to both PVE compartments and the Golgi (Kojima et al., 2012; Chi et al., 2014; Day et al., 2018), depart from maturing cisternae earlier than Kex2 and Ste13 and Stv1, which localize almost exclusively to the Golgi (Day et al., 2018; Casler et al., 2021), consistent with the existence of separate traffic pathways.

A second approach employed our original vesicle co-capture assay system (see Chapter 3) to determine which proteins travel together with Vps10. When Vps10 was tagged with both FRB and GFP, an average of 15% of the fusion protein could be captured at the bud neck after 5 min of rapamycin treatment (Figure 4.5A). For this experiment, the Golgi mask was extended by appending a HaloTag label to Vps8, which marks PVE compartments (Arlt et al., 2015; Day et al., 2018). The Golgi/PVE mask was subtracted before making the measurements, so the Vps10 fluorescence signal at the bud neck presumably represented captured vesicles that were traveling between PVE compartments and the Golgi. The GFP-tagged PVE marker Hse1 (Bilodeau et al., 2003; Henne et al., 2011) showed only very weak rapamycin-dependent co-capture with Vps10 (Figure 4.5B and Figure 4.6A), indicating that the Golgi/PVE mask removed most of the fluorescence signal from PVE compartments at the bud neck. As expected, Nhx1 was efficiently co-captured with Vps10 (Figure 4.5C), indicating that the two proteins travel in the same vesicles. Ste13 was not detectably co-captured (Figure 4.5C). Kex2 showed some co-capture with Vps10, consistent with low-level missorting of Kex2 to PVE compartments, but this signal was much weaker than the Nhx1 signal (Figure 4.5C). These results support the conclusion that the primary recycling pathway of Kex2 and Ste13 differs from that of Vps10 and Nhx1.

We also performed a complementary experiment by tagging Kex2 with FRB (Figure 4.6B). As previously shown (see Chapter 3), Ste13 was co-captured with Kex2. Vps10 and Nhx1 were also co-captured, although less strongly. We suspect that the signals from Vps10 and Nhx1

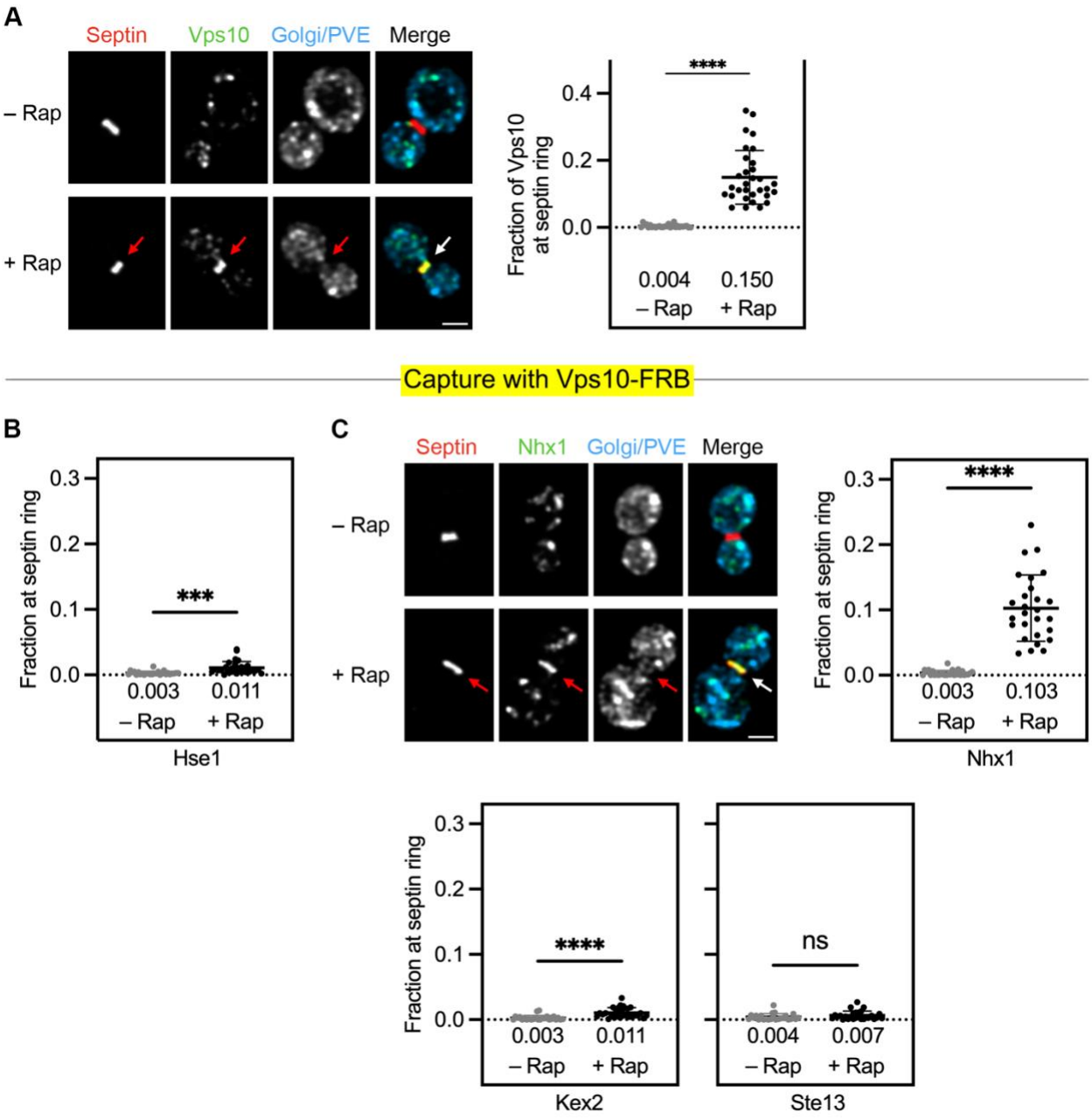

Figure 4.5: **A vesicle capture assay distinguishes two classes of TGN proteins.** For the statistical analyses: ****, significant at P value <0.0001; ***, significant at P value = 0.0001; ns, not significant. **(A)** Rapamycin-dependent capture by an FKBP-tagged septin (red) of Vps10-FRB-GFP (green). HaloTag-labeled Ric1, Sec7, and Vps8 (blue) marked Golgi cisternae and PVE compartments. Representative images are shown. Arrows indicate non-Golgi and non-PVE signal at the bud neck after treatment for 5 min with rapamycin ("Rap"). Capture of Vps10-FRB-GFP at the bud neck was quantified by measuring the fraction of the total Vps10 signal present within a septin mask that had been modified by subtraction of a Golgi/PVE mask. The mean capture values are displayed as thick horizontal bars and are listed numerically below the plots, and the standard deviations are displayed as thin horizontal bars. *(continued on next page)*

Figure 4.5: **(B)** Control experiment showing that capture of Vps10-FRB-containing vesicles at the bud neck resulted in minimal co-capture of PVE compartments marked by GFP-tagged Hse1. Quantification was performed as in (A). **(C)** Rapamycin-dependent capture with Vps10-FRB of GFP-tagged Nhx1, and weak or undetectable capture of GFP-tagged Kex2 or Ste13. Quantification was performed as in (A). Representative images are shown for Nhx1. Arrows indicate non-Golgi and non-PVE signal at the bud neck.

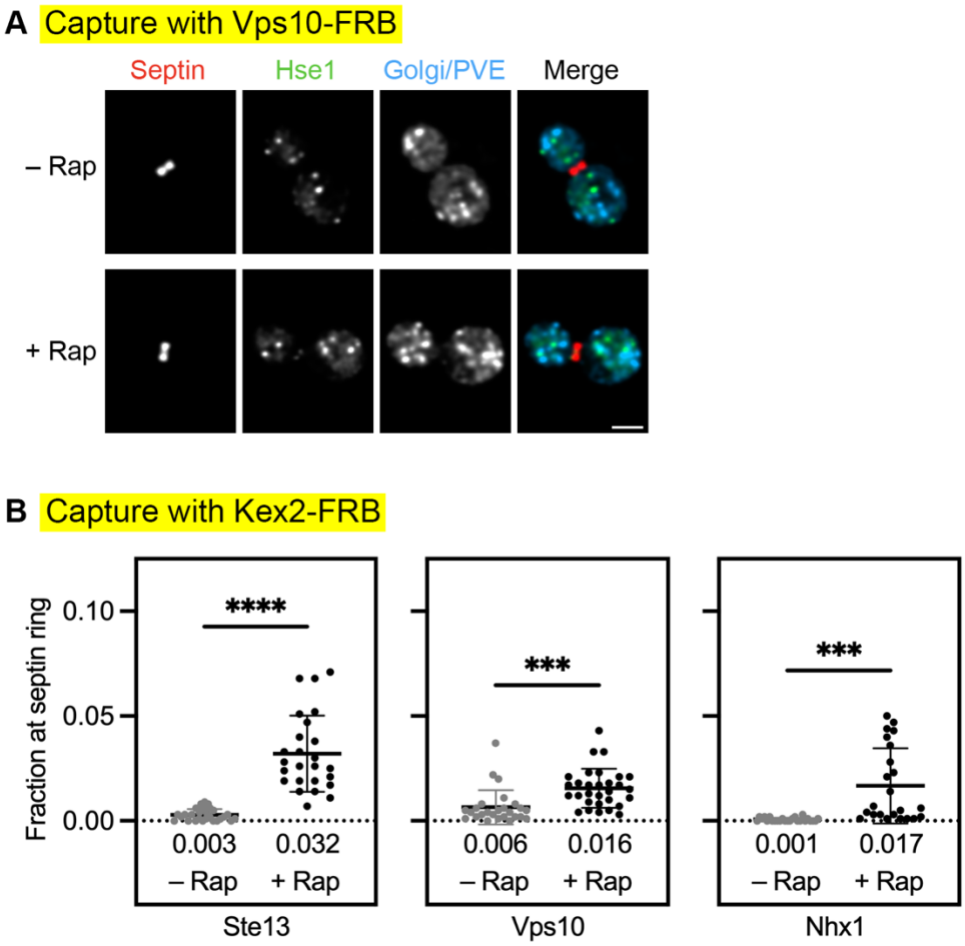

Figure 4.6: **Vesicle capture assays can be used to examine the traffic pathways of TGN proteins. (A)** Control experiment confirming minimal co-capture of the PVE marker Hse1 when Vps10-FRB is captured at the bud neck. Representative images show that capture of Vps10-FRB-containing vesicles at the FKBP-tagged septin (red) resulted in very little rapamycin-dependent accumulation of GFP-tagged Hse1 (green) at the bud neck. HaloTag-labeled Ric1, Sec7, and Vps8 (blue) marked Golgi cisternae and PVE compartments. These images accompany the quantification shown in Figure 4.5B. **(B)** Weak co-capture of Vps10 and Nhx1 when Kex2-FRB is captured at the bud neck. As a control, Ste13 shows strong co-capture. Fluorescence at the bud neck was quantified with or without a 5-min rapamycin treatment as in Figure 4.1B. ****, significant at P value <0.0001; ***, significant at P value = 0.0003 (Vps10 and Nhx1).

reflect occasional missorting of Kex2 to PVE compartments followed by retrieval. Evidence for such missorting includes weak Kex2 signals in the PVE compartments of wild-type cells (Day et al., 2018) and strong Kex2 signals in the PVE compartments of mutant cells defective in retrieving Kex2 to the Golgi (Nothwehr and Hindes, 1997; Voos and Stevens, 1998). Even a single Kex2 molecule in a vesicle traveling between a PVE compartment and the Golgi could lead to rapamycin-dependent capture at the bud neck. This argument illustrates that individual vesicle capture assays have limitations, which we have tried to address by evaluating the data in a holistic way.

GARP localizes to Golgi cisternae during a late stage of maturation and can be relocalized to the septin ring

The Golgi-associated retrograde protein (GARP) complex is a multi-subunit tether that localizes to the late Golgi (Bonifacino and Hierro, 2011; Khakurel et al., 2021), but the precise time when GARP is present during cisternal maturation has not been reported. GARP is a heterotetramer composed of the proteins Vps51, Vps52, Vps53, and Vps54 (Siniossoglou and Pelham, 2002; Conibear et al., 2003; Reggiori et al., 2003). We kinetically mapped Vps52 relative to Vps10, Kex2, and Imh1 (Figure 4.7A). GARP arrived and departed almost synchronously with Vps10, although GARP initially accumulated somewhat more slowly than Vps10. GARP began to arrive at about the same time as Kex2 and accumulated slightly faster than Kex2. GARP departed earlier than Kex2, but it was present throughout the arrival phase of Kex2. Finally, GARP arrived and departed about 10-20 sec after Imh1, resulting in partial kinetic overlap between these two tethers.

To achieve ectopic localization of GARP, Vps52 was tagged with FRB. Relocalization of GARP was assayed by tagging Vps54 with GFP. Treatment with rapamycin for 10 min eliminated

most of the punctate Golgi signal and redistributed GARP to the bud neck (Figure 4.7B). We conclude that the GARP complex can be concentrated at the septin ring for tests of its putative vesicle tethering activity.

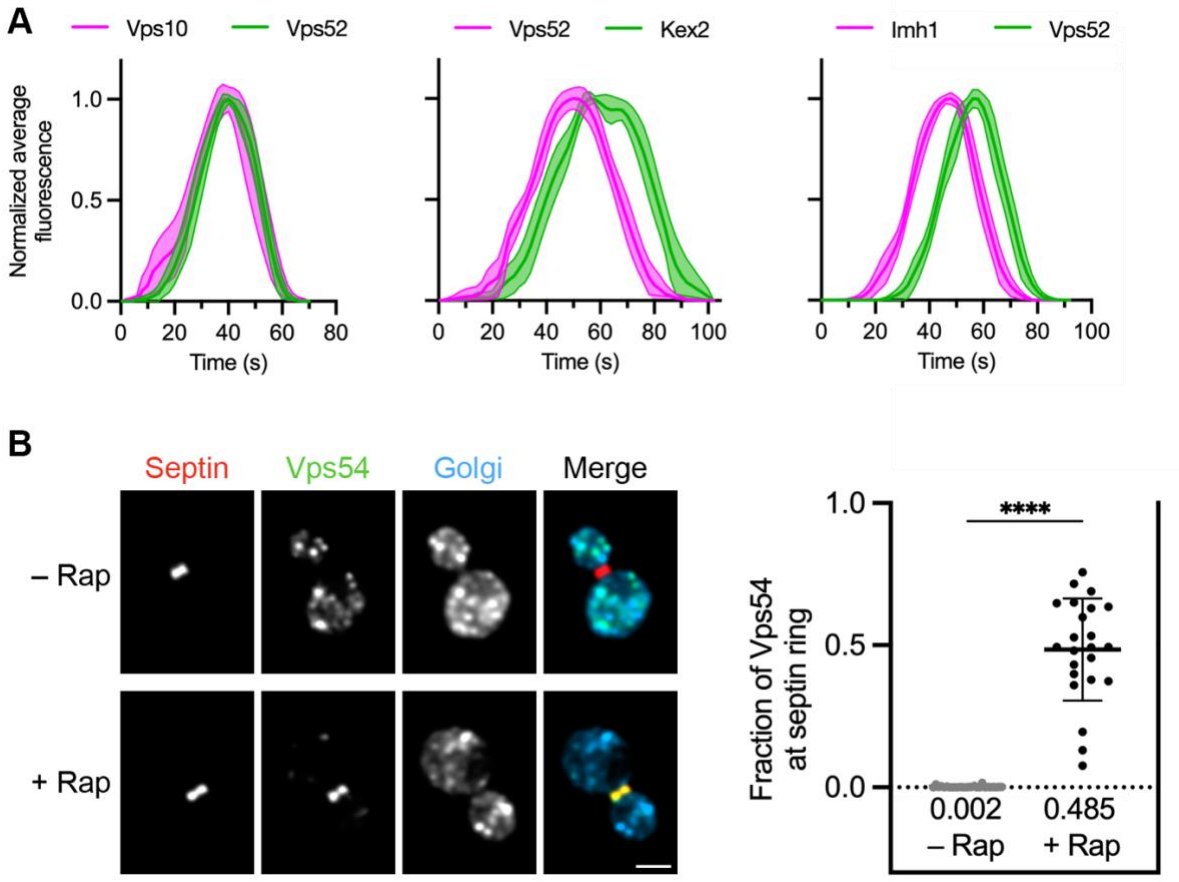

Figure 4.7: **GARP is present on cisternae during a late stage of maturation, and FRB-tagged GARP can be ectopically localized to the bud neck. (A)** Golgi maturation kinetics of the GARP subunit Vps52 relative to Vps10, Kex2, and Imh1. Green represents a GFP label and magenta represents a HaloTag label. Shown are normalized and averaged traces. **(B)** Capture by an FKBP-tagged septin (red) of a GARP complex containing Vps52-FRB and Vps54-GFP (green). HaloTag-labeled Ric1 and Sec7 (blue) marked Golgi cisternae. Representative images are shown. Vps54-GFP levels at the bud neck were quantified as in Figure 4.1B. ****, significant at P value <0.0001.

Ectopically localized GARP tethers vesicles carrying cargoes of the AP-1/Ent5 pathway

The next question was whether GARP could tether one or both of the vesicle types that recycle TGN proteins. A control experiment showed no rapamycin-dependent capture of Gga2 by GARP (Figure 4.8A), confirming that the Golgi mask eliminated contaminating signal from cisternae. GARP captured significant amounts of Kex2 and Ste13, which follow the AP-1/Ent5 pathway (Figure 4.9A). Because GARP is likely to capture endocytic vesicles that fuse directly with the Golgi, and because Kex2 contains an endocytosis signal (Tan et al., 1996), we wondered if capture of Kex2 by GARP might reflect occasional exocytosis followed by endocytosis. This explanation is unlikely because capture of Kex2 by GARP was unaffected by CK-666, which potently inhibits endocytosis (Burke et al., 2014; Casler et al., 2021) (Figure 4.9A). We infer that GARP can bind to AP-1/Ent5 vesicles.

The mechanism that recruits GARP to the Golgi is poorly understood, and we considered the possibility that soluble GARP binds in the cytosol to AP-1/Ent5 vesicles, which then deliver GARP to Golgi cisternae. This idea was tested by using a vesicle co-capture assay with Kex2-FRB to determine if GARP would bind to Kex2-containing vesicles at the septin ring. No such binding was seen (Figure 4.8B), suggesting that GARP is recruited to Golgi membranes rather than to vesicles. The most likely interpretation is that GARP normally associates with Golgi membranes and then tethers AP-1/Ent5 vesicles.

With Vps10 and Nhx1, which travel from PVE compartments to the Golgi, capture by GARP was minimal (Figure 4.9B and Figure 4.8C). This result is at odds with previous interpretations about the function of yeast GARP (Conibear and Stevens, 2000; Conibear et al., 2003; Bonifacino and Hierro, 2011). However, those studies were based on analysis of GARP

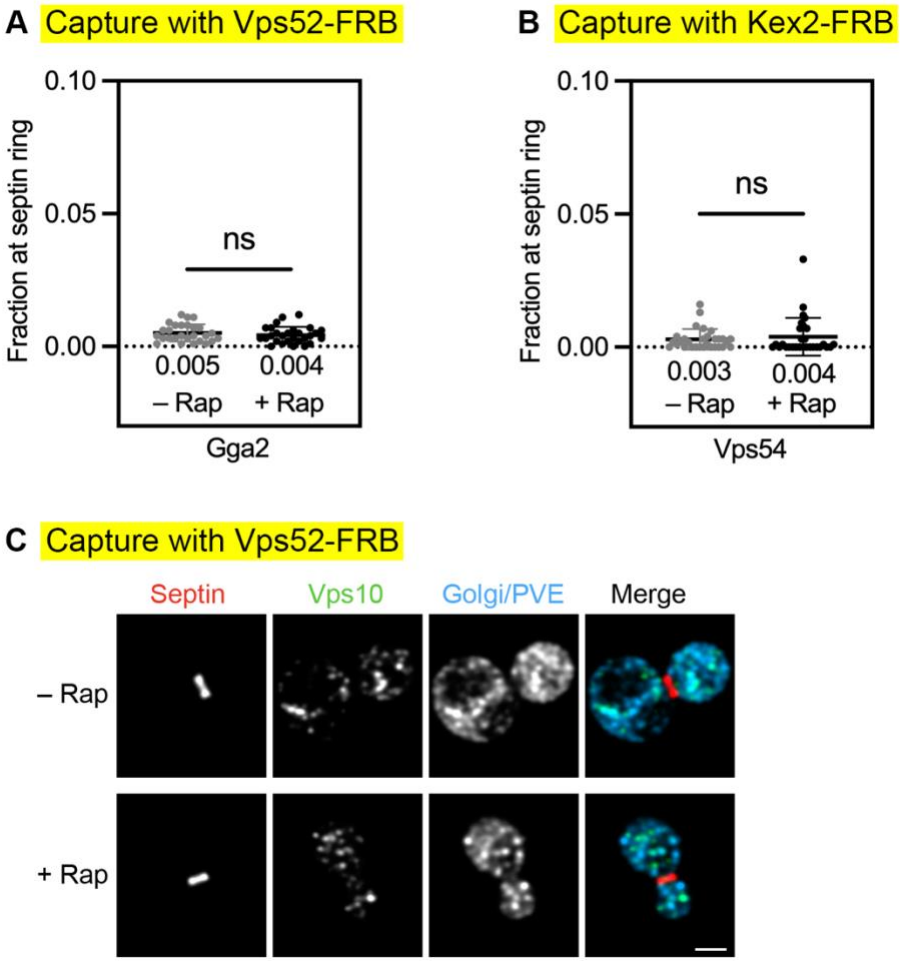

Figure 4.8: **Control experiments confirm the specificity of capture by ectopically localized GARP. (A)** Control experiment showing that ectopic localization of GARP (Vps52-FRB) to the FKBP-tagged septin did not result in detectable fluorescence at the bud neck from TGN cisternae marked by Gga2. Fluorescence of GFP-tagged Gga2 at the bud neck was quantified with or without a 10-min treatment with rapamycin ("Rap") as in Figure 4.1B. ns, not significant. **(B)** Control experiment showing that capture of vesicles containing Kex2-FRB did not result in co-capture of the GARP subunit Vps54. Fluorescence of GFP-tagged Vps54 at the bud neck was quantified with or without a 5-min rapamycin treatment as in Figure 4.1B. ns, not significant. **(C)** Undetectable capture of Vps10 by ectopically localized GARP. Representative images show that localization of GARP (Vps52-FRB) to the FKBP-tagged septin (red) resulted in no rapamycin-dependent accumulation of GFP-tagged Vps10 (green) at the bud neck. HaloTag-labeled Ric1, Sec7, and Vps8 (blue) marked Golgi cisternae and PVE compartments. These images accompany the quantification shown in Figure 4.9B.

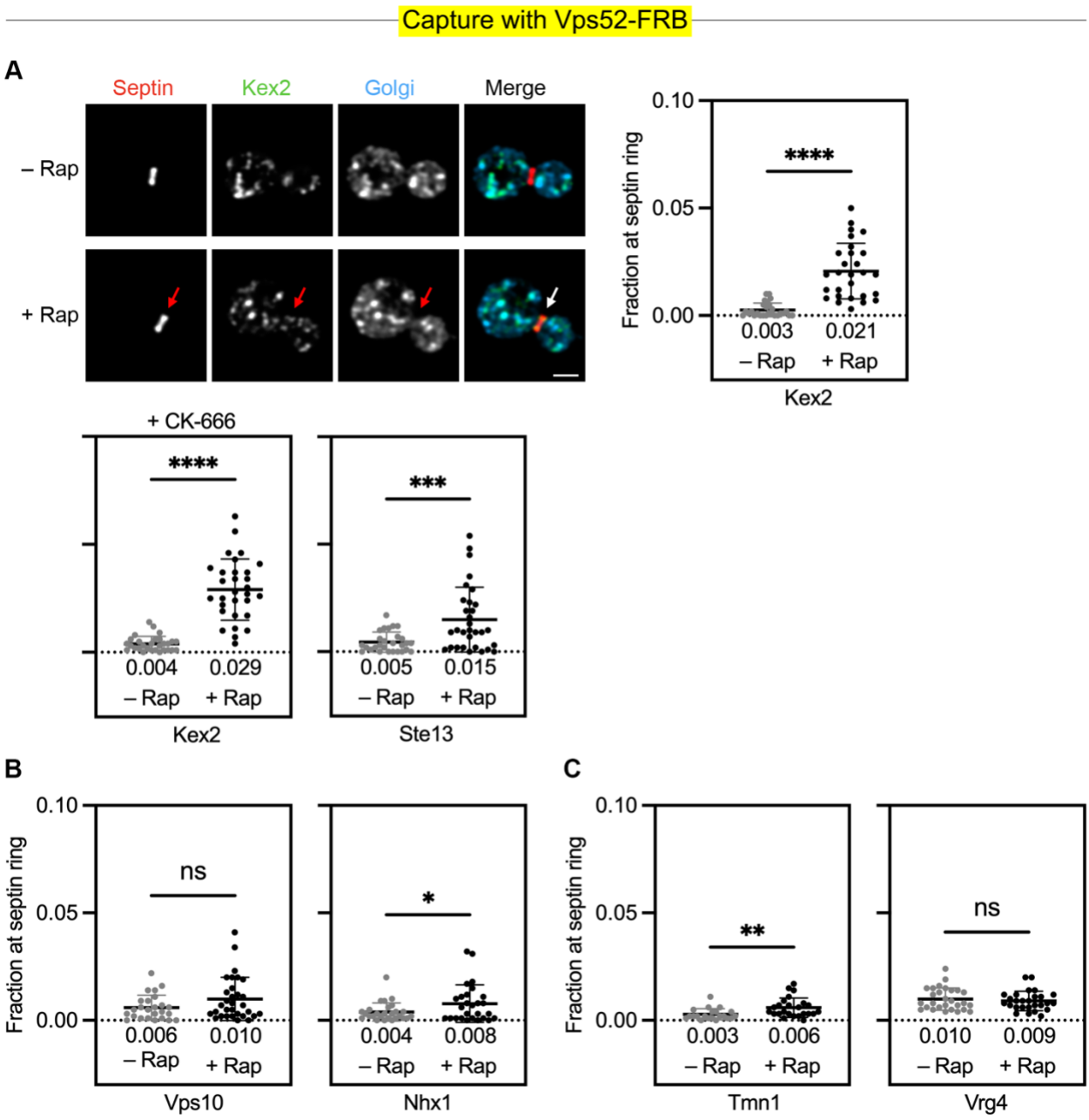

Figure 4.9: **Ectopically localized GARP captures AP-1/Ent5 cargoes.** For the statistical analyses: ****, significant at P value <0.0001; ***, significant at P value = 0.0007; **, significant at P value = 0.0065; *, significant at P value = 0.0446; ns, not significant. **(A)** Strong capture of AP-1/Ent5 cargoes by ectopically localized GARP. Representative images show that localization of GARP to the FKBP-tagged septin (red) resulted in rapamycin-dependent accumulation of GFP-tagged Kex2 (green) at the bud neck. HaloTag-labeled Ric1 and Sec7 (blue) marked Golgi cisternae. Arrows indicate non-Golgi signal at the bud neck. Kex2 fluorescence at the bud neck was quantified with or without a 10-min rapamycin treatment as in Figure 4.1B. A similar quantification was performed for GFP-tagged Kex2 after treating the cells for 15 min with CK-666 and for GFP-tagged Ste13. *(continued on next page)*

Figure 4.9: **(B)** Weak or undetectable capture of PVE-derived cargoes by ectopically localized GARP. Fluorescence at the bud neck for GFP-tagged Vps10 or Nhx1 was quantified with or without a 10-min rapamycin treatment as in Figure 4.1B. **(C)** Weak or undetectable capture of COPI cargoes by ectopically localized GARP. The experiment was performed as in (B) but with GFP-tagged Tmn1 or Vrg4.

knockout strains, and we found that such strains have abnormal early and late Golgi structures that presumably reflect both direct and indirect effects of the GARP deficiency (data not shown). Taken together, our observations suggest that Imh1 and GARP cooperate to tether AP-1/Ent5 vesicles, but that Imh1 tethers PVE-derived vesicles without assistance from GARP.

Because GARP arrives downstream of cargoes that follow the COPI-dependent intra-Golgi recycling pathways, GARP was not expected to capture cargoes of those pathways. No capture was seen with Vrg4, which follows the early recycling pathway (Figure 4.9C). Some capture was seen with Tmn1, which follows the intermediate recycling pathway (Figure 4.9C), but this weak signal is reminiscent of the weak capture of Tmn1 by Imh1 (see Figure 4.3E) and it likely reflects occasional missorting of Tmn1 into the AP-1/Ent5 pathway. We conclude that GARP tethers vesicles from the AP-1/Ent5 pathway but not from the other pathways examined in this study.

Sgm1 localizes to Golgi cisternae during an early stage of maturation and can be relocalized to the septin ring

The golgin Sgm1 is an effector of the Rab GTPase Ypt6, which is present on Golgi cisternae during early and intermediate stages of maturation (Suda et al., 2013) (Figure 4.10A). As expected, Sgm1 accumulated on Golgi cisternae at about the same time as Ypt6 (Figure 4.10A). A surprising result is that Sgm1 departed well before Ypt6 (Figure 4.10A). The departure of Sgm1 coincided with that of Vrg4 (Figure 4.10B), perhaps indicating that Golgi association of Sgm1 requires a second

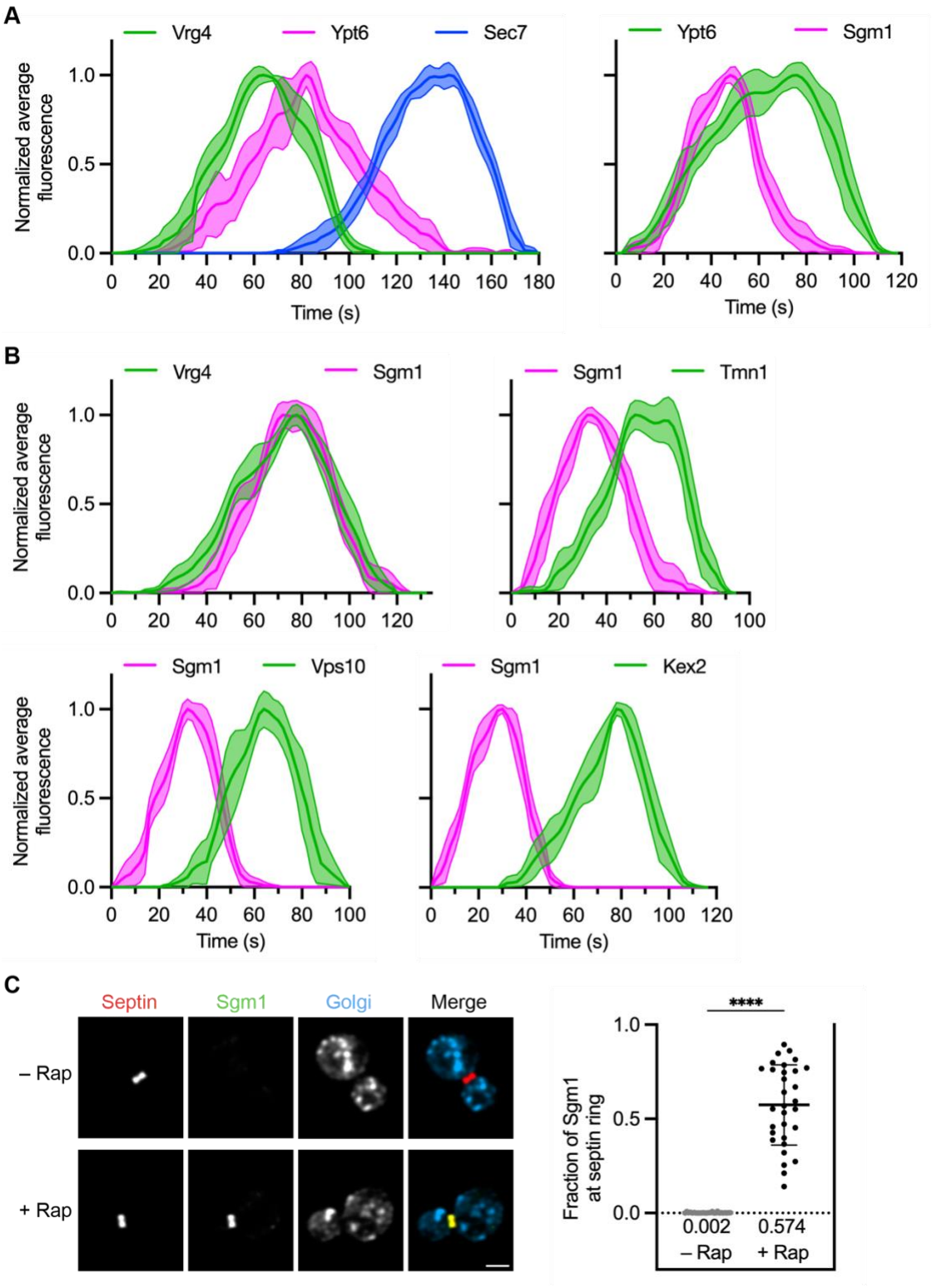

Figure 4.10: **Sgm1 is present on maturing cisternae during the arrival of proteins that follow the intermediate intra-Golgi recycling pathway, and a mutant Sgm1 can be ectopically localized to the bud neck.** *(continued on next page)*

Figure 4.10: **(A)** Golgi maturation kinetics of Ypt6 relative to the early and late Golgi markers Vrg4 and Sec7, respectively, and relative to Sgm1. Green represents a GFP label, magenta represents a HaloTag label, and blue represents an mScarlet label. Shown are normalized and averaged traces. **(B**) Golgi maturation kinetics of Sgm1 relative to Vrg4, Tmn1, Vps10, and Kex2. The display format is as in (A). **(C)** Capture by an FKBP-tagged septin (red) of a truncated Sgm1 tagged with FRB-GFP (green). HaloTag-labeled Ric1 and Sec7 (blue) marked Golgi cisternae. Representative images are shown. Sgm1-FRB-GFP levels at the bud neck were quantified as in Figure 4.1B. ****, significant at P value <0.0001.

factor that recycles synchronously with Vrg4. In any case, the net result is that Sgm1 was present on cisternae during an early stage of maturation.

We compared the kinetic signature of Sgm1 with the arrival phases of Vrg4, Tmn1, Vps10, and Kex2 (Figure 4.10B). Accumulation of Sgm1 lagged behind that of Vrg4 (Figure 4.10B), making it unlikely that Sgm1 tethers vesicles of the COPI-dependent early intra-Golgi recycling pathway. Sgm1 was present throughout the arrival phase of Tmn1 (Figure 4.10B), so Sgm1 is a candidate tether for the COPI-dependent intermediate intra-Golgi recycling pathway. Sgm1 was largely absent during the arrival phases of Vps10 and Kex2 (Figure 4.10B), so Sgm1 is not a candidate tether for PVE-derived vesicles or AP-1/Ent5 vesicles.

For the tethering assay, Sgm1 was endogenously tagged to enable ectopic localization. A control strain replaced the C-terminal Ypt6-binding domain of Sgm1 with GFP plus two copies of FRB. The resulting Sgm1 fusion protein was largely cytosolic, but it could be ectopically localized to the septin ring after addition of rapamycin (Figure 4.10C). We conclude that Sgm1 can be concentrated at the septin ring for tests of its vesicle tethering capability.

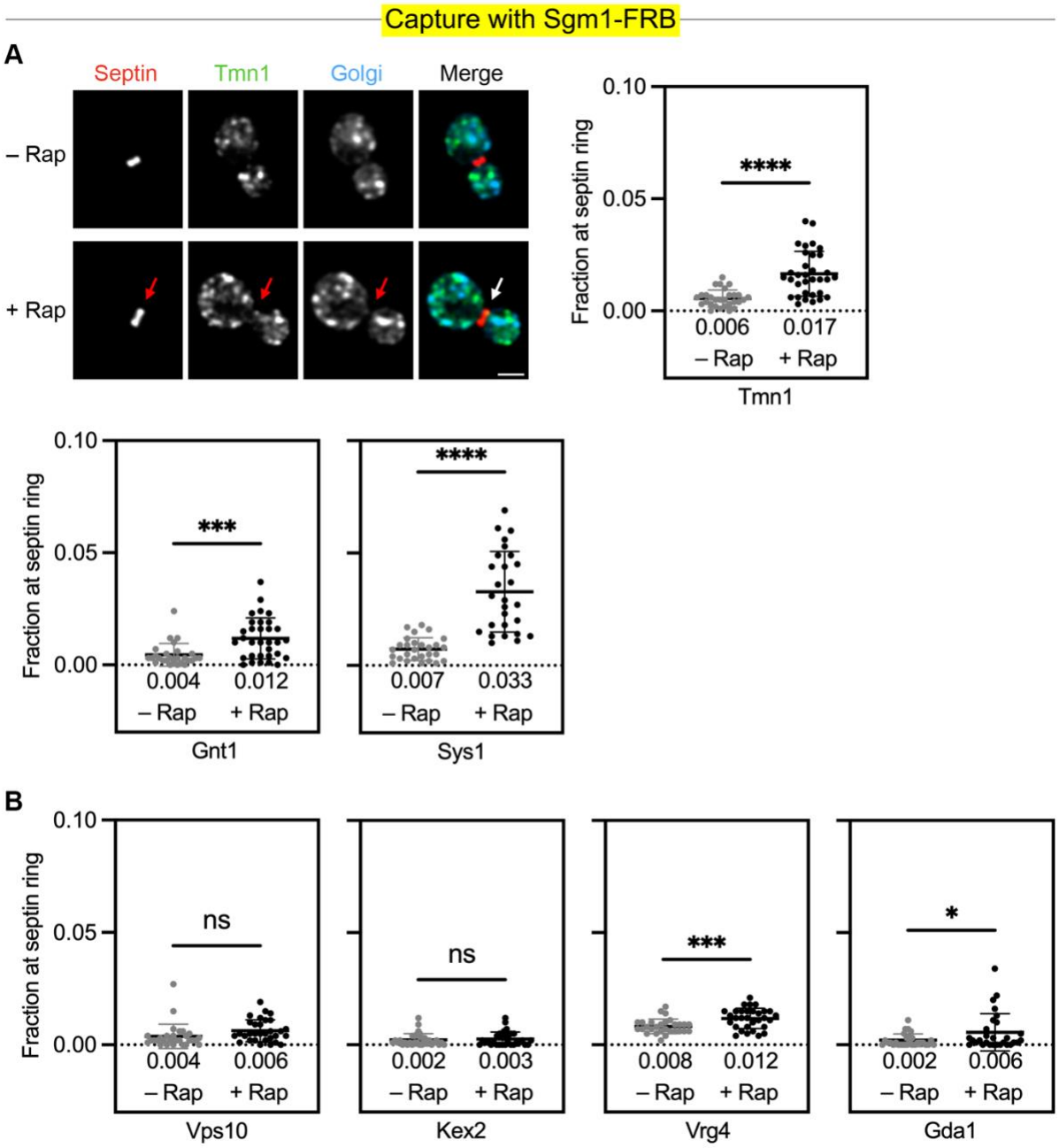

Figure 4.11: **Ectopically localized Sgm1 captures proteins that follow the intermediate intra-Golgi recycling pathway.** For the statistical analyses: ****, significant at P value <0.0001; ***, significant at P value = 0.0003 (Gnt1) or 0.0009 (Vrg4); *, significant at P value = 0.0357; ns, not significant. **(A)** Moderate to strong capture of three cargoes by ectopically localized Sgm1. Representative images show that localization of Sgm1 to the FKBP-tagged septin (red) resulted in rapamycin-dependent accumulation of GFP-tagged Tmn1 (green) at the bud neck. HaloTag-labeled Ric1 and Sec7 (blue) marked Golgi cisternae. Arrows indicate non-Golgi signal at the bud neck. Tmn1 fluorescence at the bud neck was quantified with or without a 10-min rapamycin treatment as in Figure 4.1B. Similar quantifications were performed for GFP-tagged Gnt1 and Sys1. *(continued on next page)*

Figure 4.11: **(B)** Weak or undetectable capture of cargoes that follow other recycling pathways. Fluorescence at the bud neck for GFP-tagged Vps10, Kex2, Vrg4, or Gda1 was quantified with or without a 10-min rapamycin treatment as in Figure 4.1B.

Ectopically localized Sgm1 tethers vesicles of the COPI-dependent intermediate intra-Golgi recycling pathway

The next step was to tag Sgm1 with FRB alone and to tag a transmembrane Golgi protein of interest with GFP. After addition of rapamycin, ectopically localized Sgm1 captured Tmn1, Gnt1, and Sys1 (Figure 4.11A), all of which follow the COPI-dependent intermediate intra-Golgi recycling pathway (see Chapter 3). For unknown reasons, capture of Sys1 was particularly strong. No capture was seen for Vps10 or Kex2 (Figure 4.11B). Minimal capture was seen for Gda1, which follows the COPI-dependent early intra-Golgi recycling pathway (see Chapter 3), but weak capture was seen for Vrg4 (Figure 4.11B), probably because Vrg4 occasionally fails to recycle in the COPI-dependent early pathway and then undergoes salvage in the COPI-dependent intermediate pathway (see Chapter 3). These results fit with the kinetic analysis, and they suggest that Sgm1 uniquely tethers vesicles of the COPI-dependent intermediate intra-Golgi recycling pathway.

Rud3 localizes to Golgi cisternae during the earliest stage of maturation and tethers vesicles of the COPI-dependent early intra-Golgi recycling pathway

The golgin Rud3 is an effector of the Arf1 GTPase, and Rud3 was reportedly present on early Golgi cisternae (Kim, 2003; Gillingham et al., 2004). Indeed, Rud3 arrived about 40 sec before Vrg4, at the time when Golgi cisternae were first forming (Casler et al., 2019; Tojima et al., 2024) (Figure 4.12A). Rud3 persisted during the arrival phase of Vrg4, so it is a candidate tether for the COPI-dependent early intra-Golgi recycling pathway.

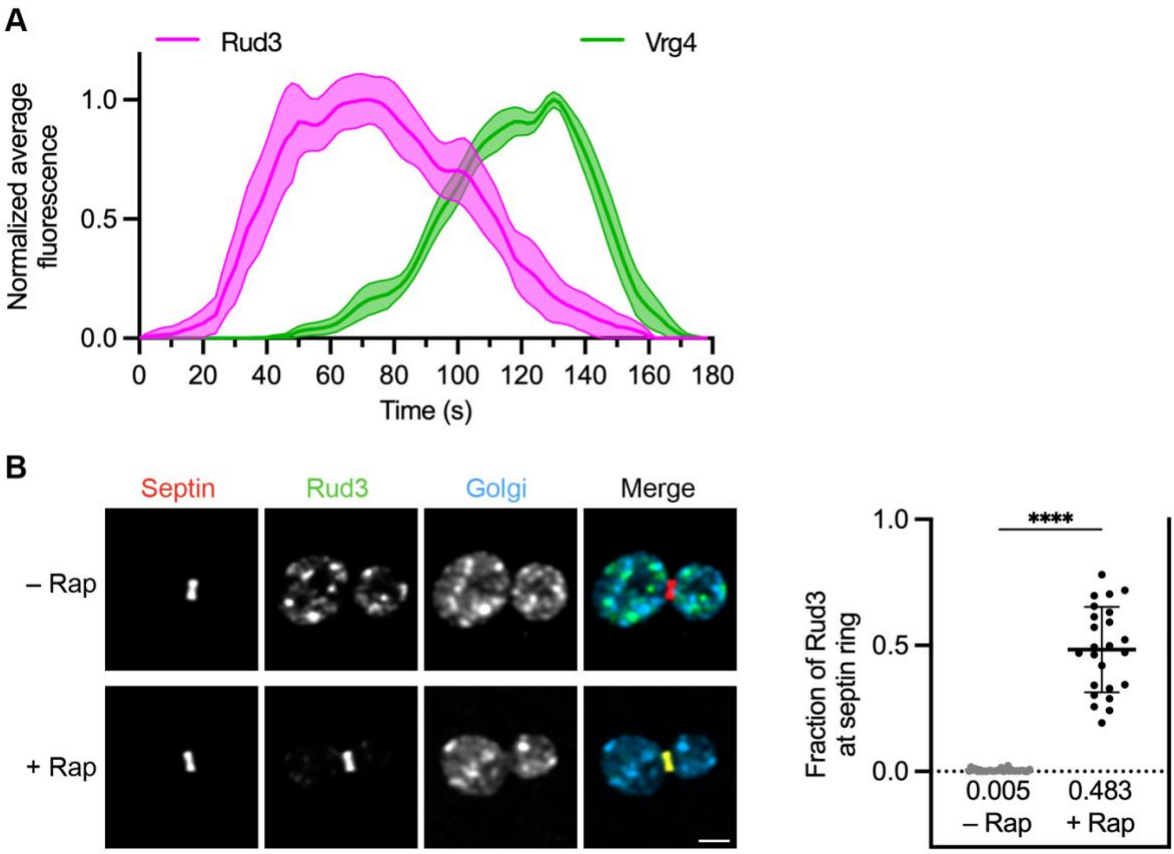

Figure 4.12: **Rud3 is present on cisternae during a very early stage of maturation, and FRB-tagged Rud3 can be ectopically localized to the bud neck. (A)** Golgi maturation kinetics of Rud3 relative to Vrg4. Green represents a GFP label and magenta represents a HaloTag label. Shown are normalized and averaged traces. **(B)** Capture by an FKBP-tagged septin (red) of full-length Rud3 tagged with FRB-GFP (green). HaloTag-labeled Ric1 and Sec7 (blue) marked Golgi cisternae. Representative images are shown. Rud3-FRB-GFP levels at the bud neck were quantified as in Figure 4.1B. ****, significant at P value <0.0001.

For ectopic localization, Rud3 was modified by appending FRB to the C-terminus of the full-length tether, because truncating Rud3 to displace it from the Golgi perturbed cell morphology (data not shown). When Rud3 was tagged with two copies of FRB plus GFP, addition of rapamycin rapidly and efficiently redistributed the fusion protein to the bud neck (Figure 4.12B). We conclude that Rud3 can be relocalized to the septin ring for tests of its tethering capability.

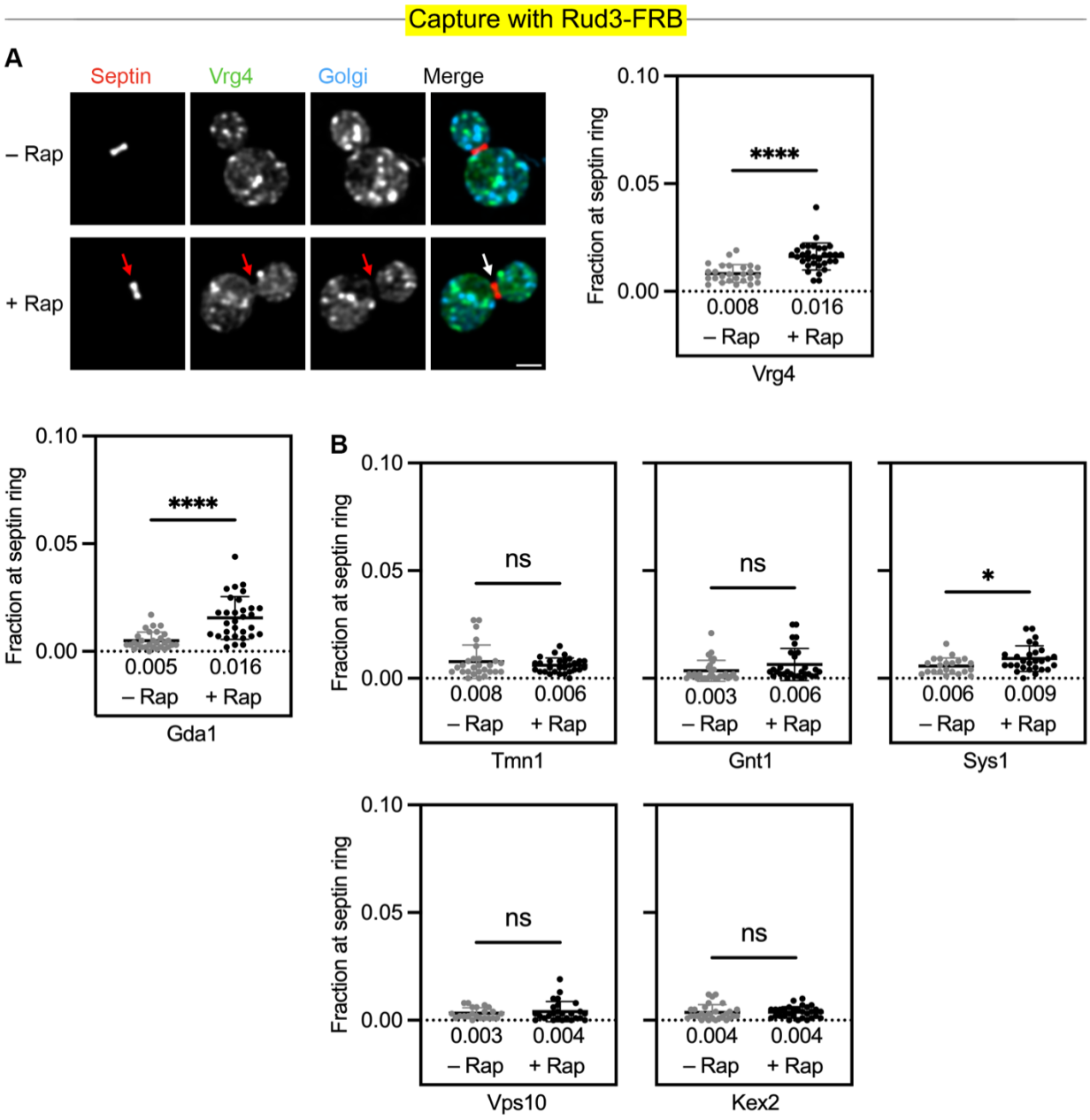

Figure 4.13: **Ectopically localized Rud3 captures proteins that follow the early intra-Golgi recycling pathway.** For the statistical analyses: ****, significant at P value <0.0001; *, significant at P value = 0.0156; ns, not significant. **(A)** Capture of two cargoes by ectopically localized Rud3. Representative images show that localization of Rud3 to the FKBP-tagged septin (red) resulted in rapamycin-dependent accumulation of GFP-tagged Vrg4 (green) at the bud neck. HaloTag-labeled Ric1 and Sec7 (blue) marked Golgi cisternae. Arrows indicate non-Golgi signal at the bud neck. Vrg4 fluorescence at the bud neck was quantified with or without a 10-min rapamycin treatment as in Figure 4.1B. A similar quantification was performed for GFP-tagged Gda1. **(B)** Weak or undetectable capture of cargoes that follow other recycling pathways. Fluorescence at the bud neck for GFP-tagged Tmn1, Gnt1, Sys1, Vps10, or Kex2 was quantified with or without a 10-min rapamycin treatment as in Figure 4.1B.

Ectopically localized Rud3 captured small but significant amounts of Vrg4 and Gda1. Under the same conditions, there was little or no capture of Tmn1, Gnt1, Sys1, Vps10, or Kex2 (Figure 4.13). These data suggest that Rud3 serves as a tether for the early intra-Golgi recycling pathway.

Discussion

We set out to assign vesicle tethers to membrane traffic pathways at the yeast Golgi. An obvious approach would have been to examine the effects of knocking out individual tethers, but such experiments have limitations depending on the strengths of the knockout phenotypes. Loss of a tether might have only a mild effect that is not detectable with our assays. Alternatively, loss of a tether might substantially compromise a given pathway, in which case additional pathways could be indirectly affected. Because of these factors, our preliminary knockout data were largely uninformative, and we chose not to pursue that line of investigation.

A more promising strategy is to have a positive readout for the function of an individual tether. The starting point was our recent development of an assay in which Golgi-derived vesicles are captured at the yeast bud neck via binding of a tagged Golgi protein in the vesicles (see Chapter 3). Here, we modified this assay by ectopically localizing a tether to the bud neck and then assessing whether particular Golgi proteins are captured by the tether. This method was inspired by earlier work on animal Golgi tethers from the Munro lab (Wong and Munro, 2014). By quantifying tether-dependent capture of Golgi proteins that have been shown to follow specific recycling pathways, we can determine which classes of vesicles are recognized by each tether.

Vesicle capture approaches also have a limitation: the fidelity of membrane traffic systems is imperfect, so a Golgi protein that follows a primary recycling pathway will undergo occasional

missorting into secondary pathways, often followed by retrieval. Missorting and retrieval are well documented for resident ER proteins (Barlowe and Miller, 2013), but these processes likely also play a key role in the Golgi. This phenomenon is illustrated by the Kex2 processing protease in the yeast TGN (Fuller et al., 1988). Kex2 was previously thought to cycle between PVE compartments and the Golgi together with the vacuolar hydrolase receptor Vps10 (Voos and Stevens, 1998; Bowers and Stevens, 2005; Bean et al., 2017), yet unlike Vps10, Kex2 shows very low steady-state localization to PVE compartments (Day et al., 2018). We have argued that Kex2 normally follows the AP-1/Ent5-dependent late intra-Golgi recycling pathway, and that Kex2 sometimes undergoes missorting to PVE compartments followed by retrieval to the Golgi. The experimental consequence is that when Kex2 is tagged with FRB, rapamycin will cause capture of AP-1/Ent5 vesicles plus less efficient capture of vesicles traveling between the Golgi and PVE compartments. Similarly, when a tether for the AP-1/Ent5 pathway is ectopically localized, the tethered vesicles will contain high levels of proteins such as Kex2 that normally follow the AP-1/Ent5 pathway plus low levels of other proteins that are occasionally missorted into that pathway. Therefore, we must try to distinguish between the relatively strong vesicle capture signals from primary recycling pathways versus the weaker signals from secondary pathways.

The vesicle capture data are complemented by kinetic analysis, in two ways. First, the kinetic signature of a resident Golgi protein provides information about the primary recycling pathway(s) for that protein (Papanikou et al., 2015; Day et al., 2018; Casler et al., 2021). Second, if a vesicle tether operates in a particular recycling pathway, then the tether must be present during the arrival phase for resident Golgi proteins that follow that pathway. By combining kinetic data with vesicle capture data, we have assigned specific recycling pathways to three golgin tethers as well as the multi-subunit tether GARP.

The first golgin we examined was Imh1, the sole GRIP domain protein in yeast (Kjer-Nielsen et al., 1999; Munro and Nichols, 1999; Tsukada et al., 1999). Association of Imh1 with the Golgi is triggered by arrival of the transmembrane protein Sys1, which initiates a biochemical cascade that recruits and activates the small GTPase Arl1 (Panic et al., 2003; Setty et al., 2003; Behnia et al., 2004; Setty et al., 2004). We showed previously that Sys1 recycles in the COPI-dependent intermediate intra-Golgi recycling pathway, although a fraction of the Sys1 molecules partition instead into the AP-1/Ent5-dependent late intra-Golgi recycling pathway (see Chapter 3). As expected, Imh1 associates with a maturing cisterna soon after the first wave of Sys1 arrival. That timing puts Imh1 in place during the arrival of both PVE-derived vesicles and AP-1/Ent5 vesicles. Indeed, ectopically localized Imh1 robustly captures multiple TGN proteins: Vps10 and Nhx1, which recycle between PVE compartments and the Golgi, as well as Kex2 and Ste13, which recycle in the AP-1/Ent5 pathway (Day et al., 2018; Casler et al., 2021).

This dual capture by Imh1 prompted us to seek concrete evidence that different classes of TGN proteins follow distinct recycling pathways. We examined five TGN proteins: Kex2, Ste13, Stv1, Vps10, and Nhx1. In wild-type cells, only Vps10 and Nhx1 show clear concentration in PVE compartments as well as the TGN (Kojima et al., 2012; Chi et al., 2014; Day et al., 2018), suggesting that those two proteins follow a different recycling pathway than the other three. Support for that interpretation came from our earlier analysis of strains carrying deletions of both Ent5 and the AP-1 subunit Apl4 (Casler et al., 2021). In *apl4*Δ *ent5*Δ mutant cells, Kex2, Ste13, and Stv1 escape from the Golgi to the plasma membrane whereas Vps10 and Nhx1 traffic normally. Further insight came from kinetic analysis. Although all five TGN proteins begin to arrive at about the same time, the departure times vary. We find that Kex2, Ste13, and Stv1 depart from a maturing cisterna synchronously, whereas Vps10 and Nhx1 depart earlier. This timing fits

with observations that the Gga and Ent3 clathrin adaptors that mediate Golgi-to-PVE traffic arrive earlier than the AP-1 and Ent5 adaptors that mediate intra-Golgi recycling (Daboussi et al., 2012; Casler and Glick, 2020). The combined data support the idea that Vps10 and Nhx1 recycle between PVE compartments and the Golgi in a pathway that involves the Gga adaptors and possibly Ent3, whereas Kex2, Ste13, and Stv1 recycle within the Golgi in a pathway that involves AP-1 and Ent5.

To explore this issue further, we used a vesicle capture assay. When Vps10 is tagged with FRB, Nhx1 is co-captured efficiently, whereas Kex2 is co-captured only very weakly and Ste13 is not detectably co-captured. This result is an additional indication that Vps10 and Nhx1 follow a different primary recycling pathway than Kex2 and Ste13. Because Imh1 captures vesicles carrying all four of these TGN proteins, Imh1 evidently recognizes two distinct types of vesicles (Figure 4.14).

A golgin such as Imh1 is expected to cooperate with a multi-subunit tether such as GARP (Chen et al., 2019), but our analysis of GARP yields a more nuanced picture. Imh1 and GARP show only a partial kinetic overlap, with Imh1 arriving and departing earlier than GARP, suggesting only a partial functional overlap. The best-established role of GARP is in the tethering and fusion of vesicles from the endocytic system (Bonifacino and Hierro, 2011). Therefore, yeast GARP likely recognizes endocytic vesicles that are directly targeted to the Golgi (Day et al., 2018). Although yeast GARP has also been proposed to tether PVE-to-Golgi vesicles that carry proteins such as Vps10 (Conibear and Stevens, 2000; Conibear et al., 2003), the evidence for that idea comes from GARP knockout strains, which show widespread defects at both early and late Golgi stages (data not shown). Our kinetic data revealed that accumulation of GARP at the Golgi lags slightly behind that of Vps10, making it unlikely that GARP acts as a tether for Vps10-containing vesicles. Indeed, ectopically localized GARP shows little or no capture of Vps10 or Nhx1. A

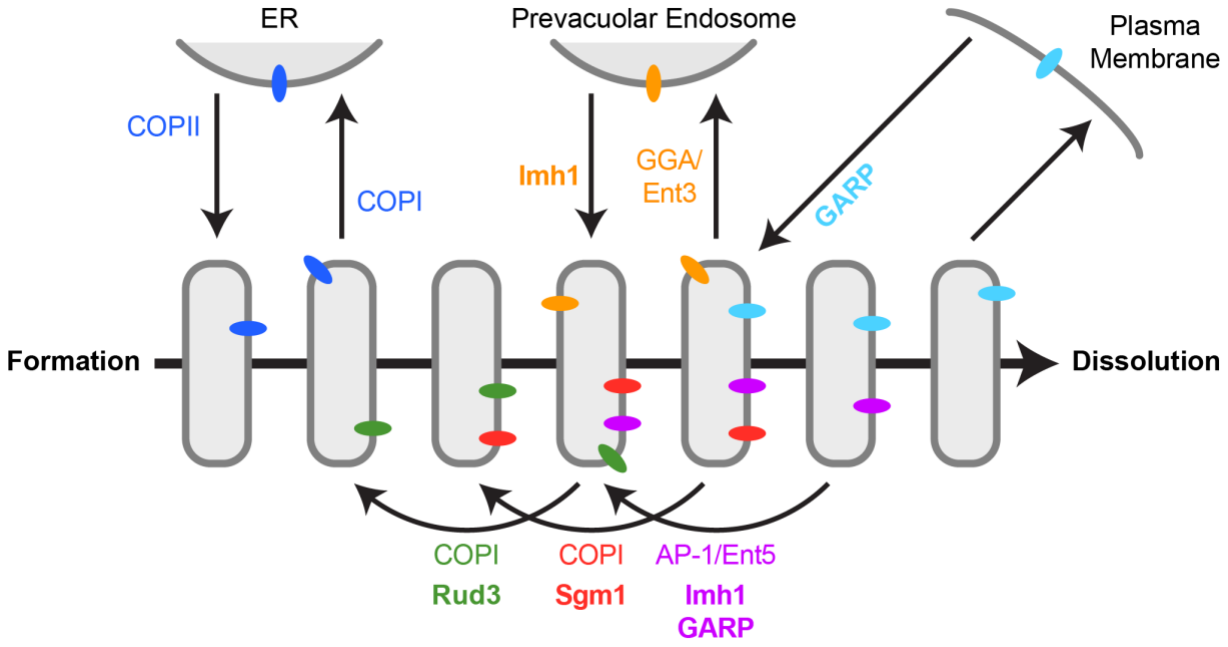

Figure 4.14: **Multiple recycling pathways deliver membrane to the yeast Golgi with the aid of vesicle tethers.** This diagram summarizes our interpretations about membrane traffic pathways at the yeast Golgi and the involvement of vesicle tethers. The thick arrow represents the timeline of cisternal maturation while the thin arrows represent vesicular traffic pathways. Transmembrane proteins are shown as colored ovals, and the tethers examined here are listed in bold. Six pathways are depicted. (i) COPII vesicles fuse with new Golgi cisternae, and some of the delivered proteins (dark blue) subsequently recycle to the ER in COPI vesicles. (ii) Some resident Golgi proteins such as Vrg4 (green) recycle within the Golgi in a COPI-dependent early pathway. (iii) Some resident Golgi proteins such as Tmn1 (red) recycle within the Golgi in a COPI-dependent intermediate pathway. (iv) Some resident Golgi proteins such as Kex2 (magenta) recycle within the Golgi in an AP-1/Ent5-dependent late pathway. (v) Some proteins such as Vps10 (orange) travel from Golgi cisternae to PVE compartments in a GGA/Ent3-dependent pathway and then recycle to the Golgi. (vi) Some proteins (light blue) travel to the plasma membrane in secretory vesicles and then recycle to the Golgi in endocytic vesicles. Although the endocytic pathway was not characterized in this study, GARP is presumed to tether endocytic vesicles based on evidence that GARP participates in the trafficking of endocytosed proteins (Bonifacino and Hierro, 2011) and that endocytic vesicles in yeast fuse directly with maturing Golgi cisternae (Day et al., 2018).

different result is seen for TGN proteins that recycle in AP-1/Ent5 vesicles. GARP arrives simultaneously with or slightly earlier than Kex2, and ectopically localized GARP captures Kex2 and Ste13, suggesting that GARP functions in AP-1/Ent5-dependent intra-Golgi recycling. We

conclude that tethering of AP-1/Ent5 vesicles involves both Imh1 and GARP while tethering of PVE-to-Golgi vesicles involves Imh1 but not GARP (Figure 4.14).

The second golgin we examined was Sgm1, the ortholog of mammalian TMF (Siniossoglou and Pelham, 2001; Fridmann-Sirkis et al., 2004). Sgm1 is an effector of the Rab GTPase Ypt6, which is present during an intermediate stage of maturation (Suda et al., 2013). We confirmed that Sgm1 arrives around the same time as Ypt6. Unexpectedly, Sgm1 departs before Ypt6, suggesting that a second component is needed to retain Sgm1 at Golgi membranes. The kinetic data indicate that Sgm1 is uniquely present during arrival of vesicles from the COPI-dependent intermediate intra-Golgi recycling pathway. As expected, ectopically localized Sgm1 shows relatively strong capture of proteins such as Tmn1 and Sys1 that follow the intermediate pathway. A weak signal is seen for proteins such as Vrg4 that follow the COPI-dependent early intra-Golgi recycling pathway, presumably due to low-level missorting of those proteins into the intermediate pathway (see Chapter 3). Sgm1 is currently the clearest example of a tether that seems to be specific to a single recycling pathway (Figure 4.14).

The third golgin we examined was Rud3, the ortholog of mammalian GMAP-210 (Kim, 2003; Gillingham et al., 2004). Rud3 associates with Golgi membranes by binding to the small GTPase Arf1 and to a second unidentified component (Gillingham et al., 2004). Like GMAP-210, Rud3 was reported to be present on early Golgi cisternae (Gillingham et al., 2004), and we detect Rud3 on maturing cisternae well before the arrival of Vrg4. A possible explanation for this early appearance is that Rud3 resembles GMAP-210 by having a second role in tethering ER-derived COPII vesicles (Wong and Munro, 2014). In any case, Rud3 is present during arrival of vesicles from the COPI-dependent early intra-Golgi recycling pathway. Rud3 shows capture of proteins that follow this early pathway but virtually no capture of proteins that follow downstream

pathways (Figure 4.14). Thus, once again, the kinetic data match the functional data from the ectopic tether localization assay.

Our overall conclusion is that vesicle tethers at the yeast Golgi can be assigned to specific membrane traffic pathways (Figure 4.14). Some tethers, such as Imh1 and GARP, seem to operate in more than one pathway while other tethers, such as Sgm1, seem to operate in a single pathway. The various tethers and membrane traffic pathways are functionally interconnected. For example, the golgin Sgm1 recognizes vesicles of the COPI-dependent intermediate intra-Golgi recycling pathway, which delivers the transmembrane protein Sys1, which triggers a biochemical cascade that recruits the golgin Imh1, which recognizes vesicles of the PVE-to-Golgi and AP-1/Ent5 pathways. Future experiments will flesh out these links by examining additional tethers, most notably the multi-subunit tether COG, which likely functions in multiple membrane traffic pathways at the Golgi (Blackburn et al., 2019). The ultimate goal is to elucidate the molecular logic circuit that regulates Golgi maturation by switching membrane traffic pathways on and off and by triggering the association and dissociation of GTPases, tethers, and other peripheral membrane proteins (Pantazopoulou and Glick, 2019; Thomas and Fromme, 2020).

The findings presented here extend work from the Munro lab, who ectopically localized golgins in mammalian cells (Wong and Munro, 2014; Gillingham and Munro, 2016). Mammalian golgins probably function similarly to their yeast counterparts, based on the following reasoning: (1) Like Imh1, the mammalian GRIP domain-containing golgin-97 and golgin-245 capture TGN proteins that recycle from endosomes or recycle within the TGN in an AP-1-dependent pathway (Shin et al., 2017; Navarro Negredo et al., 2018; Cattin-Ortolá et al., 2024). (2) Like Sgm1, mammalian TMF captures resident intermediate Golgi proteins that probably recycle with the aid of COPI (Wong and Munro, 2014). (3) Like Rud3, mammalian GMAP-210 captures resident early

Golgi proteins that probably recycle with the aid of COPI (Wong and Munro, 2014). With the yeast system, the major step forward is that we have characterized the recycling pathways for resident Golgi proteins and so we can assign vesicle tethers to specific pathways.

The conserved multi-subunit GARP complex can now be added to the list of tethers studied by ectopic localization. GARP was previously implicated in capturing vesicles from the endocytic system (Bonifacino and Hierro, 2011). In yeast, endocytic vesicles apparently fuse directly with maturing Golgi cisternae, which also serve as early endosomes (Day et al., 2018), and GARP likely operates in that pathway (Conde et al., 2003; Takagi et al., 2012; Eising et al., 2019). By contrast, GARP does not seem to tether PVE-to-Golgi vesicles. Extrapolating to mammalian cells, GARP might promote the tethering and fusion of early endosome-derived vesicles but not of late endosome-derived vesicles. We also find evidence for a novel role of GARP in capturing intra-Golgi AP-1/Ent5 vesicles. Future work will seek to clarify how multi-subunit tethers cooperate with golgins to ensure specificity during Golgi membrane traffic.

Material and Methods

The majority of the reagents and methods used in this study were described in Chapter 3, including yeast protein tagging by chromosomal gene replacement, yeast cell growth, labeling of proteins with fluorescent HaloTag ligands (Grimm et al., 2021), preparation and use of rapamycin and CK-666, live-cell 4D confocal imaging of yeast cells attached to coverglass-bottom dishes, processing and averaging of fluorescence kinetic traces, detection and quantification of rapamycin-dependent vesicle capture at the yeast bud neck, and statistical analysis. Specific to the current study are the following:

1. Cells expressing an N-terminally tagged golgin tether were from a pop-in strain that contained both the untagged, functional wild-type golgin and the tagged golgin. Both versions of the golgin were expressed from the native promoter. The same pop-in approach was used for N-terminal tagging of the Rab GTPase Ypt6.
2. Each averaged kinetic trace was generated by combining 8-16 individual kinetic traces.
3. Most of the representative fluorescence images chosen for display in the figures were scaled to the full RGB dynamic range, and then the pixel values were multiplied by 1.5 to make the labeled structures easier to visualize. An exception is the analyses of Imh1 localization (Figure 4.1B) and Sgm1 localization (Figure 4.10C), where the images taken in the absence or presence of rapamycin were scaled identically to illustrate that the cytosolic signals in the absence of rapamycin were weak and diffuse.
4. The original vesicle capture assays employed a 5-min rapamycin treatment (see Chapter 3), and that method was used here for experiments involving Vps10-FRB and Kex2-FRB. The new vesicle capture assays in which tethers were ectopically localized employed a 10-min rapamycin treatment. Where indicated, the cells were treated for 15 min with CK-666 prior to the 10-min rapamycin treatment.

Video Associated with Chapter 4

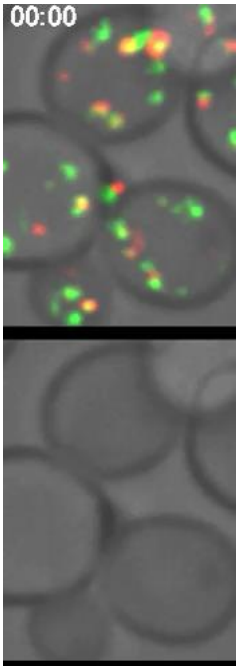

Video 4.1: **Representative 4D confocal movie of HaloTag-Imh1 and Kex2-GFP.** 3D z-stacks for the individual time points were average projected. The upper row shows the complete projections, and the lower row shows edited projections that include only the cisterna that was tracked. Intervals between frames are 2 s. The overlaid numbers represent the time in seconds after the cisterna that was tracked first became detectable. See Figure 4.2A for further details.

CHAPTER 5

DISCUSSION AND FUTURE RESEARCH OBJECTIVES

Concrete evidence of Golgi-associated vesicular transport first emerged over four decades ago. The membrane trafficking research field has since expanded greatly, leading to countless discoveries detailing the mechanisms of vesicular transport within the Golgi and between the Golgi and other organelles. We now understand the importance of vesicle coats, cargo adapters, GTPases, SNAREs, tethers, and a host of other regulatory proteins in organizing and driving vesicular transport. Many of these molecular machinery components have been individually characterized in detail at the structural and functional levels. It is now time to put the pieces of the Golgi machine together by uncovering which parts collaborate to operate each distinct trafficking pathway. Only when this task is accomplished will we obtain a mechanistically clear picture of Golgi self-organization and functionality.

The data presented in this thesis are sufficient to create a compelling model of vesicular transport pathways at the *S. cerevisiae* Golgi. As shown in Table 5.1, at least three distinct intra-Golgi transport pathways exist. The first two pathways employ COPI to form their respective vesicle populations with largely distinct cargos, including Vrg4 for the early pathway and Tmn1 for the intermediate pathway. The third pathway is operated by the clathrin coat and its AP-1 and Ent5 adaptors. A subset of late Golgi resident proteins including Kex2 are present in the vesicle population of this pathway. In addition, separate vesicular transport pathways carry proteins such as Vps10 bidirectionally between the late Golgi and the yeast prevacuolar endosome (PVE). The Golgi-to-PVE pathway is known to depend on the Gga and Ent3 clathrin coat adaptors, while the pathway back to the Golgi depends on the retromer complex and sorting nexin (SNX) proteins

(Myers and Payne, 2013; Ma and Burd, 2020). This knowledge provides a mechanistic explanation for the formation of distinct clathrin coated vesicle types of the AP-1/Ent5 and Golgi-to-PVE trafficking pathways.

Pathway Name	Example Cargos	Vesicle Packaging and Fission Machinery	Vesicle Tethering Machinery
Early Intra-Golgi (COPI)	Vrg4, Gda1	COPI, Vps74? (Wood et al., 2009; Sardana et al., 2021)	Rud3, COG? (Blackburn et al., 2019)
Intermediate Intra-Golgi (COPI)	Tmn1, Gnt1	COPI, Vps74? (Wood et al., 2009; Sardana et al., 2021)	Sgm1, COG? (Blackburn et al., 2019)
Late Intra-Golgi (AP-1/Ent5)	Kex2, Ste13	AP-1, Ent5, Clathrin	Imh1, GARP, COG? (Blackburn et al., 2019)
Golgi-to-PVE	Vps10, Nhx1	Gga1, Gga2, Ent3	CORVET? (Dubuke and Munson, 2016; Nagano et al., 2019)
PVE-to-Golgi	Vps10, Nhx1	Retromer, Sorting Nexins	Imh1, COG? (Blackburn et al., 2019)

Table 5.1: **Budding yeast possesses at least three intra-Golgi trafficking pathways and at least two pathways operating between the Golgi and PVE.** Listed are the assigned pathway names, two cargos identified for each pathway, molecular machinery used in vesicle packaging and fission, and tethers used by each pathway. Question marks denote proteins or protein complexes that may function in the specified pathway based on the references provided.

Kinetic and functional analyses of Golgi-associated tethers have allowed us to further delineate each trafficking pathway in molecular terms. The early COPI intra-Golgi pathway apparently utilizes the Rud3 golgin to tether its vesicles and facilitate their fusion. The downstream intermediate COPI pathway employs the Sgm1 golgin for this same purpose. At the late Golgi, Imh1 plays a dual role in tethering AP-1/Ent5 vesicles as well as vesicles arriving from the PVE. The GARP multi-subunit tether exhibits tethering activity for AP-1/Ent5 vesicles, but it apparently does not tether vesicular carriers arriving from the PVE. Given the widely presumed role of GARP

in facilitating endocytic traffic, we additionally hypothesize that GARP tethers endocytic vesicles with proteins internalized from the plasma membrane. We are currently testing this hypothesis and will publish our results in an upcoming manuscript.

Vesicular Trafficking Pathways at the Late Golgi

Historically, research studies examining vesicular transport at the yeast late Golgi were confounded by the assumption that *S. cerevisiae* contains distinct early and/or recycling endosomes. Trafficking pathways operating between these endosomes and the late Golgi were hypothesized by scientists who used gene deletion experiments to find evidence of their existence (Ma and Burd, 2020). Such experiments can be difficult to interpret as they allow time for cellular adaptations and/or indirect phenotypes to manifest. In 2018, our lab demonstrated that many *S. cerevisiae* early and recycling endosome proteins tightly colocalize with Sec7, a protein widely accepted to localize exclusively to the late Golgi (Day et al., 2018). Indeed, Day et al. were unable to find distinct early and recycling endosomes in wild type yeast by fluorescence microscopy. Our current understanding is that budding yeast possesses a minimal endomembrane system with a late Golgi that performs the functions of early and recycling endosomes. This model is currently shared by many albeit not all members of the yeast membrane trafficking research community. Nevertheless, I have chosen to use the minimal endomembrane system model as a basis for data interpretation in this thesis. My discussion of late Golgi trafficking therefore assumes that budding yeast possesses a minimal endomembrane system with maturing Golgi cisternae and distinct PVE (late endosome) organelles. This interpretive framework is crucial for defining trafficking pathways at the late Golgi. For example, we consider any proteins previously thought to recycle from early endosomes to the late Golgi (e.g. Kex2) as candidates for intra-Golgi recycling instead.

A complete understanding of vesicular transport pathways requires an examination of the vesicles' content, as well as molecular machineries for vesicle formation, tethering and fusion (see Chapter 1). The combined vesicle capture and tethering data presented in my thesis demonstrate the existence of at least two distinct late Golgi-related vesicle populations. One vesicle population contains the PVE and late Golgi residents Vps10 and Nhx1. These vesicles are tethered by the golgin Imh1 but apparently not by GARP. Ample data from the literature indicate that Vps10 and Nhx1 recycle between the PVE and late Golgi (Kojima et al., 2012; Chi et al., 2014; Casler et al., 2021). Based on these combined data, it may seem that a single pathway operates between these organelles. There are nevertheless additional layers of complexity that complicate interpretions. For example, the Vps10 based vesicle capture assays likely detect two vesicle subpopulations, one destined for fusion with the PVE and the other for fusion with the late Golgi. Vps10 is therefore present in two vesicle types if not more. There are also reports that at least two pathways retrieving proteins from the PVE may exist, one utilizing the retromer complex and sorting nexins, and the other depending on the SNX4 protein family but not retromer (Ma and Burd, 2020). Proteins such as Neo1 and Any1 (see Appendix E) not assayed by vesicle capture may be major cargos of these pathways. It is therefore unclear how many trafficking pathways operate between the PVE and late Golgi, and future studies will need to search for and define them by their molecular characteristics.

The second Golgi vesicle population examined contains the late Golgi residents Kex2, Stv1, and Ste13. Vesicles with these proteins are tethered by both Imh1 and GARP. We believe this vesicle population recycles intra-Golgi rather than through the PVE for the following reasons. First, Stv1, Ste13, and Kex2 are largely absent from the PVE in wild-type yeast while Nhx1 and Vps10, known to cycle between the late Golgi and PVE, are abundantly present there (Day et al., 2018; Casler et al., 2021; Kojima et al., 2012; Chi et al., 2014). Second, the seemingly

contradictory observation that Stv1, Ste13, and Kex2 substantially accumulate at the PVE and vacuole when retrieval factors are removed or inactivated for tens of minutes can be explained if these proteins only occasionally missort to the PVE (Bryant and Stevens, 1997; Voos and Stevens, 1998; Finnigan et al., 2012; Bean et al., 2017). Finally, Stv1, Ste13, and Kex2 exhibit AP-1 and Ent5 dependency; they are secreted from the late Golgi in the absence of these adapters while Vps10 and Nhx1 are not (Casler et al., 2021). Our interpretation of these data is that Stv1, Ste13, and Kex2 recycle intra-Golgi with the aid of AP-1 and Ent5. When these proteins occasionally missort to the PVE, they must be returned to the late Golgi by retromer and sorting nexins. Nevertheless, it is still formally possible that Stv1, Ste13, and Kex2 may primarily traffic between the late Golgi and PVE using anterograde and retrograde trafficking pathways distinct from those taken by Vps10 and Nhx1. If so, these three proteins should quickly accumulate at the PVE upon rapid inactivation of their retrieval pathway. To test this alternate hypothesis, distinct pathways from the PVE to late Golgi need to be definitively identified and a method to rapidly shut off each individual pathway will be required. These are nontrivial tasks that will likely necessitate multiple studies to complete.

Vesicle Tethering at the Late Golgi

My thesis work has demonstrated the ability of ectopically localized Imh1 to tether vesicles destined for fusion at the late Golgi. Imh1 tethers vesicles with cargos of both the PVE-to-Golgi and AP-1/Ent5 pathways, making it the only yeast golgin demonstrated to function in multiple trafficking routes. This is not surprising given that three mammalian, TGN-localized golgins tether vesicles with similar yet not identical cargo compositions (Wong and Munro, 2014; Shin et al., 2020). These mammalian golgins may tether vesicles from multiple pathways, and their associated

bridging factors (e.g. WDR11 complex) (Lowe, 2019; Navarro Negredo et al., 2018) could specify which vesicle type(s) they tether. With Imh1, the situation is less clear. No golgin bridging factors have been identified in yeast, and it is possible these appeared later in evolution after a gene duplication of an ancestral golgin of the late Golgi. Regardless, Imh1 must possess a molecular means of recognizing and tethering vesicles. This may be a protein receptor on the vesicle (e.g. a SNARE). To identify such a receptor, proximity biotinylation experiments can be performed with biotin ligase tagged Imh1. It will be interesting to see if Imh1 employs two different receptors, one for each pathway, or instead utilizes a single receptor common to both pathways.

The GARP complex ectopically tethers vesicles with AP-1/Ent5 dependent cargos, but it is notably unable to tether vesicles with Vps10 and Nhx1 arriving from the PVE. Aside from reinforcing the distinction between these two vesicle populations, this revelation suggests that GARP likely coordinates with Imh1 to mediate the fusion of AP-1/Ent5 vesicles. In contrast, GARP may not coordinate with Imh1 to facilitate PVE-to-Golgi vesicle fusion. One caveat is that ectopically localizing GARP in my experiments may cause a partial loss of its tethering function and yield false negative experimental results. This might occur, for example, if bud neck localized GARP loses one or more protein partners required to stably tether vesicles with Vps10 and Nhx1. However, the kinetics of GARP mirror rather than precede those of Vps10, casting some doubt on this possible scenario and rather suggesting that one or more factors arriving from the PVE may help recruit GARP to cisternae. The latter hypothesis could be tested by performing a genetic screen to identify proteins required for GARP localization at the late Golgi.

To resolve the remaining uncertainties outlined above, future experiments should examine the Conserved Oligomeric Golgi (COG) complex for its likely role in tethering vesicles at the *S. cerevisiae* Golgi. It is possible that COG may independently tether PVE-to-Golgi vesicles, or work

with GARP to do so. Indeed, both COG lobes A and B are capable of tethering vesicles in mammalian cells (Willett et al., 2013). Vesicle tethering experiments with each COG lobe could be performed at the bud neck, which is likely a better location for visualizing vesicles than the yeast mitochondria (Ishii et al., 2018). Assuming COG tethers vesicles, a possible molecular cooperation between COG and GARP can be investigated. Experiments demonstrating co-recruitment of GARP with either COG lobe at the bud neck as well as colocalization at maturing cisternae would provide initial evidence that COG and GARP coordinate to promote vesicle fusion at the Golgi.

Vesicle Formation at the Late Golgi by AP-1, Ent3, Ent5, and Gga Adapters

S. cerevisiae possesses at least five identified clathrin adaptors that aid in the formation and packaging of vesicles budding from the late Golgi. These adaptors include the adaptor protein complex 1 (AP-1), Golgi-localized γ ear-containing Arf-binding proteins 1 and 2 (Gga1 and Gga2), and the epsin-related proteins Ent3 and Ent5 (Myers and Payne, 2013; Tan and Gleeson, 2019). Gga1, Gga2, and Ent3 mediate the transport of proteins such as carboxypeptidase Y (CPY) and Pep12 from the late Golgi to the PVE (Hirst et al., 2000; Black and Pelham, 2000; Zhdankina et al., 2001). Ent3 depends on Gga1 and Gga2 for its Golgi localization, and an *in vivo* interaction has been documented between Gga2 and Ent3 (Duncan et al., 2003; Costaguta et al., 2006). AP-1 and Ent5 arrive together at maturing cisternae after Gga2, interact with each other, and are required for the intra-cellular recycling of TGN resident proteins that are largely absent from the PVE (Duncan et al., 2003; Casler and Glick, 2020; Casler et al., 2021). The totality of this evidence points toward the formation of two types of vesicles by these five clathrin adapters. As stated

previously, we believe one vesicle type (Gga1/Gga2/Ent3) carries proteins to the PVE and the other type (AP-1/Ent5) recycles proteins within the Golgi.

The above considerations notwithstanding, some evidence suggests that additional TGN-derived vesicle types may exist. In particular, Ent5 may form vesicles with Gga proteins. Multiple reports have confirmed that Ent5 colocalizes substantially with Gga2 and physically interacts with it (Duncan et al., 2003; Daboussi et al., 2012; Hung et al., 2012; Casler et al., 2021). Several studies have found partial functional redundancies for Ent3 and Ent5 in regulating protein transport at the TGN (Chidambaram et al., 2004; Copic et al., 2007; Petersen et al., 2023). These observations are suggestive of compensatory *in vivo* Gga-Ent5 interactions when Ent3 is absent, although such interactions may be enhanced in *ent3Δ* cells. In wild type yeast, peak levels of Ent5 at maturing cisternae occur between those of Gga2 and AP-1, although Ent5 colocalizes more with AP-1 than Gga2 by structured illumination microscopy (Daboussi et al., 2012). In view of these collective data, it appears that Ent5 is a functionally multifaceted adapter that mainly forms vesicles with AP-1, but may also do so with the Gga adapters.

A handful of interesting observations suggest that Ent5 could independently form clathrin coated vesicles at the late Golgi. Ent5 does not depend on the Gga adaptors or AP-1 for its Golgi localization (Costaguta et al., 2006). Additionally, unlike Ent3, Ent5 directly binds clathrin *in vivo* as demonstrated by co-immunoprecipitation experiments (Duncan et al., 2003). Notably, the binding affinity of Ent5 for clathrin is stronger than that of the AP-1 subunit, Apl2 (Defelipe et al., 2024). From the perspective of vesicle cargo packaging, Ent5 but not AP-1 is responsible for the proper localization of the late Golgi SNAREs, Tlg1 and Tlg2 (Hung and Duncan, 2016; Casler et al., 2021; Petersen et al., 2023). A direct interaction between Ent5 and Tlg2 was identified in one of these studies, so it is likely that Ent5 vesicles contain this important Qa-SNARE. Most

importantly, Ent5 can mediate the intracellular recycling of Tlg1, Kex2, Ste13, and Stv1 in the absence of AP-1, demonstrating its competency to form vesicles with these cargo proteins by itself and/or with the aid of Gga adapters (Casler et al., 2021).

In summary, it is plausible that three or four types of clathrin coated vesicles may form at the *S. cerevisiae* late Golgi. Apart from the well evidenced Gga/Ent3 and AP-1/Ent5 vesicles examined in this thesis, vesicles with Ent5 and Gga adapters and/or only Ent5 might also exist. In the scenario where Ent5 forms vesicles with Gga adapters, its interaction with Gga1 or Gga2 might exclude Ent3 and AP-1 from a budding vesicle. In this model, Ent3/Gga vesicles would initially form at cisternae followed by a brief wave of Gga/Ent5 vesicles, and finally a larger wave of AP-1/Ent5 vesicles. The presence of Ent3 may target vesicles to the PVE since Ent3 apparently interacts with the PVE localized SNAREs Pep12, Vti1, and Syn8 (Chidambaram et al., 2008). With regards to interpreting experiments in this thesis, if the Gga/Ent5 vesicle population exists, the vesicle capture assay would have conflated it with the AP-1/Ent5 vesicle population if the cargo proteins examined are common to both. Alternatively, the assay would have missed a Gga/Ent5 or Ent5 only vesicle population if no cargo trafficking in those vesicles was examined. Future studies will need to more precisely interrogate which Golgi-localized clathrin adaptors function together in vesicle formation. To this end, proximity biotinylation experiments and a proteomics analysis of isolated, clathrin coated Golgi-derived vesicles could be employed. Such experiments would additionally serve to expand our knowledge of which proteins are trafficked in each vesicle type. A verification of vesicle protein content could be achieved with vesicle capture assays, which might also serve to detect some vesicle-associated adapters *in vivo* (Robinson et al., 2024).

Ent4, a Putative Late Golgi Vesicle Cargo Adapter

In addition to the five adapters discussed above, a third epsin-related protein, Ent4, may also act as a cargo adaptor at the yeast late Golgi. Ent4 is poorly studied, and minimal experimental evidence suggests that it functions similarly to Ent3. Deletion of either Ent3 or Ent4 (but not Ent5) causes a partial mislocalization of the Arn1 ferrichrome transporter to the plasma membrane instead of the vacuole (Deng et al., 2009). The loss of Ent4 in yeast strains lacking Ent3 or Ent5 further increases an aberrant secretion of CPY (Chidambaram et al., 2004). It is noteworthy that Ent4 is shorter than Ent3 and Ent5, and does not possess C-terminal homology to these better characterized adapters (Wendland et al., 1999). Given that Ent5 binds clathrin through motifs in its C-terminus (Hung et al., 2012), it is unclear whether Ent4 binds clathrin directly or instead relies on other adaptors for its incorporation into budding vesicles. Future studies characterizing Ent4 should examine its localization, mechanism of membrane recruitment, interaction partners, and precise functions in vesicular transport at the late Golgi.

Vesicular Trafficking Pathways at the Early and Intermediate Golgi

Our analysis of COPI dependent cargos that recycle intra-Golgi revealed two vesicle populations that are formed at early and intermediate stages of cisternal maturation. The early COPI vesicle population contains the proteins Vrg4, Gda1, and Pmr1. These proteins have similar kinetics, and all of them depart substantially before COPI leaves maturing cisternae. The intermediate COPI vesicle population contains the proteins Tmn1, Gnt1, Sys1, and Aur1. The first two proteins are exclusive to this vesicle population, while Sys1 and Aur1 also recycle in AP-1/Ent5 vesicles (Casler et al., 2021). All four proteins appear at and disappear from cisternae after early COPI vesicle cargoes appear and disappear. Tmn1 and Gnt1 disappear from cisternae coincident with or

shortly before COPI leaves, while Sys1 and Aur1 apparently disappear shortly after COPI (Tojima et al., 2019). The later departure of Sys1 and Aur1 is readily explained by their presence in AP-1/Ent5 vesicles with Kex2. In total, the vesicle capture and kinetic data presented in this thesis agree with each other and provide evidence for the existence of two COPI intra-Golgi recycling pathways at the early and intermediate Golgi.

As mentioned in Chapter 1, defining trafficking pathways by vesicle cargo content alone is insufficient. An obvious reason is that some cargoes may be present in vesicles formed by multiple coats and/or adapters (e.g. Sys1). Additionally, the rapid pace of cisternal maturation and imperfections in the fidelity and completion of cargo packaging may allow proteins to leak into later cisternae and their downstream pathways. This appears to be the case with COPI dependent Golgi proteins. For example, small amounts of Vrg4 were detected in Sys1 containing vesicles, and a similar small number of Tmn1 molecules found their way into vesicles with Kex2. Low levels of early Golgi protein missorting likely occur on a regular basis in maturing cisternae, necessitating retrieval pathways. Prior to my thesis work, such secondary pathways had already been documented for late Golgi proteins escaping to the PVE and plasma membrane (Tan et al., 1996; Voos and Stevens, 1998; Ma and Burd, 2020; Casler et al., 2021). The vesicle capture data presented here suggests that COPI dependent proteins occasionally escaping their respective routes may be salvaged by subsequent intra-Golgi recycling pathways. This understanding, while intriguing by itself, highlights the need for additional criteria to clearly distinguish and define intra-Golgi COPI mediated trafficking pathways.

Vesicle Tethering at the Early and Intermediate Golgi

Identifying which golgin(s) tether each type of Golgi bound vesicles is an important step toward building a comprehensive definition for each Golgi trafficking pathway. My thesis research provides evidence that Sgm1 tethers vesicles with Tmn1, Gnt1, and Sys1 at cisternae. All other cargo proteins examined are largely absent from Sgm1 tethered vesicles. Tmn1, Gnt1, and Sys1 reside in the intermediate COPI vesicle population, indicating that Sgm1 serves as a selective vesicle tether for the intermediate COPI intra-Golgi trafficking pathway. The specificity of Sgm1 tethering stands in contrast to Imh1, which tethers two vesicle types. Our hypothesis of at least two distinct intra-Golgi COPI pathways is also supported by the tethering specificity of Sgm1. In particular, the observation that early COPI vesicle proteins (e.g. Gda1) are largely absent from Sgm1 tethered vesicles is consistent with this hypothesis.

The relatively strong capture by Sgm1 of Sys1 relative to Tmn1 and Gnt1 is surprising. A simple explanation is that Sys1 recycles more frequently in COPI vesicles than the latter two proteins. A second possibility is that Sgm1 tethers vesicles by interacting directly with Sys1, a phenomenon which would bias Sgm1 towards tethering Sys1 rich vesicles. This explanation may appear implausible given that tagged Sys1 recycles in AP-1/Ent5 vesicles and Sgm1 does not tether these. However, if untagged Sys1 only traffics in intermediate COPI vesicles (see Chapter 3 discussion), it could serve as the specificity factor for vesicle tethering by Sgm1. A tethering assay performed in cells lacking Sys1 could be used to directly test this hypothesis. Alternatively, if tagging Sys1 causes it to traffic in AP-1/Ent5 vesicles and Sgm1 tethering is mediated by Sys1, Sgm1 should be able to tether AP-1/Ent5 vesicles in the presence of tagged Sys1. A tethering experiment with non-fluorescently tagged Sys1 and a fluorescently tagged AP-1/Ent5 cargo (e.g. Kex2) would be an informative test of this idea. Otherwise, proximity biotinylation experiments

performed in the vicinity of Sgm1 vesicle tethering should provide a less biased avenue for identifying the Sgm1 specificity factor.

Like Sgm1, Rud3 also appears capable of tethering COPI vesicles at Golgi cisternae. These vesicles contain the early Golgi proteins Gda1 and Vrg4, both cargos of the hypothesized early COPI intra-Golgi trafficking pathway. Virtually no intermediate and late Golgi proteins can be detected in the Rud3 tethered vesicle population. This tethering specificity further supports our hypothesis of two distinct intra-Golgi COPI trafficking pathways.

The relatively weak ectopic tethering activity of Rud3 could simply be an intrinsic property of this golgin, or it may be due to the lack of a tethering partner such as Coy1. Along these lines, a possible interaction between Rud3 and Coy1 has been detected by yeast two-hybrid analysis and verified by bimolecular fluorescence complementation (Zhang et al., 2009). It is therefore conceivable that Rud3 and Coy1 work together from cisternae to tether incoming early COPI vesicles. Consistent with this hypothesis, gene deletion experiments show that Rud3 and Coy1 are redundant in function with regards to CPY and Gas1 glycosylation as well as overall cell growth at various temperatures (Anderson et al., 2017). This is significant as Sgm1 is not redundant with Rud3 or Coy1 by these same metrics, an observation that is additionally consistent with Sgm1 and Rud3 operating in separate trafficking pathways.

A related hypothesis is that Coy1 functions as a vesicle recognition factor for Rud3. In this case, the Rud3-Coy1 interaction would occur in *trans*, with transmembrane-anchored Coy1 operating from the vesicle. This model is compelling, because it accounts for the likely inability of Coy1 to ectopically tether vesicles, an observation made for its mammalian ortholog, CASP (Wong and Munro, 2014). The Rud3-Coy1 co-tethering hypothesis could be readily tested by deleting or mutating Coy1 and attempting to tether vesicles at the bud neck with Rud3.

Despite the apparent specificity of Rud3 tethering activity toward early COPI vesicles, the distinct identity of this intra-Golgi trafficking pathway remains the least certain for a few reasons. First, Rud3 may also function as a tether for ER-to-Golgi COPII vesicle transport similar to its mammalian ortholog, GMAP-210 (Wong and Munro, 2014). Kinetic analysis shows that Rud3 localizes to cisternae much earlier than Vrg4, almost certainly near the beginning of cisternal formation when COPII vesicle fusion occurs (Casler and Glick, 2020). Second, the time gap between the appearances of Rud3 and Vrg4 is much longer than those between Sgm1 or Imh1 and their respective vesicle cargos. This suggests a third intra-Golgi COPI pathway may exist with cargos arriving in Rud3-tethered vesicles shortly after Rud3 localizes to cisternae. Finally, some early COPI cargos like Vrg4 could at least occasionally recycle through the ER (Abe et al., 2004), complicating our task of defining the early intra-Golgi pathway by its vesicle cargos. With these uncertainties in mind, it is obvious that a comprehensive analysis of vesicular transport at the earliest stages of cisternal maturation will be required to rigorously test whether one or more early COPI intra-Golgi pathways operate during cisternal maturation.

Vesicle Formation at the Early and Intermediate Golgi by COPI

Despite decades of research on COPI, we still do not entirely understand how this important vesicle coat sorts and packages Golgi resident proteins into distinct vesicle types for inter-cisternal transport. The likely existence of two intra-Golgi COPI trafficking pathways highlights the importance of answering this question. Unfortunately, although several cargo adapters facilitating Golgi-to-ER COPI transport have been identified, very few intra-Golgi COPI adapters are known (Welch and Munro, 2019). Below, I will examine putative yeast intra-Golgi COPI cargo adapters and discuss their possible functions in the COPI trafficking pathways presented in this thesis.

The well studied intra-Golgi COPI adapter, Vps74, was first identified as a dosage suppressor of the essential SNARE Sft1 (Tu et al., 2008). Its actual function in glycosyltransferase recycling was uncovered much later in landmark 2008 studies highlighting the mislocalization of these Golgi enzymes in cells lacking Vps74 (Schmitz et al., 2008; Tu et al., 2008). Along with those observations, the researchers established Vps74 as a COPI-interacting adapter that binds glycosyltransferases through a semi-conserved cargo recognition motif present in their cytosolic tails. Subsequent studies revealed a network of interactions required for Vps74 membrane association and function. Specifically, Vps74 oligomerization as well as interactions with phosphatidylinositol 4-phosphate (PI4P) and Arf1-GTP promote its cisternal localization (Wood et al., 2009; Tu et al., 2012). The interaction with PI4P is of particular significance, as it apparently localizes Vps74 to intermediate/late Golgi cisternae where this lipid is synthesized by the PI4P kinase, Pik1 (Sardana et al., 2021; Highland and Fromme, 2021).

The relatively late presence of Vps74 at PI4P-positive cisternae hints at its specific involvement in intermediate intra-Golgi COPI transport. Curiously, some of the identified Vps74 clients are thought to be early Golgi resident proteins which largely depart before PI4P accumulates at the late Golgi (Tu et al., 2008; Sardana et al., 2021). How can these observations be reconciled? One answer is that tagging Vps74 may shift its localization to later cisternae and impact its function. This is plausible given that both termini of Vps74 are important for its Golgi localization (Schmitz et al., 2008; Tu et al., 2012). Based on my unpublished work, N-terminal tagging of Vps74 renders it at least partially dysfunctional as assessed by Vrg4 vacuolar mislocalization (data not shown). A second possibility is that Vps74 is initially recruited to early cisternae at low levels in a PI4P independent manner. In this case, interactions with Arf1-GTP and early Golgi client proteins could be sufficient for limited Vps74 membrane association. A third

explanation is that Vps74 acts as a salvage adapter for early Golgi proteins that leak into later cisternae and require the intermediate COPI pathway for retrieval. Assuming that tagging Vps74 does not change its localization, this model is appealing as it concurs with our vesicle capture data indicating a detectable level of Golgi protein leakage into downstream pathways. The second and third models presented here are not mutually exclusive, and careful kinetic analyses of functionally tagged Vps74 against its client proteins will be required to distinguish between them. In summary, the current data on Vps74 are consistent with it serving as a specific adapter for the intermediate COPI pathway and/or a salvage adapter for escaped early Golgi resident proteins.

In addition to Vps74, the early Golgi transmembrane protein Erd1 may also function as a COPI adapter. Erd1 was first identified in a genetic screen as a protein required for ER protein retention (Pelham et al., 1988; Hardwick et al., 1990), and then later as a phosphate transporter that supports glycosylation at the Golgi (Snyder et al., 2017). Most recently, Erd1 was found to assist Vps74 in the recycling of a subset of glycosyltransferases at the early Golgi (Sardana et al., 2021). In this study, loss of Vps74 or Erd1 showed similar vacuolar mislocalization of these glycosyltransferases. Erd1 and Vps74 were found to interact in co-immunoprecipitation experiments, and the loss of Vps74 caused Erd1 mislocalization to the vacuole. These experiments by themselves suggest that Vps74 and Erd1 obligately coordinate to recycle glycosyltransferases, but the story is likely more complicated. The authors of the study did not present evidence of an interaction between Erd1 and COPI, nor did they convincingly show direct interactions between Erd1 and glycosyltransferases. Furthermore, Erd1 was observed at the early Golgi with Mnn9, while Vps74 was found at the intermediate and late Golgi. Only limited kinetic overlap between Vps74 and Erd1 was demonstrated at cisternae. It is therefore premature to call Erd1 a COPI adapter, and the possibility remains that an alternate function of Erd1 is instead responsible for the

authors' observations. Regardless, it appears that Erd1 somehow promotes the operation of the early COPI intra-Golgi transport pathway. It is plausible that loss of Erd1 disrupts this pathway, overwhelms the downstream salvage capacity of Vps74, and leads to the vacuolar mislocalization of Vps74 client proteins.

Another reported intra-Golgi COPI adaptor, Cex1, may function in intra-Golgi COPI transport. Cex1 was originally reported to assist in tRNA nuclear export (McGuire and Mangroo, 2007), but a more recent study demonstrated it functions with COPI (Enkler et al., 2021). The authors found that Cex1 interacts with COPI and prevents the secretion of the transmembrane ER resident Wbp1 to the plasma membrane. Wbp1 contains a canonical dilysine motif with which it binds to COPI for retrieval to the ER (Eugster et al., 2000). It may therefore appear that Cex1 is yet another cargo adapter for COPI-mediated Golgi-to-ER transport. However, such adapters typically localize to earlier Golgi cisternae (Tojima et al., 2024), and the authors observed strong colocalization of Cex1 with both COPI and Sec7. Cex1 may therefore be a broadly utilized COPI adapter that functions in multiple COPI trafficking pathways. Future studies should examine the kinetics of Cex1 and identify any early and/or intermediate resident Golgi proteins it interacts with and helps to package into intra-Golgi recycling COPI vesicles.

Multi-pathway Trafficking of Individual Proteins at the Golgi Apparatus

The observed partitioning of proteins like Sys1 and Aur1 between the intermediate COPI and late AP-1/Ent5 pathways was surprising at first, and merits further discussion. As mentioned in Chapter 3, the cytosolic tags on Sys1 and Aur1 could cause the missorting of a fraction of these proteins into the AP-1/Ent5 pathway. While a formal possibility, I do not favor this hypothesis as the

cytosolic tags on Vrg4 and Pmr1 apparently do not force them into downstream Golgi pathways. Additionally, AlphaFold v2.0 predicts that Pmr1 possesses three large cytosolic domains, arguing that bulky cytosolic domains do not hamper COPI cargo packaging by default. Nevertheless, we cannot rule out the possibility that tagging Sys1 or any vesicle cargo protein alters its precise Golgi localization and trafficking route(s) taken. The development of smaller fluorogenic tags or a proteomics analysis of isolated vesicles with untagged cargos would be useful in resolving this concern.

On the other hand, if proteins like Sys1 and Aur1 truly partition between the intermediate COPI and AP-1/Ent5 pathways, the robustness of Golgi function could be enhanced. In general, the ability of a Golgi resident protein to take multiple pathways may be advantageous for several reasons. First, the protein would not have to rely on a single high-fidelity pathway to maintain its Golgi localization. Each molecule would essentially get two molecular windows of opportunity to be recycled and could, at least partially, miss the first one without penalty. Second, a protein recycling in multiple pathways would experience an increase in its average residence time at maturing cisternae. This would allow the protein to function longer in cisternae before being packaged into vesicles, a process which should temporarily decrease or halt its function. For example, Aur1 is an inositol phosphorylceramide synthase that may be functionally required at both the early and late Golgi. Aur1 broadly localized by multi-pathway recycling would be better positioned to modify ceramide transferred to cisternae from the ER by vesicular (at the early Golgi) and non-vesicular (at the intermediate and late Golgi) transport (Funato and Riezman, 2001; Liu et al., 2017; Ikeda et al., 2020; Schlarmann et al., 2021). Finally, multi-pathway trafficking is advantageous from an evolutionary perspective. A Golgi system possessing this attribute would likely demonstrate greater fitness under conditions of environmental duress or alternations in

metabolic flux. For example, decreases in the rate of ER-to-Golgi trafficking due to ER stress change Golgi structure by slowing cisternal formation (Amodio et al., 2009). A rapid recovery from such stress would benefit from multi-pathway trafficking, because it would more efficiently recycle proteins localized to older cisternae and rapidly re-establish Golgi polarity.

Multi-pathway trafficking may be employed by the mammalian Golgi to retain its resident proteins and maintain their proper polarization across Golgi stacks. Microscopy based imaging of mammalian Golgi proteins in mini-stacks have revealed their centers of mass vary along a continuum rather than cluster in groups (Tie et al., 2016, 2018). Assuming a discrete number of trafficking pathways exist at the mammalian Golgi, this provides circumstantial evidence that some of these proteins take multiple pathways. If so, these proteins may further differ among themselves in the frequency with which they take one pathway over another. The result would be the observed gradient of protein centers of mass across the Golgi stack. We have already demonstrated this concept at the *S. cerevisiae* Golgi, where the multi-pathing Aur1 and Sys1 possess kinetic peaks (i.e. centers of mass) that lie between those of Tmn1 and Kex2. How exactly a protein becomes a cargo of more than one pathway is unclear. However, it is conceivable that evolution has adjusted the biochemical properties of Golgi resident proteins to fine tune their trafficking preferences and resulting distributions across the Golgi stack for optimal function.

Additional circumstantial evidence for the muti-pathway trafficking of mammalian Golgi proteins comes from the studies of mammalian golgins. These studies noted that golgins tether vesicles with overlapping cargo compositions (Wong and Munro, 2014; Shin et al., 2020). One interpretation is that golgins exhibit partial functional redundancy by sometimes teaming up to tether vesicles from the same pathway. However, given that the *S. cerevisiae* golgins Imh1, Sgm1, and Rud3 all capture vesicle populations with different cargo proteins, an alternative interpretation

presents itself. Some mammalian Golgi proteins may traffic in multiple pathways, and this would explain their appearance in vesicles tethered by multiple golgins. If true, every mammalian golgin could actually function in a different pathway, and the perceived redundancy would be due to multi-pathway transport. Distinguishing between these interpretations will require a thorough identification and definition of mammalian Golgi trafficking pathways. To this end, a proteomic profiling of Golgi destined vesicles will be invaluable.

A Case for Bidirectional Intra-Golgi COPI Vesicle Transport

The intriguing hypothesis of intra-Golgi COPI bidirectional transport was originally proposed by Hugh Pelham and James Rothman in an attempt to settle the debate between the cisternal maturation and stable compartment models of Golgi transport (Pelham and Rothman, 2000). The former model postulated exclusively retrograde COPI vesicle transport while the latter model contended for anterograde COPI vesicle transport. The hypothesis of COPI bidirectional transport allows that both models are partially correct by suggesting that COPI vesicles may fuse with either neighboring cisterna in the context of a Golgi stack. These "percolating" vesicles would allow cargos to gradually transit through the stack until they reach their appropriate cisternal distributions in the case of Golgi residents, or exit the Golgi in the case of secretory cargos (Orci et al., 2000; Pelham and Rothman, 2000). Intra-Golgi COPI bidirectional transport was proposed before definitive evidence of cisternal maturation was obtained in *S. cerevisiae* (Losev et al., 2006; Matsuura-Tokita et al., 2006), but it remains a valid hypothesis if modified for the context of cisternal maturation. Below, I will discuss how data in this thesis can be viewed as evidence supporting a model of Golgi trafficking that includes intra-Golgi bidirectional COPI transport.

To begin, a definition of intra-Golgi bidirectional COPI transport is required for maturing cisternae that are unstacked in *S. cerevisiae*. I propose that such bidirectional transport occurs when the fusion and fission time windows of COPI vesicles carrying the same cargo overlap at maturing cisternae. This would, in theory, mean that a single protein molecule could leave a younger cisterna and arrive at an older one (anterograde transport) or vice versa (retrograde transport). Data presented in this thesis readily demonstrate that overlapping COPI vesicle fusion and fission windows exist in *S. cerevisiae*. First, COPI is present on cisternae for a lengthy duration, arriving before intra-Golgi cargos appear and leaving at nearly the halfway point of Sec7 late Golgi residency. This broad distribution of COPI is also present in mammalian cells (Orci et al., 1997). Second, by comparison between kinetic experiments, the COPI vesicle golgin tethers Rud3 and Sgm1 colocalize with COPI. These observations establish that some COPI vesicle fission and fusion machinery components co-exist on cisternae at the same time, a basic requirement for the bidirectional intra-Golgi transport of COPI vesicles.

Some kinetics of COPI cargos themselves are useful for assessing the likelihood of bidirectional COPI intra-Golgi transport. Previously, we had hypothesized that distinct, transmembrane COPI cargo kinetic signatures represent individual trafficking pathways. My thesis research has invalidated this view for proteins such as the Gda1 and Sys1. In the case of Gda1, its earlier disappearance from cisternae relative to Vrg4 did not indicate its absence in Vrg4 containing vesicles. Likewise, the distinct arrival and departure kinetics of Sys1 relative to Tmn1 did not imply its absence from Tmn1 containing vesicles. If the Vrg4 and Tmn1 kinetic traces encompass the entire arrival and departure windows for early and intermediate COPI vesicles respectively, we can ask whether the deviant kinetics of Gda1 and Sys1 relative to those of Vrg4 and Tmn1 provide evidence of bidirectional COPI transport.

First, I will consider whether Gda1 kinetics provide evidence of early COPI vesicle bidirectional transport. A close look at these kinetics reveals that the Gda1 peak of abundance at cisternae precedes that of Vrg4 by about twenty seconds in the averaged traces. From this peak, Gda1 departure in early COPI vesicles causes an approximate, average twenty-five percent reduction in its cisternal abundance by the time Vrg4 levels peak. The earlier drop in Gda1 levels relative to those of Vrg4 indicate that the departure phase of early COPI vesicles overlaps partially with the Vrg4 (and early COPI vesicle) arrival phase. If some Vrg4 molecules depart with Gda1 prior to maximal Vrg4 abundance, then Vrg4 undergoes bidirectional transport according to my definition above. Similar logic can be used to posit that Gda1 undergoes bidirectional transport by arriving with Vrg4 until the latter reaches its peak abundance. To refute the existence of bidirectional transport, one could suppose that only vesicles with Vrg4 and no Gda1 fuse over the time window between the peak abundances of each protein. Yet this seems implausible, as it would require an inhibitory mechanism preventing Gda1 positive early COPI vesicles from fusing with cisternae over that time period. In conclusion, the kinetics of Gda1 and Vrg4 imply that early COPI vesicle cargos likely undergo bidirectional transport.

Next, I will examine the kinetics of Sys1 for evidence of intermediate COPI vesicle bidirectional transport. It is first important to realize that the COPI vesicle departure kinetics of Sys1 are obscured by its concurrent arrival in AP-1/Ent5 vesicles. Indeed, the multi-pathway transport of Sys1 renders only the initial arrival phase of Sys1 informative for this analysis. We can therefore appreciate and analyze the delay in Sys1 appearance relative to Tmn1. This delay is shown accurately in the averaged traces as an average of about twenty seconds. It is not otherwise misleading since Tmn1 always appears before Sys1 in all individual traces. The difference in appearance between Tmn1 and Sys1 is likely not due to its multi-pathway trafficking, as I have

identified another putative multi-pathway trafficking protein, Gos1, that appears with Tmn1 and disappears with Sys1 (see Appendix A). Rather, as suggested in the Chapter 3 discussion, it is plausibly due to the departure of Sys1 molecules shortly after their arrival in COPI vesicles. Such trafficking by Sys1 fits the definition of bidirectional transport for intermediate COPI vesicles.

If Sys1 and Gda1 both undergo bidirectional transport, then why do we not by kinetic analysis immediately detect Sys1 with Tmn1 as we do Gda1 with Vrg4? I believe the answer involves the biophysical properties of transmembrane domains as well as competition between cargos for packaging into COPI vesicles (Glick et al., 1997; Welch and Munro, 2019; Lujan and Campelo, 2021). At the late Golgi, Sys1 possesses a weaker tendency to be sorted into COPI vesicles relative to Tmn1. This is apparent from the substantial amount of Sys1 that remains in cisternae when Tmn1 (and COPI) disappears. At the early Golgi, Sys1 may outcompete Tmn1 for packaging into COPI vesicles. The result would be a later appearance of Sys1 at cisternae relative to Tmn1. The biophysical properties (e.g. length) of the Sys1 transmembrane domains likely grant it an affinity for the thicker lipid bilayer environment of the late Golgi (Welch and Munro, 2019; Lujan and Campelo, 2021). This could explain its change in ability to compete with Tmn1 for packaging into COPI vesicles as cisternae mature. From this perspective, any bidirectional COPI vesicle transport of Sys1 molecules can be attributed to its biophysical 'dissatisfaction' with the early Golgi lipid environment. More generally, the principles of COPI cargo competition and cisternal membrane affinity probably impact all resident Golgi proteins. They likely contribute to the multi-pathway trafficking and divergent kinetics we are observing for Golgi proteins such as Drs2 (Casler et al., 2021). In conclusion, I find the bidirectional intra-Golgi COPI transport hypothesis to be compelling as it is supported by data in this thesis and can explain the observed differences in kinetics of proteins that we find follow the same pathways. Additional work defining

early Golgi COPI trafficking pathways and the kinetics of their cargos will be required to further test this model of intra-Golgi transport.

Perspectives on Researching Vesicular Transport at the Golgi

Decades of Golgi-related research studies have given us numerous intellectual footholds that are enabling our ascent to a comprehensive understanding of trafficking at the Golgi. My thesis work is yet another foothold, providing us with further insights into the molecular organization and definition of intra-Golgi vesicular transport pathways. As highlighted throughout this discussion, many questions and hypotheses remain to be answered and tested by thorough experimentation. Below, I offer my general perspectives on and recommendations for future research efforts in the field of Golgi transport across all commonly studied cell types.

As stated in Chapter 1, a complete understanding of vesicular trafficking at the Golgi requires that we molecularly identify and define each transport pathway. It will be important to systematically differentiate vesicle populations in the cell by lipid and protein content. To this end, quantitative proteomic and lipidomic profiling of purified vesicles will be invaluable for the identification of distinct vesicle populations. As with the vesicle capture assays presented here, a molecular hook such as a cargo or molecular tether will be required to purify the vesicle fraction of interest prior to analysis. These high throughput vesicle profiling experiments can be designed and cross-validated with the aid of *in vivo* vesicle capture assays. The result will be a set of identified vesicle populations representing putative vesicular trafficking pathways.

Once vesicle populations have been differentiated, hypotheses can be generated regarding their molecular means of fission and fusion as well as their origin and destination. Experiments testing these hypotheses can then be performed in live cells. For example, the hypothetical

identification of two vesicle populations carrying proteins to the Golgi from endosomes could guide investigations into defining their respective trafficking pathways. The targeted removal, degradation, and/or inactivation of endosomal vesicle fission proteins could be used to identify how each vesicle type is formed. Experiments such as *in vivo* tethering assays can examine which fusion machinery proteins at the Golgi act on each vesicle type. Finally, a precise microscopy-based assessment of cargo protein localization at endosomes and cisternae will specify the origin and destination of the trafficking pathways between these organelles. With such analyses concluded, reasonably complete molecular definitions for the two hypothetical endosome-to-Golgi trafficking pathways can be generated.

To motivate, guide, and expedite progress in defining Golgi-associated transport pathways in higher eukaryotes, the identification of all trafficking pathways at the *S. cerevisiae* Golgi must be prioritized. The relatively simpler Golgi in budding yeast likely requires fewer transport pathways than the Golgi complexes in multi-cellular eukaryotes. It will therefore be easier and faster to comprehensively define vesicular trafficking pathways in yeast using the approaches described above. Since much of the Golgi trafficking machinery is evolutionarily conserved, subsequent research efforts in higher eukaryotes can apply the knowledge gained about the yeast Golgi to inform and facilitate intelligent experiment design. It will certainly be interesting to see if the trafficking pathways identified in yeast are themselves conserved in other eukaryotes.

I will now conclude by highlighting some particularly large gaps in our knowledge of *S. cerevisiae* Golgi trafficking that must be rectified to advance the field. In particular, the number and molecular nature of the earliest intra-Golgi transport pathways as well as those operating between the Golgi and ER or PVE are unclear. Trafficking machinery components specifying transport steps, particularly those between the Golgi and PVE, must be identified and assigned to

specific pathways. It is probable that SNAREs play the primary role in specifying a vesicle for fusion with the ER, PVE, or appropriately mature Golgi cisternae. The cell must have a way of packing the appropriate SNARE(s) into vesicles with the correct cargos and associated adapter and coat proteins. At present, it remains unclear precisely how this fission and fusion machinery cooperation is coordinated during the vesicle packaging process. As many SNAREs are present at the Golgi, this question may be even more relevant for the further molecular clarification of distinct intra-Golgi trafficking pathways. An additional area requiring investigation is the molecular means by which tethers recognize their specific vesicle populations. Whatever factors facilitate tethering, they must also coordinate with the vesicle packaging machinery for incorporation into the appropriate vesicles. In summary, future research efforts should prioritize identifying new mechanisms of vesicle packaging (especially for cargos regulating vesicle fusion), determining which SNARE complexes act in each trafficking pathway, and discovering the molecular mechanisms of tethering. These challenges must be overcome if we are to achieve deeper insights into the mechanistically complex and microscopically beautiful world of vesicular transport at the Golgi.

REFERENCES

Abascal-Palacios, G., C. Schindler, A.L. Rojas, J.S. Bonifacino, and A. Hierro. 2013. Structural Basis for the Interaction of the Golgi-Associated Retrograde Protein Complex with the t-SNARE Syntaxin 6. *Structure*. 21:1698–1706. doi:10.1016/j.str.2013.06.025.

Abe, M., Y. Noda, H. Adachi, and K. Yoda. 2004. Localization of GDP-mannose transporter in the Golgi requires retrieval to the endoplasmic reticulum depending on its cytoplasmic tail and coatomer. *J. Cell Sci.* 117:5687–5696. doi:10.1242/jcs.01491.

Abramson, J., J. Adler, J. Dunger, R. Evans, T. Green, A. Pritzel, O. Ronneberger, L. Willmore, A.J. Ballard, J. Bambrick, S.W. Bodenstein, D.A. Evans, C.-C. Hung, M. O'Neill, D. Reiman, K. Tunyasuvunakool, Z. Wu, A. Žemgulytė, E. Arvaniti, C. Beattie, O. Bertolli, A. Bridgland, A. Cherepanov, M. Congreve, A.I. Cowen-Rivers, A. Cowie, M. Figurnov, F.B. Fuchs, H. Gladman, R. Jain, Y.A. Khan, C.M.R. Low, K. Perlin, A. Potapenko, P. Savy, S. Singh, A. Stecula, A. Thillaisundaram, C. Tong, S. Yakneen, E.D. Zhong, M. Zielinski, A. Žídek, V. Bapst, P. Kohli, M. Jaderberg, D. Hassabis, and J.M. Jumper. 2024. Accurate structure prediction of biomolecular interactions with AlphaFold 3. *Nature*. 630:493–500. doi:10.1038/s41586-024-07487-w.

Adarska, P., L. Wong-Dilworth, and F. Bottanelli. 2021. ARF GTPases and Their Ubiquitous Role in Intracellular Trafficking Beyond the Golgi. *Front. Cell Dev. Biol.* 9:1977. doi:10.3389/fcell.2021.679046.

Adolf, F., M. Rhiel, B. Hessling, Q. Gao, A. Hellwig, J. Béthune, and F.T. Wieland. 2019. Proteomic Profiling of Mammalian COPII and COPI Vesicles. *Cell Rep.* 26:250-265.e5. doi:10.1016/j.celrep.2018.12.041.

Amodio, G., M. Renna, S. Paladino, C. Venturi, C. Tacchetti, O. Moltedo, S. Franceschelli, M. Mallardo, S. Bonatti, and P. Remondelli. 2009. Endoplasmic reticulum stress reduces the export from the ER and alters the architecture of post-ER compartments. *Int. J. Biochem. Cell Biol.* 41:2511–2521. doi:10.1016/j.biocel.2009.08.006.

Anderson, N.S., and C. Barlowe. 2019. Conserved juxtamembrane domains in the yeast golgin Coy1 drive assembly of a megadalton-sized complex and mediate binding to tethering and SNARE proteins. *J. Biol. Chem.* 294:9690–9705. doi:10.1074/jbc.RA119.008107.

Anderson, N.S., I. Mukherjee, C.M. Bentivoglio, and C. Barlowe. 2017. The Golgin protein Coy1 functions in intra-Golgi retrograde transport and interacts with the COG complex and Golgi SNAREs. *Mol. Biol. Cell*. 28:2686–2700. doi:10.1091/mbc.E17-03-0137.

Ang, A.L., T. Taguchi, S. Francis, H. Fölsch, L.J. Murrells, M. Pypaert, G. Warren, and I. Mellman. 2004. Recycling endosomes can serve as intermediates during transport from the Golgi to the plasma membrane of MDCK cells. *J. Cell Biol.* 167:531–543. doi:10.1083/jcb.200408165.

Annaert, W., and C. Kaether. 2020. Bring it back, bring it back, don't take it away from me – the sorting receptor RER1. *J. Cell Sci.* 133. doi:10.1242/jcs.231423.

Antebi, A., and G.R. Fink. 1992. The yeast Ca(2+)-ATPase homologue, PMR1, is required for normal Golgi function and localizes in a novel Golgi-like distribution. *Mol. Biol. Cell*. 3:633–654. doi:10.1091/mbc.3.6.633.

Appenzeller-Herzog, C., and H.-P. Hauri. 2006. The ER-Golgi intermediate compartment (ERGIC): in search of its identity and function. *J. Cell Sci.* 119:2173–2183. doi:10.1242/jcs.03019.

Arab, M., T. Chen, and M. Lowe. 2024. Mechanisms governing vesicle traffic at the Golgi apparatus. *Curr. Opin. Cell Biol.* 88:102365. doi:10.1016/j.ceb.2024.102365.

Arlt, H., K. Auffarth, R. Kurre, D. Lisse, J. Piehler, and C. Ungermann. 2015. Spatiotemporal dynamics of membrane remodeling and fusion proteins during endocytic transport. *Mol. Biol. Cell*. 26:1357–1370. doi:10.1091/mbc.E14-08-1318.

Ayala, I., F. Mascanzoni, and A. Colanzi. 2020. The Golgi ribbon: mechanisms of maintenance and disassembly during the cell cycle. *Biochem. Soc. Trans.* 48:245–256. doi:10.1042/BST20190646.

Bai, L., B.K. Jain, Q. You, H.D. Duan, M. Takar, T.R. Graham, and H. Li. 2021. Structural basis of the P4B ATPase lipid flippase activity. *Nat. Commun.* 12:5963. doi:10.1038/s41467-021-26273-0.

Baker, R.W., and F.M. Hughson. 2016. Chaperoning SNARE assembly and disassembly. *Nat. Rev. Mol. Cell Biol.* 17:465–479. doi:10.1038/nrm.2016.65.

Barlowe, C., and A. Helenius. 2016. Cargo Capture and Bulk Flow in the Early Secretory Pathway. *Annu. Rev. Cell Dev. Biol.* 32:197–222. doi:10.1146/annurev-cellbio-111315-125016.

Barlowe, C.K., and E.A. Miller. 2013. Secretory Protein Biogenesis and Traffic in the Early Secretory Pathway. *Genetics*. 193:383–410. doi:10.1534/genetics.112.142810.

Barrero, J.J., E. Papanikou, J.C. Casler, K.J. Day, and B.S. Glick. 2016. An improved reversibly dimerizing mutant of the FK506-binding protein FKBP. *Cell. Logist.* 6:e1204848. doi:10.1080/21592799.2016.1204848.

Bean, B.D.M., M. Davey, and E. Conibear. 2017. Cargo selectivity of yeast sorting nexins. *Traffic*. 18:110–122. doi:10.1111/tra.12459.

Becker, B., B. Bölinger, and M. Melkonian. 1995. Anterograde transport of algal scales through the Golgi complex is not mediated by vesicles. *Trends Cell Biol.* 5:305–307. doi:10.1016/s0962-8924(00)89047-9.

Behnia, R., F.A. Barr, J.J. Flanagan, C. Barlowe, and S. Munro. 2007. The yeast orthologue of GRASP65 forms a complex with a coiled-coil protein that contributes to ER to Golgi traffic. *J. Cell Biol.* 176:255–261. doi:10.1083/jcb.200607151.

Behnia, R., B. Panic, J.R.C. Whyte, and S. Munro. 2004. Targeting of the Arf-like GTPase Arl3p to the Golgi requires N-terminal acetylation and the membrane protein Sys1p. *Nat. Cell Biol.* 6:405–413. doi:10.1038/ncb1120.

Bekier, M.E., L. Wang, J. Li, H. Huang, D. Tang, X. Zhang, and Y. Wang. 2017. Knockout of the Golgi stacking proteins GRASP55 and GRASP65 impairs Golgi structure and function. *Mol. Biol. Cell*. 28:2833–2842. doi:10.1091/mbc.E17-02-0112.

Benjamin, J.J.R., P.P. Poon, J.D. Drysdale, X. Wang, R.A. Singer, and G.C. Johnston. 2011. Dysregulated Arl1, a regulator of post-Golgi vesicle tethering, can inhibit endosomal transport and cell proliferation in yeast. *Mol. Biol. Cell*. 22:2337–2347. doi:10.1091/mbc.E10-09-0765.

Bentson, L.F., V.A. Agbor, L.N. Agbor, A.C. Lopez, L.E. Nfonsam, S.S. Bornstein, M.A. Handel, and C.C. Linder. 2013. New point mutation in Golga3 causes multiple defects in spermatogenesis. *Andrology*. 1:440–450. doi:10.1111/j.2047-2927.2013.00070.x.

Berninsone, P., J.J. Miret, and C.B. Hirschberg. 1994. The Golgi guanosine diphosphatase is required for transport of GDP-mannose into the lumen of Saccharomyces cerevisiae Golgi vesicles. *J. Biol. Chem.* 269:207–211.

Bertin, A., M.A. McMurray, J. Pierson, L. Thai, K.L. McDonald, E.A. Zehr, G. García, P. Peters, J. Thorner, and E. Nogales. 2012. Three-dimensional ultrastructure of the septin filament network in Saccharomyces cerevisiae. *Mol. Biol. Cell*. 23:423–432. doi:10.1091/mbc.E11-10-0850.

Best, J.T., P. Xu, and T.R. Graham. 2019. Phospholipid flippases in membrane remodeling and transport carrier biogenesis. *Curr. Opin. Cell Biol.* 59:8–15. doi:10.1016/j.ceb.2019.02.004.

Best, J.T., P. Xu, J.G. McGuire, S.N. Leahy, and T.R. Graham. 2020. Yeast synaptobrevin, Snc1, engages distinct routes of postendocytic recycling mediated by a sorting nexin, Rcy1-COPI, and retromer. *Mol. Biol. Cell*. 31:944–962. doi:10.1091/mbc.E19-05-0290.

Bevis, B.J., A.T. Hammond, C.A. Reinke, and B.S. Glick. 2002. De novo formation of transitional ER sites and Golgi structures in Pichia pastoris. *Nat. Cell Biol.* 4:750–756. doi:10.1038/ncb852.

Beznoussenko, G.V., S. Parashuraman, R. Rizzo, R. Polishchuk, O. Martella, D. Di Giandomenico, A. Fusella, A. Spaar, M. Sallese, M.G. Capestrano, M. Pavelka, M.R. Vos, Y.G. Rikers, V. Helms, A.A. Mironov, and A. Luini. 2014. Transport of soluble proteins through the Golgi occurs by diffusion via continuities across cisternae. *eLife*. 3:e02009. doi:10.7554/eLife.02009.

Bilodeau, P.S., S.C. Winistorfer, W.R. Kearney, A.D. Robertson, and R.C. Piper. 2003. Vps27-Hse1 and ESCRT-I complexes cooperate to increase efficiency of sorting ubiquitinated proteins at the endosome. *J. Cell Biol.* 163:237–243. doi:10.1083/jcb.200305007.

Bindels, D.S., L. Haarbosch, L. van Weeren, M. Postma, K.E. Wiese, M. Mastop, S. Aumonier, G. Gotthard, A. Royant, M.A. Hink, and T.W.J. Gadella. 2017. mScarlet: a bright monomeric red fluorescent protein for cellular imaging. *Nat. Methods*. 14:53–56. doi:10.1038/nmeth.4074.

Black, M.W., and H.R. Pelham. 2000. A selective transport route from Golgi to late endosomes that requires the yeast GGA proteins. *J. Cell Biol.* 151:587–600. doi:10.1083/jcb.151.3.587.

Blackburn, J.B., Z. D'Souza, and V.V. Lupashin. 2019. Maintaining order: COG complex controls Golgi trafficking, processing, and sorting. *Febs Lett.* 593:2466–2487. doi:10.1002/1873-3468.13570.

von Blume, J., and A. Hausser. 2019. Lipid-dependent coupling of secretory cargo sorting and trafficking at the trans-Golgi network. *FEBS Lett.* 593:2412–2427. doi:10.1002/1873-3468.13552.

Bonfanti, L., A.A. Mironov, J.A. Martínez-Menárguez, O. Martella, A. Fusella, M. Baldassarre, R. Buccione, H.J. Geuze, A.A. Mironov, and A. Luini. 1998. Procollagen traverses the Golgi stack without leaving the lumen of cisternae: evidence for cisternal maturation. *Cell*. 95:993–1003. doi:10.1016/s0092-8674(00)81723-7.

Bonifacino, J.S., and A. Hierro. 2011. Transport according to GARP: receiving retrograde cargo at the trans-Golgi network. *Trends Cell Biol.* 21:159–167. doi:10.1016/j.tcb.2010.11.003.

Bowers, K., and T.H. Stevens. 2005. Protein transport from the late Golgi to the vacuole in the yeast Saccharomyces cerevisiae. *Biochim. Biophys. Acta*. 1744:438–454. doi:10.1016/j.bbamcr.2005.04.004.

Bräuer, P., J.L. Parker, A. Gerondopoulos, I. Zimmermann, M.A. Seeger, F.A. Barr, and S. Newstead. 2019. Structural basis for pH-dependent retrieval of ER proteins from the Golgi by the KDEL receptor. *Science*. 363:1103–1107. doi:10.1126/science.aaw2859.

Brown, F.C., C.H. Schindelhaim, and S.R. Pfeffer. 2011. GCC185 plays independent roles in Golgi structure maintenance and AP-1–mediated vesicle tethering. *J. Cell Biol.* 194:779–787. doi:10.1083/jcb.201104019.

Bryant, N.J., and T.H. Stevens. 1997. Two Separate Signals Act Independently to Localize a Yeast Late Golgi Membrane Protein through a Combination of Retrieval and Retention. *J. Cell Biol.* 136:287–297. doi:10.1083/jcb.136.2.287.

Budnik, A., and D.J. Stephens. 2009. ER exit sites--localization and control of COPII vesicle formation. *FEBS Lett.* 583:3796–3803. doi:10.1016/j.febslet.2009.10.038.

Burke, T.A., J.R. Christensen, E. Barone, C. Suarez, V. Sirotkin, and D.R. Kovar. 2014. Homeostatic actin cytoskeleton networks are regulated by assembly factor competition for monomers. *Curr. Biol. CB*. 24:579–585. doi:10.1016/j.cub.2014.01.072.

Burkhardt, J.K. 1998. The role of microtubule-based motor proteins in maintaining the structure and function of the Golgi complex. *Biochim. Biophys. Acta*. 1404:113–126. doi:10.1016/s0167-4889(98)00052-4.

Cao, X., N. Ballew, and C. Barlowe. 1998. Initial docking of ER-derived vesicles requires Uso1p and Ypt1p but is independent of SNARE proteins. *EMBO J.* 17:2156–2165. doi:10.1093/emboj/17.8.2156.

Carosi, J.M., D. Denton, S. Kumar, and T.J. Sargeant. 2023. Receptor Recycling by Retromer. *Mol. Cell. Biol.* 43:317–334. doi:10.1080/10985549.2023.2222053.

Casler, J.C., and B.S. Glick. 2020. A microscopy-based kinetic analysis of yeast vacuolar protein sorting. *eLife*. 9:e56844. doi:10.7554/eLife.56844.

Casler, J.C., N. Johnson, A.H. Krahn, A. Pantazopoulou, K.J. Day, and B.S. Glick. 2021. Clathrin adaptors mediate two sequential pathways of intra-Golgi recycling. *J. Cell Biol.* 221. doi:10.1083/jcb.202103199.

Casler, J.C., E. Papanikou, J.J. Barrero, and B.S. Glick. 2019. Maturation-driven transport and AP-1-dependent recycling of a secretory cargo in the Golgi. *J. Cell Biol.* 218:1582–1601. doi:10.1083/jcb.201807195.

Cattin-Ortolá, J., J.G.G. Kaufman, A.K. Gillingham, J.L. Wagstaff, S.-Y. Peak-Chew, T.J. Stevens, J. Boulanger, D.J. Owen, and S. Munro. 2024. Cargo selective vesicle tethering: The structural basis for binding of specific cargo proteins by the Golgi tether component TBC1D23. *Sci. Adv.* 10:eadl0608. doi:10.1126/sciadv.adl0608.

Chen, K.-Y., P.-C. Tsai, J.-W. Hsu, H.-C. Hsu, C.-Y. Fang, L.-C. Chang, Y.-T. Tsai, C.-J. Yu, and F.-J.S. Lee. 2010. Syt1p promotes activation of Arl1p at the late Golgi to recruit Imh1p. *J. Cell Sci.* 123:3478–3489. doi:10.1242/jcs.074237.

Chen, Y., D.C. Gershlick, S.Y. Park, and J.S. Bonifacino. 2017. Segregation in the Golgi complex precedes export of endolysosomal proteins in distinct transport carriers. *J. Cell Biol.* 216:4141–4151. doi:10.1083/jcb.201707172.

Chen, Y.-T., I.-H. Wang, Y.-H. Wang, W.-Y. Chiu, J.-H. Hu, W.-H. Chen, and F.-J.S. Lee. 2019. Action of Arl1 GTPase and golgin Imh1 in Ypt6-independent retrograde transport from endosomes to the trans-Golgi network. *Mol. Biol. Cell*. 30:1008–1019. doi:10.1091/mbc.E18-09-0579.

Cheung, P.P., C. Limouse, H. Mabuchi, and S.R. Pfeffer. 2015. Protein flexibility is required for vesicle tethering at the Golgi. *eLife*. 4:e12790. doi:10.7554/eLife.12790.

Cheung, P.-Y.P., and S.R. Pfeffer. 2016. Transport Vesicle Tethering at the Trans Golgi Network: Coiled Coil Proteins in Action. *Front. Cell Dev. Biol.* 4:18. doi:10.3389/fcell.2016.00018.

Chi, R.J., J. Liu, M. West, J. Wang, G. Odorizzi, and C.G. Burd. 2014. Fission of SNX-BAR-coated endosomal retrograde transport carriers is promoted by the dynamin-related protein Vps1. *J. Cell Biol.* 204:793–806. doi:10.1083/jcb.201309084.

Chidambaram, S., N. Müllers, K. Wiederhold, V. Haucke, and G.F. von Mollard. 2004. Specific interaction between SNAREs and epsin N-terminal homology (ENTH) domains of epsin-related proteins in trans-Golgi network to endosome transport. *J. Biol. Chem.* 279:4175–4179. doi:10.1074/jbc.M308667200.

Chidambaram, S., J. Zimmermann, and G.F. von Mollard. 2008. ENTH domain proteins are cargo adaptors for multiple SNARE proteins at the TGN endosome. *J. Cell Sci.* 121:329–338. doi:10.1242/jcs.012708.

Chou, H.-T., D. Dukovski, M.G. Chambers, K.M. Reinisch, and T. Walz. 2016. CATCHR, HOPS and CORVET tethering complexes share a similar architecture. *Nat. Struct. Mol. Biol.* 23:761–763. doi:10.1038/nsmb.3264.

Christis, C., and S. Munro. 2012. The small G protein Arl1 directs the trans-Golgi-specific targeting of the Arf1 exchange factors BIG1 and BIG2. *J. Cell Biol.* 196:327–335. doi:10.1083/jcb.201107115.

Clermont, Y., A. Rambourg, and L. Hermo. 1992. Segregation of secretory material in all elements of the Golgi apparatus in principal epithelial cells of the rat seminal vesicle. *Anat. Rec.* 232:349–358. doi:10.1002/ar.1092320304.

Cole, N.B., N. Sciaky, A. Marotta, J. Song, and J. Lippincott-Schwartz. 1996. Golgi dispersal during microtubule disruption: regeneration of Golgi stacks at peripheral endoplasmic reticulum exit sites. *Mol. Biol. Cell*. 7:631–650. doi:10.1091/mbc.7.4.631.

Conboy, M.J., and M.S. Cyert. 2000. Luv1p/Rki1p/Tcs3p/Vps54p, a yeast protein that localizes to the late Golgi and early endosome, is required for normal vacuolar morphology. *Mol. Biol. Cell*. 11:2429–2443. doi:10.1091/mbc.11.7.2429.

Conde, R., G. Pablo, R. Cueva, and G. Larriba. 2003. Screening for new yeast mutants affected in mannosylphosphorylation of cell wall mannoproteins. *Yeast Chichester Engl.* 20:1189–1211. doi:10.1002/yea.1032.

Conibear, E., J.N. Cleck, and T.H. Stevens. 2003. Vps51p Mediates the Association of the GARP (Vps52/53/54) Complex with the Late Golgi t-SNARE Tlg1p. *Mol. Biol. Cell*. 14:1610–1623. doi:10.1091/mbc.e02-10-0654.

Conibear, E., and T.H. Stevens. 2000. Vps52p, Vps53p, and Vps54p Form a Novel Multisubunit Complex Required for Protein Sorting at the Yeast Late Golgi. *Mol. Biol. Cell*. 11:305–323. doi:10.1091/mbc.11.1.305.

Cooper, A.A., and T.H. Stevens. 1996. Vps10p cycles between the late-Golgi and prevacuolar compartments in its function as the sorting receptor for multiple yeast vacuolar hydrolases. *J. Cell Biol.* 133:529–541. doi:10.1083/jcb.133.3.529.

Copic, A., T.L. Starr, and R. Schekman. 2007. Ent3p and Ent5p exhibit cargo-specific functions in trafficking proteins between the trans-Golgi network and the endosomes in yeast. *Mol. Biol. Cell*. 18:1803–1815. doi:10.1091/mbc.e06-11-1000.

Cosson, P., and F. Letourneur. 1997. Coatomer (COPI)-coated vesicles: role in intracellular transport and protein sorting. *Curr. Opin. Cell Biol.* 9:484–487. doi:10.1016/s0955-0674(97)80023-3.

Costaguta, G., M.C. Duncan, G.E. Fernández, G.H. Huang, and G.S. Payne. 2006. Distinct roles for TGN/endosome epsin-like adaptors Ent3p and Ent5p. *Mol. Biol. Cell*. 17:3907–3920. doi:10.1091/mbc.e06-05-0410.

Cottam, N.P., K.M. Wilson, B.G. Ng, C. Körner, H.H. Freeze, and D. Ungar. 2014. Dissecting functions of the conserved oligomeric Golgi tethering complex using a cell-free assay. *Traffic Cph. Den.* 15:12–21. doi:10.1111/tra.12128.

Daboussi, L., G. Costaguta, R. Ghukasyan, and G.S. Payne. 2017. Conserved role for Gga proteins in phosphatidylinositol 4-kinase localization to the trans-Golgi network. *Proc. Natl. Acad. Sci.* 114:3433–3438. doi:10.1073/pnas.1615163114.

Daboussi, L., G. Costaguta, and G.S. Payne. 2012. Phosphoinositide-mediated clathrin adaptor progression at the trans-Golgi network. *Nat. Cell Biol.* 14:239–248. doi:10.1038/ncb2427.

Dahara, R., and D. Bhattacharyya. 2025. Intra-Golgi Golgin PpSgm1 and GRIP domain Golgin PpImh1 synergistically mediate Golgi cisternal stacking. *J. Cell Sci.* jcs.263612. doi:10.1242/jcs.263612.

Dalton, L.E., B.D.M. Bean, M. Davey, and E. Conibear. 2017. Quantitative high-content imaging identifies novel regulators of Neo1 trafficking at endosomes. *Mol. Biol. Cell*. 28:1539–1550. doi:10.1091/mbc.e16-11-0772.

D'Angelo, G., S. Capasso, L. Sticco, and D. Russo. 2013. Glycosphingolipids: synthesis and functions. *FEBS J.* 280:6338–6353. doi:10.1111/febs.12559.

Day, K.J., J.C. Casler, and B.S. Glick. 2018. Budding Yeast Has a Minimal Endomembrane System. *Dev. Cell*. 44:56-72.e4. doi:10.1016/j.devcel.2017.12.014.

Defelipe, L.A., K. Veith, O. Burastero, T. Kupriianova, I. Bento, M. Skruzny, K. Kölbel, C. Uetrecht, R. Thuenauer, and M.M. García-Alai. 2024. Subtleties in Clathrin heavy chain binding boxes provide selectivity among adaptor proteins of budding yeast. *Nat. Commun.* 15:9655. doi:10.1038/s41467-024-54037-z.

Del Bel, L.M., and J.A. Brill. 2018. Sac1, a lipid phosphatase at the interface of vesicular and nonvesicular transport. *Traffic Cph. Den.* 19:301–318. doi:10.1111/tra.12554.

Dell'Angelica, E.C., R. Puertollano, C. Mullins, R.C. Aguilar, J.D. Vargas, L.M. Hartnell, and J.S. Bonifacino. 2000. GGAs: a family of ADP ribosylation factor-binding proteins related to adaptors and associated with the Golgi complex. *J. Cell Biol.* 149:81–94. doi:10.1083/jcb.149.1.81.

Deng, Y., Y. Guo, H. Watson, W.-C. Au, M. Shakoury-Elizeh, M.A. Basrai, J.S. Bonifacino, and C.C. Philpott. 2009. Gga2 Mediates Sequential Ubiquitin-independent and Ubiquitin-dependent Steps in the Trafficking of ARN1 from the trans-Golgi Network to the Vacuole. *J. Biol. Chem.* 284:23830–23841. doi:10.1074/jbc.M109.030015.

Di Martino, R., L. Sticco, and A. Luini. 2019. Regulation of cargo export and sorting at the trans-Golgi network. *FEBS Lett.* 593:2306–2318. doi:10.1002/1873-3468.13572.

Diao, A., D. Rahman, D.J.C. Pappin, J. Lucocq, and M. Lowe. 2003. The coiled-coil membrane protein golgin-84 is a novel rab effector required for Golgi ribbon formation. *J. Cell Biol.* 160:201–212. doi:10.1083/jcb.200207045.

Donohoe, B.S., B.-H. Kang, and L.A. Staehelin. 2007. Identification and characterization of COPIa- and COPIb-type vesicle classes associated with plant and algal Golgi. *Proc. Natl. Acad. Sci. U. S. A.* 104:163–168. doi:10.1073/pnas.0609818104.

Duan, H.D., B.K. Jain, H. Li, T.R. Graham, and H. Li. 2024. Structural insight into an Arl1-ArfGEF complex involved in Golgi recruitment of a GRIP-domain golgin. *Nat. Commun.* 15:1942. doi:10.1038/s41467-024-46304-w.

Dubuke, M.L., and M. Munson. 2016. The Secret Life of Tethers: The Role of Tethering Factors in SNARE Complex Regulation. *Front. Cell Dev. Biol.* 4. doi:10.3389/fcell.2016.00042.

Duncan, M.C. 2022. New directions for the clathrin adaptor AP-1 in cell biology and human disease. *Curr. Opin. Cell Biol.* 76:102079. doi:10.1016/j.ceb.2022.102079.

Duncan, M.C., G. Costaguta, and G.S. Payne. 2003. Yeast epsin-related proteins required for Golgi-endosome traffic define a gamma-adaptin ear-binding motif. *Nat. Cell Biol.* 5:77–81. doi:10.1038/ncb901.

Dunphy, W.G., and J.E. Rothman. 1985. Compartmental organization of the Golgi stack. *Cell*. 42:13–21. doi:10.1016/s0092-8674(85)80097-0.

Dürr, G., J. Strayle, R. Plemper, S. Elbs, S.K. Klee, P. Catty, D.H. Wolf, and H.K. Rudolph. 1998. The medial-Golgi ion pump Pmr1 supplies the yeast secretory pathway with Ca2+ and Mn2+ required for glycosylation, sorting, and endoplasmic reticulum-associated protein degradation. *Mol. Biol. Cell*. 9:1149–1162. doi:10.1091/mbc.9.5.1149.

Eising, S., L. Thiele, and F. Fröhlich. 2019. A systematic approach to identify recycling endocytic cargo depending on the GARP complex. *eLife*. 8:e42837. doi:10.7554/eLife.42837.

Enkler, L., B. Rinaldi, J.O. de Craene, P. Hammann, O. Nureki, B. Senger, S. Friant, and H.D. Becker. 2021. Cex1 is a component of the COPI intracellular trafficking machinery. *Biol. Open*. 10:bio058528. doi:10.1242/bio.058528.

Eugster, A., G. Frigerio, M. Dale, and R. Duden. 2000. COP I domains required for coatomer integrity, and novel interactions with ARF and ARF-GAP. *EMBO J.* 19:3905–3917. doi:10.1093/emboj/19.15.3905.

Farquhar, M.G., and H.-P. Hauri. 1997. Protein sorting and vesicular traffic in the Golgi apparatus. *In* The Golgi Apparatus. E.G. Berger and J. Roth, editors. Birkhäuser, Basel. 63–129.

Fegan, A., B. White, J.C.T. Carlson, and C.R. Wagner. 2010. Chemically controlled protein assembly: techniques and applications. *Chem. Rev.* 110:3315–3336. doi:10.1021/cr8002888.

Feinstein, M., H. Flusser, T. Lerman-Sagie, B. Ben-Zeev, D. Lev, O. Agamy, I. Cohen, R. Kadir, S. Sivan, E. Leshinsky-Silver, B. Markus, and O.S. Birk. 2014. VPS53 mutations cause progressive cerebello-cerebral atrophy type 2 (PCCA2). *J. Med. Genet.* 51:303–308. doi:10.1136/jmedgenet-2013-101823.

Feng, Z., K. Yang, and J.C. Pastor-Pareja. 2021. Tales of the ER-Golgi Frontier: Drosophila-Centric Considerations on Tango1 Function. *Front. Cell Dev. Biol.* 8:619022. doi:10.3389/fcell.2020.619022.

Finger, F.P., T.E. Hughes, and P. Novick. 1998. Sec3p is a spatial landmark for polarized secretion in budding yeast. *Cell*. 92:559–571. doi:10.1016/s0092-8674(00)80948-4.

Finnigan, G.C., G.E. Cronan, H.J. Park, S. Srinivasan, F.A. Quiocho, and T.H. Stevens. 2012. Sorting of the yeast vacuolar-type, proton-translocating ATPase enzyme complex (V-ATPase): identification of a necessary and sufficient Golgi/endosomal retention signal in Stv1p. *J. Biol. Chem.* 287:19487–19500. doi:10.1074/jbc.M112.343814.

Fitzgerald, I., and B.S. Glick. 2014. Secretion of a foreign protein from budding yeasts is enhanced by cotranslational translocation and by suppression of vacuolar targeting. *Microb. Cell Factories*. 13:125. doi:10.1186/s12934-014-0125-0.

Fölsch, H. 2015. Role of the epithelial cell-specific clathrin adaptor complex AP-1B in cell polarity. *Cell. Logist.* 5:e1074331. doi:10.1080/21592799.2015.1074331.

Ford, C., A. Parchure, J. von Blume, and C.G. Burd. 2021. Cargo sorting at the trans-Golgi network at a glance. *J. Cell Sci.* 134:jcs259110. doi:10.1242/jcs.259110.

Fourriere, L., A.J. Jimenez, F. Perez, and G. Boncompain. 2020. The role of microtubules in secretory protein transport. *J. Cell Sci.* 133:jcs237016. doi:10.1242/jcs.237016.

Franke, W.W., J. Kartenbeck, S. Krien, W.J. Vander Woude, U. Scheer, and D.J. Morré. 1972. Inter- and intracisternal elements of the Golgi apparatus. *Z. Für Zellforsch. Mikrosk. Anat.* 132:365–380. doi:10.1007/BF02450714.

Fridmann-Sirkis, Y., H.M. Kent, M.J. Lewis, P.R. Evans, and H.R.B. Pelham. 2006. Structural analysis of the interaction between the SNARE Tlg1 and Vps51. *Traffic Cph. Den.* 7:182–190. doi:10.1111/j.1600-0854.2005.00374.x.

Fridmann-Sirkis, Y., S. Siniossoglou, and H.R. Pelham. 2004. TMF is a golgin that binds Rab6 and influences Golgi morphology. *BMC Cell Biol.* 5:18. doi:10.1186/1471-2121-5-18.

Fritzler, M.J., J.C. Hamel, R.L. Ochs, and E.K. Chan. 1993. Molecular characterization of two human autoantigens: unique cDNAs encoding 95- and 160-kD proteins of a putative family in the Golgi complex. *J. Exp. Med.* 178:49–62. doi:10.1084/jem.178.1.49.

Fröhlich, F., C. Petit, N. Kory, R. Christiano, H.-K. Hannibal-Bach, M. Graham, X. Liu, C.S. Ejsing, R.V. Farese, and T.C. Walther. 2015. The GARP complex is required for cellular sphingolipid homeostasis. *eLife*. 4. doi:10.7554/eLife.08712.

Froquet, R., N. Cherix, R. Birke, M. Benghezal, E. Cameroni, F. Letourneur, H.-U. Mösch, C. De Virgilio, and P. Cosson. 2008. Control of Cellular Physiology by TM9 Proteins in Yeast and *Dictyostelium**. *J. Biol. Chem.* 283:6764–6772. doi:10.1074/jbc.M704484200.

Fuller, R.S., R.E. Sterne, and J. Thorner. 1988. Enzymes required for yeast prohormone processing. *Annu. Rev. Physiol.* 50:345–362. doi:10.1146/annurev.ph.50.030188.002021.

Funato, K., and H. Riezman. 2001. Vesicular and nonvesicular transport of ceramide from ER to the Golgi apparatus in yeast. *J. Cell Biol.* 155:949–959. doi:10.1083/jcb.200105033.

Gan, L., C.T. Ng, C. Chen, and S. Cai. 2019. A collection of yeast cellular electron cryotomography data. *GigaScience*. 8:giz077. doi:10.1093/gigascience/giz077.

Gao, J., R. Franzkoch, C. Rocha-Roa, O.E. Psathaki, M. Hensel, S. Vanni, and C. Ungermann. 2025. Any1 is a phospholipid scramblase involved in endosome biogenesis. *J. Cell Biol.* 224:e202410013. doi:10.1083/jcb.202410013.

Gaynor, E.C., T.R. Graham, and S.D. Emr. 1998. COPI in ER/Golgi and intra-Golgi transport: do yeast COPI mutants point the way? *Biochim. Biophys. Acta*. 1404:33–51. doi:10.1016/s0167-4889(98)00045-7.

Gerrard, S.R., N.J. Bryant, and T.H. Stevens. 2000. VPS21 controls entry of endocytosed and biosynthetic proteins into the yeast prevacuolar compartment. *Mol. Biol. Cell*. 11:613–626. doi:10.1091/mbc.11.2.613.

Gershlick, D.C., M. Ishida, J.R. Jones, A. Bellomo, J.S. Bonifacino, and D.B. Everman. 2019. A neurodevelopmental disorder caused by mutations in the VPS51 subunit of the GARP and EARP complexes. *Hum. Mol. Genet.* 28:1548–1560. doi:10.1093/hmg/ddy423.

Gerst, J.E. 1997. Conserved alpha-helical segments on yeast homologs of the synaptobrevin/VAMP family of v-SNAREs mediate exocytic function. *J. Biol. Chem.* 272:16591–16598. doi:10.1074/jbc.272.26.16591.

Ghosh, P., N.M. Dahms, and S. Kornfeld. 2003. Mannose 6-phosphate receptors: new twists in the tale. *Nat. Rev. Mol. Cell Biol.* 4:202–213. doi:10.1038/nrm1050.

Gillingham, A.K. 2017. At the ends of their tethers! How coiled-coil proteins capture vesicles at the Golgi. *Biochem. Soc. Trans.* 46:43–50. doi:10.1042/BST20170188.

Gillingham, A.K., and S. Munro. 2016. Finding the Golgi: Golgin Coiled-Coil Proteins Show the Way. *Trends Cell Biol.* 26:399–408. doi:10.1016/j.tcb.2016.02.005.

Gillingham, A.K., and S. Munro. 2019. Transport carrier tethering - how vesicles are captured by organelles. *Curr. Opin. Cell Biol.* 59:140–146. doi:10.1016/j.ceb.2019.04.010.

Gillingham, A.K., A.H.Y. Tong, C. Boone, and S. Munro. 2004. The GTPase Arf1p and the ER to Golgi cargo receptor Erv14p cooperate to recruit the golgin Rud3p to the cis-Golgi. *J. Cell Biol.* 167:281–292. doi:10.1083/jcb.200407088.

Glick, B.S. 2014. Integrated self-organization of transitional ER and early Golgi compartments. *BioEssays News Rev. Mol. Cell. Dev. Biol.* 36:129–133. doi:10.1002/bies.201300131.

Glick, B.S., T. Elston, and G. Oster. 1997. A cisternal maturation mechanism can explain the asymmetry of the Golgi stack. *FEBS Lett.* 414:177–181. doi:10.1016/s0014-5793(97)00984-8.

Glick, B.S., and A. Luini. 2011. Models for Golgi traffic: a critical assessment. *Cold Spring Harb. Perspect. Biol.* 3:a005215. doi:10.1101/cshperspect.a005215.

Glick, B.S., and V. Malhotra. 1998. The Curious Status of the Golgi Apparatus. *Cell*. 95:883–889. doi:10.1016/S0092-8674(00)81713-4.

Glick, B.S., and A. Nakano. 2009. Membrane Traffic Within the Golgi Apparatus. *Annu. Rev. Cell Dev. Biol.* 25:113–132. doi:10.1146/annurev.cellbio.24.110707.175421.

Goud, B., and P.A. Gleeson. 2010. TGN golgins, Rabs and cytoskeleton: regulating the Golgi trafficking highways. *Trends Cell Biol.* 20:329–336. doi:10.1016/j.tcb.2010.02.006.

Goud, B., S. Liu, and B. Storrie. 2018. Rab proteins as major determinants of the Golgi complex structure. *Small GTPases*. 9:66–75. doi:10.1080/21541248.2017.1384087.

Grant, B.D., and J.G. Donaldson. 2009. Pathways and mechanisms of endocytic recycling. *Nat. Rev. Mol. Cell Biol.* 10:597–608. doi:10.1038/nrm2755.

Grimm, J.B., L. Xie, J.C. Casler, R. Patel, A.N. Tkachuk, N. Falco, H. Choi, J. Lippincott-Schwartz, T.A. Brown, B.S. Glick, Z. Liu, and L.D. Lavis. 2021. A General Method to Improve Fluorophores Using Deuterated Auxochromes. *JACS Au*. 1:690–696. doi:10.1021/jacsau.1c00006.

Grissom, J.H., V.A. Segarra, and R.J. Chi. 2020. New Perspectives on SNARE Function in the Yeast Minimal Endomembrane System. *Genes*. 11:899. doi:10.3390/genes11080899.

Gurunathan, S., D. Chapman-Shimshoni, S. Trajkovic, and J.E. Gerst. 2000. Yeast exocytic v-SNAREs confer endocytosis. *Mol. Biol. Cell*. 11:3629–3643. doi:10.1091/mbc.11.10.3629.

Gut, A., F. Kappeler, N. Hyka, M.S. Balda, H.P. Hauri, and K. Matter. 1998. Carbohydrate-mediated Golgi to cell surface transport and apical targeting of membrane proteins. *EMBO J.* 17:1919–1929. doi:10.1093/emboj/17.7.1919.

Hagen, W.J.H., W. Wan, and J.A.G. Briggs. 2017. Implementation of a cryo-electron tomography tilt-scheme optimized for high resolution subtomogram averaging. *J. Struct. Biol.* 197:191–198. doi:10.1016/j.jsb.2016.06.007.

Hammond, A.T., and B.S. Glick. 2000. Dynamics of transitional endoplasmic reticulum sites in vertebrate cells. *Mol. Biol. Cell*. 11:3013–3030. doi:10.1091/mbc.11.9.3013.

Hardwick, K.G., M.J. Lewis, J. Semenza, N. Dean, and H.R. Pelham. 1990. ERD1, a yeast gene required for the retention of luminal endoplasmic reticulum proteins, affects glycoprotein processing in the Golgi apparatus. *EMBO J.* 9:623–630. doi:10.1002/j.1460-2075.1990.tb08154.x.

Haruki, H., J. Nishikawa, and U.K. Laemmli. 2008. The Anchor-Away Technique: Rapid, Conditional Establishment of Yeast Mutant Phenotypes. *Mol. Cell*. 31:925–932. doi:10.1016/j.molcel.2008.07.020.

Hausman-Kedem, M., S. Ben-Shachar, S. Menascu, K. Geva, L. Sagie, and A. Fattal-Valevski. 2019. VPS53 gene is associated with a new phenotype of complicated hereditary spastic paraparesis. *Neurogenetics*. 20:187–195. doi:10.1007/s10048-019-00586-1.

Hegelund, J.N., T.P. Jahn, L. Baekgaard, M.G. Palmgren, and J.K. Schjoerring. 2010. Transmembrane nine proteins in yeast and Arabidopsis affect cellular metal contents without changing vacuolar morphology. *Physiol. Plant.* 140:355–367. doi:10.1111/j.1399-3054.2010.01404.x.

Hein, M.Y., D. Peng, V. Todorova, F. McCarthy, K. Kim, C. Liu, L. Savy, C. Januel, R. Baltazar-Nunez, M. Sekhar, S. Vaid, S. Bax, M. Vangipuram, J. Burgess, L. Njoya, E. Wang, I.E. Ivanov, J.R. Byrum, S. Pradeep, C.G. Gonzalez, Y. Aniseia, J.S. Creery, A.H. McMorrow, S. Sunshine, S. Yeung-Levy, B.C. DeFelice, S.B. Mehta, D.N. Itzhak, J.E. Elias, and M.D. Leonetti. 2025. Global organelle profiling reveals subcellular localization and remodeling at proteome scale. *Cell*. 188:1137-1155.e20. doi:10.1016/j.cell.2024.11.028.

Henne, W.M., N.J. Buchkovich, and S.D. Emr. 2011. The ESCRT Pathway. *Dev. Cell*. 21:77–91. doi:10.1016/j.devcel.2011.05.015.

Highland, C.M., and J.C. Fromme. 2021. Arf1 directly recruits the Pik1-Frq1 PI4K complex to regulate the final stages of Golgi maturation. *Mol. Biol. Cell*. mbc.E21-02-0069. doi:10.1091/mbc.E21-02-0069.

Hinners, I., and S.A. Tooze. 2003. Changing directions: clathrin-mediated transport between the Golgi and endosomes. *J. Cell Sci.* 116:763–771. doi:10.1242/jcs.00270.

Hirata, T., M. Fujita, S. Nakamura, K. Gotoh, D. Motooka, Y. Murakami, Y. Maeda, and T. Kinoshita. 2015. Post-Golgi anterograde transport requires GARP-dependent endosome-to-TGN retrograde transport. *Mol. Biol. Cell*. 26:3071–3084. doi:10.1091/mbc.E14-11-1568.

Hirst, J., G.H.H. Borner, R. Antrobus, A.A. Peden, N.A. Hodson, D.A. Sahlender, and M.S. Robinson. 2012. Distinct and Overlapping Roles for AP-1 and GGAs Revealed by the "Knocksideways" System. *Curr. Biol.* 22:1711–1716. doi:10.1016/j.cub.2012.07.012.

Hirst, J., J.R. Edgar, G.H.H. Borner, S. Li, D.A. Sahlender, R. Antrobus, and M.S. Robinson. 2015. Contributions of epsinR and gadkin to clathrin-mediated intracellular trafficking. *Mol. Biol. Cell*. 26:3085–3103. doi:10.1091/mbc.E15-04-0245.

Hirst, J., W.W. Lui, N.A. Bright, N. Totty, M.N. Seaman, and M.S. Robinson. 2000. A family of proteins with gamma-adaptin and VHS domains that facilitate trafficking between the trans-Golgi network and the vacuole/lysosome. *J. Cell Biol.* 149:67–80. doi:10.1083/jcb.149.1.67.

Homma, Y., and M. Fukuda. 2021. Knockout analysis of Rab6 effector proteins revealed the role of VPS52 in the secretory pathway. *Biochem. Biophys. Res. Commun.* 561:151–157. doi:10.1016/j.bbrc.2021.05.009.

Hong, W., and S. Lev. 2014. Tethering the assembly of SNARE complexes. *Trends Cell Biol.* 24:35–43. doi:10.1016/j.tcb.2013.09.006.

Hsu, J.-W., P.-H. Tang, I.-H. Wang, C.-L. Liu, W.-H. Chen, P.-C. Tsai, K.-Y. Chen, K.-J. Chen, C.-J. Yu, and F.-J.S. Lee. 2016. Unfolded protein response regulates yeast small GTPase Arl1p activation at late Golgi via phosphorylation of Arf GEF Syt1p. *Proc. Natl. Acad. Sci. U. S. A.* 113:E1683-1690. doi:10.1073/pnas.1518260113.

Hua, Z., P. Fatheddin, and T.R. Graham. 2002. An essential subfamily of Drs2p-related P-type ATPases is required for protein trafficking between Golgi complex and endosomal/vacuolar system. *Mol. Biol. Cell*. 13:3162–3177. doi:10.1091/mbc.e02-03-0172.

Huh, W.-K., J.V. Falvo, L.C. Gerke, A.S. Carroll, R.W. Howson, J.S. Weissman, and E.K. O'Shea. 2003. Global analysis of protein localization in budding yeast. *Nature*. 425:686–691. doi:10.1038/nature02026.

Humphreys, I.R., J. Pei, M. Baek, A. Krishnakumar, I. Anishchenko, S. Ovchinnikov, J. Zhang, T.J. Ness, S. Banjade, S.R. Bagde, V.G. Stancheva, X.-H. Li, K. Liu, Z. Zheng, D.J. Barrero, U. Roy, J. Kuper, I.S. Fernández, B. Szakal, D. Branzei, J. Rizo, C. Kisker, E.C. Greene, S. Biggins, S. Keeney, E.A. Miller, J.C. Fromme, T.L. Hendrickson, Q. Cong, and D. Baker. 2021. Computed structures of core eukaryotic protein complexes. *Science*. doi:10.1126/science.abm4805.

Hung, C.-W., Q.L. Aoh, A.P. Joglekar, G.S. Payne, and M.C. Duncan. 2012. Adaptor autoregulation promotes coordinated binding within clathrin coats. *J. Biol. Chem.* 287:17398–17407. doi:10.1074/jbc.M112.349035.

Hung, C.-W., and M.C. Duncan. 2016. Clathrin binding by the adaptor Ent5 promotes late stages of clathrin coat maturation. *Mol. Biol. Cell*. 27:1143–1153. doi:10.1091/mbc.E15-08-0588.

Huotari, J., and A. Helenius. 2011. Endosome maturation. *EMBO J.* 30:3481–3500. doi:10.1038/emboj.2011.286.

Ikeda, A., P. Schlarmann, K. Kurokawa, A. Nakano, H. Riezman, and K. Funato. 2020. Tricalbins Are Required for Non-vesicular Ceramide Transport at ER-Golgi Contacts and Modulate Lipid Droplet Biogenesis. *iScience*. 23:101603. doi:10.1016/j.isci.2020.101603.

Ishida, M., and J.S. Bonifacino. 2019. ARFRP1 functions upstream of ARL1 and ARL5 to coordinate recruitment of distinct tethering factors to the trans-Golgi network. *J. Cell Biol.* 218:3681–3696. doi:10.1083/jcb.201905097.

Ishida, R., A. Yamamoto, K. Nakayama, M. Sohda, Y. Misumi, T. Yasunaga, and N. Nakamura. 2015. GM130 is a parallel tetramer with a flexible rod-like structure and N-terminally open (Y-shaped) and closed (I-shaped) conformations. *FEBS J.* 282:2232–2244. doi:10.1111/febs.13271.

Ishii, M., V.V. Lupashin, and A. Nakano. 2018. Detailed analysis of the interaction of yeast COG complex. *Cell Struct. Funct.* 43:119–127. doi:10.1247/csf.18014.

Iwase, M., J. Luo, E. Bi, and A. Toh-e. 2007. Shs1 Plays Separable Roles in Septin Organization and Cytokinesis in Saccharomyces cerevisiae. *Genetics*. 177:215–229. doi:10.1534/genetics.107.073007.

Jackson, L.P. 2014. Structure and mechanism of COPI vesicle biogenesis. *Curr. Opin. Cell Biol.* 29:67–73. doi:10.1016/j.ceb.2014.04.009.

Jain, B.K., R. Dahara, and D. Bhattacharyya. 2019. The golgin PpImh1 mediates reversible cisternal stacking in the Golgi of the budding yeast Pichia pastoris. *J. Cell Sci.* 132. doi:10.1242/jcs.230672.

Jain, B.K., P.S. Thapa, A. Varma, and D. Bhattacharyya. 2018. Identification and characterization of GRIP domain Golgin PpImh1 from Pichia pastoris. *Yeast Chichester Engl.* 35:499–506. doi:10.1002/yea.3317.

Jensen, D., and R. Schekman. 2011. COPII-mediated vesicle formation at a glance. *J. Cell Sci.* 124:1–4. doi:10.1242/jcs.069773.

Jin, Y., A. Sultana, P. Gandhi, E. Franklin, S. Hamamoto, A.R. Khan, M. Munson, R. Schekman, and L.S. Weisman. 2011. Myosin V transports secretory vesicles via a Rab GTPase cascade and interaction with the exocyst complex. *Dev. Cell*. 21:1156–1170. doi:10.1016/j.devcel.2011.10.009.

Johnson, N., and B.S. Glick. 2019. 4D Microscopy of Yeast. *J. Vis. Exp. JoVE*. doi:10.3791/58618.

Khakurel, A., T. Kudlyk, J.S. Bonifacino, and V.V. Lupashin. 2021. The Golgi-associated retrograde protein (GARP) complex plays an essential role in the maintenance of the Golgi glycosylation machinery. *Mol. Biol. Cell*. 32:1594–1610. doi:10.1091/mbc.E21-04-0169.

Khakurel, A., T. Kudlyk, I. Pokrovskaya, Z. D'Souza, and V.V. Lupashin. 2022. GARP dysfunction results in COPI displacement, depletion of Golgi v-SNAREs and calcium homeostasis proteins. *Front. Cell Dev. Biol.* 10.

Khakurel, A., and V.V. Lupashin. 2023. Role of GARP Vesicle Tethering Complex in Golgi Physiology. *Int. J. Mol. Sci.* 24:6069. doi:10.3390/ijms24076069.

Khan, Y.A., K.I. White, and A.T. Brunger. 2022. The AAA+ superfamily: a review of the structural and mechanistic principles of these molecular machines. *Crit. Rev. Biochem. Mol. Biol.* 57:156–187. doi:10.1080/10409238.2021.1979460.

Kim, D.-W. 2003. Characterization of Grp1p, a novel cis-Golgi matrix protein. *Biochem. Biophys. Res. Commun.* 303:370–378. doi:10.1016/S0006-291X(03)00341-3.

Kim, D.W., M. Sacher, A. Scarpa, A.M. Quinn, and S. Ferro-Novick. 1999. High-copy suppressor analysis reveals a physical interaction between Sec34p and Sec35p, a protein implicated in vesicle docking. *Mol. Biol. Cell*. 10:3317–3329. doi:10.1091/mbc.10.10.3317.

Kim, J.J., Z. Lipatova, U. Majumdar, and N. Segev. 2016. Regulation of Golgi Cisternal Progression by Ypt/Rab GTPases. *Dev. Cell*. 36:440–452. doi:10.1016/j.devcel.2016.01.016.

Kjer-Nielsen, L., R.D. Teasdale, C. van Vliet, and P.A. Gleeson. 1999. A novel Golgi-localisation domain shared by a class of coiled-coil peripheral membrane proteins. *Curr. Biol.* 9:385–390. doi:10.1016/S0960-9822(99)80168-7.

Koike, S., and R. Jahn. 2019. SNAREs define targeting specificity of trafficking vesicles by combinatorial interaction with tethering factors. *Nat. Commun.* 10:1608. doi:10.1038/s41467-019-09617-9.

Kojima, A., J.Y. Toshima, C. Kanno, C. Kawata, and J. Toshima. 2012. Localization and functional requirement of yeast Na+/H+ exchanger, Nhx1p, in the endocytic and protein recycling pathway. *Biochim. Biophys. Acta*. 1823:534–543. doi:10.1016/j.bbamcr.2011.12.004.

Kremer, J.R., D.N. Mastronarde, and J.R. McIntosh. 1996. Computer visualization of three-dimensional image data using IMOD. *J. Struct. Biol.* 116:71–76. doi:10.1006/jsbi.1996.0013.

Krogh, A., B. Larsson, G. von Heijne, and E.L. Sonnhammer. 2001. Predicting transmembrane protein topology with a hidden Markov model: application to complete genomes. *J. Mol. Biol.* 305:567–580. doi:10.1006/jmbi.2000.4315.

Kulkarni-Gosavi, P., C. Makhoul, and P.A. Gleeson. 2019. Form and function of the Golgi apparatus: scaffolds, cytoskeleton and signalling. *FEBS Lett.* 593:2289–2305. doi:10.1002/1873-3468.13567.

Kurokawa, K., M. Okamoto, and A. Nakano. 2014. Contact of cis-Golgi with ER exit sites executes cargo capture and delivery from the ER. *Nat. Commun.* 5:3653. doi:10.1038/ncomms4653.

Kurokawa, K., H. Osakada, T. Kojidani, M. Waga, Y. Suda, H. Asakawa, T. Haraguchi, and A. Nakano. 2019. Visualization of secretory cargo transport within the Golgi apparatus. *J. Cell Biol.* 218:1602–1618. doi:10.1083/jcb.201807194.

Lai, C.-C., W.-Y. Chiu, Y.-T. Chen, C.-L. Wu, and F.-J.S. Lee. 2023. The SNARE-associated protein Sft2 functions in Imh1-mediated SNARE recycling transport upon ER stress. *Mol. Biol. Cell*. 34:ar112. doi:10.1091/mbc.E23-01-0019.

Lavieu, G., M.H. Dunlop, A. Lerich, H. Zheng, F. Bottanelli, and J.E. Rothman. 2014. The Golgi ribbon structure facilitates anterograde transport of large cargoes. *Mol. Biol. Cell*. 25:3028–3036. doi:10.1091/mbc.E14-04-0931.

Lázaro-Diéguez, F., N. Jiménez, H. Barth, A.J. Koster, J. Renau-Piqueras, J.L. Llopis, K.N.J. Burger, and G. Egea. 2006. Actin filaments are involved in the maintenance of Golgi cisternae morphology and intra-Golgi pH. *Cell Motil. Cytoskeleton*. 63:778–791. doi:10.1002/cm.20161.

Leblond, C.P. 1989. Synthesis and secretion of collagen by cells of connective tissue, bone, and dentin. *Anat. Rec.* 224:123–138. doi:10.1002/ar.1092240204.

Lee, I., N. Tiwari, M.H. Dunlop, M. Graham, X. Liu, and J.E. Rothman. 2014. Membrane adhesion dictates Golgi stacking and cisternal morphology. *Proc. Natl. Acad. Sci.* 111:1849–1854. doi:10.1073/pnas.1323895111.

van Leeuwen, J., C. Pons, J.C. Mellor, T.N. Yamaguchi, H. Friesen, J. Koschwanez, M.M. Ušaj, M. Pechlaner, M. Takar, M. Ušaj, B. VanderSluis, K. Andrusiak, P. Bansal, A. Baryshnikova, C.E. Boone, J. Cao, A. Cote, M. Gebbia, G. Horecka, I. Horecka, E. Kuzmin, N. Legro, W. Liang, N. van Lieshout, M. McNee, B.-J. San Luis, F. Shaeri, E. Shuteriqi, S. Sun, L. Yang, J.-Y. Youn, M. Yuen, M. Costanzo, A.-C. Gingras, P. Aloy, C. Oostenbrink, A. Murray, T.R. Graham, C.L. Myers, B.J. Andrews, F.P. Roth, and C. Boone. 2016. Exploring genetic suppression interactions on a global scale. *Science*. 354:aag0839. doi:10.1126/science.aag0839.

Lerer-Goldshtein, T., S. Bel, S. Shpungin, E. Pery, B. Motro, R.S. Goldstein, S.I. Bar-Sheshet, H. Breitbart, and U. Nir. 2010. TMF/ARA160: A key regulator of sperm development. *Dev. Biol.* 348:12–21. doi:10.1016/j.ydbio.2010.07.033.

Lesa, G.M., J. Seemann, J. Shorter, J. Vandekerckhove, and G. Warren. 2000. The Amino-terminal Domain of the Golgi Protein Giantin Interacts Directly with the Vesicle-tethering Protein p115*. *J. Biol. Chem.* 275:2831–2836. doi:10.1074/jbc.275.4.2831.

Lewis, M.J., B.J. Nichols, C. Prescianotto-Baschong, H. Riezman, and H.R. Pelham. 2000. Specific retrieval of the exocytic SNARE Snc1p from early yeast endosomes. *Mol. Biol. Cell*. 11:23–38. doi:10.1091/mbc.11.1.23.

Lewis, M.J., and H.R. Pelham. 1992. Ligand-induced redistribution of a human KDEL receptor from the Golgi complex to the endoplasmic reticulum. *Cell*. 68:353–364. doi:10.1016/0092-8674(92)90476-s.

Liewen, H., I. Meinhold-Heerlein, V. Oliveira, R. Schwarzenbacher, G. Luo, A. Wadle, M. Jung, M. Pfreundschuh, and F. Stenner-Liewen. 2005. Characterization of the human GARP (Golgi associated retrograde protein) complex. *Exp. Cell Res.* 306:24–34. doi:10.1016/j.yexcr.2005.01.022.

Lipatova, Z., and N. Segev. 2019. Ypt/Rab GTPases and their TRAPP GEFs at the Golgi. *FEBS Lett.* 593:2488–2500. doi:10.1002/1873-3468.13574.

Lipatova, Z., A.A. Tokarev, Y. Jin, J. Mulholland, L.S. Weisman, and N. Segev. 2008. Direct interaction between a myosin V motor and the Rab GTPases Ypt31/32 is required for polarized secretion. *Mol. Biol. Cell*. 19:4177–4187. doi:10.1091/mbc.e08-02-0220.

Liu, C., M. Mei, Q. Li, P. Roboti, Q. Pang, Z. Ying, F. Gao, M. Lowe, and S. Bao. 2017a. Loss of the golgin GM130 causes Golgi disruption, Purkinje neuron loss, and ataxia in mice. *Proc. Natl. Acad. Sci.* 114:346–351. doi:10.1073/pnas.1608576114.

Liu, K., K. Surendhran, S.F. Nothwehr, and T.R. Graham. 2008. P4-ATPase requirement for AP-1/clathrin function in protein transport from the trans-Golgi network and early endosomes. *Mol. Biol. Cell*. 19:3526–3535. doi:10.1091/mbc.e08-01-0025.

Liu, L., B. Doray, and S. Kornfeld. 2018. Recycling of Golgi glycosyltransferases requires direct binding to coatomer. *Proc. Natl. Acad. Sci. U. S. A.* 115:8984–8989. doi:10.1073/pnas.1810291115.

Liu, L.-K., V. Choudhary, A. Toulmay, and W.A. Prinz. 2017b. An inducible ER-Golgi tether facilitates ceramide transport to alleviate lipotoxicity. *J. Cell Biol.* 216:131–147. doi:10.1083/jcb.201606059.

Losev, E., C.A. Reinke, J. Jellen, D.E. Strongin, B.J. Bevis, and B.S. Glick. 2006. Golgi maturation visualized in living yeast. *Nature*. 441:1002–1006. doi:10.1038/nature04717.

Lowe, M. 2011. Structural organization of the Golgi apparatus. *Curr. Opin. Cell Biol.* 23:85–93. doi:10.1016/j.ceb.2010.10.004.

Lowe, M. 2019. The Physiological Functions of the Golgin Vesicle Tethering Proteins. *Front. Cell Dev. Biol.* 7:94. doi:10.3389/fcell.2019.00094.

Lujan, P., and F. Campelo. 2021. Should I stay or should I go? Golgi membrane spatial organization for protein sorting and retention. *Arch. Biochem. Biophys.* 707:108921. doi:10.1016/j.abb.2021.108921.

Luo, Z., and D. Gallwitz. 2003. Biochemical and genetic evidence for the involvement of yeast Ypt6-GTPase in protein retrieval to different Golgi compartments. *J. Biol. Chem.* 278:791–799. doi:10.1074/jbc.M209120200.

Ma, M., and C.G. Burd. 2020. Retrograde trafficking and plasma membrane recycling pathways of the budding yeast Saccharomyces cerevisiae. *Traffic*. 21:45–59. doi:10.1111/tra.12693.

Magdeleine, M., R. Gautier, P. Gounon, H. Barelli, S. Vanni, and B. Antonny. 2016. A filter at the entrance of the Golgi that selects vesicles according to size and bulk lipid composition. *eLife*. 5:e16988. doi:10.7554/eLife.16988.

Makhoul, C., P. Gosavi, R. Duffield, B. Delbridge, N.A. Williamson, and P.A. Gleeson. 2019. Intersectin-1 interacts with the golgin GCC88 to couple the actin network and Golgi architecture. *Mol. Biol. Cell*. 30:370–386. doi:10.1091/mbc.E18-05-0313.

Manzer, K.M., and J.C. Fromme. 2023. The Arf-GAP Age2 localizes to the late-Golgi via a conserved amphipathic helix. *Mol. Biol. Cell*. 34:ar119. doi:10.1091/mbc.E23-07-0283.

de Marcos Lousa, C., and J. Denecke. 2016. Lysosomal and vacuolar sorting: not so different after all! *Biochem. Soc. Trans.* 44:891–897. doi:10.1042/BST20160050.

Marcusson, E.G., B.F. Horazdovsky, J.L. Cereghino, E. Gharakhanian, and S.D. Emr. 1994. The sorting receptor for yeast vacuolar carboxypeptidase Y is encoded by the VPS10 gene. *Cell*. 77:579–586. doi:10.1016/0092-8674(94)90219-4.

Mari, M., W.J.C. Geerts, and F. Reggiori. 2014. Immuno- and correlative light microscopy-electron tomography methods for 3D protein localization in yeast. *Traffic Cph. Den.* 15:1164–1178. doi:10.1111/tra.12192.

Marijuán, P.C., R. del Moral, and J. Navarro. 2013. On eukaryotic intelligence: Signaling system's guidance in the evolution of multicellular organization. *Biosystems*. 114:8–24. doi:10.1016/j.biosystems.2013.06.005.

Matsudaira, T., T. Niki, T. Taguchi, and H. Arai. 2015. Transport of the cholera toxin B-subunit from recycling endosomes to the Golgi requires clathrin and AP-1. *J. Cell Sci.* 128:3131–3142. doi:10.1242/jcs.172171.

Matsuura-Tokita, K., M. Takeuchi, A. Ichihara, K. Mikuriya, and A. Nakano. 2006. Live imaging of yeast Golgi cisternal maturation. *Nature*. 441:1007–1010. doi:10.1038/nature04737.

McCaughey, J., and D.J. Stephens. 2019. ER-to-Golgi Transport: A Sizeable Problem. *Trends Cell Biol.* 29:940–953. doi:10.1016/j.tcb.2019.08.007.

McDonold, C.M., and J.C. Fromme. 2014. Four GTPases differentially regulate the Sec7 Arf-GEF to direct traffic at the trans-golgi network. *Dev. Cell*. 30:759–767. doi:10.1016/j.devcel.2014.07.016.

McGee, L.J., A.L. Jiang, and Y. Lan. 2017. Golga5 is dispensable for mouse embryonic development and postnatal survival. *genesis*. 55:e23039. doi:10.1002/dvg.23039.

McGuire, A.T., and D. Mangroo. 2007. Cex1p is a novel cytoplasmic component of the Saccharomyces cerevisiae nuclear tRNA export machinery. *EMBO J.* 26:288–300. doi:10.1038/sj.emboj.7601493.

McNally, K.E., and P.J. Cullen. 2018. Endosomal Retrieval of Cargo: Retromer Is Not Alone. *Trends Cell Biol.* 28:807–822. doi:10.1016/j.tcb.2018.06.005.

McNew, J.A., J.G. Coe, M. Søgaard, B.V. Zemelman, C. Wimmer, W. Hong, and T.H. Söllner. 1998. Gos1p, a Saccharomyces cerevisiae SNARE protein involved in Golgi transport. *FEBS Lett.* 435:89–95. doi:10.1016/s0014-5793(98)01044-8.

Miesenböck, G., and J.E. Rothman. 1995. The capacity to retrieve escaped ER proteins extends to the trans-most cisterna of the Golgi stack. *J. Cell Biol.* 129:309–319. doi:10.1083/jcb.129.2.309.

Mironov, A.A., A.A. Mironov, G.V. Beznoussenko, A. Trucco, P. Lupetti, J.D. Smith, W.J.C. Geerts, A.J. Koster, K.N.J. Burger, M.E. Martone, T.J. Deerinck, M.H. Ellisman, and A. Luini. 2003. ER-to-Golgi carriers arise through direct en bloc protrusion and multistage maturation of specialized ER exit domains. *Dev. Cell*. 5:583–594. doi:10.1016/s1534-5807(03)00294-6.

Mironov, A.A., and M. Pavelka eds. . 2008. The Golgi Apparatus: State of the art 110 years after Camillo Golgi's discovery. Springer, Vienna.

Mizuno-Yamasaki, E., F. Rivera-Molina, and P. Novick. 2012. GTPase networks in membrane traffic. *Annu. Rev. Biochem.* 81:637–659. doi:10.1146/annurev-biochem-052810-093700.

Mogelsvang, S., N. Gomez-Ospina, J. Soderholm, B.S. Glick, and L.A. Staehelin. 2003. Tomographic evidence for continuous turnover of Golgi cisternae in Pichia pastoris. *Mol. Biol. Cell*. 14:2277–2291. doi:10.1091/mbc.e02-10-0697.

Mogelsvang, S., B.J. Marsh, M.S. Ladinsky, and K.E. Howell. 2004. Predicting function from structure: 3D structure studies of the mammalian Golgi complex. *Traffic Cph. Den.* 5:338–345. doi:10.1111/j.1398-9219.2004.00186.x.

Mollenhauer, H.H., and D.J. Morré. 1991. Perspectives on Golgi apparatus form and function. *J. Electron Microsc. Tech.* 17:2–14. doi:10.1002/jemt.1060170103.

Moser, J.M., P. Bigini, and T. Schmitt-John. 2013. The wobbler mouse, an ALS animal model. *Mol. Genet. Genomics MGG*. 288:207–229. doi:10.1007/s00438-013-0741-0.

Mowbrey, K., and J.B. Dacks. 2009. Evolution and diversity of the Golgi body. *FEBS Lett.* 583:3738–3745. doi:10.1016/j.febslet.2009.10.025.

Moyer, B.D., B.B. Allan, and W.E. Balch. 2001. Rab1 Interaction with a GM130 Effector Complex Regulates COPII Vesicle cis-Golgi Tethering. *Traffic*. 2:268–276. doi:10.1034/j.1600-0854.2001.1o007.x.

Munro, S. 2011. The golgin coiled-coil proteins of the Golgi apparatus. *Cold Spring Harb. Perspect. Biol.* 3:a005256. doi:10.1101/cshperspect.a005256.

Munro, S., and B.J. Nichols. 1999. The GRIP domain - a novel Golgi-targeting domain found in several coiled-coil proteins. *Curr. Biol. CB*. 9:377–380. doi:10.1016/s0960-9822(99)80166-3.

Muschalik, N., and S. Munro. 2018. Golgins. *Curr. Biol.* 28:R374–R376. doi:10.1016/j.cub.2018.01.006.

Myers, M.D., and G.S. Payne. 2013. Clathrin, adaptors and disease: insights from the yeast Saccharomyces cerevisiae. *Front. Biosci. Landmark Ed.* 18:862–891. doi:10.2741/4149.

Nagano, M., J.Y. Toshima, D.E. Siekhaus, and J. Toshima. 2019. Rab5-mediated endosome formation is regulated at the trans-Golgi network. *Commun. Biol.* 2:419. doi:10.1038/s42003-019-0670-5.

Naslavsky, N., and S. Caplan. 2018. The enigmatic endosome – sorting the ins and outs of endocytic trafficking. *J. Cell Sci.* 131:jcs216499. doi:10.1242/jcs.216499.

Navarro Negredo, P., J.R. Edgar, P.T. Manna, R. Antrobus, and M.S. Robinson. 2018. The WDR11 complex facilitates the tethering of AP-1-derived vesicles. *Nat. Commun.* 9:596. doi:10.1038/s41467-018-02919-4.

Newman, A.P., J. Shim, and S. Ferro-Novick. 1990. BET1, BOS1, and SEC22 are members of a group of interacting yeast genes required for transport from the endoplasmic reticulum to the Golgi complex. *Mol. Cell. Biol.* 10:3405–3414. doi:10.1128/mcb.10.7.3405.

Nichols, B.J., and H.R. Pelham. 1998. SNAREs and membrane fusion in the Golgi apparatus. *Biochim. Biophys. Acta*. 1404:9–31. doi:10.1016/s0167-4889(98)00044-5.

Nicholson, D.J. 2019. Is the cell really a machine? *J. Theor. Biol.* 477:108–126. doi:10.1016/j.jtbi.2019.06.002.

Nothwehr, S.F., and A.E. Hindes. 1997. The yeast VPS5/GRD2 gene encodes a sorting nexin-1-like protein required for localizing membrane proteins to the late Golgi. *J. Cell Sci.* 110 (Pt 9):1063–1072. doi:10.1242/jcs.110.9.1063.

Odorizzi, G., C.R. Cowles, and S.D. Emr. 1998. The AP-3 complex: a coat of many colours. *Trends Cell Biol.* 8:282–288. doi:10.1016/s0962-8924(98)01295-1.

Omar-Hmeadi, M., and O. Idevall-Hagren. 2020. Insulin granule biogenesis and exocytosis. *Cell. Mol. Life Sci. CMLS*. 78:1957–1970. doi:10.1007/s00018-020-03688-4.

Ong, K., C. Wloka, S. Okada, T. Svitkina, and E. Bi. 2014. Architecture and dynamic remodelling of the septin cytoskeleton during the cell cycle. *Nat. Commun.* 5:5698. doi:10.1038/ncomms6698.

Orci, L., A. Perrelet, and J.E. Rothman. 1998. Vesicles on strings: morphological evidence for processive transport within the Golgi stack. *Proc. Natl. Acad. Sci. U. S. A.* 95:2279–2283. doi:10.1073/pnas.95.5.2279.

Orci, L., M. Ravazzola, A. Volchuk, T. Engel, M. Gmachl, M. Amherdt, A. Perrelet, T.H. Söllner, and J.E. Rothman. 2000. Anterograde flow of cargo across the Golgi stack potentially mediated via bidirectional “percolating” COPI vesicles. *Proc. Natl. Acad. Sci.* 97:10400–10405. doi:10.1073/pnas.190292497.

Orci, L., M. Stamnes, M. Ravazzola, M. Amherdt, A. Perrelet, T.H. Söllner, and J.E. Rothman. 1997. Bidirectional transport by distinct populations of COPI-coated vesicles. *Cell*. 90:335–349. doi:10.1016/s0092-8674(00)80341-4.

Orlean, P. 2012. Architecture and biosynthesis of the Saccharomyces cerevisiae cell wall. *Genetics*. 192:775–818. doi:10.1534/genetics.112.144485.

Paczkowski, J.E., B.C. Richardson, and J.C. Fromme. 2015. Cargo adaptors: structures illuminate mechanisms regulating vesicle biogenesis. *Trends Cell Biol.* 25:408–416. doi:10.1016/j.tcb.2015.02.005.

Palmgren, M.G., and P. Nissen. 2011. P-type ATPases. *Annu. Rev. Biophys.* 40:243–266. doi:10.1146/annurev.biophys.093008.131331.

Panic, B., O. Perisic, D.B. Veprintsev, R.L. Williams, and S. Munro. 2003a. Structural basis for Arl1-dependent targeting of homodimeric GRIP domains to the Golgi apparatus. *Mol. Cell*. 12:863–874. doi:10.1016/s1097-2765(03)00356-3.

Panic, B., J.R.C. Whyte, and S. Munro. 2003b. The ARF-like GTPases Arl1p and Arl3p act in a pathway that interacts with vesicle-tethering factors at the Golgi apparatus. *Curr. Biol. CB*. 13:405–410. doi:10.1016/s0960-9822(03)00091-5.

Pantazopoulou, A., and B.S. Glick. 2019. A Kinetic View of Membrane Traffic Pathways Can Transcend the Classical View of Golgi Compartments. *Front. Cell Dev. Biol.* 0. doi:10.3389/fcell.2019.00153.

Papanikou, E., K.J. Day, J. Austin II, and B.S. Glick. 2015. COPI selectively drives maturation of the early Golgi. *eLife*. 4:e13232. doi:10.7554/eLife.13232.

Papanikou, E., and B.S. Glick. 2009. The yeast Golgi apparatus: insights and mysteries. *FEBS Lett.* 583:3746–3751. doi:10.1016/j.febslet.2009.10.072.

Park, S., S. Kim, M.J. Kim, Y. Hong, A.Y. Lee, H. Lee, Q. Tran, M. Kim, H. Cho, J. Park, K.P. Kim, J. Park, and M.-H. Cho. 2018. GOLGA2 loss causes fibrosis with autophagy in the mouse lung and liver. *Biochem. Biophys. Res. Commun.* 495:594–600. doi:10.1016/j.bbrc.2017.11.049.

Park, S.Y., N. Muschalik, J. Chadwick, and S. Munro. 2022. In vivo characterization of Drosophila golgins reveals redundancy and plasticity of vesicle capture at the Golgi apparatus. *Curr. Biol. CB*. 32:4549-4564.e6. doi:10.1016/j.cub.2022.08.054.

Parmar, H.B., C. Barry, F. Kai, and R. Duncan. 2014. Golgi complex-plasma membrane trafficking directed by an autonomous, tribasic Golgi export signal. *Mol. Biol. Cell*. 25:866–878. doi:10.1091/mbc.E13-07-0364.

Paumet, F., B. Brügger, F. Parlati, J.A. McNew, T.H. Söllner, and J.E. Rothman. 2001. A t-SNARE of the endocytic pathway must be activated for fusion. *J. Cell Biol.* 155:961–968. doi:10.1083/jcb.200104092.

Pelham, H.R. 1995. Sorting and retrieval between the endoplasmic reticulum and Golgi apparatus. *Curr. Opin. Cell Biol.* 7:530–535. doi:10.1016/0955-0674(95)80010-7.

Pelham, H.R., K.G. Hardwick, and M.J. Lewis. 1988. Sorting of soluble ER proteins in yeast. *EMBO J.* 7:1757–1762. doi:10.1002/j.1460-2075.1988.tb03005.x.

Pelham, H.R., and J.E. Rothman. 2000. The debate about transport in the Golgi--two sides of the same coin? *Cell*. 102:713–719. doi:10.1016/s0092-8674(00)00060-x.

Pellett, P.A., F. Dietrich, J. Bewersdorf, J.E. Rothman, and G. Lavieu. 2013. Inter-Golgi transport mediated by COPI-containing vesicles carrying small cargoes. *eLife*. 2:e01296. doi:10.7554/eLife.01296.

Peplowska, K., D.F. Markgraf, C.W. Ostrowicz, G. Bange, and C. Ungermann. 2007. The CORVET tethering complex interacts with the yeast Rab5 homolog Vps21 and is involved in endo-lysosomal biogenesis. *Dev. Cell*. 12:739–750. doi:10.1016/j.devcel.2007.03.006.

Pérez-Victoria, F.J., and J.S. Bonifacino. 2009. Dual Roles of the Mammalian GARP Complex in Tethering and SNARE Complex Assembly at the trans-Golgi Network. *Mol. Cell. Biol.* 29:5251–5263. doi:10.1128/MCB.00495-09.

Pérez-Victoria, F.J., G.A. Mardones, and J.S. Bonifacino. 2008. Requirement of the human GARP complex for mannose 6-phosphate-receptor-dependent sorting of cathepsin D to lysosomes. *Mol. Biol. Cell*. 19:2350–2362. doi:10.1091/mbc.e07-11-1189.

Petersen, L., R. Bachmann, S. Meinerz, A. Tanz, and G. Fischer von Mollard. 2023. Distinct functional domains of the epsin-related Ent5p, a cargo adaptor for the SNARE Tlg2p in transport between endosomes and Golgi. *Traffic Cph. Den.* 24:475–488. doi:10.1111/tra.12910.

Pfeffer, S.R. 2010. How the Golgi works: A cisternal progenitor model. *Proc. Natl. Acad. Sci.* 107:19614–19618. doi:10.1073/pnas.1011016107.

Popoff, V., F. Adolf, B. Brügger, and F. Wieland. 2011. COPI Budding within the Golgi Stack. *Cold Spring Harb. Perspect. Biol.* 3:a005231. doi:10.1101/cshperspect.a005231.

Prinz, W.A., A. Toulmay, and T. Balla. 2020. The functional universe of membrane contact sites. *Nat. Rev. Mol. Cell Biol.* 21:7–24. doi:10.1038/s41580-019-0180-9.

Protopopov, V., B. Govindan, P. Novick, and J.E. Gerst. 1993. Homologs of the synaptobrevin/VAMP family of synaptic vesicle proteins function on the late secretory pathway in S. cerevisiae. *Cell*. 74:855–861. doi:10.1016/0092-8674(93)90465-3.

Pruyne, D., A. Legesse-Miller, L. Gao, Y. Dong, and A. Bretscher. 2004. Mechanisms of polarized growth and organelle segregation in yeast. *Annu. Rev. Cell Dev. Biol.* 20:559–591. doi:10.1146/annurev.cellbio.20.010403.103108.

Rabouille, C., N. Hui, F. Hunte, R. Kieckbusch, E.G. Berger, G. Warren, and T. Nilsson. 1995. Mapping the distribution of Golgi enzymes involved in the construction of complex oligosaccharides. *J. Cell Sci.* 108 (Pt 4):1617–1627. doi:10.1242/jcs.108.4.1617.

Rabouille, C., and J. Klumperman. 2005. The maturing role of COPI vesicles in intra-Golgi transport. *Nat. Rev. Mol. Cell Biol.* 6:812–817. doi:10.1038/nrm1735.

Ramazanov, B.R., M.L. Tran, and J. von Blume. 2021. Sending out molecules from the TGN. *Curr. Opin. Cell Biol.* 71:55–62. doi:10.1016/j.ceb.2021.02.005.

Rambourg, A., and Y. Clermont. 1997. Three-dimensional structure of the Golgi apparatus in mammalian cells. *In* The Golgi Apparatus. E.G. Berger and J. Roth, editors. Birkhäuser, Basel. 37–61.

Raote, I., and V. Malhotra. 2021. Tunnels for Protein Export from the Endoplasmic Reticulum. *Annu. Rev. Biochem.* 90:605–630. doi:10.1146/annurev-biochem-080120-022017.

Raote, I., S. Saxena, F. Campelo, and V. Malhotra. 2021. TANGO1 marshals the early secretory pathway for cargo export. *Biochim. Biophys. Acta Biomembr.* 1863:183700. doi:10.1016/j.bbamem.2021.183700.

Ravichandran, Y., B. Goud, and J.-B. Manneville. 2020. The Golgi apparatus and cell polarity: Roles of the cytoskeleton, the Golgi matrix, and Golgi membranes. *Curr. Opin. Cell Biol.* 62:104–113. doi:10.1016/j.ceb.2019.10.003.

Reddy, J.V., A.S. Burguete, K. Sridevi, I.G. Ganley, R.M. Nottingham, and S.R. Pfeffer. 2006. A functional role for the GCC185 golgin in mannose 6-phosphate receptor recycling. *Mol. Biol. Cell*. 17:4353–4363. doi:10.1091/mbc.e06-02-0153.

Reggiori, F., C.-W. Wang, P.E. Stromhaug, T. Shintani, and D.J. Klionsky. 2003. Vps51 is part of the yeast Vps fifty-three tethering complex essential for retrograde traffic from the early endosome and Cvt vesicle completion. *J. Biol. Chem.* 278:5009–5020. doi:10.1074/jbc.M210436200.

Rios, R.M. 2014. The centrosome-Golgi apparatus nexus. *Philos. Trans. R. Soc. Lond. B. Biol. Sci.* 369:20130462. doi:10.1098/rstb.2013.0462.

Rivera-Molina, F.E., and P.J. Novick. 2009. A Rab GAP cascade defines the boundary between two Rab GTPases on the secretory pathway. *Proc. Natl. Acad. Sci. U. S. A.* 106:14408–14413. doi:10.1073/pnas.0906536106.

Rizzo, R., D. Russo, K. Kurokawa, P. Sahu, B. Lombardi, D. Supino, M.A. Zhukovsky, A. Vocat, P. Pothukuchi, V. Kunnathully, L. Capolupo, G. Boncompain, C. Vitagliano, F. Zito Marino, G. Aquino, D. Montariello, P. Henklein, L. Mandrich, G. Botti, H. Clausen, U. Mandel, T. Yamaji, K. Hanada, A. Budillon, F. Perez, S. Parashuraman, Y.A. Hannun, A. Nakano, D. Corda, G. D'Angelo, and A. Luini. 2021. Golgi maturation-dependent glycoenzyme recycling controls glycosphingolipid biosynthesis and cell growth via GOLPH3. *EMBO J.* 40:e107238. doi:10.15252/embj.2020107238.

Robinson, M., P.P. Poon, C. Schindler, L.E. Murray, R. Kama, G. Gabriely, R.A. Singer, A. Spang, G.C. Johnston, and J.E. Gerst. 2006. The Gcs1 Arf-GAP mediates Snc1,2 v-SNARE retrieval to the Golgi in yeast. *Mol. Biol. Cell*. 17:1845–1858. doi:10.1091/mbc.e05-09-0832.

Robinson, M.S., R. Antrobus, A. Sanger, A.K. Davies, and D.C. Gershlick. 2024. The role of the AP-1 adaptor complex in outgoing and incoming membrane traffic. *J. Cell Biol.* 223:e202310071. doi:10.1083/jcb.202310071.

Rosa-Ferreira, C., C. Christis, I.L. Torres, and S. Munro. 2015. The small G protein Arl5 contributes to endosome-to-Golgi traffic by aiding the recruitment of the GARP complex to the Golgi. *Biol. Open*. 4:474–481. doi:10.1242/bio.201410975.

Rossanese, O.W., J. Soderholm, B.J. Bevis, I.B. Sears, J. O'Connor, E.K. Williamson, and B.S. Glick. 1999. Golgi Structure Correlates with Transitional Endoplasmic Reticulum

Organization in Pichia pastoris and Saccharomyces cerevisiae. *J. Cell Biol.* 145:69–81. doi:10.1083/jcb.145.1.69.

Rothstein, R. 1991. Targeting, disruption, replacement, and allele rescue: integrative DNA transformation in yeast. *Methods Enzymol.* 194:281–301. doi:10.1016/0076-6879(91)94022-5.

Roy Chowdhury, S., C. Bhattacharjee, J.C. Casler, B.K. Jain, B.S. Glick, and D. Bhattacharyya. 2020. ER arrival sites associate with ER exit sites to create bidirectional transport portals. *J. Cell Biol.* 219:e201902114. doi:10.1083/jcb.201902114.

Sahu, P., A. Balakrishnan, R. Di Martino, A. Luini, and D. Russo. 2022. Role of the Mosaic Cisternal Maturation Machinery in Glycan Synthesis and Oncogenesis. *Front. Cell Dev. Biol.* 10:842448. doi:10.3389/fcell.2022.842448.

Sanders, A.A.W.M., and I. Kaverina. 2015. Nucleation and dynamics of Golgi-derived microtubules. *Front. Neurosci.* 9. doi:10.3389/fnins.2015.00431.

Santiago-Tirado, F.H., A. Legesse-Miller, D. Schott, and A. Bretscher. 2011. PI4P and Rab inputs collaborate in myosin-V-dependent transport of secretory compartments in yeast. *Dev. Cell*. 20:47–59. doi:10.1016/j.devcel.2010.11.006.

Sardana, R., C.M. Highland, B.E. Straight, C.F. Chavez, J.C. Fromme, and S.D. Emr. 2021. Golgi membrane protein Erd1 Is essential for recycling a subset of Golgi glycosyltransferases. *eLife*. 10:e70774. doi:10.7554/eLife.70774.

Sarmento, M.J., A. Llorente, T. Petan, D. Khnykin, I. Popa, M. Nikolac Perkovic, M. Konjevod, and M. Jaganjac. 2023. The expanding organelle lipidomes: current knowledge and challenges. *Cell. Mol. Life Sci. CMLS*. 80:237. doi:10.1007/s00018-023-04889-3.

Sato, K., P. Roboti, A.A. Mironov, and M. Lowe. 2015. Coupling of vesicle tethering and Rab binding is required for in vivo functionality of the golgin GMAP-210. *Mol. Biol. Cell*. 26:537–553. doi:10.1091/mbc.E14-10-1450.

Sato, K., M. Sato, and A. Nakano. 2001. Rer1p, a retrieval receptor for endoplasmic reticulum membrane proteins, is dynamically localized to the Golgi apparatus by coatomer. *J. Cell Biol.* 152:935–944. doi:10.1083/jcb.152.5.935.

Schimmöller, F., E. Díaz, B. Mühlbauer, and S.R. Pfeffer. 1998. Characterization of a 76 kDa endosomal, multispanning membrane protein that is highly conserved throughout evolution. *Gene*. 216:311–318. doi:10.1016/s0378-1119(98)00349-7.

Schindler, C., Y. Chen, J. Pu, X. Guo, and J.S. Bonifacino. 2015. EARP is a multisubunit tethering complex involved in endocytic recycling. *Nat. Cell Biol.* 17:639–650. doi:10.1038/ncb3129.

Schjoldager, K.T., Y. Narimatsu, H.J. Joshi, and H. Clausen. 2020. Global view of human protein glycosylation pathways and functions. *Nat. Rev. Mol. Cell Biol.* 21:729–749. doi:10.1038/s41580-020-00294-x.

Schlarmann, P., A. Ikeda, and K. Funato. 2021. Membrane Contact Sites in Yeast: Control Hubs of Sphingolipid Homeostasis. *Membranes*. 11:971. doi:10.3390/membranes11120971.

Schmitt-John, T. 2015. VPS54 and the wobbler mouse. *Front. Neurosci.* 9:381. doi:10.3389/fnins.2015.00381.

Schmitz, K.R., J. Liu, S. Li, T.G. Setty, C.S. Wood, C.G. Burd, and K.M. Ferguson. 2008. Golgi Localization of Glycosyltransferases Requires a Vps74p Oligomer. *Dev. Cell*. 14:523–534. doi:10.1016/j.devcel.2008.02.016.

Schoppe, J., E. Schubert, A. Apelbaum, E. Yavavli, O. Birkholz, H. Stephanowitz, Y. Han, A. Perz, O. Hofnagel, F. Liu, J. Piehler, S. Raunser, and C. Ungermann. 2021. Flexible open conformation of the AP-3 complex explains its role in cargo recruitment at the Golgi. *J. Biol. Chem.* 297. doi:10.1016/j.jbc.2021.101334.

Schröter, S., S. Beckmann, and H.D. Schmitt. 2016. Coat/Tether Interactions—Exception or Rule? *Front. Cell Dev. Biol.* 4. doi:10.3389/fcell.2016.00044.

Schüller, C., Y.M. Mamnun, H. Wolfger, N. Rockwell, J. Thorner, and K. Kuchler. 2007. Membrane-active compounds activate the transcription factors Pdr1 and Pdr3 connecting pleiotropic drug resistance and membrane lipid homeostasis in saccharomyces cerevisiae. *Mol. Biol. Cell*. 18:4932–4944. doi:10.1091/mbc.e07-06-0610.

Seaman, M.N., J.M. McCaffery, and S.D. Emr. 1998. A membrane coat complex essential for endosome-to-Golgi retrograde transport in yeast. *J. Cell Biol.* 142:665–681. doi:10.1083/jcb.142.3.665.

Seaman, M.N.J., A. Gautreau, and D.D. Billadeau. 2013. Retromer-mediated endosomal protein sorting: all WASHed up! *Trends Cell Biol.* 23:522–528. doi:10.1016/j.tcb.2013.04.010.

Settembre, C., and R.M. Perera. 2024. Lysosomes as coordinators of cellular catabolism, metabolic signalling and organ physiology. *Nat. Rev. Mol. Cell Biol.* 25:223–245. doi:10.1038/s41580-023-00676-x.

Setty, S.R.G., M.E. Shin, A. Yoshino, M.S. Marks, and C.G. Burd. 2003. Golgi recruitment of GRIP domain proteins by Arf-like GTPase 1 is regulated by Arf-like GTPase 3. *Curr. Biol. CB*. 13:401–404. doi:10.1016/s0960-9822(03)00089-7.

Setty, S.R.G., T.I. Strochlic, A.H.Y. Tong, C. Boone, and C.G. Burd. 2004. Golgi targeting of ARF-like GTPase Arl3p requires its Nalpha-acetylation and the integral membrane protein Sys1p. *Nat. Cell Biol.* 6:414–419. doi:10.1038/ncb1121.

Shamseldin, H.E., A.H. Bennett, M. Alfadhel, V. Gupta, and F.S. Alkuraya. 2016. GOLGA2, encoding a master regulator of golgi apparatus, is mutated in a patient with a neuromuscular disorder. *Hum. Genet.* 135:245–251. doi:10.1007/s00439-015-1632-8.

Shin, H.-W., H. Kobayashi, M. Kitamura, S. Waguri, T. Suganuma, Y. Uchiyama, and K. Nakayama. 2005. Roles of ARFRP1 (ADP-ribosylation factor-related protein 1) in post-Golgi membrane trafficking. *J. Cell Sci.* 118:4039–4048. doi:10.1242/jcs.02524.

Shin, J.J.H., O.M. Crook, A.C. Borgeaud, J. Cattin-Ortolá, S.Y. Peak-Chew, L.M. Breckels, A.K. Gillingham, J. Chadwick, K.S. Lilley, and S. Munro. 2020. Spatial proteomics defines the content of trafficking vesicles captured by golgin tethers. *Nat. Commun.* 11:5987. doi:10.1038/s41467-020-19840-4.

Shin, J.J.H., A.K. Gillingham, F. Begum, J. Chadwick, and S. Munro. 2017. TBC1D23 is a bridging factor for endosomal vesicle capture by golgins at the trans-Golgi. *Nat. Cell Biol.* 19:1424–1432. doi:10.1038/ncb3627.

Shomron, O., I. Nevo-Yassaf, T. Aviad, Y. Yaffe, E.E. Zahavi, A. Dukhovny, E. Perlson, I. Brodsky, A. Yeheskel, M. Pasmanik-Chor, A. Mironov, G.V. Beznoussenko, A.A. Mironov, E.H. Sklan, G.H. Patterson, Y. Yonemura, M. Sannai, C. Kaether, and K. Hirschberg. 2021. COPII collar defines the boundary between ER and ER exit site and does not coat cargo containers. *J. Cell Biol.* 220:e201907224. doi:10.1083/jcb.201907224.

Singer-Krüger, B., R. Frank, F. Crausaz, and H. Riezman. 1993. Partial purification and characterization of early and late endosomes from yeast. Identification of four novel proteins. *J. Biol. Chem.* 268:14376–14386.

Singer-Krüger, B., M. Lasić, A.-M. Bürger, A. Hausser, R. Pipkorn, and Y. Wang. 2008. Yeast and human Ysl2p/hMon2 interact with Gga adaptors and mediate their subcellular distribution. *EMBO J.* 27:1423–1435. doi:10.1038/emboj.2008.75.

Siniossoglou, S., S.Y. Peak-Chew, and H.R.B. Pelham. 2000. Ric1p and Rgp1p form a complex that catalyses nucleotide exchange on Ypt6p. *EMBO J.* 19:4885–4894. doi:10.1093/emboj/19.18.4885.

Siniossoglou, S., and H.R.B. Pelham. 2001. An effector of Ypt6p binds the SNARE Tlg1p and mediates selective fusion of vesicles with late Golgi membranes. *EMBO J.* 20:5991–5998. doi:10.1093/emboj/20.21.5991.

Siniossoglou, S., and H.R.B. Pelham. 2002. Vps51p Links the VFT Complex to the SNARE Tlg1p. *J. Biol. Chem.* 277:48318–48324. doi:10.1074/jbc.M209428200.

Sinka, R., A.K. Gillingham, V. Kondylis, and S. Munro. 2008. Golgi coiled-coil proteins contain multiple binding sites for Rab family G proteins. *J. Cell Biol.* 183:607–615. doi:10.1083/jcb.200808018.

Smits, P., A.D. Bolton, V. Funari, M. Hong, E.D. Boyden, L. Lu, D.K. Manning, N.D. Dwyer, J.L. Moran, M. Prysak, B. Merriman, S.F. Nelson, L. Bonafé, A. Superti-Furga, S. Ikegawa, D. Krakow, D.H. Cohn, T. Kirchhausen, M.L. Warman, and D.R. Beier. 2010. Lethal Skeletal Dysplasia in Mice and Humans Lacking the Golgin GMAP-210. *N. Engl. J. Med.* 362:206–216. doi:10.1056/NEJMoa0900158.

Snyder, N.A., C.P. Stefan, C.T. Soroudi, A. Kim, C. Evangelista, and K.W. Cunningham. 2017. H+ and Pi Byproducts of Glycosylation Affect Ca2+ Homeostasis and Are Retrieved from the Golgi Complex by Homologs of TMEM165 and XPR1. *G3 Bethesda Md*. 7:3913–3924. doi:10.1534/g3.117.300339.

Song, H., T.L. Torng, A.S. Orr, A.T. Brunger, and W.T. Wickner. 2021. Sec17/Sec18 can support membrane fusion without help from completion of SNARE zippering. *eLife*. 10:e67578. doi:10.7554/eLife.67578.

Spang, A. 2016. Membrane Tethering Complexes in the Endosomal System. *Front. Cell Dev. Biol.* 4:35. doi:10.3389/fcell.2016.00035.

Staehelin, L.A., and B.-H. Kang. 2008. Nanoscale Architecture of Endoplasmic Reticulum Export Sites and of Golgi Membranes as Determined by Electron Tomography. *Plant Physiol.* 147:1454–1468. doi:10.1104/pp.108.120618.

Stagg, S.M., P. LaPointe, A. Razvi, C. Gürkan, C.S. Potter, B. Carragher, and W.E. Balch. 2008. Structural Basis for Cargo Regulation of COPII Coat Assembly. *Cell*. 134:474–484. doi:10.1016/j.cell.2008.06.024.

Stanley, P. 2011. Golgi Glycosylation. *Cold Spring Harb. Perspect. Biol.* 3:a005199. doi:10.1101/cshperspect.a005199.

Stevenson, N.L., D.J.M. Bergen, R.E.H. Skinner, E. Kague, E. Martin-Silverstone, K.A. Robson Brown, C.L. Hammond, and D.J. Stephens. 2017. Giantin-knockout models reveal a feedback loop between Golgi function and glycosyltransferase expression. *J. Cell Sci.* 130:4132–4143. doi:10.1242/jcs.212308.

Stoops, E.H., and M.J. Caplan. 2014. Trafficking to the apical and basolateral membranes in polarized epithelial cells. *J. Am. Soc. Nephrol. JASN*. 25:1375–1386. doi:10.1681/ASN.2013080883.

Su, M., A. Radhakrishnan, Y. Yan, Y. Tian, H. Zheng, O. M'Saad, M. Graham, J. Coleman, J.N.D. Goder, X. Liu, Y. Zhang, J. Bewersdorf, and J.E. Rothman. 2025. The Golgi Rim is a Precise Tetraplex of Golgin Proteins that Can Self-Assemble into Filamentous Bands. 2025.03.27.645134. doi:10.1101/2025.03.27.645134.

Suda, Y., K. Kurokawa, R. Hirata, and A. Nakano. 2013. Rab GAP cascade regulates dynamics of Ypt6 in the Golgi traffic. *Proc. Natl. Acad. Sci.* 110:18976–18981. doi:10.1073/pnas.1308627110.

Südhof, T.C., and J.E. Rothman. 2009. Membrane Fusion: Grappling with SNARE and SM Proteins. *Science*. 323:474–477. doi:10.1126/science.1161748.

Sun, X., H.C. Tie, B. Chen, and L. Lu. 2020. Glycans function as a Golgi export signal to promote the constitutive exocytic trafficking. *J. Biol. Chem.* 295:14750–14762. doi:10.1074/jbc.RA120.014476.

Sztul, E., P.-W. Chen, J.E. Casanova, J. Cherfils, J.B. Dacks, D.G. Lambright, F.-J.S. Lee, P.A. Randazzo, L.C. Santy, A. Schürmann, I. Wilhelmi, M.E. Yohe, and R.A. Kahn. 2019. ARF GTPases and their GEFs and GAPs: concepts and challenges. *Mol. Biol. Cell*. 30:1249–1271. doi:10.1091/mbc.E18-12-0820.

Takagi, K., K. Iwamoto, S. Kobayashi, H. Horiuchi, R. Fukuda, and A. Ohta. 2012. Involvement of Golgi-associated retrograde protein complex in the recycling of the putative Dnf aminophospholipid flippases in yeast. *Biochem. Biophys. Res. Commun.* 417:490–494. doi:10.1016/j.bbrc.2011.11.147.

Takar, M., Y. Huang, and T.R. Graham. 2019. The PQ-loop protein Any1 segregates Drs2 and Neo1 functions required for viability and plasma membrane phospholipid asymmetry. *J. Lipid Res.* 60:1032–1042. doi:10.1194/jlr.M093526.

Takar, M., Y. Wu, and T.R. Graham. 2016. The Essential Neo1 Protein from Budding Yeast Plays a Role in Establishing Aminophospholipid Asymmetry of the Plasma Membrane*. *J. Biol. Chem.* 291:15727–15739. doi:10.1074/jbc.M115.686253.

Tan, J.Z.A., and P.A. Gleeson. 2019. Cargo Sorting at the trans-Golgi Network for Shunting into Specific Transport Routes: Role of Arf Small G Proteins and Adaptor Complexes. *Cells*. 8:531. doi:10.3390/cells8060531.

Tan, P.K., J.P. Howard, and G.S. Payne. 1996. The sequence NPFXD defines a new class of endocytosis signal in Saccharomyces cerevisiae. *J. Cell Biol.* 135:1789–1800. doi:10.1083/jcb.135.6.1789.

Thattai, M. 2023. Molecular and cellular constraints on vesicle traffic evolution. *Curr. Opin. Cell Biol.* 80:102151. doi:10.1016/j.ceb.2022.102151.

Thomas, L.L., and J.C. Fromme. 2020. Extensive GTPase crosstalk regulates Golgi trafficking and maturation. *Curr. Opin. Cell Biol.* 65:1–7. doi:10.1016/j.ceb.2020.01.014.

Thomas, L.L., C.M. Highland, and J.C. Fromme. 2021. Arf1 orchestrates Rab GTPase conversion at the trans-Golgi network. *Mol. Biol. Cell*. 32:1104–1120. doi:10.1091/mbc.E20-10-0664.

Thyberg, J., and S. Moskalewski. 1999. Role of microtubules in the organization of the Golgi complex. *Exp. Cell Res.* 246:263–279. doi:10.1006/excr.1998.4326.

Tie, H.C., A. Ludwig, S. Sandin, and L. Lu. 2018. The spatial separation of processing and transport functions to the interior and periphery of the Golgi stack. *eLife*. 7:e41301. doi:10.7554/eLife.41301.

Tie, H.C., D. Mahajan, B. Chen, L. Cheng, A.M.J. VanDongen, and L. Lu. 2016. A novel imaging method for quantitative Golgi localization reveals differential intra-Golgi trafficking of secretory cargoes. *Mol. Biol. Cell*. 27:848–861. doi:10.1091/mbc.E15-09-0664.

Tojima, T., Y. Suda, M. Ishii, K. Kurokawa, and A. Nakano. 2019. Spatiotemporal dissection of the trans-Golgi network in budding yeast. *J. Cell Sci.* 132:jcs231159. doi:10.1242/jcs.231159.

Tojima, T., Y. Suda, N. Jin, K. Kurokawa, and A. Nakano. 2024. Spatiotemporal dissection of the Golgi apparatus and the ER-Golgi intermediate compartment in budding yeast. *eLife*. 13:e92900. doi:10.7554/eLife.92900.

Trautwein, M., C. Schindler, R. Gauss, J. Dengjel, E. Hartmann, and A. Spang. 2006. Arf1p, Chs5p and the ChAPs are required for export of specialized cargo from the Golgi. *EMBO J.* 25:943–954. doi:10.1038/sj.emboj.7601007.

Tsukada, M., E. Will, and D. Gallwitz. 1999. Structural and functional analysis of a novel coiled-coil protein involved in Ypt6 GTPase-regulated protein transport in yeast. *Mol. Biol. Cell*. 10:63–75. doi:10.1091/mbc.10.1.63.

Tu, L., L. Chen, and D.K. Banfield. 2012. A Conserved N-terminal Arginine-Motif in GOLPH3-Family Proteins Mediates Binding to Coatomer. *Traffic*. 13:1496–1507. doi:https://doi.org/10.1111/j.1600-0854.2012.01403.x.

Tu, L., W.C.S. Tai, L. Chen, and D.K. Banfield. 2008a. Signal-mediated dynamic retention of glycosyltransferases in the Golgi. *Science*. 321:404–407. doi:10.1126/science.1159411.

Tu, L., W.C.S. Tai, L. Chen, and D.K. Banfield. 2008b. Signal-Mediated Dynamic Retention of Glycosyltransferases in the Golgi. *Science*. 321:404–407. doi:10.1126/science.1159411.

Turkewitz, A.P. 2004. Out with a bang! Tetrahymena as a model system to study secretory granule biogenesis. *Traffic Cph. Den.* 5:63–68. doi:10.1046/j.1600-0854.2003.00155.x.

Ungermann, C., and D. Kümmel. 2019. Structure of membrane tethers and their role in fusion. *Traffic Cph. Den.* 20:479–490. doi:10.1111/tra.12655.

Ungermann, C., and A. Moeller. 2025. Structuring of the endolysosomal system by HOPS and CORVET tethering complexes. *Curr. Opin. Cell Biol.* 94:102504. doi:10.1016/j.ceb.2025.102504.

Uwineza, A., J.-H. Caberg, J. Hitayezu, S. Wenric, L. Mutesa, Y. Vial, S. Drunat, S. Passemard, A. Verloes, V. El Ghouzzi, and V. Bours. 2019. VPS51 biallelic variants cause

microcephaly with brain malformations: A confirmatory report. *Eur. J. Med. Genet.* 62:103704. doi:10.1016/j.ejmg.2019.103704.

Valbuena, F.M., I. Fitzgerald, R.L. Strack, N. Andruska, L. Smith, and B.S. Glick. 2020. A photostable monomeric superfolder green fluorescent protein. *Traffic*. 21:534–544. doi:https://doi.org/10.1111/tra.12737.

Valdivia, R.H., D. Baggott, J.S. Chuang, and R.W. Schekman. 2002. The yeast clathrin adaptor protein complex 1 is required for the efficient retention of a subset of late Golgi membrane proteins. *Dev. Cell*. 2:283–294. doi:10.1016/s1534-5807(02)00127-2.

VanRheenen, S.M., X. Cao, V.V. Lupashin, C. Barlowe, and M.G. Waters. 1998. Sec35p, a novel peripheral membrane protein, is required for ER to Golgi vesicle docking. *J. Cell Biol.* 141:1107–1119. doi:10.1083/jcb.141.5.1107.

VanRheenen, S.M., X. Cao, S.K. Sapperstein, E.C. Chiang, V.V. Lupashin, C. Barlowe, and M.G. Waters. 1999. Sec34p, a protein required for vesicle tethering to the yeast Golgi apparatus, is in a complex with Sec35p. *J. Cell Biol.* 147:729–742. doi:10.1083/jcb.147.4.729.

Vasile, E., T. Oka, M. Ericsson, N. Nakamura, and M. Krieger. 2006. IntraGolgi distribution of the Conserved Oligomeric Golgi (COG) complex. *Exp. Cell Res.* 312:3132–3141. doi:10.1016/j.yexcr.2006.06.005.

Venditti, R., M.C. Masone, and M.A. De Matteis. 2020. ER-Golgi membrane contact sites. *Biochem. Soc. Trans.* 48:187–197. doi:10.1042/BST20190537.

Voos, W., and T.H. Stevens. 1998. Retrieval of Resident Late-Golgi Membrane Proteins from the Prevacuolar Compartment of Saccharomyces cerevisiae Is Dependent on the Function of Grd19p. *J. Cell Biol.* 140:577–590. doi:10.1083/jcb.140.3.577.

Walch-Solimena, C., and P. Novick. 1999. The yeast phosphatidylinositol-4-OH kinase pik1 regulates secretion at the Golgi. *Nat. Cell Biol.* 1:523–525. doi:10.1038/70319.

Wei, J.-H., and J. Seemann. 2010. Unraveling the Golgi ribbon. *Traffic Cph. Den.* 11:1391–1400. doi:10.1111/j.1600-0854.2010.01114.x.

Weigel, A.V., C.-L. Chang, G. Shtengel, C.S. Xu, D.P. Hoffman, M. Freeman, N. Iyer, J. Aaron, S. Khuon, J. Bogovic, W. Qiu, H.F. Hess, and J. Lippincott-Schwartz. 2021. ER-to-Golgi protein delivery through an interwoven, tubular network extending from ER. *Cell*. 184:2412-2429.e16. doi:10.1016/j.cell.2021.03.035.

Welch, L.G., and S. Munro. 2019. A tale of short tails, through thick and thin: investigating the sorting mechanisms of Golgi enzymes. *FEBS Lett.* 593:2452–2465. doi:10.1002/1873-3468.13553.

Welch, L.G., S.-Y. Peak-Chew, F. Begum, T.J. Stevens, and S. Munro. 2021. GOLPH3 and GOLPH3L are broad-spectrum COPI adaptors for sorting into intra-Golgi transport vesicles. *J. Cell Biol.* 220. doi:10.1083/jcb.202106115.

Welz, T., J. Wellbourne-Wood, and E. Kerkhoff. 2014. Orchestration of cell surface proteins by Rab11. *Trends Cell Biol.* 24:407–415. doi:10.1016/j.tcb.2014.02.004.

Wendland, B., K.E. Steece, and S.D. Emr. 1999. Yeast epsins contain an essential N-terminal ENTH domain, bind clathrin and are required for endocytosis. *EMBO J.* 18:4383–4393. doi:10.1093/emboj/18.16.4383.

Wicky, S., H. Schwarz, and B. Singer-Krüger. 2004. Molecular interactions of yeast Neo1p, an essential member of the Drs2 family of aminophospholipid translocases, and its role in membrane trafficking within the endomembrane system. *Mol. Cell. Biol.* 24:7402–7418. doi:10.1128/MCB.24.17.7402-7418.2004.

Willett, R., T. Kudlyk, I. Pokrovskaya, R. Schönherr, D. Ungar, R. Duden, and V. Lupashin. 2013a. COG complexes form spatial landmarks for distinct SNARE complexes. *Nat. Commun.* 4:1553. doi:10.1038/ncomms2535.

Willett, R., D. Ungar, and V. Lupashin. 2013b. The Golgi puppet master: COG complex at center stage of membrane trafficking interactions. *Histochem. Cell Biol.* 140:271–283. doi:10.1007/s00418-013-1117-6.

Wilson, C., R. Venditti, L.R. Rega, A. Colanzi, G. D'Angelo, and M.A. De Matteis. 2010. The Golgi apparatus: an organelle with multiple complex functions. *Biochem. J.* 433:1–9. doi:10.1042/BJ20101058.

Witkos, T.M., and M. Lowe. 2016. The Golgin Family of Coiled-Coil Tethering Proteins. *Front. Cell Dev. Biol.* 3:86. doi:10.3389/fcell.2015.00086.

Witkos, T.M., and M. Lowe. 2017. Recognition and tethering of transport vesicles at the Golgi apparatus. *Curr. Opin. Cell Biol.* 47:16–23. doi:10.1016/j.ceb.2017.02.003.

Wong, E.D., S.R. Miyasato, S. Aleksander, K. Karra, R.S. Nash, M.S. Skrzypek, S. Weng, S.R. Engel, and J.M. Cherry. 2023. Saccharomyces genome database update: server architecture, pan-genome nomenclature, and external resources. *Genetics*. 224:iyac191. doi:10.1093/genetics/iyac191.

Wong, M., A.K. Gillingham, and S. Munro. 2017. The golgin coiled-coil proteins capture different types of transport carriers via distinct N-terminal motifs. *BMC Biol.* 15:3. doi:10.1186/s12915-016-0345-3.

Wong, M., and S. Munro. 2014. The specificity of vesicle traffic to the Golgi is encoded in the golgin coiled-coil proteins. *Science*. 346:1256898. doi:10.1126/science.1256898.

Woo, C.H., C. Gao, P. Yu, L. Tu, Z. Meng, D.K. Banfield, X. Yao, and L. Jiang. 2015. Conserved function of the lysine-based KXD/E motif in Golgi retention for

endomembrane proteins among different organisms. *Mol. Biol. Cell*. 26:4280–4293. doi:10.1091/mbc.E15-06-0361.

Wood, C.S., K.R. Schmitz, N.J. Bessman, T.G. Setty, K.M. Ferguson, and C.G. Burd. 2009. PtdIns4P recognition by Vps74/GOLPH3 links PtdIns 4-kinase signaling to retrograde Golgi trafficking. *J. Cell Biol.* 187:967–975. doi:10.1083/jcb.200909063.

Wooding, S., and H.R. Pelham. 1998. The dynamics of golgi protein traffic visualized in living yeast cells. *Mol. Biol. Cell*. 9:2667–2680. doi:10.1091/mbc.9.9.2667.

Wu, B., and W. Guo. 2015. The Exocyst at a Glance. *J. Cell Sci.* 128:2957–2964. doi:10.1242/jcs.156398.

Wu, Y., M. Takar, A.A. Cuentas-Condori, and T.R. Graham. 2016. Neo1 and phosphatidylethanolamine contribute to vacuole membrane fusion in Saccharomyces cerevisiae. *Cell. Logist.* 6:e1228791. doi:10.1080/21592799.2016.1228791.

Xiang, Y., and Y. Wang. 2011. New components of the Golgi matrix. *Cell Tissue Res.* 344:365–379. doi:10.1007/s00441-011-1166-x.

Xu, P., H.M. Hankins, C. MacDonald, S.J. Erlinger, M.N. Frazier, N.S. Diab, R.C. Piper, L.P. Jackson, J.A. MacGurn, and T.R. Graham. 2017. COPI mediates recycling of an exocytic SNARE by recognition of a ubiquitin sorting signal. *eLife*. 6:e28342. doi:10.7554/eLife.28342.

Yadav, S., M.A. Puthenveedu, and A.D. Linstedt. 2012. Golgin160 recruits the dynein motor to position the Golgi apparatus. *Dev. Cell*. 23:153–165. doi:10.1016/j.devcel.2012.05.023.

Yoko-o, T., C.A.R. Wiggins, J. Stolz, S.Y. Peak-Chew, and S. Munro. 2003. An N-acetylglucosaminyltransferase of the Golgi apparatus of the yeast Saccharomyces cerevisiae that can modify N-linked glycans. *Glycobiology*. 13:581–589. doi:10.1093/glycob/cwg063.

Zahn, C., A. Hommel, L. Lu, W. Hong, D.J. Walther, S. Florian, H.-G. Joost, and A. Schürmann. 2006. Knockout of Arfrp1 leads to disruption of ARF-like1 (ARL1) targeting to the trans-Golgi in mouse embryos and HeLa cells. *Mol. Membr. Biol.* 23:475–485. doi:10.1080/09687860600840100.

Zanetti, G., S. Prinz, S. Daum, A. Meister, R. Schekman, K. Bacia, and J.A.G. Briggs. 2013. The structure of the COPII transport-vesicle coat assembled on membranes. *eLife*. 2:e00951. doi:10.7554/eLife.00951.

Zhang, H., J. Chen, Y. Wang, L. Peng, X. Dong, Y. Lu, A.E. Keating, and T. Jiang. 2009. A computationally guided protein-interaction screen uncovers coiled-coil interactions involved in vesicular trafficking. *J. Mol. Biol.* 392:228–241. doi:10.1016/j.jmb.2009.07.006.

Zhang, Y., and F.M. Hughson. 2021. Chaperoning SNARE Folding and Assembly. *Annu. Rev. Biochem.* 90:581–603. doi:10.1146/annurev-biochem-081820-103615.

Zhdankina, O., N.L. Strand, J.M. Redmond, and A.L. Boman. 2001. Yeast GGA proteins interact with GTP-bound Arf and facilitate transport through the Golgi. *Yeast Chichester Engl.* 18:1–18. doi:10.1002/1097-0061(200101)18:1%3C1::AID-YEA644%3E3.0.CO;2-5.

Zhu, L., J.R. Jorgensen, M. Li, Y.-S. Chuang, and S.D. Emr. 2017. ESCRTs function directly on the lysosome membrane to downregulate ubiquitinated lysosomal membrane proteins. *eLife*. doi:10.7554/eLife.26403.

APPENDIX A

GOS1 IS A BROADLY LOCALIZED GOLGI SNARE THAT LIKELY FUNCTIONS WITH COY1 TO PROMOTE THE FUSION OF INTERMEDIATE COPI VESICLES

The Qb SNARE Gos1 was originally implicated in both intra-Golgi and Golgi-to-ER transport (McNew et al., 1998), but is now considered to be primarily involved in the fusion of intra-Golgi vesicles (Grissom et al., 2020). Gos1 localizes to the medial Golgi, colocalizing partially with the early Golgi protein Rer1 and the late Golgi protein Sec7 during cisternal maturation (Matsuura-Tokita et al., 2006). Loss of Gos1 causes a slight growth defect and improper secretion of Carboxypeptidase Y as well as the ER-resident Kar2 (McNew et al., 1998). The endocytic SNAREs Tlg1, Tlg2, and Snc1 are also mislocalized in *gos1Δ* cells (Siniossoglou and Pelham, 2001). These rather broad phenotypes suggest that Gos1 may function in multiple trafficking pathways at Golgi.

To more precisely investigate Gos1 localization and function, I kinetically mapped it against both Sys1 and Tmn1 (Figure A.1). Gos1 appears simultaneously with the intermediate COPI pathway cargo Tmn1 (Figure A.1A), then persists until its disappearance with Sys1 (Figure A.1B). The apparent near simultaneous appearance of Gos1 and Sys1 in Figure A.1B is mostly due to the weak signal exhibited by GFP-Gos1 relative to HaloTag-Gos1 used for the experiment in Figure A.1B. Gos1 evidently appears earlier than Sys1 and simultaneously with Tmn1 when its signal is optimized for imaging (Figure A.1A and Figure 3.4A). These kinetic data reveal that Gos1 broadly localizes to both early and late Golgi cisternae.

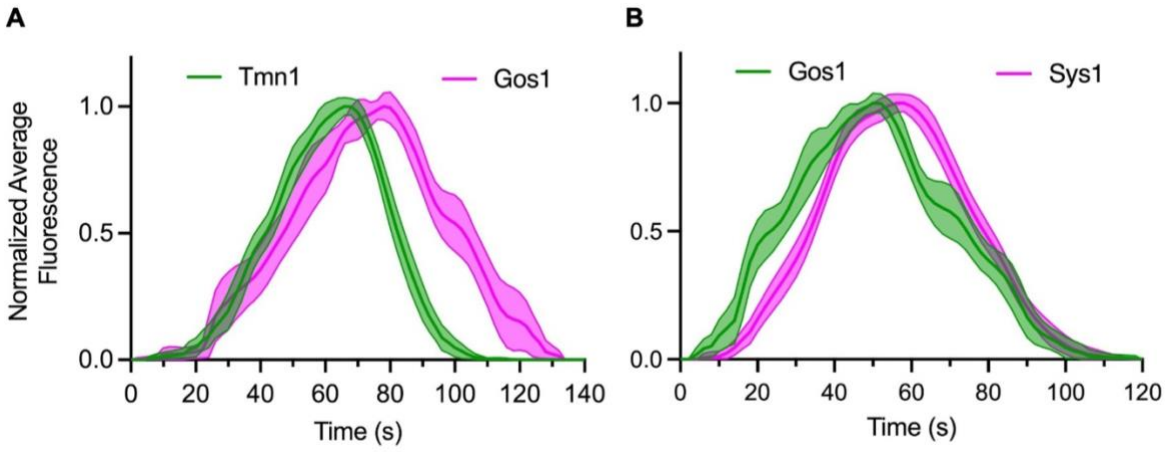

Figure A.1: **Gos1 appears with Tmn1 and disappears with Sys1 during cisternal maturation. (A)** *S. cerevisiae* cells expressing HaloTag-Gos1 and GFP-Tmn1 from their endogenous loci were grown to mid log phase in NSD, stained with JFx650 dye, and imaged on a Leica Stellaris confocal microscope. Thirteen spatially isolated cisternae were tracked over time, and their fluorescence intensities were averaged as described in Chapter 3. **(B)** As in (A), except cells expressing Sys1-HaloTag and GFP-Gos1 from their endogenous loci were stained with JFx646 and imaged. Fourteen spatially isolated cisternae were tracked over time.

The arrival of Gos1 with Tmn1 suggests that Gos1 may act as a v-SNARE that aids in the fusion of intermediate COPI vesicles. The departure of Gos1 with Sys1 implies it additionally recycles in AP-1/Ent5 vesicles. Intriguingly, I observed a biphasic departure of Gos1 which was reproduced in the averages of both experiments. The first phase is suggestive of Gos1 departure in intermediate COPI vesicles while the second phase may represent departure in AP-1/Ent5 vesicles. I also observed HaloTag-Gos1 at the limiting membrane of the vacuole, hinting that it may play a secondary role in fusogenic events with this organelle (data not shown). In total, my data implicate Gos1 as a SNARE that may function in the intermediate COPI pathway.

Coy1 is a transmembrane containing golgin that interacts with the COG multisubunit tether and its associated SNAREs (e.g. Gos1) to promote the fusion of intra-Golgi vesicles (Anderson et al., 2017). Coy1 also genetically interacts with Gos1 (Anderson and Barlowe, 2019), so I

kinetically mapped Coy1 to better understand when it functions during cisternal maturation. Surprisingly, Coy1 appears at and disappears from cisternae before the early COPI pathway cargo Vrg4 (Figure A.2A). These kinetics are not altered in a strain expressing HaloTag-Coy1 as a second genetic copy from its endogenous locus (Figure A.2B). The early localization of Coy1 indicates only a partial kinetic overlap with Gos1, which appears with Tmn1 about 20 seconds on average after Vrg4 (Figure A.1A and Figure 3.4A). In summary, Coy1 localizes exclusively to the early Golgi and may only function with Gos1 during the second half of its cisternal residency.

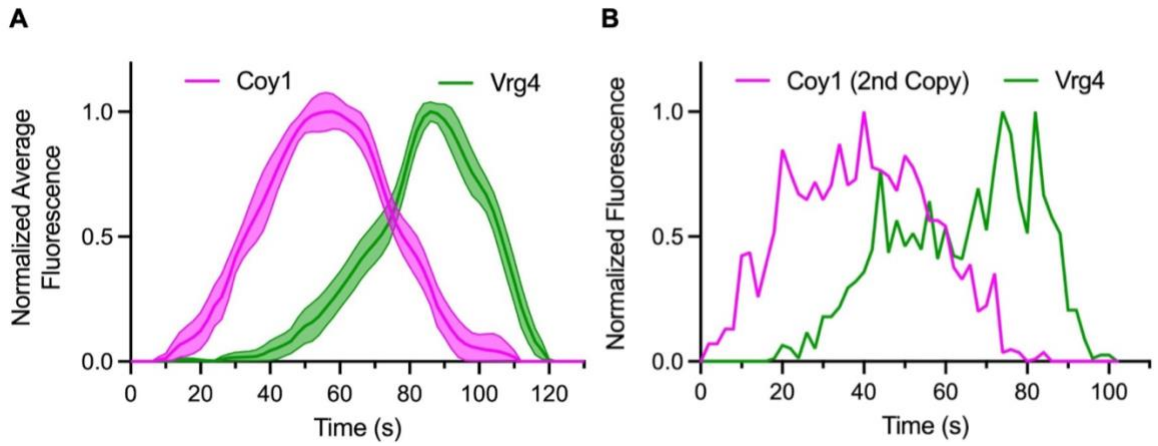

Figure A.2: **Coy1 appears and disappears before Vrg4 during cisternal maturation. (A)** *S. cerevisiae* cells expressing HaloTag-Coy1 and GFP-Vrg4 from their endogenous loci were grown to mid log phase in NSD, stained with JFx646 dye, and imaged on a Leica Stellaris confocal microscope. Twelve spatially isolated cisternae were tracked over time, and their fluorescence intensities were averaged as described in Chapter 3. **(B)** As in (A), except an individual trace is shown from an experiment using cells with HaloTag-Coy1 expressed as a second copy from its endogenous locus.

Since Coy1 assists in the fusion of intra-Golgi vesicles (Anderson et al., 2017), I asked whether deletion of Coy1 affects the kinetics of early and intermediate COPI cargos. An analysis of Vrg4 and Tmn1 kinetics in *coy1Δ* cells showed that they were not noticeably altered relative to each other (compare Figure A.3A to Figure 3.4A). Coy1 and Gos1 physically interact (Anderson et al., 2017), so I next asked whether the kinetics of Gos1 were altered in *coy1Δ* cells. An analysis

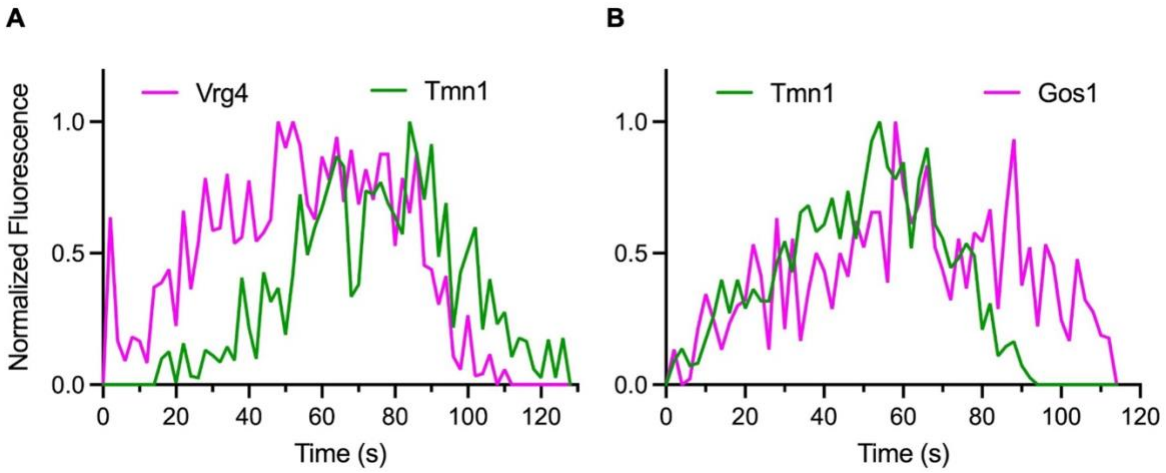

Figure A.3: **Loss of Coy1 does not noticeably alter the kinetics of Vrg4, Tmn1, and Gos1 relative to each other. (A)** *S. cerevisiae* cells lacking the Coy1 open reading frame and expressing HaloTag-Vrg4 and GFP-Tmn1 from their endogenous loci were grown to mid log phase in NSD, stained with JFx650 dye, and imaged on a Leica Stellaris confocal microscope. A spatially isolated cisterna was tracked over time, and the normalized fluorescence intensities of the two tagged proteins were quantified. **(B)** As in (A), except HaloTag-Gos1 was expressed from its endogenous locus instead of HaloTag-Vrg4.

of relative Tmn1 and Gos1 kinetics showed no apparent change due to loss of Coy1 (compare Figure A.3B to Figure A.1A). While analyzing data from this experiment, I noticed a hazy cytosolic GFP-Tmn1 signal in the vast majority of *coy1Δ* cells imaged (Figure A.4). This signal was only present in cells lacking Coy1 and expressing HaloTag-Gos1 as a single copy from its locus. A plausible interpretation of my observation is that the N-terminal tagging of Gos1 partially inhibits its function. When coupled with the removal of Coy1, this partial inhibition of Gos1 causes a noticeably slower rate of intermediate COPI vesicle fusion. The result is an increased cytosolic haze of GFP-Tmn1, which presumably originates from vesicles. If my interpretation is accurate, these data evidence roles for both Coy1 and Gos1 in assisting with the fusion of Tmn1-containing, intermediate COPI vesicles. Regardless, Coy1 by itself is apparently not required for intermediate COPI vesicle fusion. Future experiments should test whether Gos1 plays an essential role in this

process, perhaps by coupling kinetic analysis with a depletion of Gos1 using the rapamycin-induced degradation system (Zhu et al., 2017).

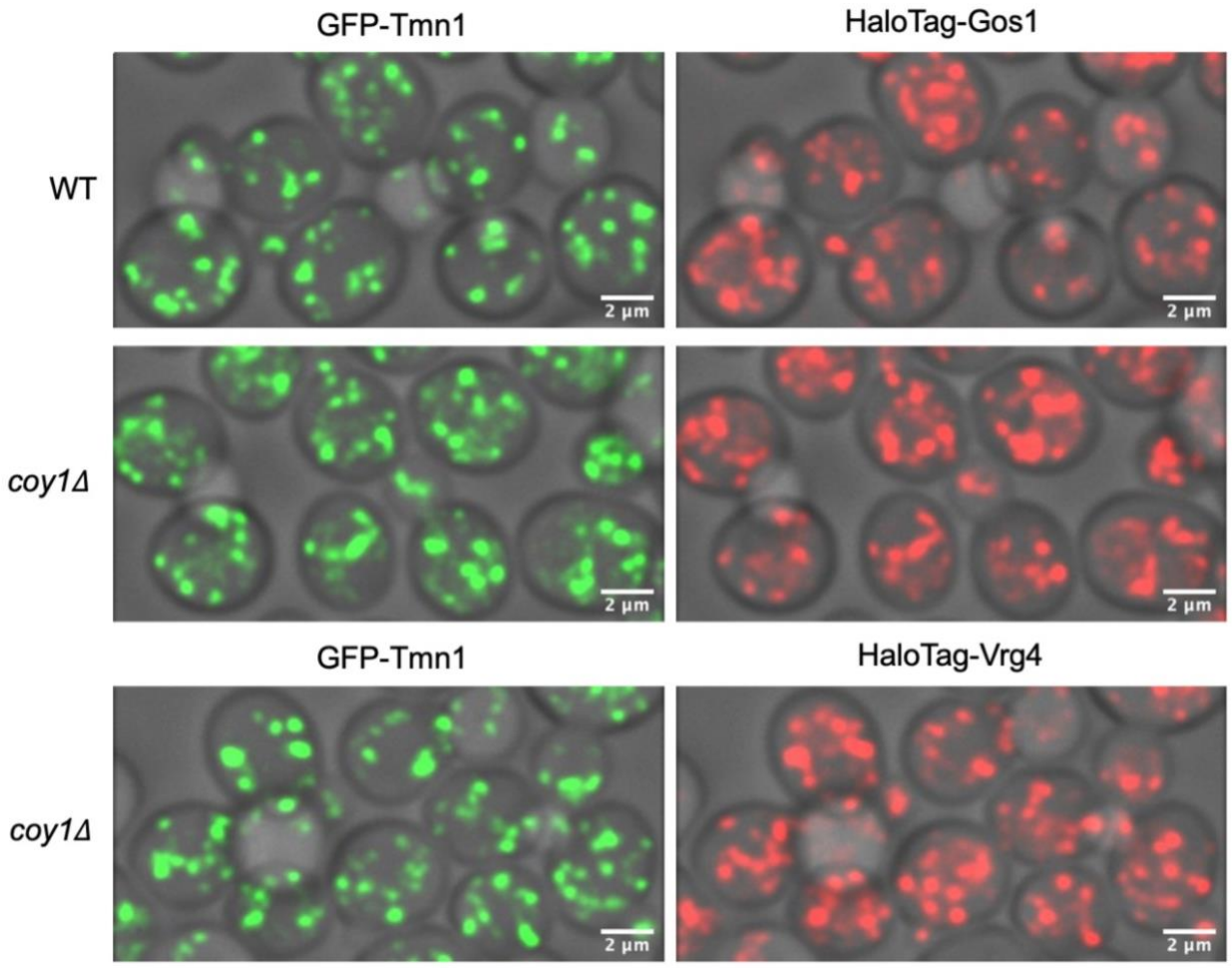

Figure A.4: **Loss of Coy1 partially delocalizes Tmn1 from cisternae when Gos1 is N-terminally tagged.** Representative images showing the selective impact of COY1 deletion on Tmn1 Golgi localization when Gos1 is N-terminally tagged with HaloTag. *S. cerevisiae* cells containing or lacking the Coy1 open reading frame and expressing the indicated fusion proteins from their endogenous loci were grown to mid log phase in NSD, stained with JFx650 dye, and imaged on a Leica Stellaris confocal microscope. Z stacks of temporally identical time points were deconvolved using Huygens software and average projected. Each channel was identically contrasted in ImageJ for fair visual comparison. Note the hazy cytosolic GFP-Tmn1 signal that occurs upon simultaneous COY1 deletion and Halo-tagging of Gos1. Scale bar 2µm.

APPENDIX B

EARLY GOLGI PROTEINS THAT ESCAPE TO THE LATE GOLGI MAY BE FREQUENTLY SALVAGED BY SUBSEQUENT TRAFFICKING PATHWAYS

The intermediate COPI intra-Golgi trafficking pathway described in this thesis initially eluded our detection. In particular, the kinetics and partial AP-1/Ent5 dependencies of proteins like Sys1 confounded our efforts to assign such proteins to distinct trafficking pathways (Casler et al., 2021). We now know that unique kinetic traces do not always represent single trafficking pathways. Apparently, the trafficking mechanisms underlying our kinetic observations are more complex than we imagined (see Chapter 5).

While examining the kinetics of intermediate COPI pathway proteins, I noticed that Tmn1 appearance at and disappearance from cisternae preceded that of Sys1 (Figure 3.4A). The same is true of Gnt1, an N-acetylglucosaminyltransferase with reported medial Golgi localization (Figure B.1A) (Yoko-o et al., 2003). The kinetics of Gnt1 are indicative of when Sys1 may arrive and depart in intermediate COPI vesicles. They are consistent with Sys1 additionally recycling in the AP-1/Ent5 pathway. As Gnt1 levels drop, Sys1 levels continue to rise due to its arrival in AP-1/Ent5 vesicles. To test this understanding, I performed a GARP tethering assay with Sys1, expecting it to be tethered in vesicles like Kex2 (Figure 4.6A). I did observe Sys1 in GARP tethered vesicles and noted it was less abundant than Kex2 (compare Figure B.1B and Figure 4.6A). This is consistent with our understanding that the pool of cellular Sys1 molecules is split between the AP-1/Ent5 and intermediate COPI pathways.

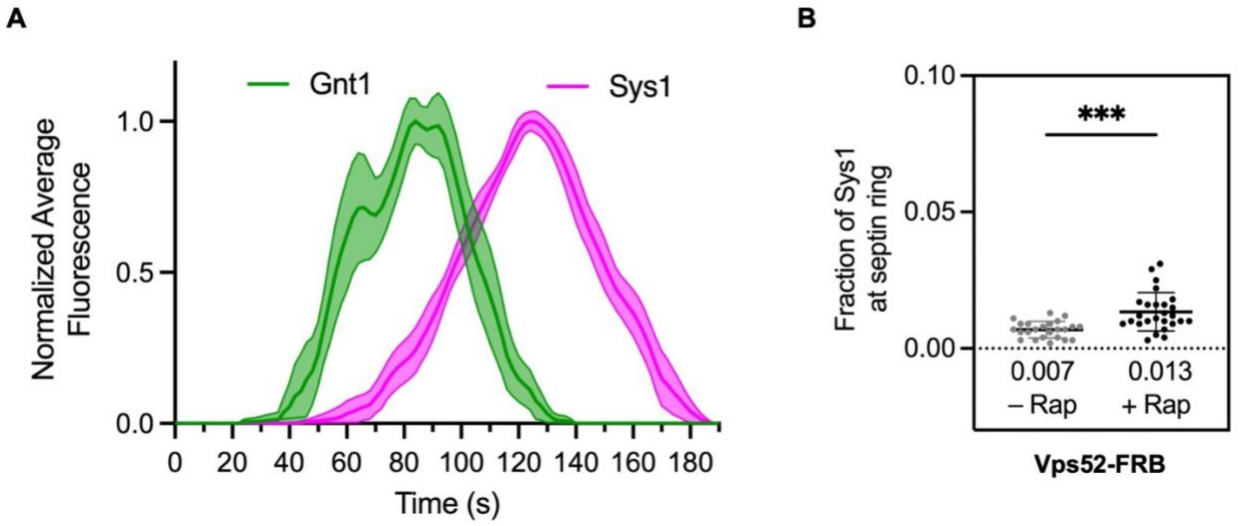

Figure B.1: **Sys1 appears after Gnt1 during cisternal maturation and traffics in vesicles tethered by GARP. (A)** *S. cerevisiae* cells expressing Sys1-HaloTag, and Gnt1-GFP from their endogenous loci were grown to mid log phase in NSD, stained with JFx650 dye, and imaged on a Leica Stellaris confocal microscope. Eleven spatially isolated cisternae were tracked over time, and their fluorescence intensities were averaged as described in Chapter 3. **(B)** GARP tethering assay with endogenously expressed Sys1-GFP performed as described in Chapter 4. ***, significant at P value =0.0001.

While characterizing recycling pathways by direct vesicle capture, we recognized that missorting of proteins into other pathways likely occurs on a regular basis. For example, small amounts of Vrg4 are captured in vesicles with Sys1 (Figure 3.3C). Such a phenomenon is not surprising given that individual trafficking pathways operate on a timescale of seconds during cisternal maturation. As discussed in Chapter 5, it is likely that downstream intra-Golgi trafficking pathways salvage proteins that escape their intended, timely packaging into vesicles of their primary pathway. Additional experiments presented here show that the early COPI cargo proteins Gda1 and Pmr1 are trafficked in significant quantities in Sys1 vesicles (Figure B.2A). In particular, Pmr1 substantially leaks into this vesicle population, presumably because it also occasionally takes the AP-1/Ent5 pathway with Kex2 and Sys1 (Figure B.2B). These results suggest that Pmr1 is not

as efficiently packaged into COPI vesicles and compensates by taking multiple downstream intra-Golgi pathways for Golgi retention.

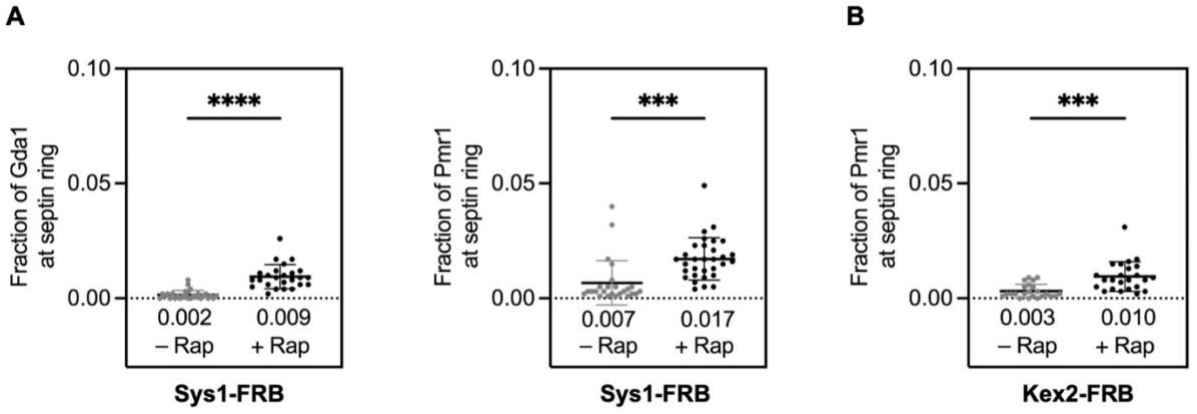

Figure B.2: **Early COPI cargos leak into downstream intra-Golgi trafficking pathways.** Sys1 based **(A)** and Kex2 based **(B)** vesicle capture assays performed as described in Chapter 3. GFP-Pmr1 and Gda1-GFP were expressed from their endogenous loci. ****, significant at P value <0.0001; ***, significant at P value <0.001.

The Pmr1 vesicle capture data imply that this protein leaks into downstream pathways more frequently than Vrg4 and Gda1. Pmr1 is a P-type ATPase transporter that shuttles calcium and manganese into the Golgi lumen (Antebi and Fink, 1992; Dürr et al., 1998). It is presumably monomeric and possesses three large cytosolic domains that undergo substantial movement during ion translocation (Palmgren and Nissen, 2011). These dynamic domains may slow the rate of Pmr1 packaging into COPI vesicles relative to other cargos, causing it to leak into downstream pathways. While collecting data for Chapter 3, I attempted to use FRB tagged Pmr1 as a means for vesicle capture. I was able to capture Pmr1 in vesicles at the septin ring but could only detect minimal amounts of Vrg4 or Sys1 in this vesicle population (Figure B.3). These observations are challenging to explain. However, the leakage of Pmr1 into downstream pathways coupled with the normally low signal levels of cargo co-capture in my assays may be sufficient in combination to prevent efficient and readily apparent co-capture by Pmr1.

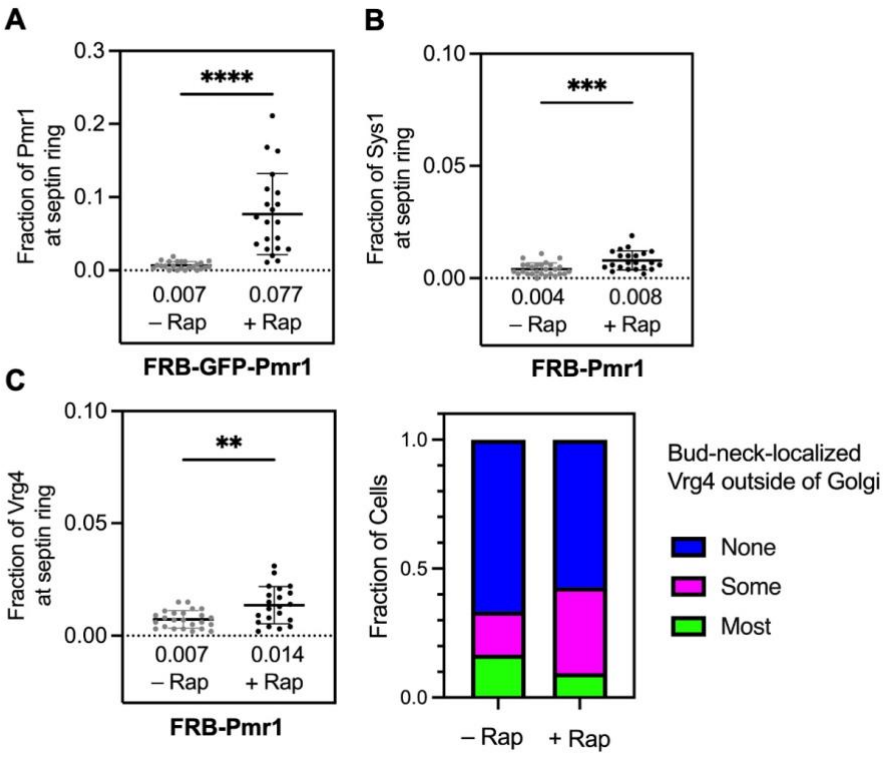

Figure B.3: **Pmr1 does not efficiently co-capture Vrg4 and Sys1 in vesicle capture assays. (A)** The FRB-GFP-Pmr1 fusion protein was expressed from its endogenous locus and used for a self-vesicle capture control experiment as described in Chapter 3. **(B)** The FRB-Pmr1 fusion protein was expressed from its locus, and a vesicle capture experiment was performed with endogenously expressed Sys1-GFP as described in Chapter 3. **(C)** As in (B), except GFP-Vrg4 was endogenously expressed instead of Sys1-GFP. Both numerical and categorical quantification plots are shown for this experiment. ****, significant at P value <0.0001; ***, significant at P value <0.001; **, significant at P value <0.01.

Given the unexpected Pmr1 vesicle capture data, I wanted to verify that this protein primarily traffics in the early COPI pathway as stated in Chapter 3. I therefore performed tethering assays with the early COPI pathway golgin Rud3 and the intermediate COPI pathway golgin Sgm1. As expected, Rud3 but not Sgm1 tethered vesicles with detectable levels of Pmr1 (Figure B.4). The apparent lack of Pmr1 in Sgm1 tethered vesicles is likely due to lower vesicle accumulation by the tethering assay compared to the vesicle capture assay with Sys1 (Figure B.2A). In summary, the trafficking dynamics of Pmr1 are incompletely understood at present, but

the totality of its kinetic, vesicle capture, and tethering data indicate that it primarily recycles in the early COPI trafficking pathway.

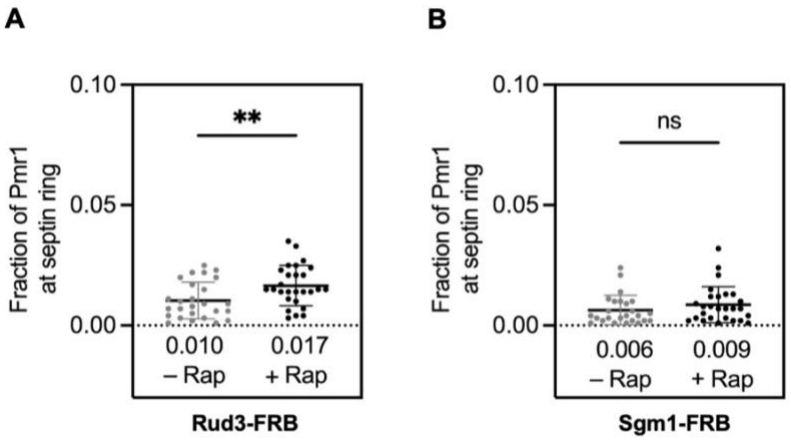

Figure B.4: **Pmr1 mostly traffics in vesicles tethered by Rud3 but not Sgm1.** Rud3 based **(A)** and Sgm1 based **(B)** vesicle tethering assays performed as described in Chapter 4. GFP-Pmr1 was expressed from its endogenous locus. **, significant at P value <0.01; ns, not significant.

APPENDIX C

VESICULAR TRANSPORT BETWEEN THE GOLGI AND PREVACUOLAR ENDOSOME MAINTAINS THEIR ORGANELLAR IDENTITIES

Vesicular transport occurs between the Golgi and PVE, beginning at the early-to-late Golgi transition during cisternal maturation (Casler and Glick, 2020). As discussed in Chapter 5, the precise identities of the trafficking pathways between these organelles are unclear. We nevertheless understand the functional relevance of these pathways for sorting proteins destined for degradation in the vacuole. As an integral membrane receptor, Vps10 assists in protein degradation by transporting hydrolases from the Golgi to the PVE en route to the vacuole (Cooper and Stevens, 1996). Upon reaching the PVE and unloading its hydrolase cargos, Vps10 is recycled to the Golgi with the aid of the retromer complex (Seaman et al., 1998). Vps10 is therefore a cargo that recycles in at least two carrier types between the Golgi and PVE.

While performing vesicle capture experiments with FRB-tagged Vps10, I noticed that the Golgi proteins Pmr1, Tmn1, and Sys1 are detectable at low levels in Vps10 vesicles (Figure C.1). My observations may evidence the slow, steady state turnover rates of these proteins as they occasionally travel to the PVE and then vacuole. Alternatively, these data may be highlighting proteins capable of returning to the Golgi after escaping to the PVE at a greater than needed frequency. At least for Sys1, this is plausible as it requires the retromer complex for its proper steady state Golgi localization (Bean et al., 2017). Regardless of which explanation proves more accurate, these Vps10 vesicle capture data are a reminder of the roles trafficking pathways

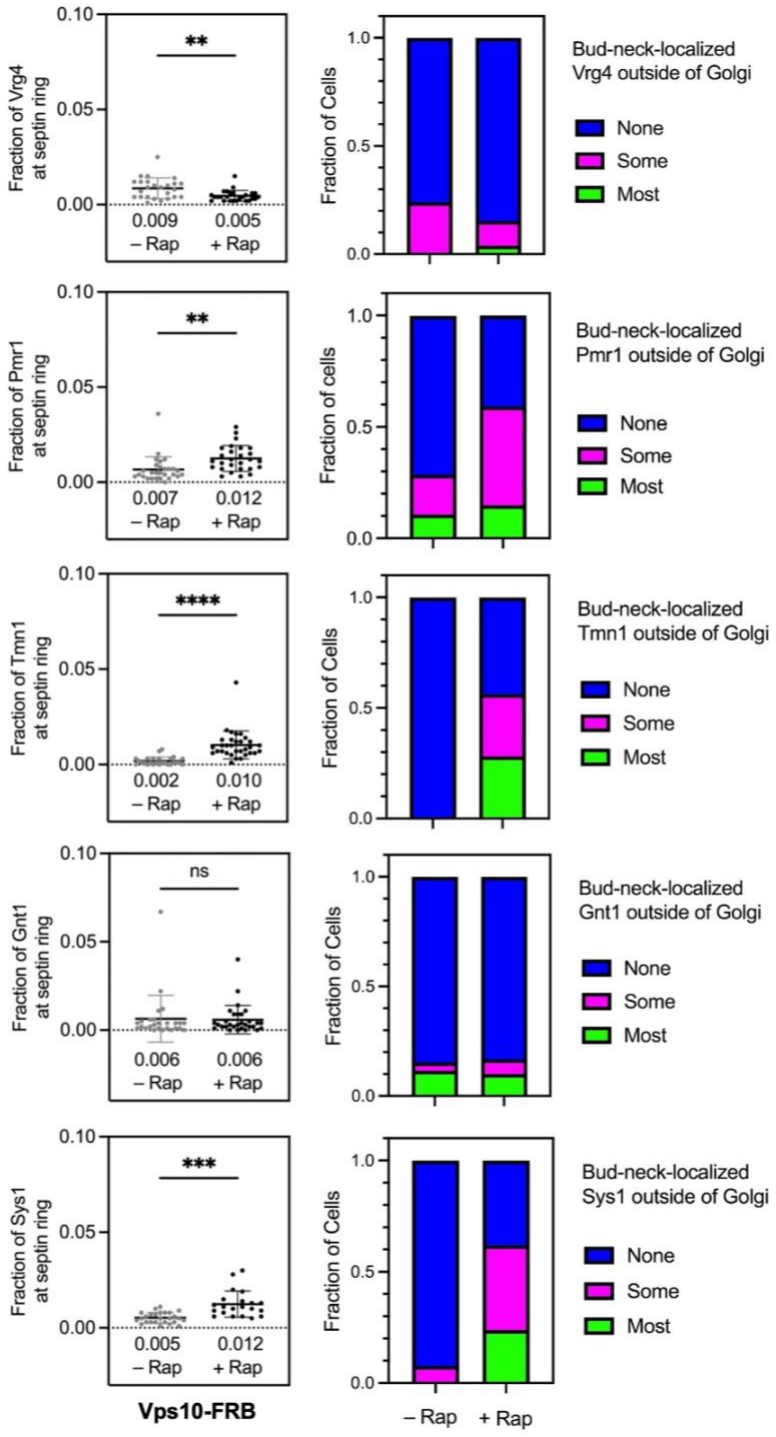

Figure C.1: **Small amounts of Golgi resident proteins are present in Vps10 containing vesicles.** Vps10-based vesicle capture assays were performed as stated in Chapter 4 with the listed GFP-tagged proteins expressed from their endogenous loci. Both numerical and categorical quantification plots are shown for these experiments. ****, significant at P value <0.0001; ***, significant at P value =0.0001; **, significant at P value <0.01; ns, not significant.

between the Golgi and PVE play in maintaining Golgi identity, protein localization, and proteostasis.

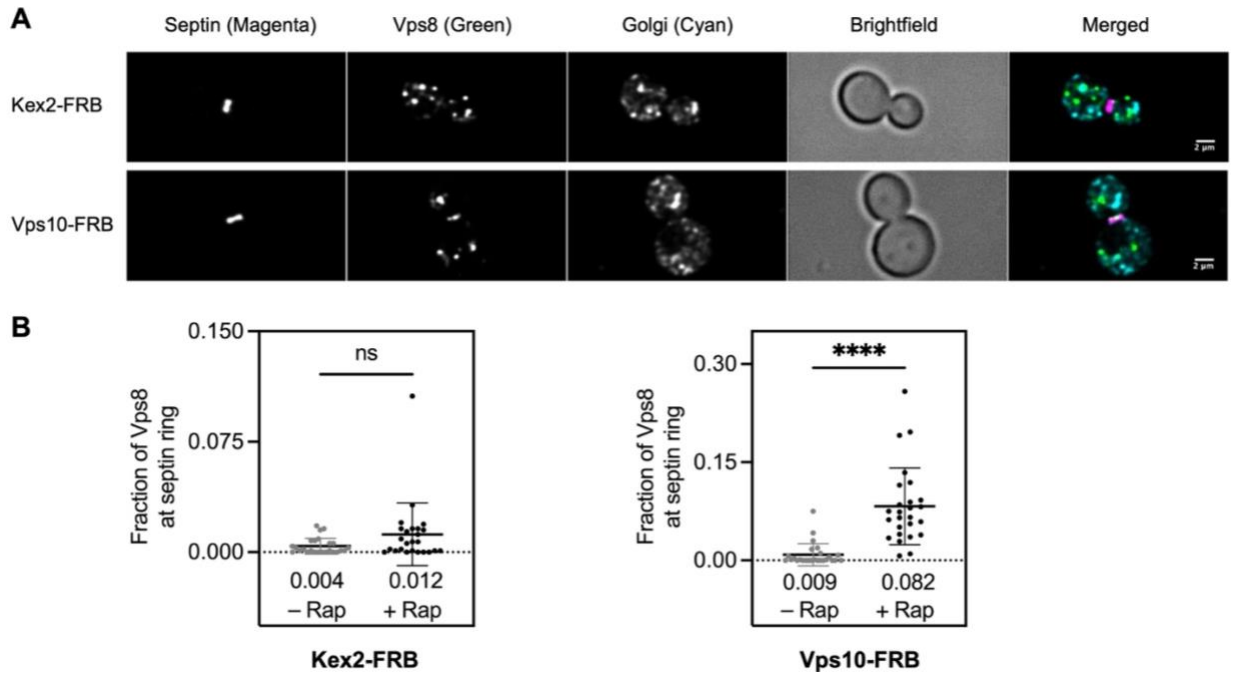

Figure C.2: **Prevacuolar endosomes can be relocalized to the septin ring in the context of Kex2 and Vps10-based vesicle capture assays. (A)** Representative images from Kex2 and Vps10-based vesicle capture assays performed as described in Chapters 3 and 4 respectively. Vps8-GFP was expressed from its endogenous locus. Note the Vps8 positive structures colocalizing with or adjacent to the septin ring. **(B)** Quantifications from (A) performed as described in Chapters 3 and 4. ****, significant at P value <0.0001; ns, not significant. Scale bar 2µm.

Yeast PVEs often associate with the vacuole in order to deliver cargo destined for degradation via kiss-and-run fusogenic events (Casler and Glick, 2020). The multisubunit HOPS complex and its SNARE partner proteins are responsible for tethering PVEs to the vacuole and opening fusion pores between these organelles (Ungermann and Moeller, 2025). The duration of PVE-to-vacuole tethering and its regulation have not been thoroughly investigated. While performing vesicle capture assays, I discovered that Vps8 positive PVEs can be captured at the

septin ring (Figure C.2). This suggests that some PVEs are untethered from the vacuole and can relocate to the septin ring within the five-minute time window of this experiment. PVE capture by Vps10 occurs much more frequently than capture by Kex2 (Figure C.2B). This difference in frequency of PVE capture is consistent with the respective high and low abundances of Vps10 and Kex2 at PVEs (Papanikou et al., 2015). Altogether, these data indicate that continuous association with the vacuole may not be an obligate feature of PVE organellar identity.

The PVE localized GTPase, Vps21, promotes the import of cargo from the Golgi, likely through its recruitment of the CORVET multisubunit tether (Gerrard et al., 2000; Peplowska et al., 2007). Many cargos recycling back to the Golgi depend on the SNX-BAR-retromer complex, which contains the sorting nexin Vps17 (Carosi et al., 2023). While performing Vps10-based vesicle capture assays, I made the serendipitous discovery that Vps21 and Vps17 are both present on Vps10 containing carriers (Figure C.3). For Vps17, the simple interpretation is that this sorting nexin remains on Vps10 laden carriers transiting from the PVE to the Golgi. The presence of Vps21 is more challenging to explain. A 2019 study claimed that the Vps21 guanine nucleotide exchange factor, Vps9, is recruited to vesicles budding from TGN (Nagano et al., 2019). The authors provided evidence that Golgi-associated vesicle fission machinery such as Arf1 and the Ent3 and Ent5 adapters are responsible for promoting the homotypic fusion of Vps21 positive PVEs. They proposed that Golgi-to-PVE transport delivers Vps9 on vesicles to PVEs for activation of Vps21. My vesicle capture data agree with their model and refine it by suggesting that Vps21 can be activated by Vps9 on Vps10-containing, PVE-destined vesicles that bud from the late Golgi. Such a model would account for the mostly cytosolic distribution of Vps9 in wild type cells (Nagano et al., 2019). To further test my hypothesis of vesicle-localized Vps21 activation, an experiment examining Vps10-containing vesicles for the presence of Vps9 could be performed. If

this promising model holds up to future scrutiny, it will demonstrate how Golgi-to-PVE transport helps maintain the distinct identity of the PVE.

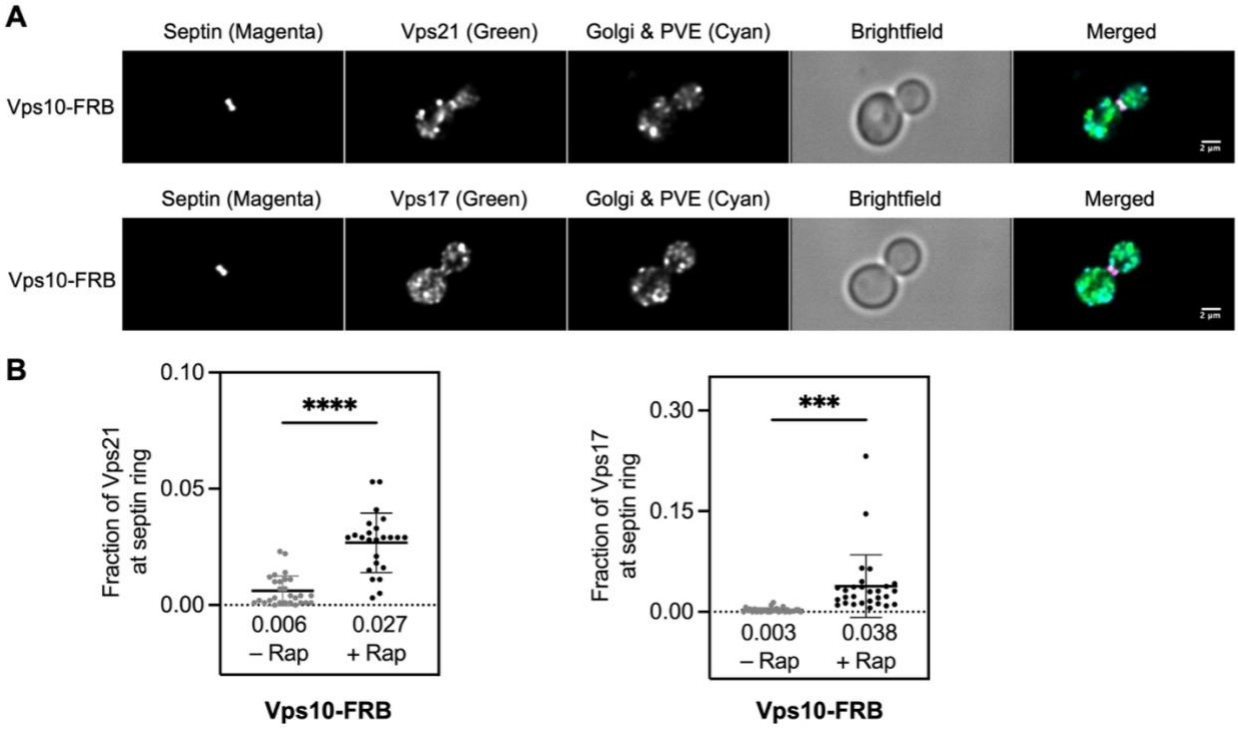

Figure C.3: **Vps17 and Vps21 are present on Vps10 containing vesicles. (A)** Representative images from Vps10-based vesicle capture assays performed as described in Chapter 4. Vps17-GFP and GFP-Vps21 were expressed from their endogenous loci. **(B)** Quantifications from (A) performed as described in Chapter 4. ****, significant at P value <0.0001; ***, significant at P value <0.001. Scale bar 2µm.

APPENDIX D

IMH1 CATALYZES AP-1/ENT5 VESICLE FUSION AND TETHERS VESICLES CONTAINING MINIMAL AMOUNTS OF THE R-SNARE SNC2

As demonstrated in Chapter 4, the golgin Imh1 localizes to the late Golgi and tethers incoming AP-1/Ent5 vesicles as well as carriers arriving from the PVE. Mechanistically, Imh1 is thought to help position such vesicles close to cisternae where other membrane-proximal components of the fusion machinery are localized (Gillingham, 2017). If this understanding is accurate, Imh1 could accelerate the fusion of vesicles it tethers and thereby increase the concentration of vesicle cargos in cisternae. I unintentionally tested this hypothesis while examining the effects of cytosolically localized Imh1 on Golgi maturation. As shown here, Imh1 removal from cisternae does not alter the timing of Kex2 arrival relative to Sys1 (compare Figure D.1A and Figure 3.3A). However, while imaging, I noticed that Kex2 signals at cisternae were dimmer compared to those in cells with wild type, Golgi-localized Imh1. This is reflected by the larger than usual standard error throughout most of the Kex2 averaged trace (Figure D.1A). I examined the individual traces which comprise the average, and observed that many of them possess especially weak Kex2 signals during its arrival phase. An example of this is shown in Figure D.1B. Since this experiment was performed in cells with cytosolically localized Imh1, it is possible these Imh1 molecules could have interfered with the other machinery proteins and slowed vesicle fusion. However, I did not observe residual Imh1 associated with Golgi cisternae, and a subsequent experiment performed by Natalie Johnson also demonstrated lower Kex2 cisternal abundance in *imh1Δ* cells (data not shown). Therefore, our data collectively suggest that Imh1, although dispensable for AP-1/Ent5

vesicle fusion at the Golgi, catalyzes this process and allows for a higher concentration of late Golgi resident proteins in cisternae.

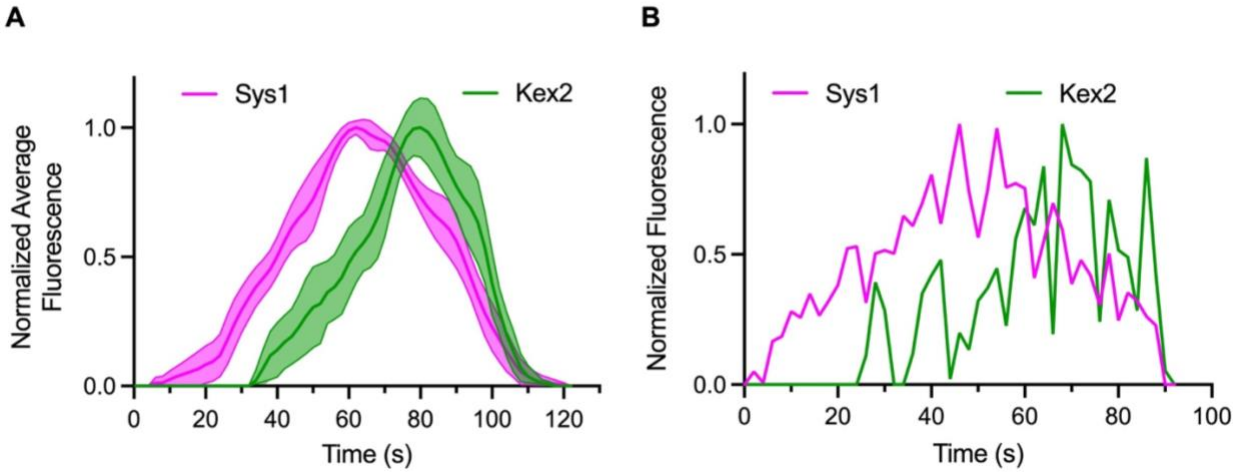

Figure D.1: **Imh1 accelerates the accumulation of Kex2 at the late Golgi. (A)** *S. cerevisiae* cells expressing Imh1(−GRIP domain)-FRBx2, Sys1-HaloTag, and Kex2-GFP from their endogenous loci were grown to mid log phase in NSD, stained with JFx646 dye, and imaged on a Leica Stellaris confocal microscope. Nine spatially isolated cisternae were tracked over time, and their fluorescence intensities were averaged as described in Chapter 3. **(B)** A representative individual trace from the dataset in (A). Note the large standard error in the average Kex2 trace in (A) and the inconsistent, weak signal during the first half of the Kex2 trace in (B).

The R-SNARE paralogs Snc1 and Snc2 function in SNARE complexes mediating exocytic and endocytic vesicle fusion events in yeast (Protopopov et al., 1993; Gerst, 1997; Gurunathan et al., 2000). Snc1 and Snc2 largely localize to the late Golgi and plasma membrane (Robinson et al., 2006), and their trafficking itineraries have been debated in recent years. For example, some researchers have suggested Snc1 traffics through multiple pathways from endosomes to the Golgi using retromer, sorting nexins, and even COPI (Xu et al., 2017; Best et al., 2020). Our view of the yeast minimal endomembrane system implies that Snc1 and Snc2 can directly traffic between the late Golgi and plasma membrane (Day et al., 2018). However, this does not exclude the possibility

Snc1 and Snc2 may also take other intra-cellular recycling pathways such as those between the PVE and Golgi.

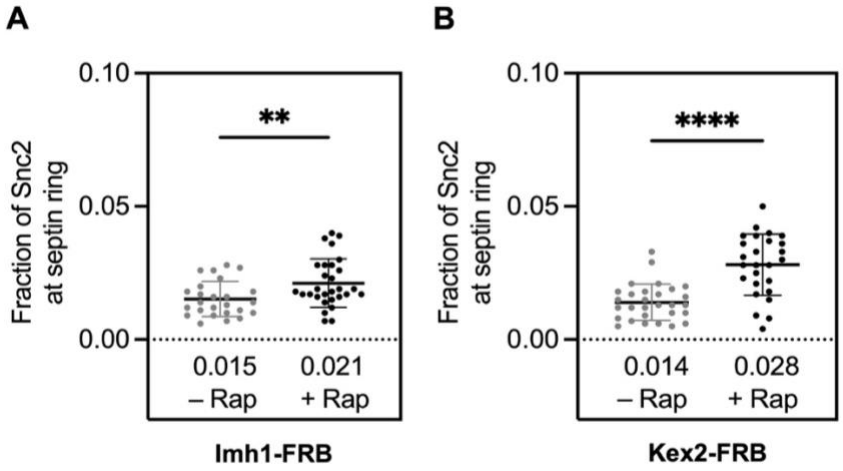

Figure D.2: **Minor populations of Snc2 molecules traffic in vesicles with Kex2 and vesicles tethered by Imh1.** The Imh1 based vesicle tethering assay (A) and Kex2 based vesicle capture assay (B) were performed as described in Chapters 4 and 3 respectively. GFP-Snc2 was expressed from its endogenous locus. Note that the high GFP-Snc2 levels quantified in control cells are due to normal Snc2 residence at the plasma membrane. **, significant at P value <0.01; ****, significant at P value <0.0001.

I was curious whether Imh1 could tether vesicles with Snc2, and which trafficking pathway(s) Snc2 commonly utilizes. Upon Imh1 localization to the bud neck, I observed minimal recruitment of Snc2 (Figure D.2A). This suggests that Imh1 does not tether vesicles enriched with Snc2, and further implies that Snc2 does not primarily traffic in the Imh1-tethered vesicles of the AP1/Ent5 and/or PVE-to-Golgi pathways. To further test this interpretation, I performed Kex2-based vesicle capture of Snc2 and observed a somewhat higher GFP-Snc2 signal at the bud neck than with the Imh1 experiment (Figure D.2B). This result is more challenging to interpret. If we consider that Kex2 sometimes recycles through the PVE and usually recycles in the AP-1/Ent5 pathway, it is plausible that the detected Snc2 could be from vesicles of these trafficking routes. However, another explanation is that Kex2 molecules are occasionally missorted to the plasma

membrane and then retrieved by endocytosis in vesicles with Snc2. Either or both of these explanations could account for the non-trivial signal observed upon Kex2-based vesicle capture. In summary, it appears that a minor population of Snc2 molecules traffic with Kex2 in vesicles, and at least some of these vesicles can be tethered by Imh1. To put these data and interpretations into context, future experiments should examine the vesicle population(s) enriched with Snc2 and characterize the corresponding trafficking pathway(s).

APPENDIX E

ANY1 AND NEO1 LOCALIZE TO THE INTERMEDIATE AND LATE GOLGI WHERE THEY MAY COOPERATE IN LIPID BILAYER REMODELING

The P-type ATPase Neo1 is a lipid flippase that translocates phosphatidylserine (PS) and phosphatidylethanolamine (PE) from the lumenal (or extracellular) leaflet of membranes to the cytosolic leaflet (Takar et al., 2016; Bai et al., 2021). The resulting phospholipid asymmetry is important for endomembrane homeostasis, vesicular transport, and associated protein sorting within the cell (Hua et al., 2002; Wicky et al., 2004; Singer-Krüger et al., 2008; Wu et al., 2016). *S. cerevisiae* possesses five P-type ATPases that flip phospholipids, yet Neo1 is the only essential member of this group (Hua et al., 2002), making it an especially intriguing protein to study. Perhaps not coincidentally, Neo1 is the only P-type ATPase known to substantially reside at both the Golgi and PVE (Dalton et al., 2017). It is therefore plausible that a critical if not essential function of Neo1 may involve facilitating vesicle formation and transport between these two organelles.

To more closely interrogate the intra-cellular localization of Neo1, I performed kinetic analysis experiments in cells with tagged Vps10, Neo1, and Sec7. I observed that Vps10 and Neo1 simultaneously appeared at Golgi cisternae which shortly thereafter acquired Sec7 (Figure E.1A). In the two cisternae analyzed, Vps10 disappeared near the peak of Sec7 abundance, and Neo1 completed its departure 15-20 seconds later. The departure kinetics of Neo1 appear similar to those of Kex2 or Nhx1 (Figure 4.3A), suggesting that Neo1 may recycle in the AP-1/Ent5 pathway and/or recycle between the PVE and Golgi. While analyzing the data, I noticed that Neo1

sometimes (but not always) resides at Vps10 containing structures which do not acquire Sec7 (Figure E.1B). These are presumptive PVEs that are sorting Vps10 for export to Golgi cisternae, possibly with the aid of Neo1. It is intriguing that not all PVEs noticeably contain Neo1, and that its Golgi residency extends well past that of Vps10. Future experiments should more closely examine Neo1 localization dynamics by kinetic analysis against well characterized markers such as Kex2, Nhx1, and Vps8. This will pave the way for further work elucidating the precise trafficking pathways that Neo1 helps operate.

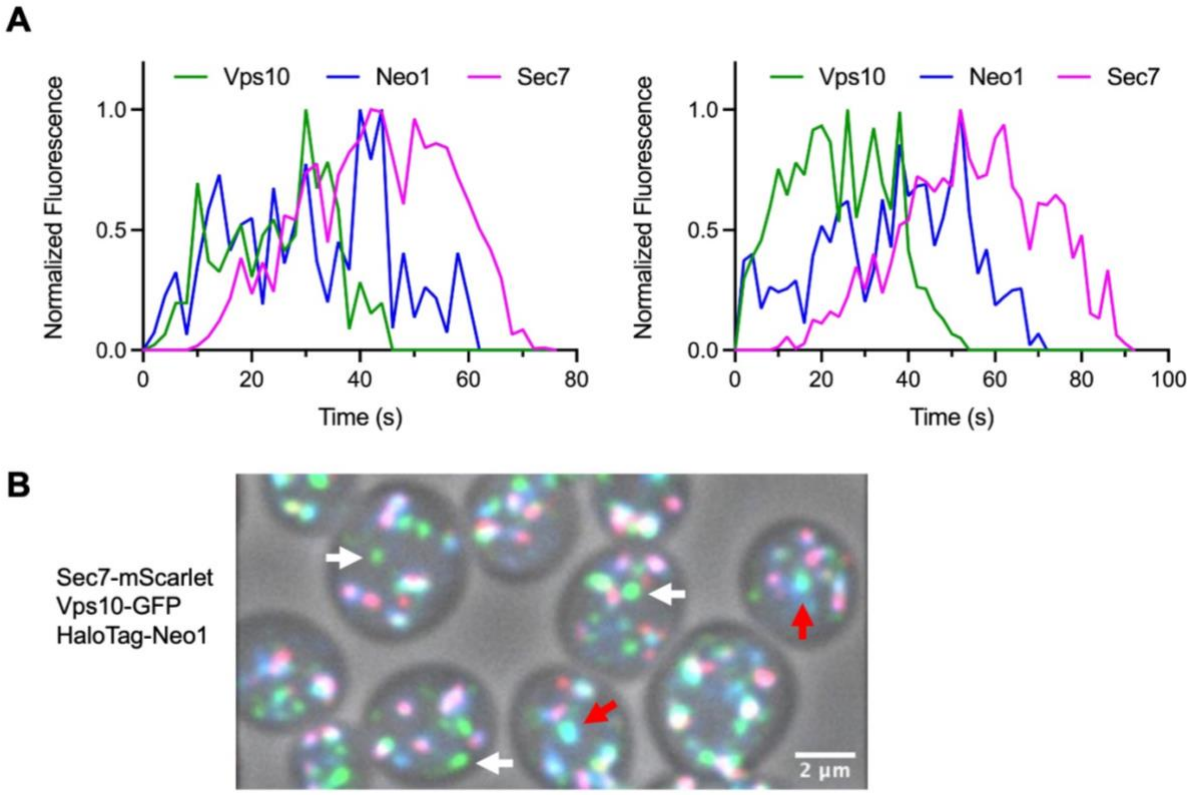

Figure E.1: **The phospholipid flippase Neo1 localizes to the late Golgi and a subset of prevacuolar endosomes. (A)** *S. cerevisiae* cells expressing Vps10-GFP, Sec7-mScarlet, and HaloTag-Neo1 from their endogenous loci were grown to mid log phase in NSD, stained with JFx650 dye, and imaged on a Leica Stellaris confocal microscope. Two spatially isolated cisternae were tracked over time, and the normalized fluorescence intensities of the three tagged proteins were quantified. **(B)** An average projected confocal Z stack from a movie obtained as described in (A). Red arrows mark structures containing Vps10-GFP and HaloTag-Neo1. White arrows mark structures containing Vps10-GFP only. Scale bar 2µm.

The transmembrane protein Any1 is a putative lipid scramblase originally identified as an antagonizer of Neo1 (van Leeuwen et al., 2016). Loss of Any1 renders *neo1Δ* cells viable, and *neo1Δ any1Δ* cells instead require the late Golgi localized P-type ATPase Drs2 for viability (Takar et al., 2019). Any1 reportedly localizes to the late Golgi as well as the PVE where its scramblase activity assists with multi-vesicular body formation (Gao et al., 2025). Nevertheless, the precise function(s) of Any1 in facilitating endomembrane homeostasis as well as its functional relationship with Neo1 are not entirely clear.

To better understand Any1 localization dynamics, I kinetically mapped it against the Golgi resident, Sys1 (Figure E.2). Data from two analyzed cisternae show that Any1 and Sys1 arrive at and depart from the Golgi concurrently. I did not see Any1 in punctate structures without Sys1 (presumptive PVEs), although the lack of a PVE marker in my experiments hampers a confident assessment. Gao and colleagues observed that Any1 colocalizes frequently with Sec7 and infrequently with Vps21, perhaps explaining my inability to observe Any1 at the PVE (Gao et al., 2025). Regardless, it will be important to clarify the localizations of Neo1 and Any1 relative to each other at the Golgi and PVE. In the meantime, my data suggest that Any1 arrives in intermediate COPI vesicles before Neo1 arrives in PVE-derived and/or AP-1/Ent5 vesicles. Neo1 likely traffics between the Golgi and PVE and may additionally utilize AP-1/Ent5 vesicles for intra-Golgi recycling. Given that Any1 and Neo1 co-immunoprecipitate together (Takar et al., 2019), they likely work in spatial proximity to remodel lipid bilayers. It is tempting to speculate that Any1 scramblase activity relieves membrane tension caused by Neo1 flippase activity, establishing an antagonistic relationship that may nevertheless be critical for vesicle formation and protein sorting at the Golgi and PVE.

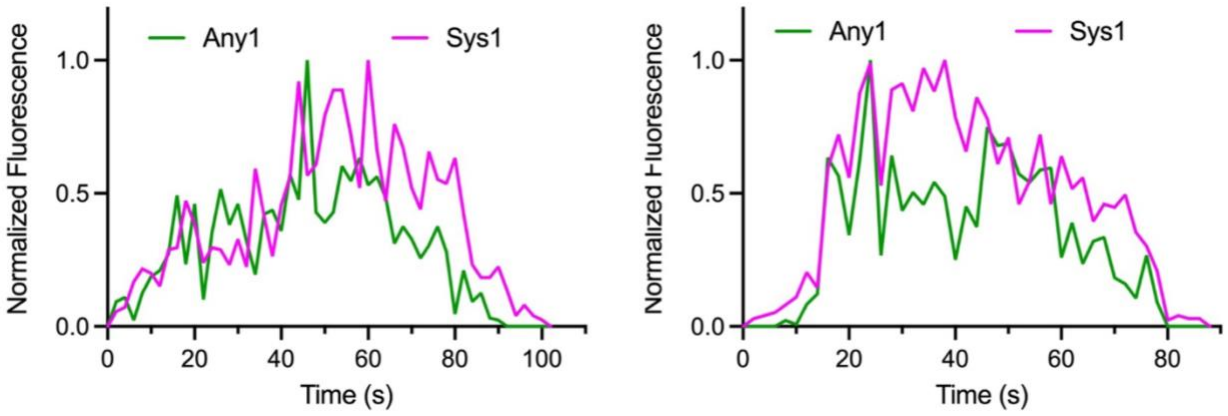

Figure E.2: **The putative lipid scramblase Any1 colocalizes with Sys1 during cisternal maturation.** *S. cerevisiae* cells expressing Sys1-HaloTag and Any1-GFP from their endogenous loci were grown to mid log phase in NSD, stained with JFx646 dye, and imaged on a Leica Stellaris confocal microscope. Two spatially isolated cisternae were tracked over time, and the normalized fluorescence intensities of the two tagged proteins were quantified.

APPENDIX F

THE TRANSMEMBRANE NINE FAMILY MEMBER TMN3 COLOCALIZES WITH VRG4 AT THE EARLY GOLGI

Little is specifically known about the *S. cerevisiae* protein Tmn3, although its sequence similarity to Tmn1 and Tmn2 has provided some insights. All three Tmn proteins are part of the transmembrane nine family which also exists in other organisms including humans. (Schimmöller et al., 1998). Tmn1 and Tmn2 are 86% similar while Tmn3 is only 41% similar to Tmn1 (Froquet et al., 2008). Tmn3 is thus a more phylogenetically distant relative of the other two. The loss of two out of three Tmn proteins causes a defect in *S. cerevisiae* filamentous growth, and the deletion of any single Tmn protein largely prevents adhesive growth (Froquet et al., 2008). Functionally, these results suggest that Tmn proteins are only partially redundant. Another study deleted all three Tmn proteins and found this substantially altered the cellular elemental profile, particularly by increasing the levels of manganese and decreasing those of copper (Hegelund et al., 2010). The above functional data and the nine transmembrane domain architecture of each Tmn protein suggest they may play roles in metabolism and ion transport.

A more complete understanding of Tmn protein functions requires a careful analysis of their subcellular localizations. A landmark study reported that Tmn1 and Tmn2 have a KXD/E motif at their C-termini that binds to COPI (Woo et al., 2015). The authors used this knowledge to properly tag Tmn1 and Tmn2 at their N-termini and observe their Golgi localization. In particular, Tmn1 was observed to colocalize with the SNARE protein Bet1 in *S. cerevisiae*. I verified the Golgi-localization of Tmn1 in Chapter 3, and further demonstrated its vesicular transport within intermediate COPI vesicles. Here, I show that Tmn3 localizes the early Golgi with Vrg4 (Figure

F.1). The signal strength of Tmn3 was very weak, likely reflecting its low abundance. Nevertheless, the two isolated cisternae analyzed possessed Tmn3 throughout almost the entire duration of Vrg4 residency. Tmn3 is therefore a likely cargo of the early COPI pathway despite not having the KxD/E motif possessed by its distant Tmn1 and Tmn2 relatives (Woo et al., 2015). Future studies should more closely interrogate the localizations and trafficking routes of Tmn proteins as well as investigate their structures and functional distinctions. It is likely that all three proteins recycle within the yeast Golgi and facilitate its metabolic contributions to cellular physiology.

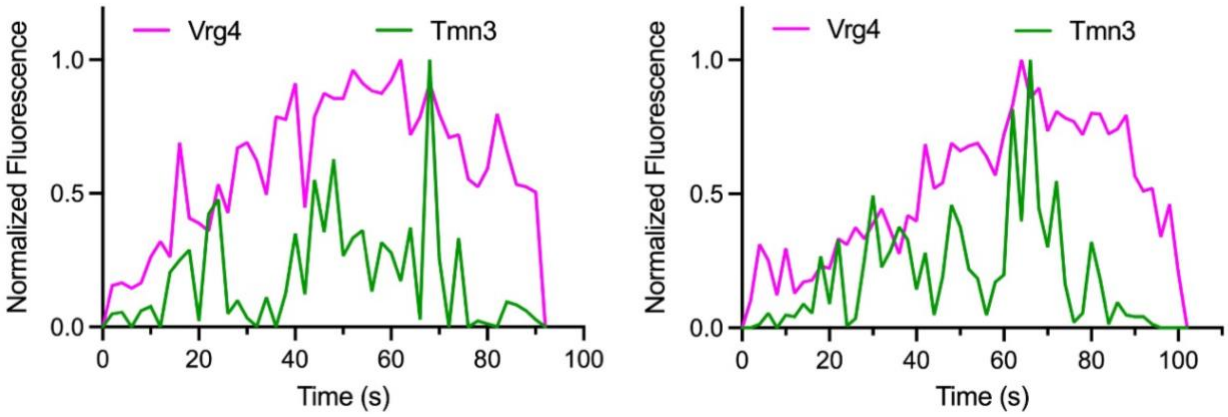

Figure F.1: **The transmembrane nine protein Tmn3 localizes to the early Golgi with Vrg4**. *S. cerevisiae* cells expressing HaloTag-Vrg4 and Tmn3-GFP from their endogenous loci were grown to mid log phase in NSD, stained with JFx650 dye, and imaged on a Leica Stellaris confocal microscope. Two spatially isolated cisternae were tracked over time, and the normalized fluorescence intensities of the two tagged proteins were quantified.

APPENDIX G

LIST OF PERFORMED EXPERIMENTS TO BE PUBLISHED

The following vesicle capture and tethering experiments will be published in upcoming manuscripts. They are listed here to finalize the complete record of all publication quality work performed during the completion of this thesis.

Vesicle Capture and Tethering Experiments

- Kex2-FRB based vesicle capture with the following GFP tagged proteins:
    - Kex1 as a test protein
        - Vrg4 as a negative control and Stv1 as a positive control
    - Tlg2, Tlg1, and Vps45 as test proteins
        - Vrg4 as a negative control
- Vps52-FRB based vesicle tethering with the following GFP tagged proteins:
    - Kex2 (+/– CK-666 drug), Snc2 (+/– CK-666 drug), Tlg1, Tlg2, and Vps45 as test proteins
        - Sec2 as a negative control
    - Control experiments testing the impact of GFP-Tlg2 tagging on GARP tethering of vesicles with the following GFP-tagged proteins:
        - Tlg1, Vps45, and Kex2